Modeling the growth of higher plants for life support systems : lettuce leaf metabolic model considering energy conversion and central carbon metabolism

Swathy Sasidharan L.

UNIVERSITÉ BLAISE PASCAL **UNIVERSITÉ D'AUVERGNE**
N° D. U. 2251 **ANNÉE : 2012**

ECOLE DOCTORALE SCIENCES DE LA VIE, SANTÉ, AGRONOMIE, ENVIRONNEMENT

N° d'ordre : 584

Thèse

Présentée à l'Université Blaise Pascal
Pour l'obtention du grade de

DOCTEUR D'UNIVERSITE

(SPÉCIALITÉ: GENIE DÉS PROCÉDÉS)

Soutenue le **4 Juillet 2012**

Swathy Sasidharan L.

Modélisation de la croissance des plantes supérieures pour les systèmes de support-vie : modèle métabolique de la feuille de laitue considérant la conversion d'énergie et le métabolisme central du carbone

---

Président	**:** M. MICHAUD Philippe, Professeur, Université Blaise Pascal, Clermont-Ferrand.
Membres	**:** M. MERGEAY Max, Directeur de Recherche, SCK-CEN, Mol, Belgique.
	Mme PAILLE Christel, Ingénieur, ESA-ESTEC, Noordwijk, Pays-Bas.
Rapporteurs	**:** M. PRUVOST Jérémy, Professeur, Université de Nantes, Saint Nazaire.
	M. BRANDAM Cédric, Maître de Conférences (HDR), Université de Toulouse, Toulouse.
Directeur de thèse	**:** M. DUSSAP Claude-Gilles, Professeur, Université Blaise Pascal, Clermont-Ferrand.

Institut Pascal, axe Génie des Procédés, Energétique et Biosystèmes – Université Blaise Pascal – CNRS UMR 6602

UNIVERSITÉ BLAISE PASCAL **UNIVERSITÉ D'AUVERGNE**
N° D. U. 2251 **YEAR : 2012**

ECOLE DOCTORALE SCIENCES DE LA VIE, SANTÉ, AGRONOMIE, ENVIRONNEMENT

Order no : 584

Thesis

Submitted to Université Blaise Pascal
To obtain the degree of

DOCTOR OF PHILOSOPHY

(SPECIALITY: CHEMICAL ENGINEERING)

Defended on **4th July 2012**

Swathy Sasidharan L.

Higher Plant Growth Modelling for Life Support Systems: Leaf Metabolic Model for lettuce involving Energy Conversion and Central Carbon Metabolism

---

President : Mr. MICHAUD Philippe, Professor, Université Blaise Pascal, Clermont-Ferrand.
Members : Mr. MERGEAY Max, Research Director, SCK-CEN, Mol, Belgium.
Mme. PAILLE Christel, Engineer, ESA-ESTEC, Noordwijk, The Netherlands.
Reporters : Mr. PRUVOST Jérémy, Professor, Université de Nantes, Saint Nazaire.
Mr. BRANDAM Cédric, Assistant Professor (HDR), Université de Toulouse, Toulouse.
Thesis director: Mr. DUSSAP Claude-Gilles, Professor, Université Blaise Pascal, Clermont-Ferrand.

Institut Pascal, axe Génie des Procédés, Energétique et Biosystèmes – Université Blaise Pascal – CNRS UMR 6602

Résumé

Pour des missions spatiales de longue durée, les plantes supérieures doivent faire partie des systèmes de support-vie. Le projet Micro-Ecological Life Support System Alternative (MELiSSA, alternative de système de support-vie micro-écologique) de l'Agence Spatiale Européenne est basé sur un système clos de support vie qui inclut, autour d'un compartiment consommateur, des compartiments microbiens et des plantes supérieures. Les plantes consomment les déchets pouvant être recyclés (les eaux usées et du CO_2) et produisent de la nourriture fraîche, de l'eau potable et de l'oxygène pour l'équipage. Un des points clé pour ce type d'étude est le maintien d'un système qui assure le recyclage de tous les éléments C, H, O, N, S, P, … C'est pourquoi la base de l'étude repose sur une modélisation des stœchiométries de conversion qui doit traduire les échanges de matière et d'énergie en fonction des limitations physiques qui sont les paramètres de contrôle du système. L'étape préliminaire a été d'établir un modèle métabolique de feuille (un sous-modèle du modèle biochimique), comprenant le métabolisme central et utilisant les techniques métaboliques d'analyse des modes élémentaires (EFMA) et d'analyse des flux métaboliques (MFA) associé à une vision intégrée de l'énergétique du métabolisme central. En l'absence de données expérimentales suffisantes, le modèle métabolique de feuille a été construit à partir de la composition de la biomasse référencée par le Département Americain de l'Agriculture (USDA) et validé avec les données expérimentales de laitues (*Lactuca sativa*) cultivées dans l'installation de recherche des systèmes à environnement contrôlé (CESRF) de l'Université de Guelph (Canada). Pour la première approche, le modèle est satisfaisant et prometteur; il peut prédire la production de biomasse une fois connecté aux facteurs physiques de la croissance de plante (lumière, disponibilité en CO_2 et en eau,…) au cours du temps et à la composition de la biomasse. Cependant, nos résultats souffrent d'un manque de données pour vérifier les modèles métaboliques; ainsi, différents types de mesures pour des prédictions plus précises sont proposés. Le futur modèle doit être en mesure de contrôler la croissance de la plante pour la survie des humains, connaissant les flux provenant des autres compartiments de la boucle MELiSSA. Par ailleurs, l'approche décrite ici peut être utilisée de manière plus générale pour tous types d'études et modélisations du métabolisme, en particulier pour étudier le fonctionnement simultané et/ou consécutif des métabolismes photosynthétique et respiratoire.

Mots-clés : Analyse des flux élémentaires, analyse des flux métaboliques, croissance des plantes supérieures, modélisation, modèle métabolique des plantes supérieures, modèle stœchiométrique.

Abstract

For long term space missions, higher plants are necessary to be included in life support systems. The Micro Ecological Life Support System Alternative (MELiSSA) project of European Space Agency (ESA) is based on a closed life support system where microbial and higher plant compartments support the consumer's compartment. Plants consume the possible recycling wastes (waste water and CO_2) and provide fresh food, potable water and oxygen to the crew. One of the key points for this kind of study is to maintain a system which recycles all the elements C, H, O, N, S, P, etc. That is why, the study is based on the modelling of conversion stoichiometries; they are the results of the control parameters of the system (physical limitations of mass and energy exchanges). As a preliminary step, we have established leaf metabolic model (a sub model of the plant biochemical model) involving central carbon metabolism using metabolic techniques, elementary flux mode analysis (EFMA) and metabolic flux analysis (MFA). It is associated to an integrated approach of energetics and central metabolism. Due to data limitations, the leaf metabolic model was constructed taking the biomass composition of lettuce (*Lactuca sativa*) from United States Department of Agriculture (USDA) and validated with the experimental data where lettuce grown in controlled Environment Systems Research Facility (CESRF) of University of Guelph (Canada). For the first approach, the model is satisfying and promising; it can predict the biomass production connecting the physical plant growth factors (light, CO_2 and water availability, etc.) along with time course growth and biomass composition. However, our results show the lack of sufficient data; hence, various kinds of measurements required for more accurate model predictions are proposed. The future model must be able to control and manage the plant growth for human survival knowing the fluxes from other compartments of MELiSSA loop. Further, the approach described here can be used more generically in all kinds of metabolic studies and modeling, especially for studying simultaneous and/or consecutive photosynthetic and respiratory metabolisms.

Key words: Elementary Flux mode analysis; higher plant growth; higher plant metabolic model, metabolic flux analysis; modelling; stoichiometric model.

Remerciements
Acknowledgements

I wish to extend my deep-felt gratitude to our **Almighty God** and to all those who made the submission of this thesis possible.

I sincerely thank my supervisor Prof. Claude Gilles Dussap, Director of Axe GePEB, for his support, coordination, patience and continued guidance over the years. Even though he was very busy, he has gone out of his way to help me. Without his ideas and tireless effort, this work would not have been possible. His encouragement, criticism and useful suggestions have helped me to submit this thesis.

I am grateful to Prof. Ashok Pandey, Deputy Director and Head of Biotechnology division, NIIST, Trivandrum, India. I could never forget him as he has given me the opportunity to study in France. I acknowledge Prof. Christian Larroche, Director of Polytech' Clermont Ferrand for introducing me to all and helping me in all of my needs.

I sincerely express my gratitude to MELiSSA project leaders: Christophe Lasseur, Christel Paille, Max Mergeay, and to all those who helped me to become a part of the same. Additionally, my sincere gatitude goes to the members of the jury, Prof. Jérémy Pruvost, Dr. Cédric Brandam and Prof. Philippe Michaud for accepting my thesis evaluation and providing stimulative and constructive criticism.

My heartfelt thanks to all faculty members of Axe GePEB: especially to Sky for my work related doubts and friendly discussions; Catherine, Agnes, Jean Francois and Fabrice for their affection with ever withstanding positive energy, Jean Pierre, Helene, Pascal, David, Berengere and Gwen for their smile and support.

I acknowledge the services of Beatrice for her administrative support and granting money via EGIDE/Campus France during the period of my research without which I would not have been able to support myself.

Axe GePEB was like a home away from home to me. I deeply feel gratitude to Pauline for her constant support, encouragement and love. Thanks for the care and friendly support of my labmates Azin, Oumar and Marie-Agnes; I will surely miss our 'Repas de mercredi'; thanks to Reeta chechi, Anil, Cindie, Alain, Matthieu, Aurore, Jeremy, Kais and Numidia for their companionship. In this occasion, I remember and wish to thank my ex labmates Darine, Akhileshji, Erell and Stephanie.

I am greatly indebted to all those persons who encouraged or helped me personally or professionally during my stay in France. I am deeply obliged to Sushama aunty for making June as an unforgettable month. Also, I express my love to Dominique, Estéle and Guillaume.

I could never forget the constant love and parental care I received from Claire aunty and Patrick uncle (of course, they are 'mes parents français'), through whom I received great support for my spiritual life, 'la famille de l'Hospitaliers d'Auvergne'. I am thankful to the families who showered love on me: Patrick, Evylene, Marie Therese, Cecile, Adeline, Jean, Martin, Annelise, Pierre, Jean Marc, Bernard, Francine, Jean Luc... I have a big list of families to whom I would like to say thanks!

Further, I wish to thank all of my friends and families of our Indian-Pakistan Community who made my weekends lively. Thanks to Polkam ji, Vanaja and their families.

Also, I am extremely thankful to Emilie, Shan, Shanti and Lolo for encouraging my cultural activities and their companionship. The friendship and support provided by my friends from India is also acknowledged: Bala, Syed chettan, Smitha chechi and Jancy chechi for their understanding, love and support.

My parents and siblings with their constant support, encouragement and prayers have helped me to move on all these years. I thank Amma, Achan, Annan, chechi and Zakia for being there always for me. Special thanks to Mary aunty, Mary Antony aunty, Fr. Cyril and the parish where I belongs to.

I thank once again the Lord Almighty, for his benevolence and blessings showered upon me. Whenever I lost faith in myself, he held me in his never failing hands and I know that all along, HIS power has lead me and sure it will still lead me on.

Swathy

Table of Contents

List of Figures

List of Tables

Abbreviations

BioCyc	Biological database
CESRF	Controlled Environment Systems Research Facility (CA)
^{13}C MFA	Metabolic Flux Analysis using ^{13}C
EFM	Elementary Flux Modes
EFMA	Elementary Flux Mode Analysis
EMP	Embden Meyerhof Pathway
EP	Extreme Pathway
EPA	Extreme Pathway Analysis
ESA	European Space Agency
ETC	Electron Transport Chain
FBA	Flux Balance Analysis
FSA	Flux Spectrum Approach
Int. ref.	Internet reference
KEGG	Kyoto Encyclopedia of Genes and Genomes
LSS	Life Support System
MCA	Metabolic Control Analysis
MELiSSA	Micro-Ecological Life Support System Alternative
MetaCyc	Encyclopedia of Metabolic Pathways
MFA	Metabolic Flux Analysis
PlantCyc	Plant metabolic pathway database
TCA	Ticarboxylic acid cycle
USDA	United States Department of Agriculture

Atoms, molecules and metabolites

10-formylTHF	10-Formyltetrahydrofolate
1-3BPGA	1,3- bisphospho-D-glycerate
1-3BPGA^{4-}	Reduced form of 1,3- bisphospho-D-glycerate
2 Oxo	2-oxoglutarate or 2-ketoglutarate
2-oxobut	2-oxobutanoate
2-oxoiso	2-oxoisovalerate
2PGA	2-phospho-D-glycerate
3PGA $^{-}$	3-phospho-D-glycerate
4-hydroPhe	4-hydroxyphenylpyruvate
5p-ribosyl-1-pp	5-phospho-alpha-d-ribosyl 1-pyrophosphate
ac	Acetate
AcCoA-	Reduced form of acetyl-CoA
AcCoA	Acetyl-CoA
ADP	Adenosine diphosphate
ADP^{3-}	Reduced form of adenosine-diphosphate
Ala	Alanine
AMP	Adenosine monophosphate
AMP^{2-}	Reduced form of adenosine-monophosphate
Arg	Arginine
Asn	Asparagine
Asp	Aspartate
Asp-semialdehyde	Aspartate-semialdehyde
ATP	Adenosine-triphosphate
ATP^{3-}	Reduced form of adenosine-triphosphate
C	Carbon
Ca^{2+}	Calcium ion (oxidised)
CH2=THF	Methyltetrahydrofolate
CH3THF	5-formyl-tetrahydrofolate
Cis Aconitate^{3-}	Reduced form of cis aconitate
Cisaconitate	Cis aconitate

Cit	Citrulline
$Citrate^{3-}$	Reduced form of citrate
Cl^{-}	Chloride ion
CO_2	Carbon dioxide
CoA	Coenzyme A
Cys	Cystine
DHAP	Dihydroxyacetone phosphate
$DHAP^{2-}$	Reduced form of dihydroxyacetone phosphate
DNA	Deoxyribonucleic acid
E4P	D-erythrose-4-phosphate
$E4P^{2-}$	Reduced form of D-erythrose-4-phosphate
F6P	D-fructose-6-phosphate
$F6P^{2-}$	Reduced form of D-fructose-6-phosphate
FAD	Flavine adenine dinucleotide (oxidised form)
$FADH_2$	Flavine adenine dinucleotide (reduced form)
FBP	D-fructose-1,6-bisphosphate
FBP^{4-}	Reduced form of D-fructose-1,6-bisphosphate
Fe^{2+}	Iron ion
fum	Fumarate
$Fumarate^{2-}$	Reduced form of fumarate
G1P	D-glucose 1-phosphate
$G1P^{2-}$	Reduced D-glucose 1-phosphate
G3P	Glyceraldehyde-3-phosphate
$G3P^{2-}$	Reduced glyceraldehyde-3-phosphate
G6P	D-glucose 6-phosphate
$G6P^{2-}$	Reduced D-glucose 6-phosphate
GDP^{3-}	Reduced form of guanosine diphosphate
Gln	Glutamine
Glu	Glutamate
Glu semi	Glutamate-γ-semialdehyde
Gly	Glycine
glycerol3P	Glycerol 3-phosphate
GTP^{4-}	Reduced form of guanosine triphosphate
H	Hydrogen

H^+	Proton ion
H_2O	Water
H_2S	Hydrogen sulphide
Hexose 6-P	Hexose 6-phosphate
His	Histidine
H_N^+	Proton in N-phase
HNO_3	Nitrate
H_P^+	Proton in P-phase
icit	Isocitrate
Iso	Isoleucine
$Isocitrate^{2-}$	Reduced isocitrate
K^+	Potassium ion
Leu	Leucine
Lys	Lysine
Mal Co A	MalonylcoA
Malate	L-malate
$Malate^{2-}$	Reduced L-malate
MethenylTHF	5,10-methenyltetrahydrofolate
Mg^{2+}	Magnesium ion
N	Nitrogen
NAD^+	Nicotinamide adenine dinucleotide
NADH, H^+ or NADH	Nicotinamide adenine dinucleotide (reduced form)
$NADP^+$	Nicotinamide adenine dinucleotide phosphate
NADPH, H^+ or NADPH	Nicotinamide adenine dinucleotide phosphate (reduced form)
NADPH, H_N^+	Nicotinamide adenine dinucleotide phosphate (reduced form) at N-phase
NADPH, H_P^+	Nicotinamide adenine dinucleotide phosphate (reduced form) at P-phase
NH_3	Ammonia
O	Oxygen
O_2	Dioxygen (molecular oxygen)
OAA	Oxaloacetate
Orn	Ornithine
$Oxaloacetate^{2-}$	Reduced oxaloacetate

P	Phosphorus
PEP	Phosphoenol pyruvate
PEP^{3-}	Reduced phosphoenol pyruvate
PGA^{3-}	Reduced 3-phospho-D-glycerate
Phenyl Ala	Phenylalanine
Pi	Inorganic phosphate
Pi^{2-}	Reduced inorganic phosphate
PPi	Pyrophosphate
PPP	Pentose phosphate pathway
PQ	Plastoquinone
PQH_2	Plastoquinol
Pr & Pfr	Forms of phytochrome
Pro	Proline
Pyr	Pyruvate
Pyr 5	1-pyrroline-5-carboxylate
$pyruvate^-$	Reduced pyruvate
R5P	Alpha-D-ribose 5-phosphate
$R5P^{2-}$	Reduced alpha-D-ribose 5-phosphate
RBP	Ribose 1,5-bisphosphate
RNA	Ribonucleic acid
Ru5P	D-ribulose 5-phosphate
$Ru5P^{2-}$	Reduced D-ribulose 5-phosphate
RuBisCO	Ribulose Bisphosphate Carboxylase-Oxygenase
RuBP	D-ribulose 1,5-bisphosphate
$RuBP^{4-}$	Reduced D-ribulose 1,5-bisphosphate
S	Sulphur
S7P	Sedoheptulose 7-phosphate
$S7P^{2-}$	Reduced sedoheptulose 7-phosphate
S-ade-methionine	S-Adenosyl-L-methionine
S-ad-homocysteine	S-Adenosyl-L-homocysteine
SBP	Seduheptulose-1,7-bisphosphate
SBP^{4-}	Reduced seduheptulose-1,7-bisphosphate
Ser	Serine
Suc	Succinate

Suc CoA	Succinyl-CoA
Suc homoserine	Succinyl homoserine
Succinyl-CoA^{-}	Reduced succinyl-CoA
THF	Tetrahydrofolate
Thr	Threonine
Triose 3-P	Triose 3-phosphate
Trp	Tryptophan
Tyr	Tyrosine
UDP	Uridine-diphosphate
UDP-glucose	Uridine 5'-(trihydrogen diphosphate) alpha-D-gucopyranosyl ester
UMP	Uridine-monophosphate
UQ	Ubiquinone
$UQ^{\cdot-}$	Ubiquinone semi radical
UQH_2	Ubiquinol
$UQ_N^{\cdot-}$	Ubiquinone semi radical at N-phase
$UQ_P^{\cdot-}$	Ubiquinone semi radical at P-phase
Val	Valine
Xu5P	D-xylulose 5-phosphate
$Xu5P^{2-}$	Reduced D-xylulose 5-phosphate

Scientific parameters, variables and notations

*	Physiological conditions
A	Stoichiometric matrix of *'m'* metabolites and '*n'* reactions
aa	Amino acid
c	Velocity of light (2.998×10^8 m/s)
Cu_A	Copper site near mitochondrial P-phase
Cu_B	Copper site near mitochondrial N-phase
Cyt	Cytochrome
Cyt *b6f*	Cytochrome *b6f*
Cyt b_H	Cytochrome b_H
Cyt b_L	Cytochrome b_L
Cyt b_H^-	Reduced cytochrome b_H
Cyt b_L^-	Reduced cytochrome b_L
Cyt c_1	Cytochrome c_1
Cyt Fe^{3+}	Oxidised cytochrome
Cyt Fe^{2+}	Reduced cytochrome
e	Elementary mode
e-	Electron
E	Exchangeables
$E_{m,7}$	Mid point potential at pH 7 (mV)
$E_{m,4}$	Mid point potential at pH 4 (mV)
$E_{m,7.5}$	Mid point potential at pH 7.5 (mV)
$E_{m,6.5}$	Mid point potential at pH 6.5 (mV)
E_N	Electrical potential at N-phase (mV)
E_P	Electrical potential at P-phase (mV)
E	Total luminous energy available for one quanta of photon (kJ/mol)
ΔE	Total energy of any system (kJ/mol)
F	Faraday's constant (kJ/mol)
Fd	Ferredoxin
Fdox	Oxidised ferredoxin ($Fd(Fe^{3+})$)
Fdred	Reduced ferredoxin ($Fd(Fe^{2+})$)
ΔG	Gibbs free energy (kJ/mol)
$\Delta G_{m,7}$	Free energy at pH 7 (kJ/mol)
$\Delta G_{m,4}$	Free energy at pH 4 (kJ/mol)
$\Delta G_{m,7.5}$	Free energy at pH 7.5 (kJ/mol)
$\Delta G_{m,6.5}$	Free energy at pH 6.5 (kJ/mol)
ΔG_{physio}	Free energy at physiological condition
h	Planck's constant (6.626×10^{-34} J/s)
hν	Photon of light
$h\nu_{680}$	Photon of light at 680 nm
$h\nu_{700}$	Photon of light at 700 nm
J	Unknown vector of the reaction rates or fluxes
K_m	Kinetic parameter of Michaelis-Menton constant
m	Metabolites of a system

n Reactions of a system
n Number of electrons participated in a reaction
N Number of amino acids
NE Nonexchangeables or intermediate metabolites
N-phase Negative phase
n_e Number of protons consumed
ΔpH pH gradient between the membranes
P_{680} Reduced pheophytin
P_{680}^{+} Oxidised pheophytin
P_{680}^{*} Excited photosystem, PS II due to the photon absorption at 680 nm
P_{700}^{*} Excited photosystem, PS I due to the photon absorption at 700 nm
P_{700} Reduced photosystem, PS I
P_{700}^{+} Oxidised photosystem, PS I
PC Plastocyanine
PC (Cu^{2+}) Oxidised plastocyanin
PC (Cu^{+}) Reduced plastocyanin
P/2e- Ratio of the production rates of ATP and reduction power of two electrons for photosynthesis (ATP/NADPH, H^{+})
pH_N pH at N-phase
pH_P pH at P-phase
P/O Ratio of ATP production rate and consumption of the reduction power of two electrons for respiration (production of 1 mole of water from ½ mole O_2)
P-phase Positive phase
PS I, II Photosystem I and II
Q Net heat supplied to the system
Q_A & Q_B site Sites located at chloroplast and mitochondrial membranes
Q_N Ubiquinol binding site near N-phase
Q_P Ubiquinol binding site near P-phase
R Ideal gas constant (8.31451 J/mol K)
R Vector of rates of exchange
R_E Vector of rates of exchange for exchangeables
R_{NE} Vector of rates of exchange for nonexchangeables
r_H Ratio of oxidised and reduced forms of cytochrome b_H
r_L Ratio of oxidised and reduced forms of cytochrome b_L
T Temperature (K)
V_{max} Kinetic parameter of Michaelis-Menton equation
W Work done by the system

Greek Letters

α Stoichiometric coefficients for lipid formation
β Stoichiometric coefficients for lipid formation
γ Stoichiometric coefficients for lipid formation
δ Stoichiometric coefficients for lipid formation
λ Wavelength of light (nm)
$\tilde{\mu}_{UQ_N^-}$ Electrochemical potential of semi ubiquinone radical at N-phase
$\tilde{\mu}_{UQ_P^-}$ Electrochemical potential of semi ubiquinone radical at P-phase
ΔΨ Membrane chemical potential (mV)
η_{max} Coefficient of photosynthesis

Foreword

Foreword

The project of higher plant growth modelling for life support systems has been developed jointly for two aspects: the global model design with a specific accent on mass and energy transfers, and the simulation of the biomass production at the level of metabolism and plant growth stoichiometry. These studies are presented in the thesis manuscripts of Pauline Hézard, "Higher plant growth modelling for life support systems: global model design and simulation of mass and energy transfers at the plant level" and Swathy Sasidharan L, "Higher plant growth modelling for life support systems: Leaf metabolic model for lettuce involving energy conversion and central carbon metabolism". These two documents have a common foreword, defining the main aspects and requirements of the project.

Life support systems requirements

Space exploration includes long-term manned missions as well as planetary explorations, which require life support systems (LSS) designed with a high degree of closure and food regeneration capability. Micro-Ecological Life Support System Alternative (MELiSSA) project of European Space Agency (ESA) is designed in this objective providing a planetary base for continuous life support system of a small crew (from 2 to 6), recycling 100% of air, water and producing at least 40% of food.

This system consists of six separated compartments growing micro- and macro-organisms in order to fulfil all the different recycling steps. One of these is used for growing plants: they are in the last steps of recycling, permitting oxygen, water and food regeneration from carbon dioxide, mineralised water and light. The final aim is to be able to control whole recycling loop in order to fulfil human needs. In this objective, efficient and robust models are necessary for each compartment; they are required to control the environment (temperature, pH, light intensity, etc.) to obtain the required behaviour for the organism. Then, the compartment could provide the required amount of output in terms of gas, liquid and solid (food) to the rest of the loop. The system of control is highly constrained by two specificities: multiple levels and multiple time scales. In terms of levels, four different layers can be described (Dussap *et al*., 2005): level 0 is the closest to the process; it contains the process measurements and basic controllers for maintaining the adequate set point for an environmental parameter. For example, temperature or pH regulations rely on heater-cooler start and stop or acid-base pumps, with a simple proportional-integral-derivative (PID)

controller. Level 1 contains the system model itself, which corresponds to the present work. It states the correct value for each environmental parameter based on the system history, prediction determination and overall loop requirements. Level 2 is not specific for one compartment, but regulates all the set points in an optimisation objective in order to respond to level 3 requirements. Level 3 is the interface with the crew, who can define future events (like crew member arrival or departure) and accurate environmental tuning. This level defines the optimised response of the loop in order to fulfil these requirements. In terms of control dynamics, they are highly different depending on the different states of the matter: gas control has to be effective within few minutes, liquid control is at an hourly step, and food control is in the day scale. Moreover, depending on each compartment, the biological response kinetics to environmental adjustment is different and these various time scales have to be accounted in the models. For the output control, quality and security aspects have to be included: quality in terms of chemical and microbiological content to be provided to the consumers (human crew for the overall system, but also each compartment); and security for the backup systems that should be included at each key point, for each step of the closed loop process. Another important issue is that the life support system functions with uncontrolled inputs, for example, CO_2 production rate from the crew cannot be predicted accurately. Additionally, these inputs may be discontinuous (crew waste production) for a system that is designed for a continuous functioning; this means that all the system is constrained by the mass balance of the overall loop, for all the chemical elements. In a mass- and volume-limited environment in space, the buffer sizes have to be small for each of the consumable (oxygen, water, food, etc.), which means that the life support system must have a short response-time and a highly adaptable behaviour.

Higher plant compartment requirements

Concerning the higher plant compartment, the growth environment is designed as fully controlled, except for the supply of CO_2 and waste issued from the human habitat. The input flow rate corresponds to the flow rate of minerals (CO_2, N-NO_3 and N-NH_4) coming from the previous compartments in charge of waste degradation. Light intensity and photoperiod, temperature, humidity, pH of the nutrient solution and electro conductivity are adjusted. The higher plants' growth model should be designed for organising the cultures, and if possible, managing environment in order to control plant behaviour. The main requirements are of three ranges. First, for a closed loop, it is necessary to follow mass balance principle at each

step. Then, the model for higher plant compartment should take into account mass balance: metabolism has to be considered, even if a simplified way with few, global stoichiometric equations. Secondly, this model is only a part of MELiSSA loop control system: it has to be able to communicate information with the models of the other compartments. As it is also a long-term implementation system, it should be built in a structured form in order to be easy to modify, just changing specific functions or adding new parts, if necessary. Finally, the system will be settled in extraterrestrial places: the environmental conditions may not be similar to Earth's conditions, especially in terms of gravity and radiations. Therefore, the model has to be based upon known mechanisms and validated equations. This mechanistic approach of modelling could be based upon the understanding of rate-limiting processes for plant growth: the different mechanisms that happen in the organism have a maximum rate depending on few parameters. For example, maximum light interception depends on leaf properties (surface, absorption coefficient, etc.) and incident light intensity. These parameters have to be included in the model in order to obtain an accurate value of light energy available for plant growth. If all the maximum rates are calculated (such as water, CO_2, nutrient availability), it is possible to know which rate limits plant growth. Following all these objectives, an extensive bibliographic research was made for finding existing models of plant growth. They can be separated in three categories as described below: global models, models of physical mechanisms and models of biochemical mechanisms.

Existing plant growth models

Global models

Global models can be separated in two main types: process-based models and functional-structural models.

Process-based models consider the environment as the main driving variable for plant growth. The calculation of soil and atmosphere variations depending on climatic conditions and plant interactions permit the calculation of biomass growth and development, in a more or less detailed view. Process-based models take into account some of the growth mechanisms like light interception or water and nutrient absorption. However, plant shape is usually simplified as root and shoot, and/or edible and inedible. These models have the aim of modelling plant growth in an explanatory way linking environment characteristics to plant growth and development; however the developmental steps are included in an empirical way (Bouman *et*

al., 1996; Boote *et al*., 1998; Gabrielle *et al*., 1998; Brisson *et al*., 2008; Priesack and Gayler, 2009).

Functional-structural plant models are based upon plant architecture. They consider the plant shape (structure) in a detailed way; the internal plant mechanisms are often included in a simplified, sometimes empirical way (Fournier and Andrieu, 1998, 1999; Yan *et al*., 2004; Allen *et al*., 2005; Evers *et al*., 2005; Cournède *et al*., 2006; Bertheloot *et al*., 2008).

Of the existing global models of plant growth, all include an original approach of specific mechanisms: process-based models are usually well-structured for all of the mechanisms, and the limiting rates are calculated for predicting water or nutrient stress and eventually pests. Even if they often contain empirical simplifications for some processes, the approach and results are mainly based on extensive experimental knowledge from agriculture results. Also, soil and atmosphere dynamics can be included in an accurate mechanistic way, and the aim of guiding agricultural practices corresponds to the objective of the life support system control. Finally, functional-structural plant models include an accurate approach of morphology (even if the laws of architectural growth are not really mechanistic), and an explanatory or mechanistic approach for some of the mechanisms. Some of them calculate the exact repartition of light and its absorption in the leaves; others take into account a mass-balance approach for biomass repartition in the different organs, etc. That is why, even if none of them can be adapted directly to MELiSSA modelling approach, they can all give interesting ideas for building a new model. Consequently, it is necessary to take into account models of specific mechanisms in order to select suitable ones.

Physical models

The models of plant physical mechanisms for a general plant are studied separately and the influences of specific parameters or conditions are tested in detail. The main mechanisms are light interception, gas exchange, sap conduction and root uptake. Most of them have been built on mechanistic or explanatory laws.

Light interception is generally represented using Beer-Lambert law, at the global or local scale, eventually including the reflection and refraction indices, differentiation between leaves receiving direct or diffuse light, the leaf properties such as leaf angle, height or density (repartition in space), etc. (Govaerts, 1996; Asner and Wessman, 1997; Chelle and Andrieu, 1998; Wang and Leuning, 1998).

Another mechanism is the gas exchange; it happens through the stomata, small dynamic holes in plant cuticles; it depends on stomatal aperture, wind speed in external atmosphere, leaf shape, CO_2 concentration difference between atmosphere and leaf. Stomatal aperture is an important active mechanism based upon osmotic regulations which are controlled by sensing the parameters like light intensity, internal CO_2 concentration, atmosphere humidity or water availability at the root level. Gas exchange depends, also on the atmosphere dynamics around the leaves, leaf shape and canopy architecture. Many different types of models exist, depending if they consider atmosphere dynamics (Boulard *et al*., 2002), stomatal aperture (Aalto *et al*., 1999; Dewar, 2002; Kaiser, 2009), CO_2 diffusion (Leuning, 1995), water transpiration (Monteith, 1981) or several of these mechanisms (Tuzet *et al*., 2003; Xu and Baldocchi, 2003; Zavala, 2004).

The matter exchange between leaf and root happens via sap conduction vessels, which are separated into two different types depending on the sap composition, origin and role: phloem sap contains water and organic solutes produced by photosynthesis in the leaves and provide the organic substrates as building blocks for biomass production in the non-photosynthetic organs: buds, roots, fruits or grains and storage organs. For the movement of water and mineral nutrients from the roots, xylem vessels are made of dead lignified cells allowing a rapid upstream flow. Sap flow rate depends on vessel radius, length, sap viscosity and production (source) and demand (sink) powers, which are expressed as water potential. Only one mechanistic model of phloem exists, based on the pressure difference between production and consumption sites (Christy and Ferrier, 1973; Henton *et al*., 2002). Usually, only the source and sink powers of the organs and a resistance-to-transfer factor are taken into account in order to model directly biomass repartition in global models (Yan *et al*., 2004; Allen *et al*., 2005). For xylem, in many cases, the transport is not considered limiting compared to evaporation mechanism of transpiration, however some models consider this resistance (Tyree, 1997; Da Silva *et al*., 2011).

Last important mechanism is the root absorption. It depends on root architecture and morphology, nutrient and water availability, active uptake mechanisms, root permeability and pumping power (water potential difference). Several models exist with different parameters and structures (Fiscus and Kramer, 1975; Hopmans and Bristow, 2002; Roose, 2000).

All these mechanisms are extensively studied and most of the models have been established for more than 30 years; however, some parts remain uncertain. The mechanisms which would require some more attention for including accurate and robust mechanistic laws are the

stomatal processes, the sap flow (especially for phloem sap calculation, as it is difficult to measure it experimentally and it is rarely included in the models) and the root absorption. In any case, all the existing laws should be evaluated in order to verify the applicability in the case of controlled but extraterrestrial conditions.

Biochemical models

The biochemical mechanisms exist at two levels: (*i*) at the cell scale, metabolism, genome transcription-translation regulations, cell multiplication-differentiation, osmotic regulations, etc. (*ii*) at the plant or organ scale, hormonal signalling, environmental sensing and active transports. However, the latter are poorly described in terms of mathematical formulation, except for metabolism: the role of each hormone, the existence of the sensing systems and the signalling cascade, the cell multiplication and differentiation regulations, especially concerning transcription and translation regulations are not totally understood or known. The large variety of cultivars has given the opportunity to include the genetic variability into some process-based models in order to predict the response of each cultivar to the environment. However, the mechanisms of resistance to a specific pest or environmental stress are not known in detail and the inclusion of cultivar genetic specificities is purely empirical (Bertin *et al*., 2010). On the contrary, several modelling tools are available for metabolism; some of them follow mass-balance principle using stoichiometric equations. They provide the link between matter and energy exchange laws of the physical mechanisms and biomass growth and composition. For other biochemical mechanisms, they could be included in an explanatory way for the known mechanisms, for example, as global laws of development regulation and environmental sensing.

Design of a new model

With the knowledge of existing plant growth models and MELiSSA requirements, a global plant growth model is designed based on the physical and biochemical mechanisms. This corresponds to the structure of a process-based model. However, it should include a detailed description of plant architecture for a functional-structural model. Last requirement is to add a correct mass-balance approach with metabolic stoichiometries. The designed model is schemed in the next page: ‘Part a’ represents the plant mechanisms for the flows of matter and energy, which have to be modelled. ‘Part b’ is the description of the designed model with the details of the flows of information, separated as matter, energy and architecture information.

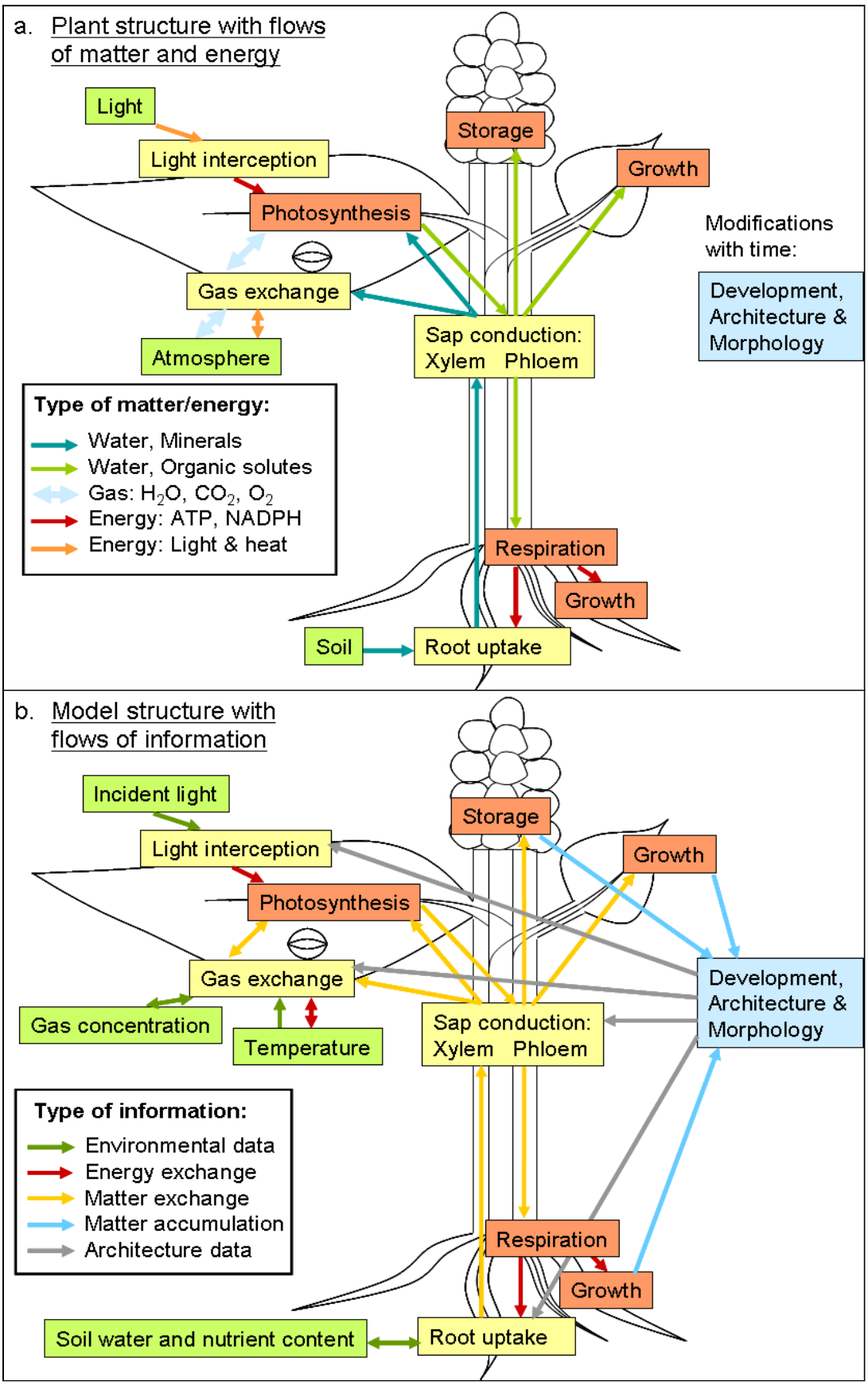

Figure: Comparison of plant and aimed model structures describing the flows of matter, energy and information.

The blue boxes represent the plant behaviour depending on growth: development and architecture mechanisms, which cannot be described with simple mechanistic laws. The yellow boxes contain physical mechanisms submodels, and the red boxes are specific for biochemical mechanisms submodels. These submodels are developed concomitantly in order to achieve the entire plant growth model; the work associated has been split into two complementary projects. These two research objectives have been realised in permanent close cooperation: architectural and physical (blue and yellow) submodels are described in the thesis of Pauline Hézard while we discuss the biochemical submodels (red).

Therefore, this document mainly concerns the biochemical model for higher plants growth. Of course, this work and manuscript has been elaborated in constant co-operation with Pauline Hezard's Ph D thesis that brings integrated views of higher plants growth model in connection with metabolic models.

Introduction

Introduction

The plant growth modelling is definitely a major task for the success of long term space exploration, because plants keep humans and other organisms alive. Without plants on long-duration missions, humans cannot survive safely. Plants consume the possible recycling wastes like waste water and atmosphere and provide fresh food, potable water and oxygen to breathe, in addition to the green and lively atmosphere. In terms of recycling functions, apart their intrinsic objective to produce edible biomass, higher plants have major capacities for recycling carbon (CO_2 assimilation by photosynthesis), producing oxygen (by photosynthesis), recycling water, nitrogen and other elements. Therefore, in conncetion with other compartments devoted to specific unit operations such as waste degradation, separation, fractionation, etc., higher plants compartment holds a central role for life support systems for recycling major elements. This is quite similar at another scale for terrestrial biosphere, the sustainability of which being listed to the photosynthetic activity of vegetation.

This thesis explores the routes to obtain the biochemical model of plant growth. The study is specifically applicable for plants that are growing in controlled environments. The development of biochemical model is mandatory in the designed higher plant growth model of Micro Ecological Life Support system Alternative (MELiSSA) loop of European Space Agency. Adopting a reductionist's point of view, our main concern is the modelling of plant metabolism linking the physical parameters such as CO_2, water, light in terms of inputs, and biomass and O_2 as outputs. The modelling requirements such as mass and energy balances, either at steady state or at pseudo steady state inside the loop are considered; then, the model stands for accounting elemental balances with the surroundings in terms of the flow of inputs and outputs. This concept gives a valid approximation for the modelling of plant growth in the controlled and predetermined environmental chamber.

Understanding the plant characteristics, the difficulty lies in the factors controlling plant growth: the biochemistry, metabolism and the associated properties and mechanisms differ in different cells, tissues and organs. Though almost all plants have the same central carbon metabolic pathways, the reactions occur at different rates. These are influenced by environmental conditions which are simulated by the physical models. Therefore, for the biochemical model validation, it is necessary to verify the experimental data (input/output flux rate and material balances) of plants grown under a predetermined/known environmental system.

Further, the degrees of freedom and complexities may increase, if we consider the whole plant metabolic network as such (as thousands of reactions are involved) to obtain the biochemical model; also, there are interactions within the cell organelles, between cell to cell and organ to organ. Hence, the first approach we plan is to divide the biochemical model of plant into different organ levels: a minimum of three biochemical sub models (leaf, root and stem models) as a generic aspect. The metabolic models for leaves and roots are obtained knowing the related plant metabolic networks: leaf model considers mainly photosynthesis and respiration, root model accounts for respiration and transport mechanisms, while stem model takes flux transport by xylem and phloem. The plant composition at organ level is necessary to connect root and leaf sub models in order to achieve the entire plant growth biochemical model.

Chapter 1 presents a trial of hierarchy. As a preliminary step, we developed a stoichiometric biochemical model for leaves taking all major pathways like photosynthesis, respiration, energy for maintenance and growth occurring in different cell organelles. This can be specifically applied for lettuce (*Lactuca sativa*) grown in controlled environments, as the experimental data for the same is already available. The stoichiometric equations involving experimental data (e.g. biomass formation equation) represent the total impact of various constraints for plant growth predicted by the physical submodel such as light energy availability, environmental stress, temperature, humidity, nutrient/water availability, CO_2/O_2 gas level, etc.

From the literature and previous developments explained in chapter 1, several metabolic modelling methods applicable for plant metabolism are studied; two methods found simpler to establish the leaf biochemical model are presented in chapter 2. The method we used is by metabolic flux analysis (MFA) and elementary flux mode (EFM) analysis; EFM stands for the topological analysis of the network, while MFA calculated the flux distribution for the same. Both techniques allow the leaf metabolic network studies under steady state and mass balance approach.

Taking the advantage of these, we study the central carbon metabolism (involving detailed mechanisms of light energy conversion in chloroplast and subsequent energy metabolism in mitochondria including thermodynamic consistencies), which can be used for general photosynthetic plant cell; this study is presented in chapter 3. It uses mathematical techniques that have been originally conceived for the study of microbial growth. This revealed *in vivo*

results without going into the experimental details and provided meaningful functional and structural properties of metabolic networks.

Finally in chapter 4, we coupled the EFM results of central carbon metabolism to the rest of the lettuce leaf cell metabolic network, assuming the initially formed metabolites transform into simple molecules such as sugars, amino acids, etc. and are moved by transport mechanisms, connecting the metabolism from one cell compartment to another. This process takes place within the cell, from cell to cell so that it connects all metabolisms, forming a large network of one leaf, which is integrated into the whole leaf canopy corresponding to the leaf model. The model is validated using the experimental data of lettuce grown in controlled Environment Systems Research Facility (CESRF) of University of Guelph, where the biomass composition used in the model was taken from another source, United States Department of Agriculture (USDA, Int. ref. 5).

Our first attempt, leaf biochemical model enabled us to couple and validate the plant biochemical perturbations and energy exchange with respect to physical limitations (e.g. light availability), thus providing, the link between matter and energy exchange laws of the physical mechanisms in addition to the biomass growth and composition exploration.

The main issues addressed in this thesis are,

a) The importance of fine understanding of the energy conversion processes including photosynthetic activity and respiration.
b) The reconciliation of a global stoichiometry from the sum of elementary biochemical conversions at the metabolic level highly connected to energy conversion processes.
c) The proof that, it is relevant to use the same techniques for metabolism investigations for microbial species and higher plants.
d) The lack of sufficient experimental data of lettuce plants grown in controlled environments including water, carbon and oxygen balances.
e) The need for a precise validation, when the whole biochemical model is coupled with the other models as designed in the general plant growth model for MELiSSA.
f) In the case of lettuce leaves, as they stand for 75% of the edible biomass at the time of harvest, the validation is obtained with the available data considering only the leaf model including data reconciliation.

At the end of the thesis, the types of data required in order to have precise and accurate validation of model in future are proposed.

Chapter 1 Biochemical approaches to study and model plant metabolism

1.1 Introduction

Plant biochemical process modelling is associated with the plant metabolic pathways: the reactions, their interactions and responses to the plant and the surroundings. Certainly, metabolic modelling reveals the plant biochemistry and this must be associated with the plants growing in controlled environmental chambers of MELiSSA higher plant compartment. The supply of metabolic energy responsible for plant growth is photosynthesis and respiration. Photosynthesis takes place mainly in leaf cells, while the roots are devoted for respiration, storage of carbohydrates, transportation of minerals and food, etc. Apparently, mineral uptake metabolism and food transportation occurs via stems and roots. This leads to a model with different metabolic behaviours from cellular level to plant organ level. In addition to this, the model contains energy and matter exchanges between several plant parts in order to control the growth and maintenance. Therefore, the metabolic model combines the details of all main metabolic pathways including cell growth, dissolved component transport and mass balances of different parts of the plant. This makes necessary to know the biochemistry of various plant parts and growth phases. In this aspect, the existing models based on plant biochemistry and metabolisms are described. Stoichiometric metabolic models were found interesting; but, some limitations were observed. Understanding the advantages and disadvantages of the methods used to develop the existing stoichiometric models, the ways to accomplish our aimed goal containing sub models are proposed. The designed plant metabolical model is only one of the efficient sub models in the general model design of the whole plant growth model. The general frame work and the structure of the possible metabolic sub models is presented in this chapter.

1.2 Biochemistry of metabolism

Though a wide diversity of plants exist in earth, the list of simple elements of which plants constructed are carbon, oxygen, hydrogen, magnesium, nitrogen, phosphorous, etc. The fundamental atomic components of plants are the same as for all life, only the details of the way in which they are assembled differ. Organisms show marked similarity in their major pathways of metabolism. For example, glycolysis and mitochondrial respiration, the metabolic pathway by which energy released from glucose and captured in the form of ATP, is common to almost every cell. All organisms, even those that can synthesise their own

glucose, are capable of glucose degradation and ATP synthesis via glycolysis. Other prominent pathways are also virtually ubiquitous among organisms.

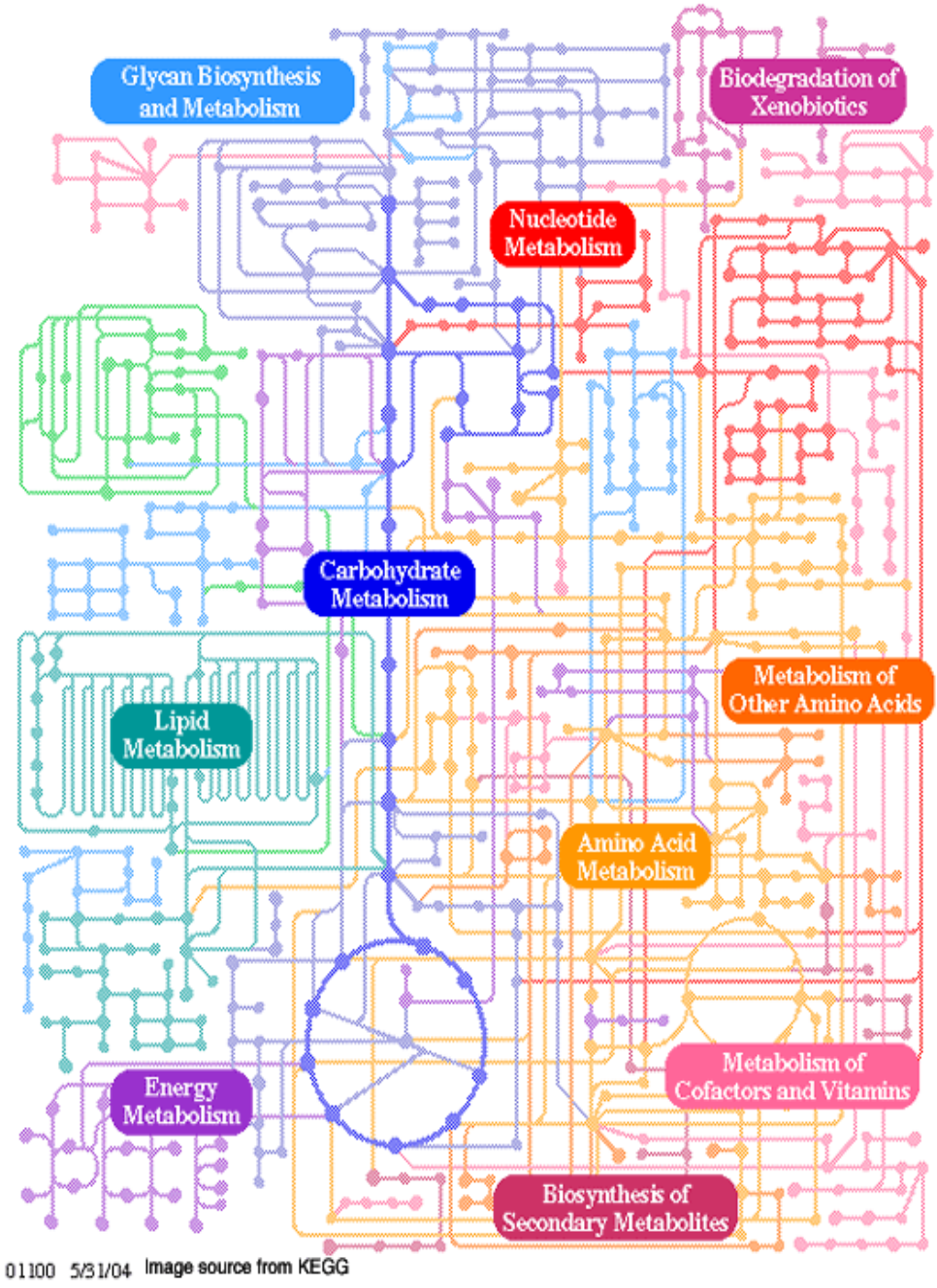

Figure 1.1: Metabolic map as a set of dots and lines. The heavy dots and lines trace the central energy-releasing pathways known as glycolysis and the citric acid cycle. (Adapted from KEGG) each intermediate = black dot, each enzyme = a line. The numbers of dots in the figure have one or two or more lines (enzymes) associated with them. A dot connected to just a single line must be either a nutrient/storage form/end product, or an excretory product of metabolism. Also, since many pathways tend to proceed in only one direction (that is, they are essentially irreversible under physiological conditions), a dot connected to just two lines is probably an intermediate in only one pathway and has only one fate in

metabolism. If three lines are connected to a dot, that intermediate has at least two possible metabolic fates; four lines, three fates; and so on.

Literally, metabolism studies started over a hundred years ago. According to Kepes, the first metabolism studied was about the conversion of glucose to ethanol (Kepes, 2007). This study was continued discovering many pathways for the synthesis of specific substances. However, the biochemical metabolic process in the cells can be represented by metabolic maps (as in Figure 1.1) which portray all of the principal reactions of the intermediary metabolism of carbohydrates, lipids, amino acids, nucleotides and their derivatives. These maps are very complex at first glance and seem to be virtually impossible to learn easily. Despite their appearance, these maps become easy to follow once the major metabolic routes are known and their functions are understood. The underlying order of metabolism and the important interrelationships between the various pathways then appear as simple patterns against the seemingly complicated background (Garrett and Grisham, 2000).

1.3 Structural analysis of plant metabolism

Metabolism serves two fundamentally different purposes: the generation of energy to drive vital functions and the synthesis of biological molecules. To achieve these, metabolism consists largely of two contrasting processes- catabolism and anabolism. These occur simultaneously in the cell. Catabolic pathways are characteristically energy-yielding, whereas anabolic pathways are energy-requiring. Catabolism involves the oxidative degradation of complex nutrient molecules like carbohydrates (sugars, starch and cellulose), lipids, proteins, etc. originally obtained from environment via photosynthesis. The breakdown of the molecules by catabolism leads to the formation of simpler molecules such as carbon dioxide and water. Therefore, respiration can be considered as catabolic reaction. Photosynthesis can be taken as an anabolic biochemical pathway, since light energy is used to synthesize sugar molecules from atmospheric carbon dioxide and water. So, light reactions in the photosystems can be considered as both catabolic and anabolic, as it breaks down water and builds up the chemical energy molecules, NADPH, H^+ and ATP; this will be studied in detail in chapter 3.

Anabolic reactions are usually endergonic, i.e. energy requiring metabolism. Catabolic reactions are exergonic. Often, the chemical energy released is captured in the form of ATP. Catabolism is oxidative for the most part; a part of the chemical energy may be conserved as energy-rich electrons transferred to the coenzymes NAD^+ and $NADP^+$. These two reduced coenzymes have very different metabolic roles: NAD^+ reduction is a part of catabolism;

NADPH, H^+ oxidation is an important aspect of anabolism. The energy released upon oxidation of NADH, H^+ is coupled to the phosphorylation of ADP in aerobic cells, and so NADH, H^+ oxidation back to NAD^+ serves to generate more ATP. In contrast, NADPH, H^+ is the source of the reducing power needed to drive reductive biosynthetic reactions. A few molecules of substrate whose catabolism yield more ATP than required, allow the cell to harvest an endless supply of energy which is necessary for the cell maintenance and growth (Garrett and Grisham, 2000). All these factors are well balanced and maintained throughout the cell and plant's life.

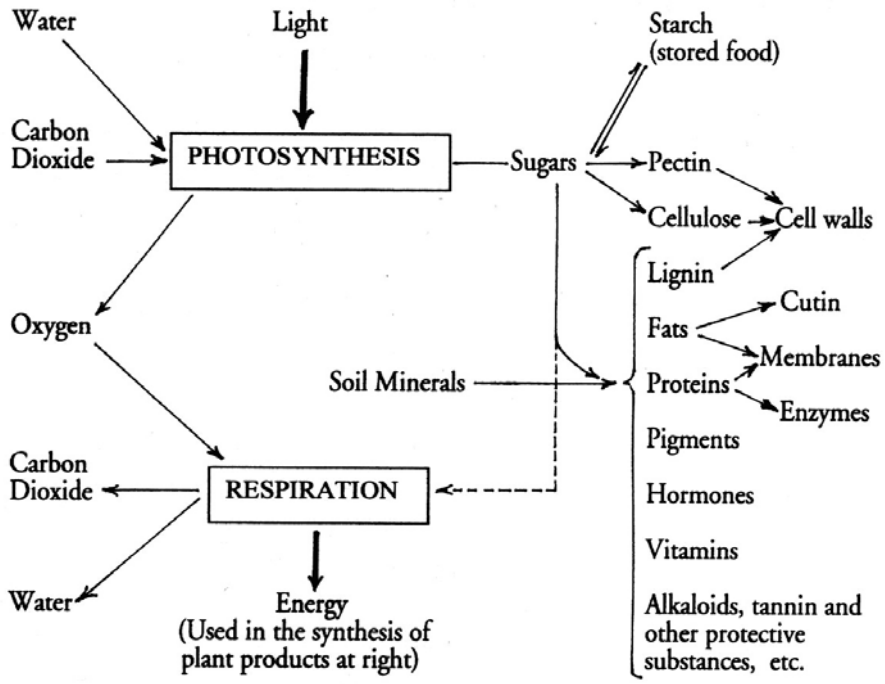

Figure 1.2: An outline of plant metabolism

The conflicting demands of catabolism and anabolism are managed by cells in two ways. First, the cell maintains tight and separate regulation of both catabolism and anabolism, so that metabolic needs are served in an immediate and orderly pattern as in the Figure 1.2. Second, competing metabolic pathways are often localized within different cellular compartments. The metabolic pathways are isolated in distinct compartments based on opposing activities, e.g. separate organelles and sub organelles. This avoids the metabolic complexities. For example, the enzymes responsible for catabolism of fatty acids and the fatty acid oxidation pathway are localized within the mitochondria. In contrast, fatty acid biosynthesis takes place in the cytosol.

Plant metabolism involves various types of metabolism specified for different functions (growth, regulation, maintenance, mechanical support, food storage, etc.). Concerning plant morphology, each plant organ is specially designed for typical metabolism. For example, metabolisms like photosynthesis happen only in green leaves, while respiration occurs throughout the plant. Numerous metabolic reactions can be seen accompanied by this; in order to balance and regulate the whole mechanism, some reactions take place very fast in some plant parts. For example, respiration rate at roots of growing plants is usually very high. In some cases, this may be influenced by the environmental stress. The respiration process at roots provides sufficient energy to uptake water and nutrients actively that is necessary for the plant growth. Inside the plant, the transport process occurs via special types of vascular tissues, as cell to cell transport is not so much effective; even though, the energy molecules ATP and NADH, H^+ are transported via cell translocators. The associated plant metabolism is very complex considering all mechanisms throughout the plant. For easiness of metabolic studies, plant metabolism can be studied separately for different plant portions or organs. This avoids the complexities caused by the transport phenomena of different plant portions, when we consider the whole plant metabolism.

1.3.1 Organ level: plant parts

Generally, all types of plants are composed of three major organ groups: leaves, stems and roots. All are comprised of tissues working together for a common goal function; each plant part has specific functions to support and maintain the plant life. In turn, tissues are made up of a number of cells, which constitutes of different elements and atoms on the most fundamental level. Plant tissues are characterized and classified according to their structure and function. As each part of the plant is different, each has different function and the main aim altogether is the growth and development. In leaves, mainly photosynthesis, transpiration, respiration, gas exchange processes, etc. take place, while in stem that contains phloem and xylem, the function is different; it transports whatever the plant needs (for the photosynthesis and food storage) from root; these are also linked with the availability of elements in the plant culture. In the case of root, it actively transports water and nutrients from where it holds and gives to the transporting tissue (xylem and phloem).

In addition to this, during the life, plant goes through different stages like germination, flowering, maturation etc. In each stage, the plant metabolism is influenced by growth hormone production, environmental responses and the whole plant physiology. The reaction

rates are also different in each stage of growth. In this aspect, it is necessary to have biochemical knowledge about what is exactly happening in plant parts at different growth stages. The following sections give an overall idea about the biochemical mechanisms in organ level.

1.3.1.1 Leaf

In most plants, leaves are the sites where transpiration takes place; at the same time, they are highly efficient solar energy converters. They capture light energy using chloroplasts, and through the process of photosynthesis they trap energy in the form of sugar molecules using carbon dioxide and water from the environmental surroundings. In addition, leaves are able to twist on their petioles, stalks, in order to maximize sun exposure and photosynthetic activity. All the energy required by living organisms is ultimately depending upon photosynthesis.

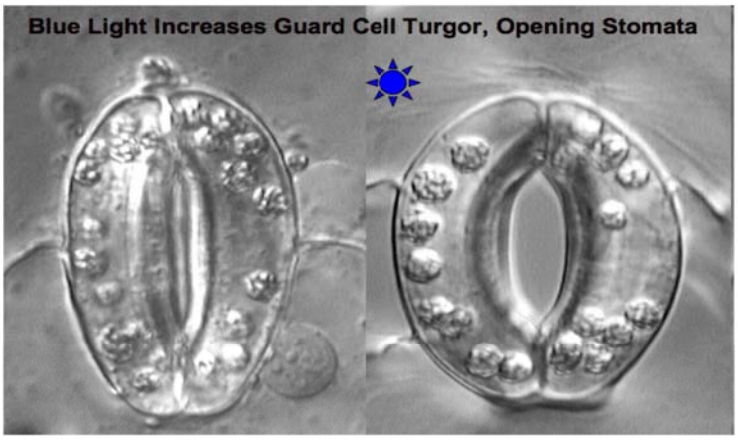

Figure 1.3: Stomatal conductance (Taiz and Zeiger, 1998)

The produced sugars are transported through leaf veins, skeleton like pattern that appear in the leaves. These are actually vascular bundles, made up of xylem and phloem vessels. In dicots, these veins run in all directions (e.g. tree leaves). In monocots, the veins are parallel (e.g. grass). In addition, monocots do not have mesophyll differentiated into two layers. Instead, some have large thin-walled special type of buliform cells surrounding the main vein. The thin-walled cells are sensitive to water conditions and will collapse in dry conditions which cause the leaf blade to fold or roll reducing transpiration. Up to a great extent, leaves are responsible for the water movement in the plant; it is transported throughout the plant since transpiration pull is one of the reasons for the uptake of water by roots.

A thin layer of epidermal cells covers leaf surface which permit light to the interior; this protects cells from physical damage. The upper epidermis is generally uninterrupted, but the lower epidermis is perforated by numerous tiny pores called stomata. The stomata are numerous; they support gas exchange between the interior part of the leaf and the environment. Each stoma is regulated by a pair of kidney-shaped guard cells with thick and less elastic inner wall, creating bending when turgid (Kwak *et al*., 2008; Schroeder *et al*., 2001) (Figure 1.3). The photosynthetic products in the guard cells provide the energy for the functioning of the cells. The walls of the guard cells are thickened, only at the side adjacent to the pore. The cells expand or contract with respect to the changes in the amount of water in the cells, availability of light and the concentration of carbon dioxide. There is a need of energy, as the water is moved into and out of the guard cells. When guard cells are full of water, the stoma pore opens and when the water is evacuated, the pore closes. Thus, guard cells perceive and process environmental and endogenous stimuli such as light, humidity, CO_2, temperature, drought and plant hormones to trigger cellular responses resulting in stomatal opening or closure. These signal transduction pathways determine for example how quickly a plant will lose water during a drought period (Kwak *et al*., 2008; Schroeder *et al*., 2001). The rate of transpiration is directly related to the stomatal behaviour. Transpiration happens when stomata are opened, and usually in sunny days the stomata close, as the water release would be too high. If the internal moisture drops below a certain level, in order to reduce drying inside the leaf, the stomata will close. Stomata accounts for only 1 percent of a leaf's surface and transpiration uses about 90 percent of the water that enters to the plant roots. The other 10 percent is used in chemical reactions and in plant tissues (De Reffye *et al*., 2008; Jarvis and McNaughton, 1986; Aalto *et al*., 1999). The amount and the rate of water loss depend on several factors such as high temperature, dry or low relative humidity and windy weather. In short, these are complex plant organs upon which life depends.

However, as per the leaf biochemistry, the leaf level modelling must account the major metabolic activities: photosynthesis, respiration, fatty acid, amino acid metabolism, light absorption, transpiration, gas exchange processes, etc. The last three terms are considered as physical process, and are treated separately in the thesis of Pauline Hezard (2012). This thesis mainly concerns the first four items. Later, this will be coupled with the physical processes.

1.3.1.2 Stem

Stem supports the plant, and in some plants, it serves as food storage. It allows the movement of water and minerals from roots to leaves and, food from leaves to different plant parts including the storage space. For the plant modelling, here we consider only herbaceous stems (soft and green stems) of plants containing transporting vessels called xylem and phloem. Through xylem, water and minerals travel up to the leaves; phloem carries sugar molecule that is made in the leaves.

Xylem is an important tissue as it is the 'plumbing part' of a plant. These are bundles of pipes running along the main axis of stems and roots. Xylem sap mainly consists of water, inorganic ions, organic chemicals and other dissolved substances.

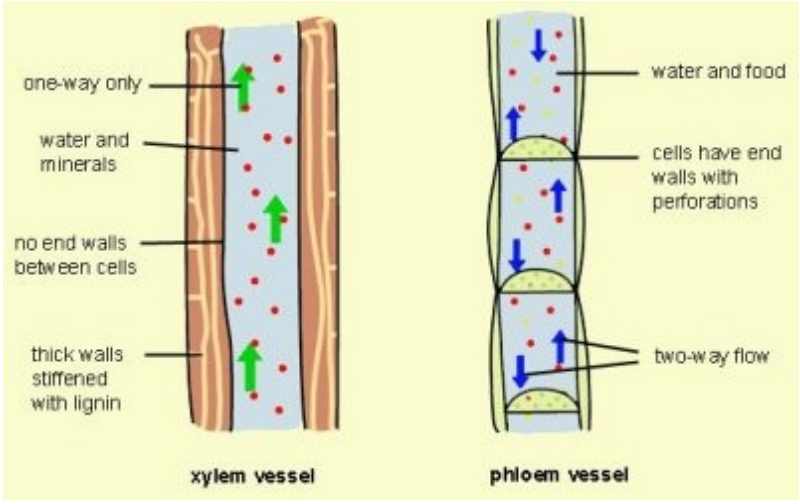

Figure 1.4: Material transport through xylem and phloem vessels [Int. ref.2]

Two phenomena cause xylem sap to flow:

1. Transpirational pull: due to the transpiration process, surface tension arises causing an equivalent 'negative pressure' or tension in the xylem. This pulls water from the roots and thereby roots uptake water from the culture. Although surprising, this is likely an effect on water chemical potential inside the xylem vessel.
2. Root pressure: if the water potential (i.e. the potential energy of water relative to pure free water) of the root cells is more negative than the culture, due to high concentrations of solute, water move by osmosis into the root. This causes a positive pressure that forces sap up the xylem towards the leaves. Root pressure is highest in the morning before the stomata opening and it allows beginning the transpiration process.

Phloem is the living tissue which carries organic nutrients and dissolved food substances (photosynthates) particularly sucrose, to all parts of the plant as per the requirements. This conduction system is composed of sieve-tube member and companion cells without secondary walls. Furthermore, xylem-phloem vessels together give mechanical strength to the plant. Xylem allows unidirectional flow, while phloem vessels allow bidirectional flow (Figure 1.4).

After the growth period, when the meristematic cells (cells in the growth zones) are dormant, the leaves act like sources, where storage organs act like sinks. The movement of phloem sap is due to the high concentration of organic substance inside cells of the phloem at a source, leaf; it creates a diffusion gradient that draws water into the cells. Movement occurs by bulk flow; phloem sap moves from sugar sources to sugar sinks by means of turgor pressure. In this way, the metabolism with respect to the stem is mainly depending on the transport processes affected by the pressure developed.

It is reported that plants with green coloured stem carry out photosynthesis using CO_2 from vascular systems (Hibberd and Quick, 2002); but, this may be relatively very small amount compared to leaves. Using the produced sugar molecules, respiration happens and it is probably utilised as per the energy demands, e.g. transport purposes (Pilarski, 1994). Stem respiration is increased by high temperature, but, limited by light availability and surface area.

Understanding the percentage of stem photosynthesis and with respect to all the above descriptions, the stem modelling of C3 plant (e.g. lettuce, tomato) can be done. Thus, photosynthetic respiration processes are necessary in addition to the active and passive transport processes. The transport processes mainly fall into the physical process modelling, while respiration and the carbon source transport in the xylem and phloem vessels are biochemical process modelling which should be coupled to the stem metabolic model.

1.3.1.3 Root

The involvement of the root in the transformation of absorbed mineral nutrients in specific biosyntheses is unquestionable. The two major functions of roots are: (1) the absorption of water and inorganic nutrients and (2) anchoring the plant body to the ground. The plant roots develop very fast; the respiration rate goes faster, especially at the root tips (up to some stages of growth). Without the knowledge of the metabolic basis of growth processes, we cannot understand the peculiarities of the formation of those metabolic systems and elements of cell structures which determine the functional differentiation of the root as an organ of uptake, transport and synthesis.

The growing root tip represents a linear sequence of cell differentiation from the apical meristem over the zone of elongation to the zone of cell maturation (Figure 1.5).

Structurally, plant root constitutes of:

a) Root cap: covers the root tip and protects tissue from damage. The root cap is having a life span of about one week; it serves in determining root growth direction. Whether the cap sloughs off or is cut off, the root will grow in random directions as opposed to downward until a new root cap is formed.

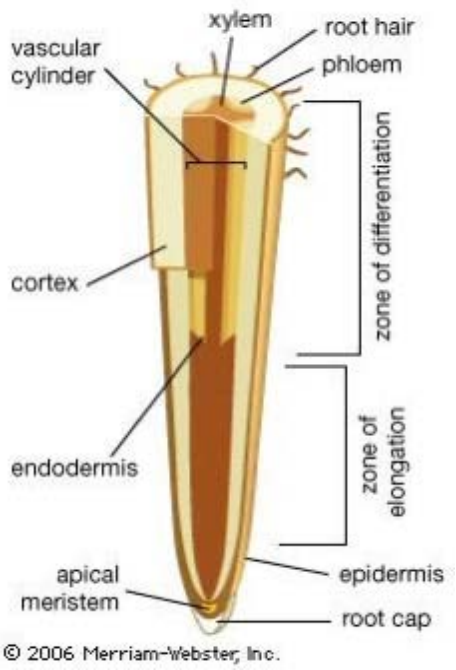

Figure 1.5: Root structure [Int. ref.1]

b) Zone of cell division (apical meristem): situated in the centre of the root tip. Cell division occurs at this portion and gives rise to the primary body of the plant. This produces xylem and phloem

c) Zone of elongation: cells become several times bigger than their original length. The cells in the zone of elongation stretch and lengthen as small vacuoles within the cytoplasm coalesce and fill with water (Int. ref.1). One or two large vacuoles occupy almost all of the cell volume in fully elongated cells. Cellular expansion in this zone is responsible for pushing the root cap and apical tip forward through the culture.

d) Zone of maturation (differentiation): cells differentiate into various distinctive cell types. At the zone of differentiation, root hairs form which absorb water and minerals and adhere tightly to hold the entire plant. They greatly increase the absorptive surface of roots during the growth period when large amounts of water and nutrients are needed. An individual root hair lives for only a day or two, but new ones form constantly nearer the tip as old one dies in the upper part of the zone (Int. ref.1).

Based on the metabolic utilization of photosynthates translocated by the phloem from the shoot to the root, during elongation and maturation, new cells formed in the root tip along

with the functional modification and other physiological functions. The transport form of assimilate is sucrose, representing the main carbon and energy source in root metabolism. The phloem transportation depends on various factors including the sucrose concentration level and acid invertase activity (Kolek and Kozinka, 1992). The level of carbohydrates in the meristem and at the onset of cell elongation is low, due to the use in the synthesis of structural polymers (mainly polysaccharides, nucleic acids, nucleoproteins, glycoproteins) associated with the formation and completion of the cell wall, cytoplasm and cell organelles and their decomposition in respiration (for energy, reducing agents and carbon skeletons for biosyntheses) and for ion uptake and transport (Kolek and Kozinka, 1992). These cells have high demand for the ions corporated into organic structures, including enzymes, along with monosaccharides and organic acids. These are very important in producing turgor potential needed for cell extension. Cell wall composition changes in the course of root growth.

In the root elongation and root hair zones, the activities of all enzymes increase. This phenomenon differs from plants to plants. In meristem of these roots, enzymes of glycolysis prevail and in the root elongation zone, activities of enzymes of the pentose cycle increases (Kolek and Kozinka, 1992). All these studies project the importance of the metabolic pathways that should be considered for root metabolic model of a particular plant species, which may be extremely different for another species. In addition to this, the metabolic pathways are influenced by environmental factors.

1.3.1.4 Storage organ/fruit

All fruits come exclusively from flowering plants. The sugars produced at leaves travel through the stem; finally, they are stored as starch or proteins. A storage organ is any part of the plant in which excess of energy or water is stored (generally, in the form of carbohydrates) in order to be used for future growth (Jenks and Bebeli, 2011). Storage organs often grow underground, where they are better protected from attack by herbivores. A fruit is a mature, or ripened, ovary that usually contains seeds. In contrast, a vegetable can consist of leaves (lettuce, cabbage), leaf petioles (celery), specialized leaves (onions), stems (white potato), stems and roots (beets), flowers and their peduncles (broccoli), flower buds (globe artichokes) and or other parts of the plant.

Green fruits can synthesize organic acids as products of photosynthesis. Most organic acids within the fruit are derived from other parts of the plant (Ulrich, 1970). Fruit development and growth are dependent on photosynthetic CO_2 fixation in leaves and the translocation of

sugars, amino acids and organic acids to the fruit cells. During the early phase of development, most fruits can be regarded as sinks because of their high metabolic activity and rapid cell division. In the later phase of development (at the time of cell expansion, seed development and maturation), most fruits accumulate high levels of carbohydrates in the form of starch and are thus more typical storage sinks (Jenks and Bebeli, 2011). During fruit maturation and ripening, significant changes in the carbohydrate composition lead to fruit softening and sweetening. The stored carbohydrate breakdowns into sugars like glucose, fructose and sucrose which are essential for fruit quality. However, the relative concentrations of individual sugars vary greatly between species and cultivars, as well as the stage of maturation and ripening.

The rate of metabolic breakdown (i.e. respiration) varies in different plant fruits. The storage lives of which have high respiration rates (broccoli, lettuce, peas, spinach and sweet corn) are short in comparison to that of which have low respiration rates (apples, limes, onions and potatoes). Respiration is affected by a wide range of environmental factors that include light, chemical stress (e.g. fumigants), radiation stress, water stress, growth regulators and pathogen attack. That is the reason why, the storage room temperature is maintained in a particular temperature range. The respiration includes glycolysis, TCA cycle and electron transfer chain in the cell membranes. The energy produced as a result of this, is released as heat.

1.3.2 Growth/developmental phases

Growing cells are metabolically active. In growing young leaves, the leaf metabolism is complex. Growth occurs over the entire leaf area; but cell division, expansion and differentiation occur pre-eminently in different zones. This is reflected in leaf metabolism and photosynthetic activity. Even in fully developed source leaves, the topography of metabolism is not uniform. In order to understand the whole plant metabolism we need to know both synthesis and degradation of all carbon sources throughout the life span of the plant. The different growth stages are the following.

1.3.2.1 Germination

Germination is the process in which a seed or spore emerges from a period of dormancy. Seed germination depends on both internal and external conditions. The external factors include temperature, water, oxygen and sometimes light or darkness. Different plant seeds require different values of distinctive variables for successful germination. Mature seeds are often

extremely dry and need to uptake significant amounts of water relative to the dry weight of the seed, before cellular metabolism and growth can resume. Most seeds need enough water to moisten (imbibition) and this leads to the swelling and breaking of the seed coat. Most plants store food in seeds such as starch, proteins or oils. This food reserve provides nourishment to the growing embryo. Most seeds are not affected by light or darkness. The breakdown of seed storage substance by respiration is necessary to release the energy. It starts only during early development of the seedling (Mohr and Schopfer, 1995). The adult seed contains mitochondria which function respiratory mechanism based on reserved sugars during imbibition. During the transition to the growth phase, metabolic activity of the embryo can be measured (since there may have an increase of respiration, the ATP level increases (Mohr and Schopfer, 1995)).

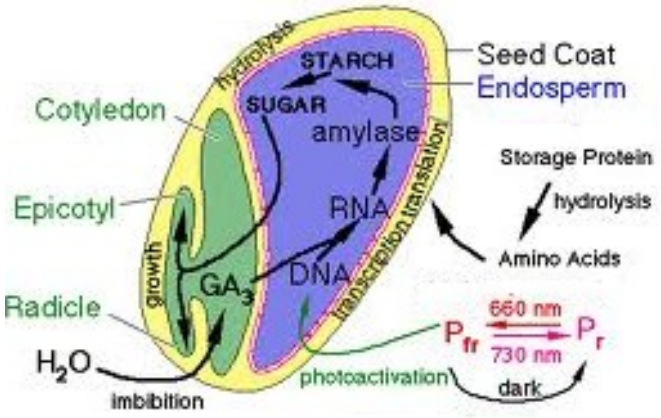

Figure 1.6: Germination mechanism in lettuce seeds (Int. ref. 5)

In lettuce seeds (which is a dicot), the activating chemical is a pigment called phytochrome. This chemical exists in two different forms: Pr and Pfr. Pfr is the form of phytochrome that photoactivates the genes for amylase in lettuce; Pr is inactive. The lettuce seed germination depends on how much of each of these two forms of phytochrome is present in each cell. Typical lettuce seed batches germinate at 30-60%, if placed in darkness because at least this percentage of seeds is enough to stimulate the germination. If the lettuce seeds are exposed to red light (660 nm), the red light causes all the Pr to change into Pfr. Then, 85-95% of the seeds can sprout, because they all have an abundance of Pfr inside. On the other hand, if lettuce seeds are kept in far-red (730 nm) light, the far-red light causes all the Pfr to change into Pr; then, all the seeds have essentially no Pfr and so very few (0-5%) sprout (Int. ref. 5).

1.3.2.2 Vegetative growth

Vegetative growth is the second stage in the life of a plant after germination. During this stage, a plant will be photosynthesising as much as possible to grow as large as it can before the onset of the flowering (generative) phase. In essence, it is the period of growth between germination and the beginning of sexual maturity characterised by flowering.

Blue light stimulates chlorophyll production more than any other colour encouraging thick leaves, strong stems and compact vegetative growth. Chlorophyll absorbs blue and red light and transmits the energy to a pigment-based electron transport chain. The energy is ultimately used to produce high-energy chemical bonds that can be used for a range of biochemical transformations including fixation of carbon dioxide into sugars.

1.3.2.3 Flowering

Flowers are modified leaves possessed only by the group known as angiosperms. For the formation of flowers, the relation between the internal physico-chemical conditions must be different from those in which vegetative growth occurs. The transition to flowering must take place at a time that is favourable for fertilization and the formation of seeds, hence ensuring maximal reproductive success. To meet these needs, a plant must be able to interpret changes in levels of plant hormones, seasonable temperature and photoperiod.

Flower, particularly at the earlier stages, usually performs very intense respiratory activity and often possesses a higher rate of oxidation (Ketsa, 2001). In some flowers, the rate of respiration decreases from relatively early stages onward; but in some cases, it undergoes increase or remains almost constant up to the time of opening. The factors like temperature, water, nutritive salts, etc. influence the occurrence of flowering. In the beginning of 20th century, Klebs found that flowering occurs in red light with limited absorption of water and salts (Klebs, 1906). Red light is very important in plant reproduction. Phytochrome pigments absorb the red and far red portions of the light spectrum and regulate seed germination, root development, tuber and bulb formation, dormancy, flowering and fruit production. Therefore, red light is essential for stimulation of flowering and fruiting.

1.3.2.4 Seed maturation and senescence

Seed maturation is an important phase of seed development during which embryo growth ceases, storage products accumulate, the protective tegument differentiates and tolerance to desiccation develops leading to seed dormancy (the state of plant seeds which prevents

germination). During senescence, proteins, antioxidants and other nutritional compounds degrade which finally limits the crop yield and biomass production.

Further, the plant hormones such as gibberellins, auxin, abscisic acid cytokinins and ethylene have great importance as they influence the growth. By knowing all these mechanisms, the rate and timing of development is determined based on different factors like species, day length (photoperiod) and temperature.

In short, the development is the process of a plant changing from one growth stage to another. The right combination of different parts and growth phases of plant lead to growth and development; in this way, the model corresponding to each plant part and growth phase can satisfy the modelling targets. Metabolic processes of senescence are important to be accounted in growth modelling as recycling processes are necessarily performed in the MELiSSA loop.

1.4 Metabolic interactions in plant level

Though plants have different organs and cells performing different functions, the entire plant metabolism is interrelated and forms a metabolic network. This operates together to achieve the particular goal - growth and development. The fundamental property of this network is the selective partitioning of organic metabolites among different organs, tissues, cells and organelles. In the peripheral level, the entire metabolic interactions take place through the plant organs – leaf to stem, stem to root, etc.; it is regulated by the transport of carbon source metabolites and energy molecules (Pessarakli, 2005). In addition to this, interactions between plants and environment also exist which may disturb the metabolic interactions within the plant. Organs of the same plant may be subject to contrasting environmental conditions, and this may result in differential responses, which may have consequences on the growth and morphology of the entire plant.

1.4.1 Metabolic interactions between organs, tissues and cells

Apparently, each organ is specifically made to perform definite functions. Undoubtedly, there is a high correlation exist within the organs, and in between. Various mechanisms accommodate the directional transport of metabolites through the organs by xylem and phloem. They are essential for long distance transport, from leaf to stem and then stem to root.

Plants assimilate inorganic carbon and nitrogen into organic compounds required for plant growth; a very large variety of metabolites are produced, and the anabolic and catabolic pathways that they feed into are complex and interconnected. Metabolism has been divided into discrete pathways which are frequently partitioned between cells or even tissues and organs. The soluble sugars circulate as a consequence of source – sink activities of plant organs. The exportation rate of carbon source like sucrose or glyceraldehydes-3-phosphate (G3P) from the source and the photosynthetic fixation may be considered as the inputs. Then, the outputs are the carbon fluxes within the plant, carbon allocation to different organs and functions, and the proportion of carbon allocated to growth, respiration and the storage. Many tightly regulated metabolic steps control the movement of photosynthetically fixed carbon to the phloem transport system. Source site is controlled by the rates of photosynthetic incorporation of CO_2. The flow of carbon in the form of soluble sugars of cytoplasm is regulated by complex biochemical interactions which altogether direct the export of fixed carbon out of the chloroplast. Carbon that is not released from the chloroplast retain as starch. This will not be available for phloem transport (Pessarakli, 2005). Measurements of these transports require labeled carbon distribution experiments.

In addition to the transport vessels, plant organs are connected through transporters which carry metabolites with respect to the associated metabolic requirements. A metabolite can be synthesised by performing many types of possible pathways; metabolites are not synthesised in isolation, rather, large sets of metabolites must often be synthesised simultaneously. Transporters participate in basic mechanism by partitioning these metabolites within and in between the organs. For example, G3P is mostly transported within the organs. The amount of G3P transportation should be fixed and regulated in order to attain the plant growth.

Furthermore, photosynthesis in leaves needs sufficient amount of water; this originally comes from roots, by water uptake using transporting vessels in stem; then, xylem vessels within the stem, connects the veins of the leaves. In this way, intracellular and long distance transport processes potentially affect the availability of substrates or products present in the plant organ and nutrient availability of the culture, where it grows (Da Silva *et al*., 2011). They also represent the critical sites at which metabolism and growth can be regulated. Hence, the transport processes in plants, particularly, the location and the kinetic properties of transporters are essential components of metabolic networks, since they frequently influence metabolic fluxes as well as partitioning of nutrients between growth and storage.

Another interesting fact comes from the supporting tissues of an organ: for example, the leaf tissue consists of multiple cell types, such as epidermis, vascular bundles and photosynthetic mesophyll tissue. Mesophyll tissue is multi layered and differentiated into spongy and palisade parenchyma cells. Photosynthesis occurs only in specified cells containing chloroplast. The rest of the tissue support the action of photosynthesis, and help the produced carbon source transportation and allocation to other plant parts. In this way, every organ is composed of tissues of different characteristics which altogether directly or indirectly assist the main functions.

1.4.2 Metabolic interactions in cell compartments

Just like the metabolic interactions in plant organ levels, cells possess some types of interactions to one another which make high degree of compartmentation within the cell. Due to this, the whole plant metabolic network seems to be complex. In contrast to other non-plant eukaryotic cells, plant cells are highly complex, with the chloroplast being the most prominent one. In such a system, the uncertainties about which metabolites are transported across organellar membranes, the lack of knowledge about kinetic constants, biochemistry of metabolites and metabolite transporters and subcellular metabolite concentration levels may interfere with the metabolic studies. This is the reason why we will study separately each and all possible plant mechanism influencing the metabolism (as described in the above sections) including the physical, metabolical and environmental factors.

In some cases, the cell requires massive flux of metabolic intermediates across cellular and organellar membranes. Since most small molecules in plant cells are not permeable, metabolite transporters are required to catalyze the transport of metabolites across the membranes. An example for such type of transporter is glucose transporter; as the name suggests, it facilitates the transport of glucose over plasma membrane. In vascular plants, long-distance transport is critical for the allocation of organic carbon and nitrogen compounds from their sites of synthesis to developing or reproductive plant organs that rely on import of the organic compounds for growth and development. Metabolite transporters play critical roles in connecting parallel and interdependent biosynthetic and catabolic pathways and thus represent the integrating elements in these metabolic networks (Atwell *et al*., 1999). These transporters act as gate keepers determining which substances may enter or leave, how fast they may move and whether their entry involves an exchange of metabolites or an input of energy. Different forms of the transporters are found in different types of plants and in

different tissues within the plants (Atwell *et al*., 1999). Chloroplast transporters are collectively called phosphate translocators; e.g. phosphoenolpyruvate/phosphate translocator, xylulose-5-phosphate/phosphate translocator, glucose-6-phosphate/phosphate translocator, etc.

Looking into the details of cellular structural level (Figure 1.7), each cell is composed of differentiated regions- endoplasmic reticulum, golgi complex, various membrane bounded vesicles such as lysosomes, plastids, nucleus, vacuoles, mitochondria, microbodies and cytosol itself. Cytosol provides an easy route for the movement of ions, small molecules (sugars and amino acids) and even for macromolecules (RNA and proteins) between the cells. Hence, the cell to cell communication happens (Robards, 1975).

Cellular compartment	% of the total volume	Main functions
Plastids (chloroplast)	16	Photosynthesis, starch and lipid synthesis, fatty acid synthesis from acetyl co A
Mitochondria	0.5	Energy production by cell respiration
Cytosol	3	Sucrose synthesis, glucose degradation
vacuole	79	Protein degradation, maintenance of cell turgor, store, water, waste products
Nucleus	0.3	Reaction site for replication and for processes in which toxic transcription intermediates are formed
Peroxisome		Fatty acid oxidation, pentose phosphate pathway, glyoxylate, photorespiration
Ribosome		Protein synthesis
Golgi bodies		Processing and sorting of proteins destined for export from the cells or transport into the vacuole
Endoplasmic reticulum		Storage of Ca^{2+} ions, participation in the export of proteins from the cell and in the transport of proteins into the vacuole.

Table 1.1: Compartmentation of cell metabolic functions (Based on spinach leaves (Winter *et al*., 1994))

The compartmentation of metabolic pathways provides additional options for regulation. Each compartment is dedicated to specialized metabolic functions; the enzymes appropriate to these specialised functions are confined together within the organelle (Held H.W. and Held F., 2005). Therefore, by knowing the compartmental function, it is possible to control a metabolic pathway by controlling only the responsible enzyme of the limiting reaction. Luckily, most of the important mechanisms are known and the rest lies on the route. In many

instances, the enzymes of a metabolic sequence occur together within the organellar membrane. Thus, the flow of metabolic intermediates in the cell is spatially as well as chemically segregated. For example, the enzymes of glycolysis are found in the cytosol, but pyruvate, the product of glycolysis, is fed into the mitochondria, which contain the citric acid cycle enzymes, which oxidize pyruvate to CO_2. But at the same time, the intermediate acetyl Co A is synthesised in both cytosol as well as mitochondria as per the requirements (Liedvogel, 1986).

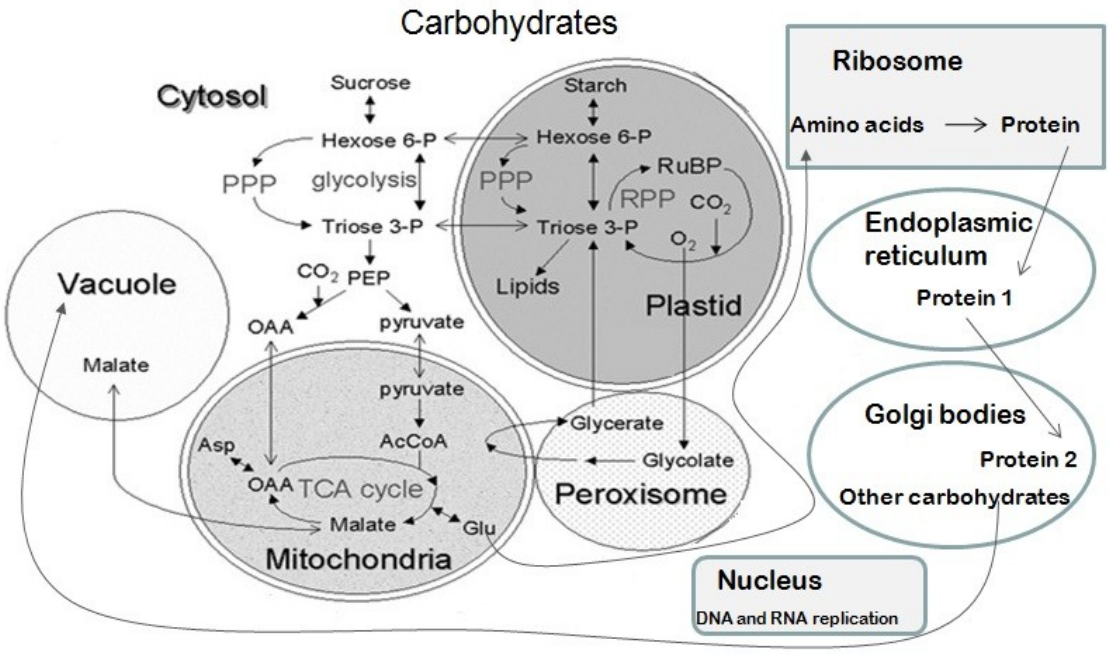

Figure 1.7: Compartmentation of metabolic processes in a leaf cell. For each subcellular compartment, some of the major metabolic processes are shown. Many processes occur exclusively in a single compartment but may obtain their substrates from, and export their products to, other compartments. Abbreviation: OAA = oxaloacetic acid, PEP = phosphoenol pyruvate, Glu = glutamine, Asp = Aspartate, AcCoA = Acetyl CoA, CO_2 = Carbon dioxide, O_2 = Oxygen, Triose 3-P = Triose 3-phophate, Hexose 6-P = Hexose-6-phophate, PPP = pentose phosphate pathway, RPP = reductive pentose phosphate pathway. (This image is inspired from Morgan and Rhodes, 2002).

The compartmentation permits simultaneous operation of pathways within the same cell avoiding futile cycles. The synthesis and degradation of biopolymers occur simultaneously in the same cell and are segregated in different compartments. For example, the oxidation of fatty acids occurs in the glyoxysomes, while synthesis takes place in the plastids. It is important to differentiate the location of these metabolic processes in this way, as the enzyme catalyze for these metabolism are different and therefore, cannot exist in the same compartment as well (Emes, 1991). The analysis of metabolic networks at a system level

depends upon the integration of data obtained from more than one level of molecular entity (DNA, RNA, proteins, metabolites, organelles, organs, cell types, etc.).

Several organelles participate in a major metabolic event and transport of specific metabolites between compartments must occur; the enzyme sequences in spherosomes, glyoxysomes, mitochondria and cytosol participate in succession in the conversion of stored fat to sucrose. This type of information defines which metabolites must move from one compartment to another, e.g. succinate from glyoxysomes to mitochondria. This also provides the availability of energy in the form of reducing equivalents (Mettler and Beevers, 1980).

Further, the function of cell organelles in different regions is different, for example, the golgi in cells engaged in cell wall synthesis or secretion (Mollenhauer and Morre, 2009) and the plastids in storage and breakdown of starch (Preiss, 1988). Neverthless, mitochondrial and chloroplast transporters are leading the way (Heldt and Flugge, 1987). It is important to understand the acquisition of nutrients and the maintenance of internal environmental properties (like pH, temperature). Changes in other regulating factors are achieved by close regulation of metabolic mechanisms of organelles and transport between cell compartments. This mostly involves the control of fluxes at compartmental level though the membranes. The organelles which are not participating in major metabolic pathways support their essential roles in the synthesis and maintenance of enzymes which require considerable amount of energy. The hydrolysis of protein in the vacuole provides energy along with amino acids. The regulation and energy balance in cellular and plant levels are necessary to be considered for plant growth modelling.

1.5 Energy metabolism and its utilization for plant growth and regulation

Energy metabolism is central to all cellular functions. Photosynthesis transduces solar energy into useful metabolic forms such as ATP; the mitochondrial oxidative respiration provides energy by exploiting the supply of assimilates of photosynthesis. A continuous supply of energy is required for all synthetic and maintenance processes and is dependent on the regulation of ions, substrates and exclusion of mineral elements (heavy metals). Heavy metals act as toxic elements; they can perturb the electron flow and thereby the synthesis levels of ATP, $NADPH/H^+$ and $NADH/H^+$. Metabolism is largely regulated by the provision of ATP as a substrate and by the amounts of ATP, ADP, AMP and Pi which serve as control molecules in many reactions. Hence, energy metabolism is related to the supply of phosphorous (P)

availability (Porter and Lawlor, 1991). Actually, it is a major determinant factor of growth and efficient uptake mechanisms. The concentration of inorganic P in the cytosol is close to 10 mol m^{-3} and the molar ratio of ATP: ADP: AMP is held at approximately 10:3:1 by the enzyme adenylate kinase (Porter and Lawlor, 1991). When ATP is consumed by processes in the cytosol and organelles, and if P is bound into metabolites, the inorganic phosphate (Pi) content falls; a flux of Pi from the vacuole maintains the concentration and provides the available energy.

Another fact is the availability of nitrogen, N. The synthesis of proteins requires amino acids demanding a large supply of energy and nitrogen. The supply of N depends on the amount of nitrate and ammonium ions from the environment and on the rate that they are metabolised to amino acids. If N supply is not limiting, protein constitutes a major regulator of whole plant growth. More generally, metabolites can only be synthesized if carbon, nitrogen, phosphorous and sulphur, and the basic building blocks generated from them in central metabolism are available. This implies that regulatory networks control metabolic activities to the availability of these basic resources.

Nevertheless for plants, the initial energy comes from the sunlight; plants convert light energy into redox energy, to change its redox potential from being moderately electropositive to highly electronegative. The electrons released from this component serve to generate an electrochemical gradient, flowing through either a cyclic pathway back to reduce the original component, or a non-cyclic pathway to reduce additional electron acceptors. This allows a fine adaptation to the energy requirements of the cell, since NADPH, H^+ reduction equivalents or ATP energy can be supplied in variable ratios. The ratio of the rate of photophosphorylation over the rate of production in reduced cofactors is named as the $P/2e^-$ ratio. A part of the produced energy, ATP and NADPH, H^+ is used for Calvin cycle reactions for the carbon assimilation. Other metabolic processes of great importance in cells are linked to the provision of energy for synthetic metabolism and for maintenance processes such as transport and ionic regulation. Since last few decades, studies have been carried out linking bioenergy and metabolism; some of the interesting studies/models which could be used for revealing plant biochemical processesy are quoted in the following sections.

1.6 Existing models for plant biochemical process

The plant biochemical process models consist of the studies concerning biochemical metabolism and energy necessary to build the biomass and for transport processes within the plant. To a great extent, the properties such as cellular interactions and molecular cell biology are affected by the physical properties (e.g. phytochemistry and environmental reactions) which altogether results into the plant morphology. Therefore, it is necessary to find an apt biochemical plant model from the existing plant models or to develop or properly reconstruct as per the requirements.

Since 1960s, several attempts have been done to study and to establish mathematical models for cellular and metabolic systems; the first model developed was for plant central metabolism containing the reactions of glucose phosphorylation and the bioenergetics including ATP utilisation (Goodwin, 1963). This was later extended by modifying some of the reactions (Garfinkel and Hess, 1964). The main limitation of this model was the lack of computational memory power and the availability of sufficient experimental data required to define the model accuracy (Garfinkel and Hess, 1964). Later, due to the developments in technologies, theories, tools and concepts, there were significant progress to overcome some of these limitations. A number of theoretical tools and concepts have emerged, notably for the analysis of controlling the flux distributions of metabolites and metabolic concentrations in a particular metabolic pathway called Metabolic Control Analysis (MCA) (Kacser and Burns, 1973; Heinrich and Rapoport, 1974). Afterwards, numerous modelling studies of plant, especially photosynthetic, metabolism have been carriedout (Laisk *et al*., 1989; Pettersson and Ryde Pettersson, 1988). Then another obstacle in modelling plant systems came at 1990's, because of the limitation in the availability of reliable data pertaining to the activity of enzymes, metabolites and reactions. However, rapid advances in molecular biology techniques and the emergence of a number of theoretical concepts in metabolic modelling and engineering aided in reducing this limitation to some extent (Stephanopoulos *et al*., 1998).

From a metabolical perspective, mathematical modelling provides insights to the general principles governing cellular function. The models of cellular metabolism and function are generally known as metabolic models; they have an important role for phenotypic analysis. It can be used for the design of optimal metabolic network structures as it originates from the metabolic network. Metabolic models can be classified into two main categories- kinetic models and stoichiometric models. If a metabolic model of a pathway of known structure is

constructed using measured kinetics of individual enzymes and/or the data recovered from literature, the developed model can be said as a kinetic model. The kinetic data together with data on the effects of co-factors, pH and ions are used to parameterise the model. Kinetic models incorporate kinetics whereas stoichiometric models rely exclusively on time invariant properties of metabolic networks (Rice, 2009). This is a straightforward type of modelling just like translating biochemistry shown in Figure 1.7 into mathematics.

It is less complicated to build stoichiometric models, compared to kinetic models. This is because, the development of latter is restricted by the lack of knowledge of the kinetics of cellular processes such as oxidative phosphorylation or electron transport in the cell mitochondria, without which is impossible to establish a metabolic model. When building kinetic models, in addition to the estimation of usual large number of kinetic parameters, it is crucial to take into account the validity of transferring reaction mechanisms of enzymes observed in vitro to in vivo conditions (Gombert *et al*., 2000; Wiechert, 2002). Kinetic models can be applied to simulate the dynamics of metabolic systems, while stoichiometric models are needed to be in pseudo steady state metabolic behaviour.

1.6.1 Kinetic models

Kinetic modelling method requires detailed knowledge of enzyme kinetics (Gombert and Nielsen, 2000). Each reaction in the model is defined in terms of its stoichiometry and enzymatic rate equation; also, the user must specify values for the various kinetic parameter (like Michaelis-Menton constant K_m, V_{max}, etc.) and individual metabolite concentrations or reaction rates (Poolman *et al*, 2004). For decades, starting with the work of Chance (who published the first numerical simulation of a biochemical system), kinetic models have been the most frequently used mathematical approach to metabolism. He could solve the equations for the behaviour of a simple enzymatic system using a mechanical differential analyser (Chance, 1943).

Kinetic models are generally applied to small segments of metabolism to explain the behaviour of metabolic subsystems in response to perturbations. For example, Laisk's model (1973) explained the interaction of photosynthesis and photorespiration; it was soon followed by many other models like Thornley (1974), Milstein and Bremermann (1979) and Kaitala *et al* (1982). The Thornley model (1974) was based on a novel approach in which a very simple mathematical model was formulated to represent the most important features of the dynamics of photosynthesis. Kaitala used the approach of Thornley to construct a kinetic model of

photosynthesis describing the effect of radiant energy and CO_2 concentration to control the CO_2 assimilation in leaves, where Milstein and Bremermann studied the kinetic parameters of the Calvin photosynthesis cycle.

Besides, the first known, efficient, mechanistic and integrated metabolic model was proposed by Farquhar *et al* (1980). He biochemically modelled the photosynthetic CO_2 assimilation in the leaves of C3 plants. The Farquhar biochemical growth model could calculate photosynthesis as a function of demand and supply of CO_2. The advantage of this model was that, they regulated photosynthesis not only by radiation and transpiration, but also by air humidity, leaf temperature, CO_2 availability and leaf nitrogen content; the plants experience radiation saturation at high levels of radiation. Therefore, though it had some limitations in some factors, this became the fundamental portion for most of the morphological and architectural (e.g. Greenlab model) models. The balance of mechanistic details with mathematical simplicity contributes to the broad use of the Farquhar, Von Caemmerer and Berry photosynthetic rate model; the model was later coupled with the stomatal conductance model proposed by Lens *et al* (Lens *et al*., 2010; Farquhar *et al*., 2001).

Various examples of efficient kinetic models for plants may be seen while going through the literature (Table 1.2). Kinetic modelling has been applied to investigate penicillin biosynthetic pathway in Penicillium chrysogenum (De Noronha *et al*., 1996; Nielsen and Jorgensen, 1996; Theilgaard and Nielsen, 1999). The model was used for calculating the fluxes through this pathway (enzyme kinetics for 10 reactions were included), as well as the concentrations of the involved metabolites, which were in agreement with experimental results. In 1997, Pettersson extended his earlier model of Calvin cycle metabolism by adding the oxygenase activity of ribulose 1,5-bisphosphate carboxylase/oxygenase (Pettersson, 1997; Pettersson and Ryde-Pettersson, 1988). Their model helped to understand the dependence of photosynthetic rate on CO_2 and O_2 concentrations and on the gradients of inorganic phosphate and triose phosphates across the chloroplast envelop, whereas Poolman *et al* have been studied the regulation of the Calvin cycle using a recently developed kinetic model with the help of an evolution-strategy algorithm (Poolman *et al*. 2000).

Eventually, it has been observed that the existing kinetic models stand for particular process, not for the entire plant metabolism. For example, Calvin Cycle, TCA cycle, glycolysis pentose phosphate pathway and photosynthesis are specified for C3 plants (Affourtit *et al*., 2001; Krab, 1995, Poolman *et al*., 2000; Thomas *et al*., 1997). In an earlier model of sucrose

accumulation in developing sugar cane (Rohwer and Botha, 2001), each reaction step was modelled with accurate kinetics by using detailed experimental and literature data.

It has been noticed that efficient kinetic models use mass balance principle. For example, the model developed by Zhu *et al*. (2007) have been used the enzyme and metabolite concentration variations followed by the reaction rate calculation. Inspiring Farquhar model, Zhu and co-workers also constructed a large compartmental model of leaf carbon metabolism comprising more than 40 reactions and transporters (Zhu *et al*., 2008). The model was capable of simulating the effect of evolutionary adaptation to higher CO_2 concentrations. They found a substantial increase in photosynthesis, suggesting that the typical partitioning in C3 leaves might be suboptimal for maximising the light-saturated rate of photosynthesis.

One of the latest established kinetic models simulates the aspartate derived amino acid pathway in *Arabidopsis thaliana* (Curien *et al*., 2009). This model is based on in vitro kinetic measurements and successfully reproduces in vivo data like metabolite concentrations and fluxes.

Kinetic modelling is undoubtedly a powerful proven technique to quantify the metabolic fluxes in compartmentalised dynamic metabolic systems and to address metabolic flux responses to environmental and genetic perturbations. But, it has some limitations; the construction of kinetic models relies on the precise knowledge of the functional form of all involved enzymatic rate equations and their associated parameter values. Furthermore, even if both are available from the literature, the parameter values usually depend on many factors such as tissue type or experimental and physiological conditions. Most enzymes – kinetic rate laws have been determined *in vitro*. Often, there is only little guidance available whether a particular rate function is still appropriate *in vivo* to overcome the difficulties and propose a bridge between structural modelling (which is based on the stoichiometry alone) (Famili *et al*., 2003; Bailey, 2001), and explicit kinetic models of cellular metabolism. However, as kinetic data was found difficult to be measured *in vivo* and stoichiometric modelling does not need this type of data, they were developed extremely fast since 1990s (Gombert and Nielsen, 2000; Stephanopoulos and Vallino, 1991).

Kinetic model	Reference
Glycolysis in plant tubers	Thomas *et al*., 1997
Mitochondrial respiration	Affourtit *et al*., 2001; Krab, 1995
C3 plants	Farquhar *et al*., 1980, 2001; Fridlyand, 1998; Fridlyand *et al*., 1998;Fridlyand and Scheibe, 1999, 2000; Gross *et al*., 1991; Pearcy *et al*., 1997; Pettersson and Ryde-Pettersson, 1988; Pettersson, 1997; Poolman *et al*., 2000; von Caemmerer, 2000
C4 plants	Chen *et al*., 1994; Collatz *et al*., 1992; Ghannoum *et al*., 1998; He and Edwards, 1996; von Caemmerer, 2000
C3–C4 intermediate plants	von Caemmerer, 2000
CAM plants	Blasius *et al*., 1997, 1999; Neff *et al*., 1998; Nungesser *et al*., 1984
Isoprene emissions	Zimmer *et al*., 2000
Xanthophyll cycle, Carotenoid metabolism	Latowski *et al*., 2000; Sielewiesiuk and Gruszecki, 1991
PHA copolymer in transgenic plants	Daae *et al*., 1999
[^{14}C] Choline metabolism in transgenic tobacco	McNeil *et al*., 2000 ; Nuccio *et al*., 2000
Choloroplast superoxide dismutase–ascorbate–glutathione pathway, redox regulation	Polle, 2001
Methionine and threonine biosynthesis pathways	Curien *et al*., 2003

Table 1.2: Kinetic models focusing plant metabolism Part of this table is adapted from Morgan and Rhodes, 2002

1.6.2 Structural models

As mentioned, structural models are based on the stoichiometry of the metabolic network. The modelling concept using structural approach is also known as stoichiometric modelling. These models account steady state approach for the intracellular components at the expense of abandoning any kinetic information (Kuepfer, 2010). The overall model structure is generally linear and represents an underdetermined system of algebraic equations in which intracellular fluxes are the unknown variables. Usually, stoichiometric models of metabolism reveal the fundamental inventory of the cell for maintenance and fuelling. Metabolic models stands for cellular metabolism at genome scale; they provide in turn a unique possibility to correlate genetic predisposition with clinical observations making them a valuable tool for model based analysis of genotype - phenotype correlations (Kuepfer, 2010). In the case of biochemical modelling of plants, stoichiometric mass balanced models are thus the centre of attraction as they account steady state mass balance principle for the whole plant metabolism. In addition,

it is relatively convenient with respect to the kinetic approach. For the stoichiometric plant model, the metabolic mass balanced equations revealing the entire plant metabolism are required. This is available in several data base (Table 1.3).

Unfortunately, some of the mechanisms of intracellular reactions are complex and still not very well understood (Bailey, 1998; Palsson, 2000) and this is why stoichiometric modelling lies on the basis of assumption of the pseudo steady state for internal metabolites (Stephanopoulos *et al*., 1998). This assumption is supported by the observation which says, intracellular dynamics are much faster than extracellular dynamics.

Name	Links
BRENDA	http://www.brenda-enzymes.info
KEGG	http://www.genome.ad.jp/kegg/pathway.html
PlantCyc	http://www.plantcyc.org/
MetaCyc	http://www.metacyc.org/
AraCyc	http://www.arabidopsis.org/biocyc/index.jsp

Table 1.3: Name and links of familiar metabolic data base

Since 1986, several metabolic modelling techniques are developed to stoichiometrically model various kinds of metabolism; first it was successfully done by Holms for the growth model of *E.coli* (Holms, 1986). Stephanopoulos and Vallino introduced the concept of network rigidity to explain the stoichiometric model of *Corynebacterium* metabolism: the yield values of lysine amino acid were found high, compared to the experimental conditions (Stephanopoulos and Vallino, 1991). Nowadays, based on mass balance stoichiometry and pseudo steady state approach, several methodologies exist to study and understand metabolism of living organism knowing few experimental data; based on this domain, recently few stoichiometric models developed for small metabolic networks (e.g. Calvin cycle, TCA cycle, etc.) which will be specifically explained in chapter 2. Of special importance in this context is, constraint based or flux based modelling approaches. These focus on the quantification of metabolic fluxes, which are accepted as the final representation of a certain physiological state of the cell resulting from different levels of cellular regulation (Stephanopoulos, 1999; Nielsen, 2003). These make use of stoichiometric models and rely on the principle of mass conservation and steady state.

1.7 Limitations of existing models

Although several models exist for specific plant processes (Table 1.2), they were not found suitable in their original form, for plant biochemical model fulfilling the requirements in the general plant growth model design. This was due to the following reasons.

1. Recent attempts to construct 'genome-scale' kinetic models of cellular metabolism (Slepchenko, 2003; Ishii *et al*., 2004; Yugi and Tomita, 2004; Jamshidi and Palsson, 2008) explicit that kinetic modelling is currently often limited to smaller (sub) systems or individual pathways. The difficulty to obtain reliable estimates of kinetic parameters is one of the main hindrances to construct kinetic models in whole plant scale.
2. Existing dynamic models were not found satisfactory for MELiSSA plants. Moreover, MELiSSA requires a stoichiometric model of plant growth which can predict output fluxes providing input fluxes and vice versa.
3. Similar to small scale kinetic metabolic models, the developed stoichiometric models are also stand for small metabolic network, not for the entire plant metabolism and the modelling methods used are different from one another. In some cases, topology is not analysed well, while in other cases, flux distributions are absent or determined by unprofitable methods (experimentally by isotopic labelling method) agreeing the period of time/conditions, in which they have used. In the case of MELiSSA plant, it may be impossible to have such type of isotopic labelling experiments during the entire plant growth.

Furthermore, the general model design is really in need of a stoichiometric model under steady state which will be perfectly suitable for the plant growth model design followed by MELiSSA loop. Among the developed models, none was fit at this context.

1.8 Our modelling approach

According to the requirements of MELiSSA loop, plant growth modelling stands for the modelling and achieving the knowledge of the factors that control and manage the plant growth. In other words, the crop composition, yield prediction and the responses to its environment in the closed loop must be related to the regenerative life support system performances. Furthermore, within a desirable regenerative system, the amount and the composition of the non-edible parts which come under waste cannot be neglected as recycling

must be necessarily performed with maximum efficiency. Hence, the development of a feasible, robust, stoichiometric model is very important which fit for the MELiSSA plant compartment requirements as well as general plant growth model design. As far as we know, not even single model is established which couple plant metabolic perturbations and energy exchange with respect to physical limitations (e.g. light or water availability); the model of our concept links matter and energy exchange laws of the physical mechanisms in addition to the biomass growth and composition exploration.

Plant metabolism includes not only the biochemical processes, but also light absorption and the subsequent processes (i.e. excitation of electron in cell level, electron transfer, energy transduction, regulation of gas exchange between leaf and atmosphere, etc.). Therefore, the stoichiometric plant metabolic model should account all these mechanisms involving the complex bioenergetics (photosynthesis and respiration), uptake of substrates (CO_2, nutrients and water), and all other secondary metabolisms in terms of mass balanced equations.

From literature, though there is not a complete stoichimetric metabolic model exists representing the whole plant metabolism, metabolic models for small networks have seen achieved by understanding the associated metabolism; these lighten the ways to obtain a realistic stoichiometric whole plant model of our target.

Furthermore, each plant species has specificity in their developmental stages. Some plants have biomass near root system (e.g. potato), while some has at shoot system (e.g. tomato). Though almost all plants have the same central carbon metabolic pathways, the reactions and transports occur in different rates, varies from tissues to tissues, organs to organs influenced by several environmental factors/conditions (light, water and nutrient availability, the gas levels, the stress caused by toxic elements, etc.). Therefore, for the metabolical model validation, it is necessary to use the experimental data (plant composition, plant inputs) of plants grown under a predetermined/known environmental system and verify with the same (plant inputs/outputs). With respect to the plant characteristics, metabolisms vary which control the growth and survival; hence, the metabolic network for each species will be (at least) slightly different from what can be seen in another. However, taking into account the usual phenomena, the general metabolic model structure for plants can be conventionally proposed in which some metabolic pathways shall be replaced/added or removed, while some equations remain the same: e.g. the central carbon metabolism remains the same for all models; at the same time, some of the reactions need to be replaced or removed. This general stoichiometric mass balanced plant model assumes pseudo steady state and can predict

biomass quantity, rate and composition with respect to the process variables such as the amount or rate of uptake of CO_2 or release of O_2 in the plant chamber for a specific period of time in a controlled predetermined environmental condition.

As described in the previous sessions, every plant has at least three organs (which are fluctuating periodically due to various growth phases) - leaves, stem and roots having three main functions: leaves for light absorption and photosynthesis; stem for transport process and to hold the plant; roots to absorb water and nutrients for plant growth and to hold the entire plant firmly vertical to the surface. Consequently, the general plant metabolical model revealing biochemical processes should include a minimum of three separate metabolic models which would be coupled in future on the basis of carbon source flux and percentage of metabolite composition (Figure 1.8).

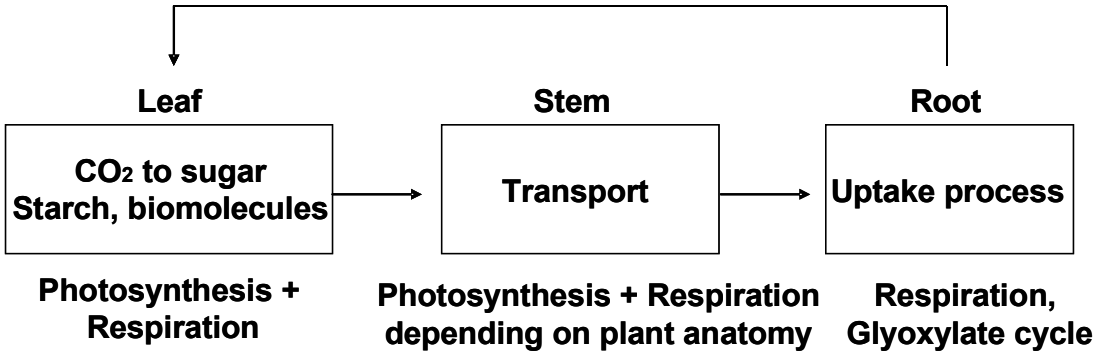

Figure 1.8: General Metabolic model structure for plant metabolic model

1.8.1 Leaf sub model

Leaf sub model takes in to account all the main metabolic processes happening in leaves starting from cellular level which reflect the metabolic and genome level summary. Leaves contain specific types of cells containing chlorophylls for performing photosynthesis. Respiration process also occurs within the same cell using a particular amount of metabolites (formed as a result of photosynthesis) and derives energy for entire plant maintenance and growth. Thus, in the case of leaves, photosynthesis and respiration are the inevitable metabolisms. Furthermore, the metabolic reactions involving macromolecule synthesis such as protein, lipid, fatty acid and carbohydrate (starch), etc. take place in leaf cell level; hence, the sub model obviously accounts those metabolisms in addition.

Usually, low rates of sucrose synthesis potentially result in high rates of starch synthesis. Several mechanisms coordinate and control the rate of sucrose synthesis in the cytosol, the rate of CO_2 assimilation in chloroplast, and hence the rate of triose phosphate (G3P and

DHAP) transport within the cell. The triose phosphate transporter in the chloroplast envelope which exchanges triose phosphate for inorganic phosphate release during sucrose synthesis, plays a central role in these mechanisms. Feedback mechanisms coordinate the rate of sucrose synthesis with the demand for sucrose in the non-photosynthetic parts of the plant to which it is exported. The control and regulation of all these mechanisms will be studied only in the final model of the MELiSSA plant after considering all other limiting factors. Nevertheless, photorespiration is not considered for the leaf metabolic model, as it is assumed that the CO_2/O_2 concentrations, light, temperature, etc. in the plant chamber are perfectly controlled.

1.8.2 Stem sub model

Stem transports materials 'to and fro' from the root and shoot using the transport tissues called xylem and phloem. These are very useful for the material supply throughout the plant. For these reasons, stem model constitutes metabolic mechanisms for component transport such as glucose, glyceraldehyde-3-phosphate (G3P), sucrose, amino acids like glutamine, etc. representing the main carbon, nitrogen and energy source in plant metabolism. Studies showed that the amino compound exchanges as well as metabolic interconversions occur in between xylem and phloem (Stoermer *et al*., 1997; Atkin *et al*., 1980).

The stem model interconnects leaf and root metabolic models. Hence, the knowledge of carbon source transport, loading - unloading, flux and composition of the material transport in each plant organ level is necessary. In order to obtain compound specific nitrogen exchange rates between xylem and phloem systems combined with information on metabolic interconversion of amino compounds, metabolic flux analysis technique (will be explained in chapter 2) with steady state labelling approaches (^{13}C and ^{15}N labelled amino acids) on the whole plant level are necessary (Ulrich *et al*., 2012).

1.8.3 Root sub model

Roots carry nutrients and water from the soil/hydroponics system of the plant culture. The nutrient absorption by plant roots is regulated relative to the plant demand. To absorb water and nutrients, roots need large amount of energy. This energy is mainly supplied by the respiration process. Hence, the rate of respiration in roots is very high compared to any other organ of the plant. Also, depending on plant species and/or the growth stage N assimilation might occur in roots or source leaves followed by the transport of amino acids.

Further, respiration limits the growth: it is reported that between one-quarter and two-thirds of all the photosynthates produced per day are respired (Poorter *et al*., 1990). A major part of this respiration occurs in the roots where carbohydrates are translocated; this is connected with the growth, maintenance and absorption of ions (Waisel *et al*., 2002). The fraction of carbohydrate translocation tends to change with the plant age/developmental stages. The percentage increases with decreasing growth rate of the plants (Poorter *et al*., 1990). Similarly, so many factors affect plant growth and root metabolic model as well. However, the general plant root metabolic model accounts respiration and related uptake metabolisms. Usually, root respiration metabolism involves the catabolism of macromolecules (protein, lipid, fatty acid and carbohydrate). In this way, root models will be different for potato, tomato and lettuce plants; moreover, it may depend on the concentration of O_2 of the nutrient solution and the quantity of physical exchange with gas phase. In cucumber plants grown in O_2 deficient nutrient solution, it has been found that O_2 in the aerial environment is transported through leaves for root respiration (Yoshida and Guchi, 1994). Nevertheless, it is assumed that MELiSSA plants are cultured in a perfect controlled atmosphere along with most suitable nutrient solution.

The proper coupling of the above discussed models constitutes the general metabolic model which reveals the bicochemical plant significance. Obviously, most of the metabolisms are connected to the physical plant processes. For example, photosynthesis is influenced by gas concentration, pressure, humidity, etc. Similarly, the uptake metabolism is related to the transpiration and gas movements with the environment which are separately studied with the physical process modelling and will be implemented in future.

Although the ways to achieve the biochemical plant growth model are described, as a preliminary step, we aimed to develop leaf metabolic model. For that, we have taken many concepts involving metabolism studies that already carried out by several people (Schwender *et al*., 2003; Provost *et al*., 2006; thesis of Balakrishnan Achuthanunni Chokkathukalam, 2010; thesis of Guillaume Cogne, 2003) along with the compartmentalised metabolic pathway studies of a photosynthetic plant cell (Morgan and Rhodes, 2002). Many more models and studies for specific plant processes exist which are outside the scope of this thesis. However, it was necessary to establish a stoichiometric metabolic model for the entire plant correlating available modelling methodologies (which will be described in chapter 2) and general plant growth model design (as mentioned in foreword). The stoichiometric metabolic models which are successfully applied for microorganisms were found interesting, as it was possible to

modify it into plant cell level and subsequent integration could satisfy our preliminary model concepts.

1.9 Conclusion

Mathematical models in the plant and crop sciences provide means of integrating different aspects of the plant system, in particular the interaction between plant metabolic processes and environmental factors. An accurate metabolic model will be systematic and well ordered, describing the current knowledge of plant biochemical processes. The aimed model focuses the response of canopy photosynthesis - respiration processes including adaptation to predetermined environmental conditions. Adaptation is obligatory while considering controlled ecological life support systems, since plant metabolical characteristics are affected by past as well as present environmental conditions of the entire loop; especially, the level of photosynthetic enzymes in a plant is generally greater for plants grown in high irradiance levels than for similar plants grown in low irradiance. Upto an extent, such an adaptation can be accomplished through a stoichiometric plant growth model, as it can directly link to the light and CO_2 availability. However, by controlling all environmental factors, the plants growing in controlled chambers are assumed to have a smooth plant growth. Nevertheless as it is concerned with the human life security, the final model validation is necessary using the experimental data of plants grown in such controlled environmental conditions in addition to the space constraints (e.g. microgravity and radiation), and if necessary, models of plant processes can be added, removed or connected to get a growth model of our target. The obtained model can be applied to 'normal' growing conditions, although the principles are applied to closed bio-regenerative systems; but, of course, this also may need some modifications.

1.10 Main outcomes of Chapter 1

- To achieve a biochemical model of plant growth, the entire plant metabolism must be studied: organ, growth/developmental phase, matter transports (organ, tissue, cell and cellular organelles), interconnections, etc.
- For plant growth modelling purpose, the energy metabolism and its utilization are important.
- The existing metabolism models use either kinetic or stoichiometric steady state approach; models were found for a specific metabolism or under some particular conditions.
- There were no stoichiometric models available for entire plant and this must be developed.

Chapter 2 Methodologies for modelling cell metabolism

2.1 Introduction

Plant biology lies within a range of principles and mechanisms. Each process happens in its own rhythmic way controlled by hormonal/gene regulations. For plant modelling, there are connections between several sciences – mathematics, chemistry, physics and biology. Biology generates complex problems while the others provide ways to understand and solve it. A large number of biological phenomena and processes can be translated into an abstract concept of a complex network making biological problem which can be mathematically solved. Most of these networks have been determined through biochemical experiments over the last few decades and can be found in various kinds of biochemistry text books. At the same time, various techniques are developed for the representation and analysis of biochemical networks establishing mathematical models. Such models suggest new enquiries that can be tested on real biological system.

In order to achieve a model revealing plant biochemical processes, it is necessary to introduce the key concepts of mathematical metabolic modelling: material balances in the living system, the mathematical representation of metabolism into metabolic stoichiometric matrices and the network analysis using steady-state assumption. Two methods are found interesting for the plant metabolic modelling purpose. Both are based on the stoichiometric metabolic network analysis. The same methods have already been successfully used for the *in silico* studies and modelling of microorganism grown in specified cultures. The efficient and relatively easy metabolic modelling techniques that can be used for modelling cell metabolism are described in this chapter.

2.2 Biochemical and mathematical basis of metabolic modelling

The biochemical basis of metabolic modelling lies on the understanding of the metabolism. The catalysts of cellular metabolism are the proteins known as enzymes. Each enzyme has a relatively high specificity in terms of metabolites on which it acts and usually it catalyses only a single reaction. This is regulated by the instructions of a set of genes. In addition to this, the enzyme activity depends on the concentration of metabolites, which may susceptible to change with respect to different types of constraints (e.g. environmental constraints like light, water, nutrient availability).

A metabolic model refers a selected list of reactions and associated properties assumed to be present in the system under investigation, along with the description of the environment within which the system is assumed to reside. Therefore, plant metabolic model accounts all major pathways such as photosynthesis, respiration, energy for maintenance, growth, transport processes not only by xylem- phloem vessels, but also within the cells. In order to attain a metabolic model, all these pathways must join up, since plants make all their constituents from a small set of precursors such as carbon dioxide (CO_2), water, light, micro nutrients, etc. In those cases, the relative material flows known as 'metabolic flux' from small cell compartments to another (e.g. from chloroplast to cytoplasm) connect the metabolic pathways. This process takes place within the cell, from cell to cell and from organ to organ so that it connects all metabolisms forming a large network which could integrate into the plant level (Cassimeris *et al*., 2011). Following Figure 2.1, mathematical model of any kind of metabolism can be easily constructed (Wiechert and Takors, 2004).

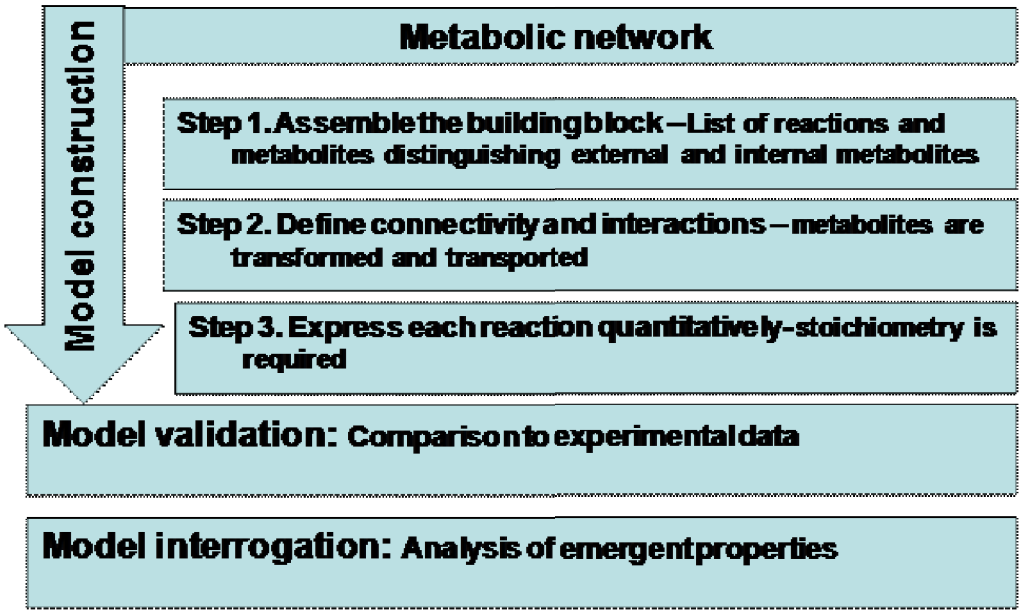

Figure 2.9: Mathematical way to construct metabolic model (Wiechert and Takors, 2004)

Concentration of research on individual components of the system, rather than on its integration may result in the lack of information on many of the important mechanisms which link the component parts and this contributes to the inability of detailed knowledge based models. Hence, for the modelling of plant metabolism, it is quite necessary to know the entire metabolism related to plants. For better understanding of plant metabolism, the metabolic compartmental studies in different levels (leaf, stem, roots, etc.) may help. The metabolic equations can be written expressing the impact of the environmental constraints mainly linked

to physical constraints, e.g. light, water, etc. But, to validate the model to be developed, it would be necessary to have experimental values for plants that grown in controlled/known environment. This means, in the absence of stress, plants grow naturally taking the advantage of environmental and nutritional factors/conditions. Furthermore, the factors such as metabolism, metabolic flow and relative growth rate with respect to the environmental stress or constraints reflect plant morphology and development.

Regarding the metabolic networks which involve sequence type reactions (which is very common), the first produced metabolite will be consumed by another reaction as substrate; then, it is known as primary metabolite; if primary metabolite is consumed by another reaction as a substrate, it is called secondary metabolite and so on. Though secondary metabolite is not directly involved in the process, it has an important ecological function. Examples include hormones, vitamins and pigments. Being the intermediates of biochemical reactions, metabolites connect many different pathways that operate in a living cell. The metabolite level, which could be determined by the activity of the enzymes that are involved in the synthesis and conversion of that metabolite represents the integrative information of the cellular function; hence it defines the phenotype of a cell or tissue in response to genetic or environmental changes. Due to the coupling of many different reactions within the metabolic network, even small perturbations in the level of biological enzymes may result in a significant change in the levels of many metabolites.

The metabolome forms the complete set of metabolites used or formed by the cell in association with the metabolism. Consequently, it comprises the intracellular metabolites as well as the metabolites excreted into the growth medium (e.g. hormones and other signalling molecules found within a biological sample). The series of metabolic reactions of metabolism are called metabolic pathways. There are a number of biological metabolic pathways that are quite common for many living organisms. For example, respiration and pentose phosphate pathway are very common in all organisms, which serve as energy conversion pathway. Other important metabolisms are fatty acid, glycogen and amino acid metabolisms. In an early study, it was found that the large scale structure of the core metabolic network from 43 organisms is identical, being dominated by the same highly connected substrates (Jeong *et al*., 2000).

However in a metabolic pathway, the reactions are organized to serve a coordinated function within the cell. The main metabolic pathways such as photosynthesis, respiration and associated metabolic processes play major roles in the plant's carbon budget (Lambers *et al*.,

2008). The biomass produced by leaves is specifically partitioned in roots and shoots accounting all plant activities. In short, the fluxes through biochemical reactions connect the entire metabolism, which can be specified as a function of the amount of enzymes catalyzing the reactions and the concentration of the metabolites. This differs from the rate of a reaction or velocity and depends on the metabolite level. The concentrations of metabolites themselves are functions of the metabolic fluxes and vice versa. Thus, there is an important feedback regulation imposed on the system (Nielsen, 2003; Schwender, 2009). Moreover, enzymes are regulated by reactants and products of many reactions. Thus, the metabolic flux is appeared to be the final outcome of genetic, enzymatic and metabolic reaction and hence stands as a valuable representation of cell physiology.

2.2.1 Theories behind metabolism

2.2.1.1 Material balance

Every biochemical system maintains material and energy balance in order to keep the growth and survival. The balance is in accordance with the law of mass and energy conservation.

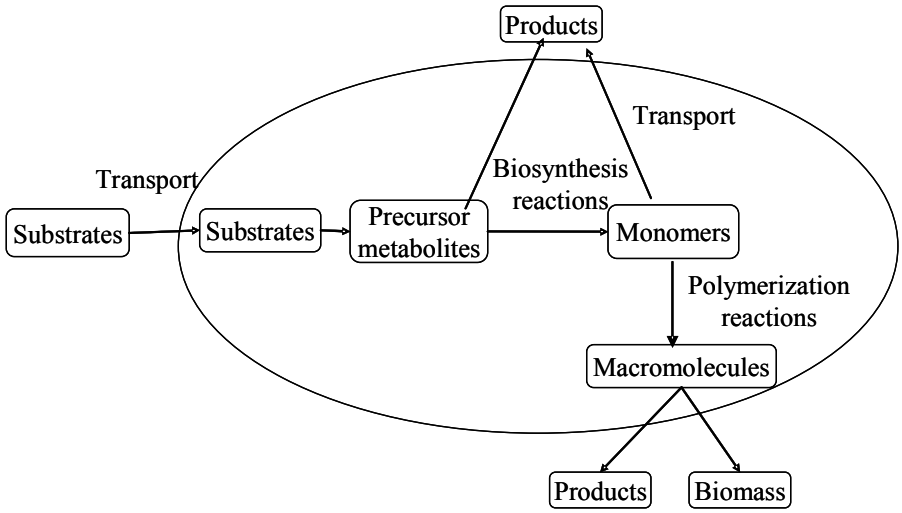

Figure 2.10 : A biochemical system

Consider an open system (as shown in Figure 2.2) separated from its surroundings by an imaginary boundary; some substrates are consuming, reactions take place and macromolecules are forming inside the cell through different stages. Then, according to mass-balance theory, the material entering into a system must, either leave the system or accumulate within the system, with or without having reaction.

Then, the simplest expression for the total mass balance for the system is given by (Himmelblau, 1967),

Input – Output + Reaction = Accumulation

Here, the substrates injected to the system are inputs, and products formed outside are outputs. The accumulation can either be positive or negative, depending on the relative magnitudes of input and output. It should be zero for a continuously operated reactor (e.g. continuous culture at steady state). As many biological systems achieve steady states at some stages of growth, the accumulation term will be considered as zero. Considering plants as a bio-system, the substrates consumed are carbon dioxide, water, nutrients, light energy, etc. and the main products are biomass, transpired water and oxygen gas. Therefore, according to mass balance theory for plant system,

$$\text{Substrates}_{(\text{consumed})} \rightarrow \text{Biomass}_{(\text{produced})} + (\text{water} + \text{gases})_{(\text{produced})}$$

While using equations for biomass transaction, in most cases we consider C, H, O and N, since other elements (S and P) participate only in small fractions and contribute only a very small quantity to the biomass. These types of mass balanced equations are also termed as stoichiometric equations. For reactions that occur inside a physical system, such as a cell or all reactions (whether they are enzyme catalysed reactions or cells grown in nutrient solution producing product) occurring inside a reactor, stoichiometric equations can be written and the metabolic feasibility can be analysed. When dealing with a physical system, the materials flow in and out of the system. Hence, the material balance involves the flow of materials (inputs and outputs) and the reactions in the system. Anyhow facilitating this, most biological reactions occur in aqueous solution.

2.2.1.2 Energy balance

The energy balance in a biological system is maintained in the form of several energy molecules (ATP^{4-}, ADP^{3-}, Pi^{2-}, $NADP^{+}$ $NADPH/H^{+}$, NAD^{+} and $NADH/H^{+}$). For a non-flow system separated from the surroundings by a boundary, the increase in the total energy 'ΔE' of the system is,

$\Delta E = Q - W$

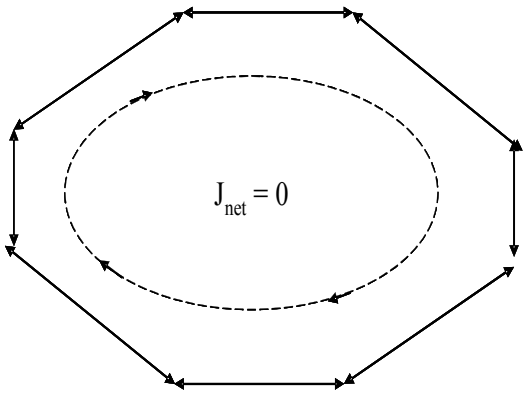

Figure 2.11: Energy balance

where ‘Q’ is the net heat supplied to the system and ‘W’ is the work done by the system (Katoh and Yoshida, 2009). Considering again plants, the light energy is the only source of energy for the whole plant metabolism (work). Plants absorb this energy directly from the environment using special pigments called chlorophylls. The light energy is then converted into chemical energy, in the form of energy molecules in order to maintain all the metabolic process and energy needed process like uptake of nutrients, water by root. The extra energy is released in the form of heat; this process is also balanced by many other mechanisms like transpiration, regulation of water, temperature balance, etc. within the plant. For example, when the temperature rises in response to sunlight, most components of the energy balance that contribute to cooling increase in magnitude until energy gain and loss are in balance. At this stage, leaves reach an equilibrium temperature and the sum of all components of the energy balance will be zero (Figure 2.3) (Lambers *et al*., 2008). Any change in the components of energy balance alters leaf temperature, which is important for gas exchange and photosynthesis.

2.2.2 Metabolic networks in steady state

One of the characteristic features of living organisms is their ability to maintain a relatively constant composition during their growth. Organisms keep the internal state constant by the flow (flux) of matter and energy through cell metabolic pathways. Biologically, it is not always necessary to reach the steady state for successive enzymatic reactions. But, the consequence of not attaining steady state by one or more intermediate metabolites may continue to accumulate in increasing or decreasing amounts which could lead to severe problems (osmotic problems or exhaustion of intermediate) for the survival of the organism (Cassimeris *et al*., 2011). All reactions in a living system are interrelated and hence, the system as a whole can be considered to be in a steady state condition.

Despite, every single reaction takes place at a particular rate. To understand the rate of several chemical reactions constituting the metabolic pathway, pseudo steady state approach can be assumed (Schwender, 2009). This means, the rate of each reaction is equaled (steady). There will be a net conversion of the starting reactant into the final product. The concentration of each of the intermediates between the initial substrate and final product remains steady; the reaction rates linking them are constant; only the concentrations of first and last molecules change with time; these are excreted or imported inside the cell. Thus, a single rate applies to all of the reactions, when the system is in steady state and the rate of a metabolic pathway is

equal to the rate of conversion of initial reactants into final products (Cassimeris *et al*., 2011). In this event, higher plants' metabolic pathways are readily modelled using pseudo steady state and mass balance approach. It must be kept in mind that the hypothesis remains valid for a time interval: not too short for averaging time course fluctuations, and not too long for accounting long time evolution of metabolism. The time interval may be 15 min - 1 day in higher plant compartment.

2.2.3 Thermodynamics of metabolic pathways

Principally, living organisms are considered as open systems that can exchange matter as well as energy with the surroundings (as in Figure 2.2). Biochemical thermodynamics is concerned with the use of energy from the source so that the necessary reactions become favourable, and thus may occur. Living systems have evolved to couple unfavourable and favourable reactions to make the overall process a thermodynamically favourable one. The primary examples for such phenomenon are metabolic pathways. The reactions that are thermodynamically favourable may not occur rapidly enough to be compatible with the demands of the organism. These reactions are made faster by biological enzymes. For example, the respiration process needs much amount of energy where as the reverse reaction, photosynthesis is thermodynamically unfavourable. But the reaction occurs in the presence of sunlight. Here, sunlight provides energy to the plants to overcome the energy barrier that is necessary for thermodynamic favourability.

At steady state, the reactions are at equilibrium ($\Delta G = 0$); the reactions with $\Delta G < 0$ are thermodynamically favourable (exergonic), while those with $\Delta G > 0$ are thermodynamically unfavourable (endergonic). In a metabolic pathway, one of the nonequilibrium reactions frequently becomes the rate determining step of that pathway and the associated kinetic regulation controls the system (Cassimeris *et al*., 2011).

2.3 Mathematical representation of plant physiology

Plant physiology is represented by a series of metabolic pathways that control the plant growth and maintenance. The internal and external factors which control and regulate the growth may be written in the form of mass balanced metabolic equations. These equations of each major and minor pathway of plant metabolism form a metabolic network corresponding

to the plant physiology. *In silico* representation of plant physiology is necessary to study the system for the modelling purpose. For that reason, we need to convert/represent the plant metabolic network into a mathematical one. This is possible by the matrix construction of mass balanced (stoichiometric) metabolic equations. Stoichiometry rests upon the law of conservation of mass because of the conservation of each element of the reaction.

Any system of biological complexities can be converted into the form of matrices. The matrix representations based on stoichiometric metabolic equations are known as stoichiometric matrices. This allows to perform various types of linear algebraic studies on the *in silico* metabolic networks.

2.3.1 Equations into matrix

If a reaction network has '*n*' reactions and '*m*' molecular species participating, then the stoichiometry matrix will have '*n*' columns and '*m*' rows. For example, consider the system of reactions shown below:

$$S_1 \rightarrow S_2$$

$$5S_3 + S_2 \rightarrow 4S_3 + 2S_2$$

$$S_3 \rightarrow S_4$$

$$S_4 \rightarrow S_5$$

This system comprises four reactions and five different molecular species (S_1, S_2, S_3, S_4 and S_5). Thus, the matrix has four columns and five rows. The stoichiometry matrix, A for this system can be written as:

$$A = \begin{bmatrix} -1 & 0 & 0 & 0 \\ 1 & 1 & 0 & 0 \\ 0 & -1 & -1 & 0 \\ 0 & 0 & 1 & -1 \\ 0 & 0 & 0 & 1 \end{bmatrix}$$

2.3.2 Representation of metabolic network under steady state

The key concepts for mathematical modelling are stoichiometric matrix and steady-state assumption. To explain these terms in a metabolic network, consider a hypothetical system of reactions having pseudo-steady state for the intermediates B, D and NADH as in Figure 2.4.

A → B; at flux J1

B → C + NADH; at flux J2

B → D; at flux J3

D → E; at flux J4 &

D + 2 NADH → F; at flux J5

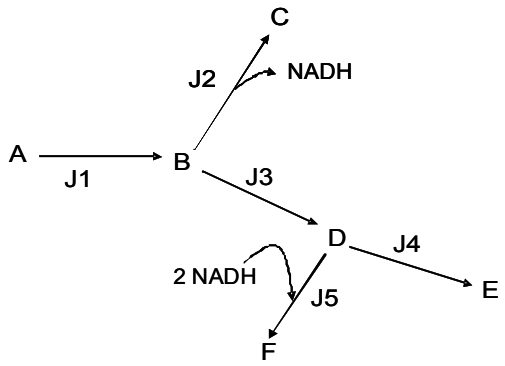

Figure 2.12: Hypothetical system at steady state

From this network, we can write the system of equations at steady state as,

$$J1 - J2 - J3 = 0$$

$$J3 - J4 - J5 = 0$$

$$J2 - 2\,J5 = 0$$

Solving for J2, J3 and J4 in terms of J1 and J5:

$$J2 = 2\,J5$$

$$J3 = J1 - 2\,J5$$

$$J4 = J1 - 3\,J5$$

Thus, using steady-state approach, all fluxes could be calculated from only two measured values; i.e. J1 and J5, which are corresponding to the exchangeables fluxes (initial and final fluxes).

2.3.3 Constraints in cell and network level

Usually, in a biological system, the number of metabolites (m) is more than that of the number of reactions (n). This makes the stoichiometric metabolic network to an underdetermined system (i.e. $m>n$), the analysis on which finds many solutions ('infinite solutions' in terms of mathematics). Hence, it is difficult to distribute the fluxes in the metabolic flux map and to model the metabolism. The use of constraints in metabolic network analysing techniques helps to find a solution in such cases (Schwender, 2009). Cellular functions also suffer different types of constraints which are inviolable and provide hard constraints on cell functions. Mainly, constraints can be classified into four different categories as below.

2.3.3.1 Physicochemical constraints

Many kinds of physicochemical constraints are found in a cell (mass and energy balance, osmotic pressure, electro neutrality, etc.); all are balanced by regulating redox potentials and osmotic pressure. Furthermore, as living systems attains steady state, in order to avoid the accumulation, the cell constraints such as osmosis and osmotic pressure are well maintained (Strange, 2004). Similarly, steady state and mass balance approaches are used while analysing metabolic networks.

Further, the diffusion rates of macromolecules inside a cell are limited by mass transport, as the cells are thickly packed. Moreover, reactions can proceed only in the direction of a negative free energy change. Regarding this context, the thermodynamics of metabolic pathways are accounted by powerful metabolic techniques.

2.3.3.2 Topological/spatial constraints

These are the constraints that affect the topology. Usually, cell is highly crowded and leads to topological constraints that affect cell structure functions. For example, bacterial DNA is about 1000 times longer than the length of a cell. Hence, the tight packing and the accessibility of the DNA constrain the physical arrangement of DNA in the cell level. Incorporating these constraints is a significant challenge. To connect topological constraints in terms of network analysis, the distribution of the number of connections per node within the network, called connectivity of a node is calculated (Jeong *et al*., 2000). Biological network of interactions, including gene expression networks of organisms have many nodes with few connections and a few nodes with many connections (Luscombe *et al*., 2004; Van Noort *et al*., 2004; Junker and Schreiber, 2008).

2.3.3.3 Environmental constraints

Environmental constraints are the constraints originally coming from the environment. These are important to determine phenotypic properties and fitness. Environmental constraints on cells are time and condition dependent. In the case of plants, these constraints include gas levels in the atmosphere such as CO_2/O_2, humidity, temperature, pressure, light availability to the canopy, light intensity, nutrient availability, pH, hydroponics solution temperature which helps the root uptake process, etc. The performance of a plant varies under different environmental conditions. Environmental constraint data from plant culture can only be compared, if the experimental conditions are identically managed.

2.3.3.4 Regulatory constraints

Regulatory constraints are the constraints that regulate the metabolism and growth of a living cell. These are self imposed constraints and involve in concentrations, fluxes or kinetic constants. On the basis of environmental conditions, regulatory constraints allow the cell to eliminate suboptimal phenotypic states and to confine itself to behaviours of increased fitness (Price *et al*., 2004). Regulatory constraints are implemented by cell in various ways, including the amount of gene products which make transcriptional, translational and enzymatic regulation (Price *et al*., 2004).

Mathematically, the stoichiometry of the reactions limits the space into a subspace which is a hyperplane. If the reactions are defined so that they are all positive, the plane is converted into a cone. If additionally the constraints in terms of upper bounds and maximum capacities are defined for the fluxes, a closed convex cone solution space will be obtained as in Figure 2.5. All possible metabolic states of an organism, the feasible flux distributions, lie in that solution space. Thus, it is the space of phenotypes which an organism can express. To further shrink the solution space, additional constraints must be set up from extracellular metabolome for condition-specific solution spaces, reaction thermodynamics (Price *et al*., 2004; Price *et al*., 2006) and experimental transcription data. The whole feasible solution space can be studied algebraically or statistically by sampling the space (Price *et al*., 2004; Palsson, 2000).

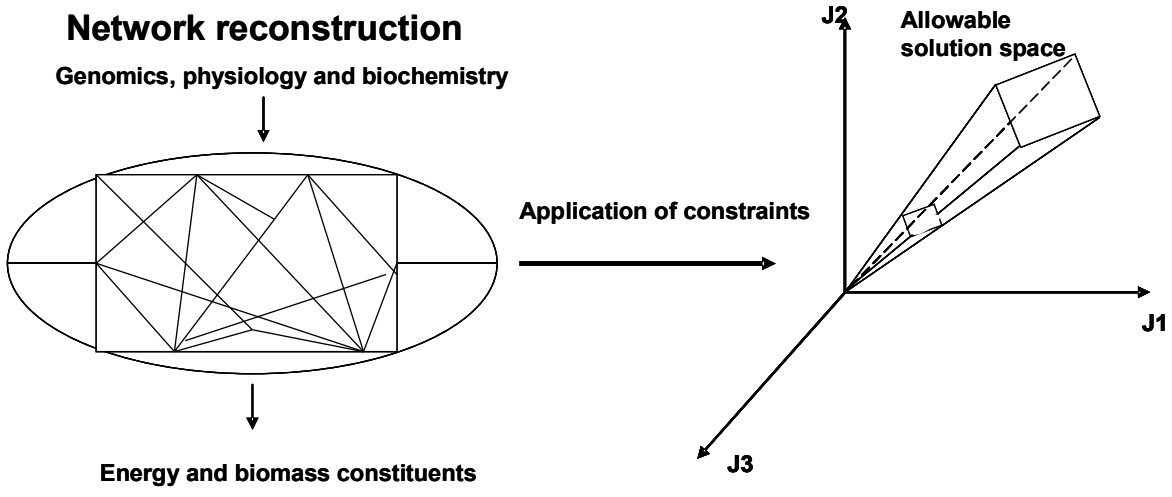

Figure 2.13: Mathematical representation of plant metabolic network The application of constraints reduces the allowable solution space which makes easier the plant modelling (Adapted from Price *et al*., 2004)

Randomized Monte Carlo sampling of the feasible solution space gives unbiased information on the shape and properties of the space where the true metabolic state lies (Price *et al.*, 2004; Schellenberger and Palsson, 2009). The null space containing all the possible flux distribution can be studied algebraically (Palsson, 2000). Investigation on the feasible solution space yields properties of the true metabolic state: the types of possible solutions, the parts of the metabolic network participated in the possible metabolic states, the factors limiting production of specific extracellular compounds, etc. Therefore, it is necessary to use constraints in the modelling level, similar to the cellular level. Fortunately, the powerful methodologies and techniques of metabolic network analysis use the above described (Paragraph 2.3.3) valuable constraints.

2.4 Methodologies for metabolic network analysis

2.4.1 General trends and techniques for system pathway analysis

The interesting fact for a biological network is that, it is arranged in such a way that linear algebra can be applied to study the system behaviour; i.e., the metabolic behaviour and thereby physiological behaviour can be studied and connected to the physical activities. The network often reflects crucial system properties, such as robustness, redundancy, constraints or other functional interdependencies between network elements.

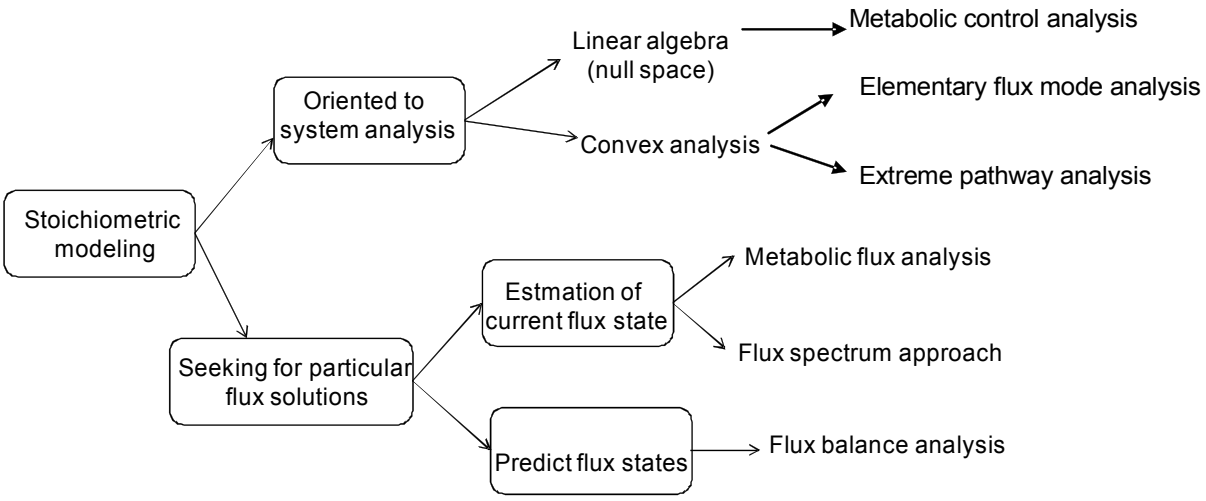

Figure 2.14: Applications and methodologies in the stoichiometric modelling framework There are two main categories – i) to study the properties of the whole space of possible flux distributions ii) determination of particular flux solutions of the allowed space. The scheme is adapted from Llaneras and Picó, 2008; Gombert and Nielsen, 2000.

Several quantitative analytical methods have been developed for the analysis of metabolic networks. Two basic approaches are kinetic approach and structural approach. Kinetic approach, the approach used for kinetic modelling, is based on the fundamental reaction engineering principles. But, as we said in the previous chapter, this requires detailed kinetic information. On the other hand, structural approach is based on the stoichiometry of the metabolic network, in which we are interested. Structural modelling or stoichiometric modelling focuses on the network topology of the system; it has no relation to the efforts of those producing impressive 3D models of the physical structure. However, the analysis uses matrix algebra to deduce the constraints implicit in metabolic networks. This matrix is of chief importance because it represents the translation of biological knowledge in mathematical terms. Once the fundamental stoichiometric matrix has been determined, mass balances involving the rest of the intracellular metabolites can be mathematically represented.

In order to build a comprehensive mathematical model of the living organism/cell, it is required to know all principal components of the system in addition to the interactions that enable metabolite flow (as described in chapter 1). Since last 10-12 years, several modelling methodologies are developed based on this information. The outline of the stochiometric modelling is shown in Figure 2.6. Each methodology has a particular purpose; either analysing the metabolic pathways of the network or seeking particular flux solutions. Each method employs different mathematical frameworks and is based on different assumptions among others. A rational classification of these methodologies can be done based on their division between, those focused on the properties of the entire space of possible flux distributions (and thereby elucidating systemic or emergent properties of the organism under investigation), and those for determining particular flux solutions (Figure 2.6) (Gombert and Nielsen, 2000).

The most frequently used classical stoichiometric modelling methods are Elementary Flux Mode Analysis (EFMA) (Schuster and Hilgetag, 1994; Schuster *et al*., 2000) and Extreme Pathway Analysis (EPA) (Schuster *et al*., 1999, 2000; Schwender, 2009) which characterise all possible flux distributions satisfying the mass balance constraints (Edwards *et al*., 2002; Klamt *et al*., 2002; Papin *et al*., 2004); additionally, Metabolic Flux Analysis (MFA) (Stephanopoulose *et al*., 1998) and Flux balance analysis (FBA) (Varma and Palsson, 1994; Bonarius *et al*., 1997; Schiling *et al*., 1999) allow the determination of particular flux solutions.

In summary, system analysis provides huge, unstructured molecular interaction network into well-defined modules describing the major information flows, which can be used for predictive dynamic modelling. These modules describe individual biological processes and signalling cascades with enough accuracy so that they can be combined into a predictive computational model for the entire system which predicts the outputs with respect to the response of the input variables. The history of pathway analysis begins since 1964 (Milner, 1964; Happel and Sellers, 1982). For the time being, various methods are known for network pathway analysis, based on linear algebra and convex analysis.

2.4.2 Pathway analysis based on convex algebra

This approach is based on the analysis of the null space of a stoichiometric matrix, which contains all cell steady states (flux distributions). One can gain an insight into pathway structures within a metabolic network by calculating biochemically meaningful basis vectors for the null space (Schilling *et al*., 1999). But, it has some limitations: it could not account for irreversibility constraints, and the linear bases were not an invariant property, because, they were not unique. Although, null space has been used in the context of plant metabolism by metabolic control analysis (MCA) technique (Reder, 1988; Heinrich and Schuster, 1996), as it uses kinetics-based tool (Poolman *et al*., 2000; Fridlyand and Scheibe, 2000; Daae *et al*., 1999), further details are not provided.

Convex analysis enables the analysis of linear systems of inequalities, thus making it possible to consider the irreversibility of fluxes (Schilling *et al*., 1999). Two similar approaches, elementary flux modes (EFMs) and extreme pathways (EP) analysis, use convex analysis to generate unique convex sets of vectors that characterise all the steady state flux distributions of a metabolic network (Papin *et al*., 2003, 2004). Both are used to elucidate systemic properties. While analysing the cell metabolic network of the organism under investigation, EFM and EP emerge from the entire network as a whole revealing the cell capabilities like pathway length, network redundancy or enzyme subsets.

2.4.3 Elementary flux mode analysis – Theory and Principle

Each elementary flux mode fulfils three conditions: steady state, feasibility and non decomposability:

- *Steady State*: the elementary mode has to be in the null space of A, which means that A.e = 0, where A is the stoichiometric matrix of order '*m*' metabolites and '*n*' reactions.
- *Feasibility*: the elementary mode, 'e' has to be thermodynamically feasible. Irreversible reactions have to operate in the correct direction.
- *Non decomposability*: the elementary modes have to be the minimal functional units in a network and each elementary mode is unique and cannot be decomposed in to smaller elementary flux modes.

Thus, an elementary mode is defined as a minimal set of reactions (at steady state) with all irreversible reactions proceeding in the appropriate direction. The set of EFM has the following properties:

a) There is a unique set to EFMs for a given network, i.e. this set is an invariant systemic property.
b) Each EFM is genetically non-decomposable. That is, it consists of a minimum number of reactions that need to exist as a functional unit; if any of the reactions of the EFM is removed, it cannot operate as a functional unit.
c) EFM is the set of all routes through a metabolic network consistent with the previous property.

Quantification of elementary flux modes is possible, if accumulation rates of external metabolites are represented as the fluxes of the elementary modes (Gayen and Venkatesh, 2006; Gayen *et al*., 2007).

For any complex biochemical reaction systems, the elementary flux modes are detected. It uses stoichiometric mass balanced equations and reaction directionalities. The matrix on which EFMA performs is represented mathematically as,

$$A\,J = R$$

where 'A' is the matrix of stoichiometric coefficients of the metabolites, J the unknown vector of fluxes and 'R' vector represents the accumulation rates of the external metabolites. It has the dimension of $(m \times n)$, where '*m*' is the number of metabolites in rows and '*n*' is the number of reactions in columns. Therefore, each column in the matrix represents a reaction (Figure 2.7). 'J' is a vector of the 'n' reaction rates. The '*n*' metabolic fluxes and '*m*' conversion rates characterise a physiological state.

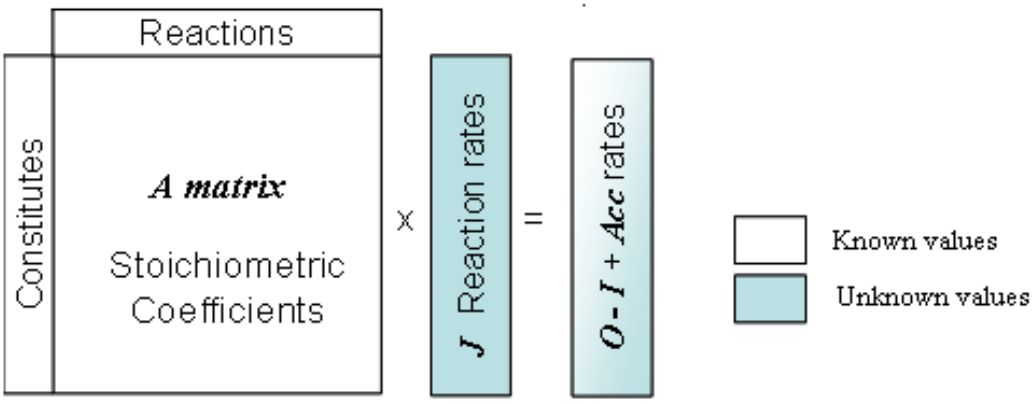

Figure 2.15: *In silico* representation of metabolic network

Due to pseudo steady state approach, the elements of vector 'R' (the rate of exchange) corresponding to the intermediate metabolites (R_{NE}) must be necessarily equal to zero. The non-zero elements of R (R_E) are the net rates of formation of substrates, metabolic products and biomass components.

2.4.3.1 Flux cone formation

The set of all pairs satisfying the conditions, $J \geq 0$ and $R_{NE} = 0$ at steady state forms a polyhedral cone (Figure 2.8), where R_{NE} is the rate of exchange of internal metabolite (intermediate or non exchangeables) (Urbanczik and Wagner, 2005). Since some biological reactions are irreversible, the space of possible flows through the network is constrained, and in mathematical terms, it corresponds to a high-dimensional polyhedral cone, which is often called the flux cone.

2.4.3.2 Computation of elementary modes

The elementary modes are given by the generating vectors of the flux cone, and thus, can be computed based on an algorithm for detecting the generating vectors of convex polyhedral cones (Nozicka *et al*., 1974). In 1981, Clarke proposed one algorithm. But, this had the drawback that the running time increases rapidly with the number of reactions (Clarke, 1981). However in 1993, Schuster R. and Schuster S. have solved this problem. The algorithm presented by them was faster than the method proposed by Clarke (Schuster R. and Schuster S, 1993). In addition, Schuster has given more mathematical description as well as references to related methods (Schuster and Hilgetag, 1994; Schuster *et al*., 1996).

The metabolic reactions, defined in terms of reversibility/irreversibility, and metabolites as exchangeables and nonexchangeables are converted into the matrix form. Transposing this matrix and augmenting it with the identity matrix gives a matrix called the initial tableau. From this, further tableaux are consecutively computed by pair-wise linear combination of rows so that the columns of the transposed stoichiometry matrix become null vectors successively. This procedure ensures the fulfilment of steady-state condition for each metabolite.

Before computing the elementary modes, it is convenient (but not necessary) to reduce the matrix by lumping the reactions that necessarily operate together. Lumping reactions in any one of the sequences gives a reduced system (Schuster *et al*., 2000). While calculating EFMs, generally linear combinations of two rows belonging to the same type of directionality (reversible or irreversible) go into the part of the respective type in the next tableau, while linear combinations of rows corresponding to different types go into the "irreversible" part as they include at least one irreversible reaction. The "irreversible" reaction can enter a linear combination only with a positive coefficient in such a way that all modes use the irreversible reactions in the appropriate direction. Then, as mentioned earlier, calculations for initial table and consecutive tables should be carried out; rows are combined so as to ensure the column of the transpose matrix should be zero. The rows of respective elements which are already zero are copied straight into the next tableau. In the course of the algorithm, calculation of duplicate modes, non-elementary modes, and flux modes violating the sign condition for the irreversible reactions is avoided by checking three conditions (Schuster *et al*., 2000):

1. First, a pair of rows is combined, only if it fulfils the condition $[S(m_i^{(j)}) \cap S(m_k^{(j)}) \not\subset S(m_l^{(j+1)})]$ for all row indices 'l' belonging to the respective

part (reversible or irreversible) of the new tableau as it has been compiled until that stage. The term $m_i^{(j)}$ stands for the i^{th} row in the submatrix of tableau $T^{(j)}$ and $S(m_i^{(j)})$ is the set of positions of zeroes in this row. This set harbours information about which enzymes are not used in the respective mode.

2. The second condition says that "irreversible" rows can only be added rather than subtracted.

3. Third condition rose to avoid the non elementarity upon constructing a new tableau. If any pair of rows pass the first condition and are combined and added to the tableau, all the rows $m_l^{(j+1)}$ previously added to the new tableau are checked to ensure that:

$$S(m_l^{(j+1)}) \not\subset S(m_i^{(j)}) \cap S(m_k^j)$$

2.4.3.3 Futile cycles and EFM

At cell level as well as in metabolic network level, futile cycles can be seen. The analysis of cyclic modes helps to understand the physiological relevance of futile cycles in metabolism. One can calculate the energy cost attributable to substrate cycling. The principle of detailed balancing cannot be applied to cycles, if exchangeables (inputs and outputs) are hidden in reaction cycles (Walz and Caplan, 1988). Therefore, the cyclic effect could be avoided by fixing the relation between the cyclic reactions understanding the significance of the metabolic pathway. Thus, the system sustains. In the biological system, this fixation takes place by many types of constraints like environmental, physicochemical constraints, etc.

2.4.4 Extreme pathway analysis – Theory and Principle

While EFMs enumerate all distinct routes from substrates to products within a metabolic network, extreme pathway analysis (EPA) focuses on enumerating the unique and minimal set of convex basis needed to describe all the possible steady state flux distributions. The EP set defines the edges of the convex cone. It is a subset of the set of EMs. It potentially represents all possible flux distributions being a basis set of vectors. Furthermore, as EPs form a convex base, they satisfy an additional property of systemic independence. The set of EP is said to be systemically independent, if no EP can be written as a non-trivial non-

negative linear combination of any other EP. The difference between this definition and linear independence is that the coefficient of the linear combination must be positive.

Analysed system	References
Analysis of photosynthate metabolism in the chloroplast	Poolman *et al*., 2003
Measurements of mass balance, Rubisco enzyme activity, stable isotope labelling and analysis of elementary flux modes	Schwender *et al*., 2004 a
Identification of pathways	Papin *et al*., 2003; Poolman *et al*., 2003; Schuster, 2000; Schuster, 1999
Detection of reactions correlations (enzyme subsets)	Schuster *et al*., 2002
Detection of infeasible circles	Gagneur and Klamt, 2004
Detection of minimal cut sets, Translation of flux distributions into EM/EP patterns	Klamt and Gilles, 2004
Particular solution methods	Schwartz. and Kanchisa, 2006
α-spectrum	Wiback *et al*., 2003; Llaneras, 2007
Determination of minimal medium requirements, Detection of network dead ends	Schilling *et al*., 2002; Schilling and Palsson, 2000
Analysis of pathway redundancy and robustness	Papin *et al*., 2002 a, b
Incorporation of information about regulation	Covert *et al*., 2001
Support in metabolic engineering, Assignment of function to orphan genes, Identification of pathways with optimal and suboptimal yields, Evaluation of effect of addition/deletion of genes	Papin *et al*., 2003
Suggest changes in flux distributions to increase product yield	Van Dien *et al*., 2006

Table 2.4 : Applications of elementary flux modes and extreme pathways analysis in plants and microbial metabolism Adapted from Llaneras and Picó, 2008.

The algorithm for the calculation of EPs and EFMs differ in terms of treatment of reversible reactions, although both analysis accounts for irreversibility of some of the reactions. EPA decouples all internal reversible reactions into two separate reactions for the forward and reverse directions, and subsequently calculates the pathways. Since EPs are a subset of EFMs, considering EPs instead of EFMs reduces not only the number of routes, but also, the required computational power. However, the result in terms of EPs does not produce the complete set of genetically independent routes within the metabolic network under consideration.

2.4.5 Techniques for flux distribution assessment

The measurements of intracellular fluxes are difficult and often damage the system. Several methodologies of stoichiometric modelling framework use experimental measurements to

estimate *in vivo* fluxes and to develop models capable of predicting unique feasible flux distribution under certain conditions. For example, the effect of measured uptake and secretion fluxes on the space of possible flux distributions has been investigated (Wiback *et al*., 2004). In order to determine the complete current flux distribution, usually, the space of possible flux distributions is coupled with experimental measurements of fluxes, commonly the extracellular ones. Such methodologies uniquely determine the exact flux distribution (Stephanopoulos *et al*., 1998). Metabolic flux analysis (MFA) is one of the popular techniques among them. Therefore, this technique has been extensively applied in recent years, and found particularly successful in the fields of microbial production and animal cell culture.

After the introduction of metabolic flux analysis, variants of classical metabolic flux analysis called ^{13}C Metabolic flux analysis (^{13}C MFA) and flux spectrum approach (FSA) have been established (Llaneras and Picó, 2007, 2008; Wiechert, 2002). Both methods provide reliable and richer estimation of unmeasured fluxes when the system is determined. In the case of FSA, it is due to the inclusion of reversibility constraints and the consideration of the intrinsic uncertainty of experimental measurements; it is useful to estimate unmeasured fluxes, even if, there is a lack of measurable species (Llaneras and Picó, 2008). Nevertheless, ^{13}C MFA always requires information regarding ^{13}C labelling experimental data. The flux ratios at branch points in the network reflect the ^{13}C labelling pattern of the metabolites, thus provide additional constraints to the stoichiometric equations which finally compensate the lack of measurements therein (Wiechert, 2001).

Modelling method	References
Isotope labelling based MFA	Fernie *et al*., 2001 ; McNeil *et al*., 2000; De Graaf *et al*., 1999
Classical MFA	Calik P *et al*., 1999; Yang *et al*.,, 1999; Shi *et al*., 1999; Hua *et al*., 1999; Follstad *et al*., 1999
FBA	Price *et al*., 2004; Edwards and Palsson, 1999, 2000 a; Schilling and Palsson, 2000; Reed *et al*., 2003; Feist *et al*., 2007; Schilling *et al*., 2002.

Table 2.5 : Isotope labelling based MFA, MFA and FBA methods applied in bacterial and plant metabolism. Adapted from Rios- Estepa and Lange, 2007; Gombert and Nielsen, 2000; Raman and Chandra, 2009.

Further, a number of organisms are metabolically modelled using flux balance analysis (FBA) methodology (Schilling *et al*., 2002, Edwards and Palsson, 1999, 2000 a; Feist *et al.*, 2006; Edwards *et al*., 2001); it involves computing a basis of the underlying polyhedral cone.

It can be carried out assuming that cell behaviour is optimal with respect to a (known) objective, and the optimal flux distribution is calculated using an optimization routine (Kauffman *et al*., 2003; Price *et al*., 2003). Table 2.2 contains a few recent models studied using the above said metabolic techniques. Many more examples exist; a full review of which is outside the scope of this thesis.

2.4.6 Metabolic Flux Analysis (MFA) – Theory and principle

MFA is aimed at estimating the extent (flux) of each reaction in the biological network using mass balance and pseudo steady state assumptions. A flux balance is written for each metabolite within a metabolic system yielding mass balance equations that interconnect various metabolites. The basic principle, stoichiometry stands same for MFA as well as EFM analyses. To perform MFA calculations, the metabolic network is represented into a mathematical one. Similar to EFM analysis, the system of equations can be represented in matrix form as,

$$A\,J = R$$

where 'A' is the matrix of the stoichiometric coefficients of all the reactions involved in the metabolism. As said before, it has the dimension of $(m \times n)$, where 'm' is the number of metabolites in rows and 'n' is the number of reactions in columns. Therefore, each column in the matrix represents a reaction. 'J' is a vector of the 'n' reaction rates, which is unknown. The 'n' metabolic fluxes and 'm' conversion rates characterise a physiological state. The matrix representation is the same as we discussed for EFMA (Figure 2.7); i.e. the metabolic matrix for EFMA and MFA can be constructed in a similar way and if we want to perform both analyses on the same metabolic network, it can be done without changing any formats/parameters.

Moreover, the elements of vector 'R' (the rate of exchange) corresponding to the intermediate metabolites (non exchangeables, NE) is partially known as pseudo steady state is assumed. The non-zero elements of R are the net rates of formation of substrates, metabolic products and biomass components.

Since biomass is treated as a product, the rate of biomass can be expressed as time rate of change in the concentration of biomass formation,

$$R_{biomass} = \frac{dC\text{biomass}}{dt}$$

For all extracellular metabolites at steady states,

$$R_E = \frac{dC_E}{dt};\ R_{NE} = 0$$

Therefore, vector 'R' is determined by measuring only the production rate of extracellular metabolite; then, the system is completely determined and can be solved. To perform MFA, experimental data are necessary in addition. Constraints in terms of directions of reactions and mass balance are also imposed on the metabolic network. Generally, the more knowledge that can be incorporated into the flux determination algorithm, the more reliable the flux estimates will be.

Taking the metabolic network in the paragraph 2.3.2 as an example, the stoichiometric matrix can be created.

$$\begin{bmatrix} 1 & -1 & -1 & 0 & 0 \\ 0 & 0 & 1 & -1 & -1 \\ 0 & 1 & 0 & 0 & -2 \\ -1 & 0 & 0 & 0 & 0 \\ 0 & 1 & 0 & 0 & 0 \\ 0 & 0 & 0 & 1 & 0 \\ 0 & 0 & 0 & 0 & 1 \end{bmatrix} \begin{bmatrix} J1 \\ J2 \\ J3 \\ J4 \\ J5 \end{bmatrix} = \begin{bmatrix} 0 \\ 0 \\ 0 \\ R_A \\ R_C \\ R_E \\ R_F \end{bmatrix}$$

The reaction stoichiometries are defined by the stoichiometric matrix, A which contains all coefficients of reactions. The reaction rate vector, J can be calculated as $J = A^{-1} R$. The rate of exchange values corresponding to B, D, NADH (intermediates) are zeros; R_A and R_F (which corresponds to J1 and J5) should be measured, while R_C and R_E (exchangeables) can be find out from steady state approximations. Such type of manual computation is surely a major task for a large network with lots of equations; but, easy to calculate using a suitable mathematical program like MATLAB. After the calculation, we will get the fluxes in terms of the measured rates. This is the systematic way of analysing fluxes in a particular metabolic network. Anyhow, before doing calculations, some of the below conditions must be satisfied.

2.4.6.1 Non-singularities (matrix of full rank)

If 'A matrix' is non-singular, a solution exists for the system. In that case, the rank of matrix A (the number of independent equations) is equal to the number of unknown fluxes, J. Mathematically saying, MFA is applicable only for a fully determined system (Schwender,

2009). But, this condition is not always possible, especially for a biological system. Due to the reaction dependence, singularities arise in the A matrix; for example, consider the simplified network depicted in Figure 2.9.

In this case, Reactions 1 and 2 are indistinguishable from the extracellular measurements of A and D, and the resulting 'A' matrix would be singular. Singularities can only be eliminated by changing the metabolic network or by adding some information; hence, reactions in the network that produce such singularities must be either lumped together or removed.

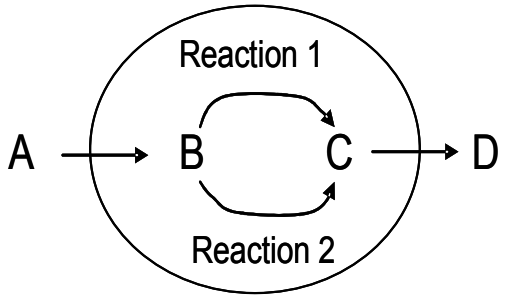

Figure 2.16 : A simplified network

Degree of freedom = No. of reactions - No. of internal metabolites

The number of degrees of freedom of the stoichiometric matrix A determines how many fluxes must be known to solve the metabolic fluxes in the network. The reaction rates can be easily calculated, if a system has zero degrees of freedom (Follstad *et al*., 1999). But, this is not the usual case as described in paragraph 2.3.3.

2.4.6.2 Futile cycles

The stoichiometric equations are selected in a way that reduces the number of futile cycles and parallel metabolites in the reaction network (Cogne *et al*., 2003). Otherwise, during matrix calculation, linear combinations of reactions will be equal to zero. Moreover, mass and energy balances should be maintained; the necessary reactions for energy producing as well as consuming should be supplied as additional constraints (Varma and Palsson, 1994). For large metabolic networks with lots of reactions, MFA becomes difficult as the number of futile cycles increases correspondingly in terms of energy (Wiechert, 2001). Additionally, the energetic costs contribute to a major part of oxygen and hydrogen (via $NADH/H^+$, $NADPH/H^+$, ATP) balance; but, they are difficult to account for. But, even then, the application of constraints aims at solving this difficulty and allows the metabolic flux calculation.

2.4.6.3 Importance of understanding metabolism

To apply MFA for the entire plant metabolism, we must understand possible metabolic reactions and pathways which are very fundamental. This helps to separate the reactants as exchangeables and intermediates knowing the compartmental metabolic informations. For example, glucose is an exchangeable in Calvin cycle reactions; but, if glucose accumulates in the form of biomass (e.g. carbohydrate or macromolecules), which is necessary for cell growth, it should be specified as nonexchangeable in the system network. Such kinds of information are available from extensive literature surveys and several online databases including substrates, products and stoichiometries of each metabolic reaction, directions of reactions, energetics, etc. All important reactions should be included in the system under study; avoiding any one of the important reactions may lead wrong result.

2.4.6.4 Importance of constraints

Application of constraints reduces the number of degrees of freedom of the system. Therefore, in addition to the elemental balances, known metabolic pathways with directionality (reversible and irreversible) of reactions are implemented to the network; the system is also influenced by the metabolites (exchangeables and nonexchangeables). The steady state assumption and lumping of the reactions help to reduce the complexity of the system. For a series of reactions in which there is no consumption or production or accumulation (means, if the products are using as the substrates for consecutive reactions and there is not at all accumulation), all the rates will be the same and the need for the rate of the reaction to be calculated will reduce. This altogether makes the possibility to calculate fluxes from relatively few measured fluxes. The intracellular fluxes, which are difficult to measure *in vivo* can thus be calculated.

2.4.7 Limitations and significance of current metabolic methods

All metabolic methods developed up to present have found both advantages and limitations, although they were successfully used for various metabolic models. The kinetic modelling method, metabolic control analysis (MCA) which was established in earlier periods has clear limits in its scope of applicability (Rice, 2009). Mathematically, the control coefficients of MCA are simply logarithmic sensitivity coefficients at a particular steady state. MCA does not account the stability of steady state and time scales, in which the system reacts to

perturbations. Moreover, the applicability of MCA as a guide to metabolic engineering is often hampered by the fact that regulation on the transcriptional and posttranscriptional level is not considered (Rice, 2009); it is also challenged by the theories proposed by Savageau (Savageau *et al*., 1987; Savageau, 1992).

Coming to the flux distribution solution techniques, FBA takes the risk to select solutions that might be optimal with respect to an objective function, as it is analysed on the basis of maximizing or minimizing a function (Rice, 2009).

Similarly, flux spectrum approach has also some limitations, though it brings some attentive advantages over classical MFA. There are combinations of fluxes within the flux-spectrum in which each individual flux cannot be varied independently. Actually, flux-spectrum itself is an overestimation (Llaneras and Picó, 2007). Unfortunately, this overestimation is unavoidable, if one wants to have an independent estimation for each flux. It is guaranteed that all the feasible solutions are captured by the flux-spectrum intervals; in fact, this is the advantage and at the same time, the limitation.

Meantime, it has been observed that classical MFA is successively applied for relatively 'small' networks; usually, this is the trend. For large networks, the available measurements would be insufficient creating network under-determinacy. Using the irreversibility constraints and isotope labelling experimental data (when available), a great extent of MFA limitations would be overcame. But, plant metabolic systems are sufficiently complex that they often demand use of multiple isotopes to achieve obvious flux determinations. Thus, ^{13}C labelling is often combined with ^{14}C labelling to provide flux constraints that cannot be deduced by ^{13}C labelling alone (Fernie *et al*., 2001). However, such types of necessarily required fluxes for plant metabolic network are not available which we can be used. The high degree of compartmentation of plant metabolism, the existence of duplicate pathways in different organelles, the occurrence of heterogeneous cell populations within a tissue or organ, the difficulty in achieving metabolic and isotopic steady state due to large, slowly turning-over polymer pools, represent the major challenges in applying isotopic labelling to plant systems (Roscher *et al*., 2000). Hence, ^{13}C MFA stays far away from our modelling concepts. Considering again the primarily discussed techniques, MFA captures the attraction where it uses thermodynamic constraints. Further, MFA is found successful in the case of microorganisms and cell cultures (Schilling *et al*., 2000; Schuster *et al*., 1999; Wittmann and de Graaf, 2005; Follstad *et al*., 1999; Schwender *et al*., 2004 b). Currently, there is a trend in

applying MFA for different plant cells and for studying specific metabolism (Williams *et al*., 2008; Beurton *et al*., 2011); but none is accounting the entire plant metabolic network.

Several applications of MFA are reported in addition to the quantification of pathway fluxes:

- MFA identifies the pathways that can reproduce the macroscopic fluxes of extracellular metabolites and can eliminate alternative pathways which are not possible by virtue of their inability to satisfy the material balances. The transhydrogenase activity of *C. glutamicum* is identified in this way (Stephanopoulos and Vallino, 1991).
- In cellular pathways, MFA is useful in determining nodal rigidity. It determines the interconnections between metabolites called nodes (Junker and Schreiber, 2008).
- It is possible to calculate the non measured extracellular fluxes. If measurements of these fluxes are available, the extent of their agreement with model predictions can be verified for model validation (Stephanopoulos *et al*., 1998).
- Helps in the calculation of maximum theoretical yields which provide a benchmark for real processes and can also identify alternative pathways with attractive features for a given application (Stephanopoulos *et al*., 1998)

Thus, metabolic flux analysis is found to be a powerful metabolic technique. As mentioned before, MFA predicts metabolic outputs along with biomass composition, if the experimentally determined inputs are provided, which is required as a part of predictive MELiSSA plant model.

2.4.8 Comparing EFM, EP and MFA - Significance and relative differences

The concepts of elementary flux modes (EFMs) and extreme pathways (EPs) have proved to be valuable tools for assessing the properties and functions of biochemical systems (Papin *et al*., 2002a, 2002b, 2004; Schwartz and Kanehisa, 2006; Junker and Schreiber, 2008). In fact, both concepts are closely related to one another. EFMs and EPs were introduced by the groups of Schuster and Palsson (Schuster *et al*., 1999, 2000; Schilling *et al*., 1999; Pfeiffer *et al*., 1999). The set of extreme pathways are systematically independent and are the subsets of the sets of EFMs. The similarities and differences are discussed in detail by Klamt and Stelling (2002).

Elementary flux modes	Extreme pathways
There is a unique set of elementary modes for a given metabolic network.	There is a unique set of extreme pathways for a given metabolic network.
Each elementary mode consists of the minimum number of reactions that it needs to exist as a functional unit. If any reaction in an elementary mode were removed, the whole elementary could not operate as a functional unit.	Each extreme pathway consists of the minimum number of reactions that it needs to exist as a functional unit.
The elementary modes are the set of all routes through a metabolic network consistent with property 2.	The extreme pathways are the systemically independent subset of elementary modes; that is, no extreme pathways can be represented as a nonnegative linear combination of any other extreme pathway.

Table 2.6 : Comparison between elementary flux modes and extreme pathways (Klamt and Stelling, 2002)

An elementary flux mode is a minimal set of enzymatic irreversible reactions knowing the appropriate direction that could operate at steady state, while, systematically independent subset of the elementary modes constitutes an extreme pathway. The common objective of elementary mode and extreme pathway analysis is to extract functionally independent units of a whole metabolic network and there is no need of genomic or kinetic details. The reactions which are not connected to the metabolic network are identified by employing EFMs and EPs (Junker and Schreiber, 2008).

Comparing with EP analysis, EFM analysis is the most promising, as it offers several advantages.

- EP analysis may neglect important routes connecting extracellular metabolites; but, EFM is capable of accounting all possible routes (Klamt and Stelling, 2002).
- Another advantage is that the connecting routes between different extracellular can be traced out and the maximum theoretical yield can readily be computed.
- It is used to predict optimal growth and optimal phenotypic space of a specific target metabolite (Gayen and Venkatesh, 2006).
- It is used to analyse biochemical networks in mixed substrates and has biomedical applications (Edwards *et al*., 2001; Gayen and Venkatesh, 2006).

- The use of elementary modes in the development of unstructured, kinetic models compatible with the underlying metabolic network provides new applications (Provost and Bastin, 2004; Gao, 2007; Provost, 2006).
- Despite being these proposals, EFMA along with alpha spectrum analysis and FBA showed one of the promising methods for modelling (Wiback *et al*., 2004). Also, studies connecting MFA and EFMA are also reported recently (Beurton *et al*., 2011)

Because of these advantages of EFM analysis over EP analysis, we have chosen EFM analysis as a stoichiometric technique to perform pathway analysis in the metabolic network of plant metabolism. The theory and principles of EFM analysis are studied in detail.

Metabolic flux analysis quantifies the metabolic capabilities of a cellular system. Elementary flux mode analysis systematically enumerates all independent minimal pathways through a network, each unique elementary mode, which are stoichiometrically and thermodynamically feasible. All possible steady state flux distributions through the metabolic network are nonnegative linear combinations of the set of elementary modes (Gagneur and Klamt, 2004). Both MFA and EFM are different techniques involving different manners of matrix calculations and conditions with different objectives, although they use mass balances and steady states. Therefore, the software that should be used for the computational analysis is also different within MATLAB.

As the number of reactions increases, the number of elementary modes normally increases. This means, a large number of elementary modes will be involving in a larger network. Usually, it is found that the number of EFMs obtained will be greater than that of the number of reactions used; it also depends on the exchangeables and non exchangeables involved. In the case of MFA analysis, it is preferable to reduce the network size by lumping reactions. Cyclic reactions differentiate both the methods. MFA will be affected by the influence of cyclic reactions (futile cycles); some reactions will get nullify because of the futile cycles. But EFM analysis can retain the effect of futile cycles. The differences and similarities of these two techniques can be summarised as follows:

2.4.8.1 Similarities

- Both the methods can be used to analyse the metabolic network of any biological complexities.
- Both use steady state and mass balance stoichiometry principles.

- The metabolic *in silico* construction principles and the separation of metabolites into exchangeables and non exchangeables for the studies are very similar and necessary.
- Both run under physico chemical, regulatory, environmental constraints, etc.
- Both methods do not need any details on genetics and kinetics.
- Hence, the same metabolic system can be used for both of the analyses.

2.4.8.2 Differences

- Obviously, matrix calculation is different for MFA and EFMA.
- Futile cycles are taken into account in the calculation of elementary flux modes. In fact, futile cycles may increase the number of elementary modes of the system. While metabolic flux analysis calculation is blocked by the influence of futile cycles (also known as cyclic reactions). But, this can be solved in another way.
- There is no need of experimental data for the calculation of the number of elementary modes of the system. But, for the calculation of intracellular fluxes using metabolic flux analysis, the experimental data (of at least, one value in terms of exchangeable rate) is essential.

2.4.9 Available Software tools

The available software tools handle the matrix computations. A number of excellent tools are available for analysing metabolic networks and to establish models (Table 2.4). GEPASI developed by Mendes is specifically designed for the analysis of biochemical systems (Mendes, 1997). This software package calculates the control coefficients and elasticities of biochemical systems, and includes various optimisation algorithms (Mendes and Kell, 1998). Two other software tools with comparable scope are SCAMP (Sauro, 1993) and DBSolve (Goryanin *et al*., 1999). The software tools Empath (Woods, Oxford), JARNAC (Sauro, 2000), ScrumPy (Poolman, 2006), FluxAnalyzer/CellNetAnalyzer (Klamt *et al*., 2002), PySCeS (Olivier *et al*., 2005), YANA (Schwarz *et al*., 2005) and METATOOL (Pfeiffer *et al*., 1999) calculate elementary modes. If flexibility is important, it is better to use algebraic software such as Maple, Mathcad, Mathematica or MATLAB (Giersch, 2000).

Software tools	Available links
GEPASI	http://www.ncgr.org/software/gepasi/index.html
SCAMP	http://www.brookes.ac.uk/bms/research/molcell/fell/mca~rg/sware.html#SCAMP
YANA	http://yana.bioapps.biozentrum.uni-wuerzburg.de/
DBSolve	http://websites.ntl.com/-igor.goryanin
Empath	ftp://bmshuxley.brookes.ac.uk/pub/mca/software/ibmpc/empath/
JARNAC	http://www.fssc.demon.co.uk
ScrumPy	http:// mudshark.brookes.ac.uk/ScrumPy
FluxAnalyzer/ CellNetAnalyzer	http://www.mpi-magdeburg.mpg.de/projects/fluxanalyzer http://www.mpi-magdeburg.mpg.de/projects/fluxanalyzer
PySCeS	http://pysces.sourceforge.net
METATOOL	ftp://bmshuxley.brookes.ac.uk/pub/mca/sof~are/ibmpc/metatool/
Maple	http://www.maplesoft.com
Mathcad	http://www.mathcad.com
Mathematica	http://www.mathematica.com
MATLAB	http://www.mathworks.com

Table 2.7 Software tools and links for metabolic network analysis

Although several software tools are available, the elementary mode calculation will be performed via available software called METATOOL; the new version, METATOOL 5.1 based on several aspects in the recent developments allows cyclic modes (von Kamp and Schuster, 2006; Klamt *et al*., 2005; Pfeiffer *et al*., 1999; Schuster *et al*., 2000; Urbanczik and Wagner, 2005) and therefore, the calculations will be performed via the same principles. In addition to the elementary modes, it can compute other structural properties of metabolic networks, such as enzyme subsets, conservation relations, etc. (Pfeiffer *et al*., 1999). Therefore, this could be used for different purposes including *in silico* metabolic reconstruction and there by metabolic modelling of any kind of organism (Covert *et al*., 2001).

2.5 *In Silico* reconstruction and analysis of plant metabolic network

As we mentioned before, *in silico* reconstruction and analysis of plant metabolic network are associated with mass balanced stoichiometric metabolic pathways of plant metabolism. Some of the stoichiometric reactions are available in several databases (e.g. KEGG, BioCyc, PlantCyc, MetaCyc, etc). In addition to the known metabolic pathways, missing reactions are necessary to connect several pathways to one another. In that cases, several literatures as well as thermodynamic feasibility should be verified before taking it into account. Similar to the

biological systems that suffers many constraints, the constructed *in silico* metabolic network also suffers constraints in the form of mass balances, reaction directions (reversibility/irreversibility), etc., while it is analyzed using any of the metabolic techniques discussed in the above sessions.

Then, from the above discussed metabolic techniques, plant modelling can be achieved by two ways. Both methods are based on stoichiometric mass balanced metabolic techniques accounted by the stoichiometric matrix, which underline the importance of understanding metabolism. One method uses elementary flux mode analysis and flux balance analysis followed by alpha spectrum analysis; while, the other is based on elementary flux mode analysis and metabolic flux analysis approach. For both methods, it is necessary to construct metabolic matrices as a preliminary step. While constructing the metabolic matrix, two types of metabolites- exchangeables (E) and non exchangeables (NE) are defined. If the formation of the metabolite is balanced by its consumption (using steady-state assumption) in the studied system, it is considered as a nonexchangeable, and if the metabolite is the source or sink (nutrient or product including waste), it is defined as an exchangeable. The definitions of external and internal metabolites (E and NE) depend on the main targets and the system nature. If we consider the entire plant metabolism, some of the energy must be considered as output, as heat will be producing as output. The *in silico* representation of metabolic network allows studying and modelling the plant system using the following methods.

2.5.1 Method 1: EFM

In this method, the constructed network is analysed using elementary flux mode analysis, flux balance analysis and then by alpha spectrum analysis. These analyses altogether on the complete network will provide a set of maximum yield giving equations. This set of relevant metabolic equations reveal the exact metabolic behaviour of the living organism without going in to the details of any kinetic or genetic information, Figure 2.10 (Gagneur and Klamt, 2004). In this way, it is possible to build the metabolic model and to estimate and predict the outputs with respect to the input values knowing few experimental values.

Once we construct the metabolic network, it is possible to compute the number of elementary modes. As it uses constraints, it can also give the range of possible values representing whole solution region. Each steady state flux distribution can be expressed as a linear combination of elementary modes (Chen *et al*., 2009). The edges of a high-dimensional convex cone formed in the flux space contain all the attainable steady state solutions or flux distributions

of the metabolic network under study. Elementary modes can be interpreted geometrically as extreme rays from a pointed convex cone corresponding to the network with split reversible reactions, as described in EFM theory.

In general, there is not a unique set of solution that produce a given steady state flux distribution, but rather a range of possible values; this is due to the underdeterminacy of the system. For a given steady state flux distribution and a set of elementary modes of flux vectors, α-spectrum approach determines the range of possible solutions of a particular elementary mode (Wiback *et al*., 2004). This can be determined using linear optimization to maximize and minimize the weightings of a particular EFM pathway in the reconstruction. Here comes the concept of flux balance analysis (FBA).

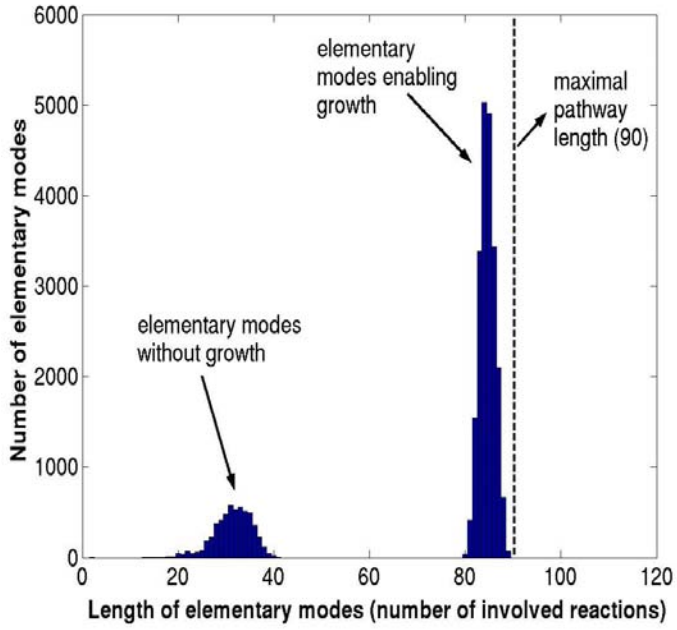

Figure 2.17 : Pathway length distribution of the *E. coli* modes on glucose. Maximum pathway length is the maximum no. of reactions involved in elementary mode (Gagneur and klamt, 2004)

Alpha spectrum specifies a range of possible weights (possibilities) for each EFM pathway, reflecting to some extent the possibility that an elementary flux mode pathway is utilized in a particular flux distribution. Thus, α-spectrum quantifies the involvement of EFM pathways in a particular flux distribution and defines which pathways can, and cannot be included in the reconstruction of a given steady state flux distribution, and to what extent they individually contribute to the reconstruction. According to Wiback *et al*, the usage of transcriptional regulatory constraints can considerably shrink the alpha-spectrum (Wiback *et al*., 2003). The alpha-spectrum is computed and successfully interpreted for human red blood cell

metabolism under various physiological and non-optimal conditions (Wiback *et al*., 2003, 2004). The detailed approach to obtain alpha spectrum is well described by Llaneras and Pico (2007).

The main limitation and advantage of this method is that, the computed alpha spectrum contains all elementary mode activity patterns corresponding to a flux distribution compatible with the available knowledge. The alpha spectrum provides a simple representation of the whole solution region, but not an exact one: it provides an overestimation which cannot be elucidated without additional assumptions. Hence, when the studied metabolic network is enlarged (more reactions), the number of elementary flux modes dramatically increase. This means, there is an increment of the pathway redundancy, and therefore, it might be difficult to determine the internal state of a cell because there can be multiple ways to produce the same behaviour (Papin *et al*., 2003). When the number of elementary modes is greater than the number of reactions, the degrees of freedom will increase. Hence, even if a complete flux distribution for a particular phenotype is known, the alpha spectrum computed from it may be wide (it may contain many possible internal states). Even though that situation makes it difficult to interpret the obtained alpha spectrum, it must be noticed that redundancy is an inherent property of large metabolic networks.

Not very long ago, a new approach of computing alpha spectrum has been introduced, which is called interval approach; it can be used when fluxes are uncertain and flux distributions are partially known. The same has been illustrated using a real example; taking the value for the cultivation of CHO cells calculated before by Provost and Bastin (Llaneras and Pico, 2007; Provost and Bastin, 2004). At the same time, Prevost and Bastin have used a method similar to the following.

2.5.2 Method 2: MFA

To obtain the metabolic model through MFA, it is necessary to collect all the metabolic reactions same as method 1, and construct the metabolic network in the form of matrices. The system is analyzed using a computational program called, 'Brume' developed in Axe GePEB, where the principles and conditions are already stored (Dussap, 2005). Both EFM and MFA calculations are performed via Brume which uses the version, METATOOL 5.1.

The convex analysis method, elementary flux mode analysis predicts possible pathways/routes producing particular biomass precursors or ultimately the biomass production pathway of plant metabolic network, while MFA calculates the intracellular

metabolic fluxes. MFA is one of the most important tools in metabolic engineering and a key measure of metabolic phenotype. As indicated before, it makes use of experimental data to study flux distribution in the system. Recently, complete (genome-scale) metabolic network models have been established for Arabidopsis (*Arabidopsis thaliana*) and flux distributions have been predicted using constraints-based modelling and optimization algorithms such as linear programming (Williams *et al*., 2008; Poolman *et al*., 2009; Masakapalli *et al*., 2010). While checking the compatibility of the predicted flux distributions with those occurring *in vivo*, it has been noticed that for the majority of the reactions, the genome scale model flux predictions were a close match for those estimated by MFA (Williams *et al*., 2008). The model was successful even in the case of Arabidopsis cells grown under stress conditions. MFA showed that the increase in temperature and hyperosmotic stress can alter the cell growth, as it affects the intracellular flux distribution. Regarding the plant system, the challenge is apart from constraints, lots of complexities lie within the system. Even though, EFM and MFA techniques can be applied exploiting available stoichiometric plant metabolic equations and network constraints knowing that, the physicochemical, environmental and regulatory cell constraints reflect on the metabolic equation of biomass formation.

The general limitations of modelling by metabolic flux analysis are the following.

- Large reaction network needs to be simplified:

A system with 10 or 15 metabolic equations is considered as a small system, since it displays only a small metabolic network. As the number of equations increases in a system, the system may have to face lots of complexities; also, it has to face underdetermined case leading many degrees of freedom. So, for the systems like plant metabolic networks, it is preferred to have much simplified system. However, the large metabolic network can be reduced by lumping equations as discussed previously and up a great extent, constraints solve the difficulties.

- Regulation of futile cycles:

As mentioned before, the energy related equations in large metabolic networks form a cycle, which nullifies the metabolic effect. For example, if the futile cycle is associated with energy production ATP, as a result of futile cycle (since the linear combination of the reactions associated with futile cycle will be equal to zero), ATP production will be cancelled. As the system cannot proceed without energy, this will stop the overall system activities and intracellular flux calculation cannot be accomplished. Therefore, during MFA studies, if futile cycles are detected, one must fix any of the reaction participating in the futile cycles to

a particular value so that it suppresses the nullifying effect of ATP production. But, this fixation must be done based on the metabolic pathway knowledge.

- Input/output measurements:

Sometimes, it may be difficult to measure the accurate rates of exchangeables like water, oxygen, carbon dioxide, ammonia, especially in the case of plants. It depends on the type of culture and the facilities one use for the measurements. Further, biomass composition is required for the model validation, if biomass is considered as an exchangeable.

The typical difficulty to perform classical MFA is the lack of available measurements; it may be insufficient to estimate the intracellular fluxes, particularly in large-scale networks of plants, because there may be different flux distributions compatible with the available measurements. To face the lack of measurements, the only solution is to perform MFA together with constraints, which is capable of estimating metabolic fluxes, based on the model and the available measurements. Thus, a flexible, reliable and usable metabolic model for MELiSSA plant can be achieved.

Briefly saying, the main advantage is that the algorithm does not require information concerning intracellular control mechanisms or kinetic rate constants for reactions occurring in the living organism. The overall network is simply a metabolic balance governed by the biochemistry of particular metabolism. By comparison, the concept of EFM is a useful tool in determining maximal and submaximal yields of biotransformations and in functional genomics. It is also helpful in MFA for determining the calculability of fluxes (Klamt *et al*., 2002). The physiological, medical and biotechnological relevance of determining elementary modes in biochemical networks has been explained by many authors (Schuster and Hilgetag, 1994; Liao *et al*., 1996; Nuno *et al*., 1997; Schuster *et al*., 1996, 2000; Dandekar *et al*., 1999; Sauro and Ingalls, 2004). In this regard, the internal fluxes adopted by higher plants could be traced out using EFM analysis. Moreover, using this, one could identify key metabolic routes that are contributing to the metabolism and how it could be modified by environmental factors. This application makes it an attractive tool for *in silico* analysis.

2.6Conclusion

The significant advances in metabolic studies and modelling by metabolic techniques are witnessed in last few years. Up to a great extent, cellular complexities can be exposed by understanding the complex networks and by using the existing metabolic modelling methods which run under stoichiometric mass balanced steady state approaches. As stoichiometric

modelling avoids the difficulties that may arise in the development of kinetic models, it is always a preferable one. The knowledge of the metabolism is fulfilled by applying the suitable and relatively easier existing stoichiometric methodologies on the metabolic network under study. For metabolism modelling, the methods, elementary flux modes and metabolic flux analysis are found relatively simple and easier methods. This can provide characteristic thermodynamically feasible pathways and intracellular flux distributions which cannot be detected *in vivo*. Although, there are some other techniques like isotopic labelling exist to measure the intracellular rates, they are difficult to use in the case of plants. Despite of all existing metabolic techniques, two methods were summarised which could be used for the modelling of plant metabolism; within that, method 2 found relatively simpler which may exploit the possible available data and establish a model of our concept. The main advantage of this method is that, it does not require much experimental data compared to any other existing methods.

2.7 Main outcomes of Chapter 2

- To achieve a biochemical model for plant leaves, the entire metabolic network constituting plant leaves is studied: the mass and energy balances, the maintenance and regulation, etc.
- The relation between steady state and thermodynamics and effects on mass and energy balanced stoichiometric reactions in the metabolic network are important.
- Mathematically, a metabolic network of any complexity can be represented in matrix form and studied using the existing methods; but it is always preferred to have small networks.
- The effects of different constraints in cell level are studied; the utilisation of constraints on metabolic techniques is required to know.
- Existing techniques to analyse metabolic networks (EFM, EP, MFA, etc.), their significances, differences, possibilities, limitations, etc. are discussed and compared.
- Methods for analysing plant metabolism are chosen; the theories, principles and the preliminary requirements to perform the analysis are described.
- The limitations and significance of current metabolic methods are mentioned; for the modelling, the method using mass balance and steady state approaches along with constraints could give valuable results.

Chapter 3 Modelling higher plants energy conversion and central carbon metabolism

3.1 Introduction

3.1.1 Two levels for modelling higher plants metabolism

In order to model plant metabolism, the generic basis of metabolism and regulatory networks for plant growth and development must be addressed. The control and regulation of photoassimilation metabolism is central in this aspect. Primarily, simple sugars are produced in photosynthetically active tissues which contain the specially designed cell organelles for photosynthesis - chloroplasts. Within the cell chloroplast, a part of the assimilated carbon accumulates as starch and the rest is transported through specific types of tissues for respiration and other biosynthetic processes including sucrose synthesis in cell cytoplasm. Similar to cell-cell communication, organ-organ communication also exists in the plant. The sugar molecules (e.g. sucrose) are transported via phloem from source organs (leaves) to support growth of sink tissues such as young leaves, roots, fruits or tubers which themselves are unable to produce assimilates. During development, sink to source ratios change which implies that assimilate production must be adjusted to the changing needs of distant tissues. In this basis, a thorough understanding of the stoichiometry and the thermodynamics as well as regulatory networks linking the entire plant metabolic pathways is required including the factors controlling the synthesis and degradation of carbohydrates and their partitioning within and in between the plant organs.

In this chapter, the current understandings of the energy conversion processes and central pathways of carbohydrate metabolism in plants are summarised. The stoichiometric modelling techniques are applied to model central carbon assimilation pathways of general plants' metabolism. With the current knowledge, metabolic modelling revealing plant biochemical process is possible with mass balance, energy balances considering steady state approaches. As plant metabolism happens in several compartments from the peripheral level to the micro level, the metabolism is separated for leaves, roots, stems and fruits or storage organs. The movement of the components between each organ must be further modelled knowing diffusion and transport processes.

It is clear that the light energy capture and its chemical conversion play a central role in higher plants metabolism. This is directly related to O_2 release and CO_2 capture that are the basic processes to consider when closed systems are considered. For this reason, the metabolic pathways involved in energy conversion in leaves are studied using the techniques

presented in the previous chapter. To analyze the network topology and thermodynamic feasibility, Elementary Flux Mode analysis (EFM) and Metabolic Flux Analysis (MFA) are used. Importantly, the description that we develop includes energetics and energy transduction processes in organelles (chloroplasts and mitochondria). This is linked to central metabolism pathways. The global aim we pursue is to integrate the stoichiometric and energy constraints generally well documented in classical textbooks at elementary level, in a global vision of plant metabolism with the sake of determining the flexibility and the adaptability of the energy metabolism. This fully mechanistic approach constitutes a lumped vision of what we call the "energy model" of higher plant metabolism.

In a second step, presented in Chapter 4, this so-called "energy model" is coupled to biomass composition, nitrogen accumulation in an integrated vision of entire plant metabolism, connecting the previous "energy model" to anabolism, i.e. building block synthesis (e.g. amino acids, carboxylic acids, lipids and carbohydrates monomers) and further, the synthesis of macromolecules (e.g. proteins, nucleic acids, etc.). This aims to achieve the whole biochemical modelling of higher plant growth and maturation. This includes leaf model, root model and stem model. These two levels are modelled and coupled together to establish the complete metabolic model.

Therefore, the first level mainly concerns photosynthesis and respiration. Photosynthesis includes light reactions (water photolysis which produces energy for carbon fixation) and carbon fixing reactions. Calvin cycle uses atmospheric CO_2 and water for the production of sugar; respiration utilises the energy that is stored as sugars through the photosynthetic processes. Photosynthesis, respiration and related pathways produce the necessary energy (ATP and NAD(P)H) for the entire plant processes. This level accounts for the main exchanges (in terms of mass) between the plant and environment (water flow, gas inputs and outputs).

The second level metabolism includes global reactions that produce and accumulate biomass from the basic constituents. In this level, accumulation of biomass leads to assess the nutriental properties of plant depending on the plant development and the environmental conditions. The experimental rates of inputs, outputs and accumulation are used and correlated using the same techniques (EFM and MFA). In a first approach, this second level will be simplified and will not consider all the secondary metabolites contributing to small percentages (e.g. vitamins). A fixed biomass composition is implemented. The

implementation will be based on the experimental data of biomass composition of plants grown in controlled environment.

3.1.2 The higher plant "energy model": modelling central carbon metabolism

As we aimed to analyse C3 plant central carbon metabolism, which is found very common in plant species, the final model can be applied to leafy vegetables like lettuce, spinach, etc. The metabolic pathways in leaves are almost known and central carbon metabolic pathways build the basis of leaf metabolism. This accounts for the main part of the "energy model" of higher plants.

In cellular levels, the biomass formation requires the interaction of three cellular compartments: chloroplast, cytosol and mitochondria. The metabolic pathways associated are called central carbon metabolic pathways; these are not only involved the conversion of the carbon source into building blocks that is needed for macromolecular biosynthesis, but also in the constant supply of Gibbs free energy via ATP and redox equivalents ($NADPH,H^+/NADH,H^+$). For the growth and maintenance process of plants, the function of central carbon metabolism is finely tuned to exactly meet the needs for building blocks and Gibbs free energy in conjunction with cell growth rate. Therefore, the metabolic fluxes and the rates of metabolic reactions through the central carbon metabolism are tightly regulated (Nielsen, 2003). Thermodynamic organization has implications for modelling the energetic efficiency of metabolic transformations. It also affects which experimental and theoretical strategies are taken to study metabolic regulation (Feist *et al*., 2007). For the same reason, when considering a metabolic reaction, it is required to analyse thermodynamical possibility of the reaction. It is possible to estimate the change in free energy *in vivo* from the standard free energy, even if the final exact calculation would require quantitative measurements, local concentrations and activities of metabolites. This determines the thermodynamic feasibility and the direction (reversibility or irreversibility) of a reaction.

Thermodynamical reversibility of the reactions at cellular level influences and directs the transport of metabolites in organelles; this is a fundamental aspect; the energy metabolism is tightly linked to membrane transports and chemiosmotic coupling. This adds a further degree of complexity in the thermodynamic description that we intend to develop for obtaining a robust understanding of energy transduction processes. This compartmentalisation of cell metabolism of course concerns chloroplast and mitochondria.

The metabolic processes concerned in photosynthesis are divided into two: light reactions – the reactions responsible for light energy into chemical energy - and Calvin cycle reactions responsible for carbon fixation using atmospheric CO_2. Similarly, respiration is also separated into three: mitochondrial electron transport and oxidative phosphorylation (which produces ATP by oxidising the reduced coenzymes NADH, H^+ and $FADH_2$), Krebs cycle and glycolysis (which convert the energy from stored sugars).

In summary, the so-called "energy model" for higher plants is composed of the following five blocks:

- Light reactions
- Calvin cycle
- Mitochondrial electron transport
- Krebs cycle
- Glycolysis

Each block has a complementary role providing the energy for overall plant growth and maintenance. Consequently, for establishing the "energy model", we study each metabolic network separately and specifically for higher plants. As these biochemical processes are connected to one another using the redox energy intermediates, we coupled the subsystems corresponding to photosynthesis and respiration separately in two ways: firstly, with the entire metabolic equations corresponding to the systems and secondly, with the stoichiometric EFM equations (will be discussed later) resulted from corresponding subsystems. The intention is to analyse the flexibility or in other words, their number of degrees of freedom for each system separately.

3.2 Light reactions

3.2.1 General overview of chloroplast function

The light energy absorption and conversion (light reactions) take place in the cell chloroplast of leaves; they are green in colour as they contain chlorophyll pigments. At first steps, electrons are energised by light of definite wavelengths for the transport of protons enabling the formation of ATP and reduced compound NADPH, H^+; this is the basic phenomena. But we must go in more details for achieving a complete description of light energy metabolism.

Structurally, chloroplasts are surrounded by two lipid-bilayer membranes: inner and outer membranes; and between the two, there is a space called intermembrane space. Similar to the

cell cytosol, chloroplast contains a liquid medium called stroma; it also contains ribosomes, small circular DNA, starch, lipids, etc. However, most of its proteins are encoded by cell nucleus with the protein products transported to the chloroplast.

Within the chloroplast stroma, the suborganelles called thylakoids are present; it consists of a thylaloid membrane surrounding thylakoid lumen. Chloroplast thylakoids frequently form stacks of disks known as grana (granam in singular), these are linked together by the connectors, lamella (Figure 3.1).

In the thylakoid grana, there are two reaction centres situated: Photosystem I (PS I) and Photosystem II (PS II); they selectively absorb photons of wavelength 700 nm and 680 nm respectively. They use light energy as initiators for the electron transport which generates a proton gradient across the thylakoid membrane and ultimately produce energy molecules ATP and NADPH, H^+. To occur this, special type of photosynthetic pigments and proteins are situated in the thylakoids other than photosystems: cytochrome *b6f* (Cyt b6f), ferredoxin-$NADP^+$ reductase (FAD) and chloroplast ATP synthase are the main protein complexes. In addition to this, the plastoquinone-plastoquinol pool and plastocyanin present in the thylakoids have also important roles to conduct the electron transport.

Since the concentration of protons in the stroma is less than that of the lumen, stroma could be considered as negative phase or N-phase, while lumen is positive phase or P-phase. Subsequently, protons at P-phase and N-phase are taken as H_P^+ and H_N^+. In the following discussions, we consider that stroma is at pH = 7.5 and lumen is at pH = 4. Furthermore, the electrical potentials of lumen and stroma are assumed to be almost equal and will be discussed in the subsequent analysis.

In the following paragraphs, we have analysed the complexes involved in light reactions.

3.2.2 Photosystem II

When light excites the chlorophyll, it fiercely releases electrons from water and passes to plastoquinone producing oxygen and plastoquinol. The reported mechanism is as follows. The manganese complex (OEC of Figure 3.2) helps the oxidation reaction of water on the thylakoid lumen of the membrane (Feyziyev, 2010). Four quanta of light are required to abstract four electrons from two molecules of water; as a result, four protons are released into the thylakoid lumen. The excited electrons have two possibilities to release/pass the energy: either it can return into their ground state releasing heat or it may be accepted by pheophytin (chlorophyll without central Mg^{2+} ion) leaving one positive charge at P_{680}.

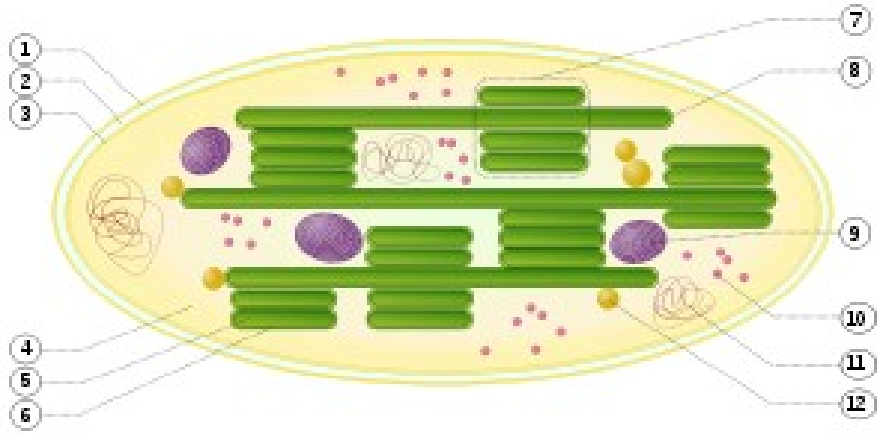

Figure 3.18: Structure of chloroplast 1. outer membrane 2. intermembrane space 3. inner membrane (1 + 2 + 3: envelope) 4. stroma (aqueous fluid) 5. thylakoid lumen (inside of thylakoid) 6. thylakoid membrane 7. granum (stack of thylakoids) 8. thylakoid (lamella) 9. starch 10. ribosome 11. plastidial DNA 12. plastoglobule (lipids)

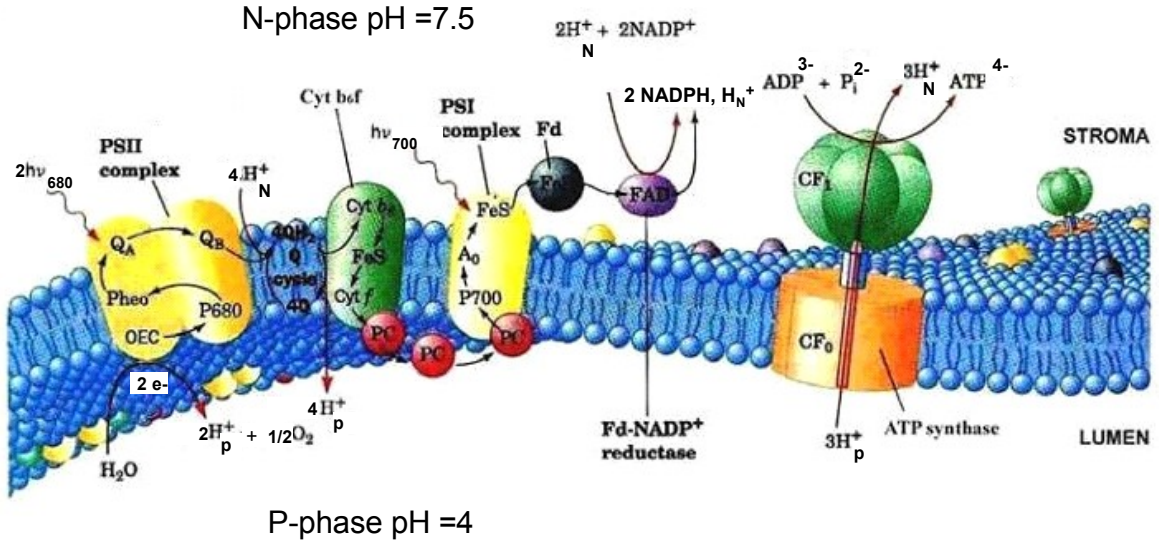

Figure 3.19: Light reactions involving photosystem I and photosystem II Abbreviations: P- phase – positive phase, N-phase – negative phase, PS I –photosystem I, PS II – photosystem II, H_P^+ - proton in P-phase, H_N^+ - proton in N-phase, PQ –plastoquinone, PQH_2 – plastoquinol, Fd- ferredoxin complex, PC-plastocyanin, OEC-Mn^{2+} complex (Adapted from Feyziyev, 2010)

The mechanism involves the oxidation of P_{680} into P^{+}_{680} by one quanta that generate one electron per quantum inside the membrane (Nobel, 2009). The P^{+}_{680}/P_{680} couple has a very high redox potential of 1300 mV (Rappaport *et al*., 2002). Gibb's free energy, ΔG is calculated for this reaction, taking 'n' number of electrons used in the reduction reaction ('n' consumed, i.e. reduction), 'F' Faraday's constant which is equal to 96.484 kJ/mol and, $E_{m,7}$ the change in midpoint potentials in Volt, V.

$$P^{+}_{680} + e^{-} \rightarrow P_{680} \qquad E_{m,7} = 1\ 300 \text{ mV} \qquad (1)$$

$$\Delta G_{m,7} = - n F E_{m,7} = - 1 \times 96.484 \times 1.3 = -125.4 \text{ kJ/mol} \qquad (2)$$

It appears that in this case, $\Delta G_{m,7}$ is independent of pH, which renders the subscript 7 facultative.

The energy, *E* available for one quanta of photon at 680 nm is given by:

$$E = h\nu = \frac{hc}{\lambda},$$

where 'h' is Planck's constant, '*c*' the velocity of light and 'λ' the wavelength of light. This leads to:

$$h\nu_{680} = \frac{6.6262 \times 10^{-34} J.s / photon . 2.9978 \times 10^{8} m/s . 6.022 \times 10^{23} photon/mol}{680 \times 10^{-9} m . 10^{3}}$$

$$= 175.9 \text{ kJ/mol} \qquad (3)$$

This means that one quanta of light energy at 680 nm wavelength represents 175.9 kJ/mol of energy. Taking into account the energy of photon, reaction (1) proceeds in the oxidation way (production of electrons),

$$h\nu_{680}: \ P_{680} \rightarrow P^{+}_{680} + e^{-} \qquad (4)$$

$\Delta G_{m,7}$ for this reaction is calculated:

$$\Delta G_{m,7} = - 175.9 - (-1 \times 96.484 \times 1.3) = - 50.5 \text{ kJ/mol}$$

Obviously this $\Delta G_{m,7}$ is strongly negative. This indicates that reaction (4) is irreversible. This is the maximum available energy for the production of P^{+}_{680} in the chloroplast at pH = 7. P_{680}^{+} is an incredibly strong oxidant, which extracts electrons from water molecules tightly bound at the manganese centre.

In the subsequent steps, the free energy for P^{+}_{680}/P_{680} couple extracts electrons; the redox centre being even more electropositive than P^{+}_{680}, it is capable of reacting

spontaneously with water. In order to analyse this process, we must consider the redox couple of water oxidation:

$$\tfrac{1}{2}\ O_2 + 2\ e^- + 2\ H^+ \rightarrow H_2O \qquad E_{m,7} = 800\ mV,\ P_{O2} = 0.21\ atm \qquad (5)$$

$$\Delta G_{m,7} = -\ 2 \times 96.484 \times 0.8 = -154.4\ kJ/mol$$

This is the free energy for equation (5) at pH 7 at an O_2 partial pressure of 0.21 atm, i.e. at the value in air (Wheeler *et al.*, 2008). Considering water oxidation happens in lumen compartment at pH = 4 (i.e. at P-phase), the reaction free energy as a function of pH is calculated. Taking the standard pH 7, the free energy at a particular pH is given by:

$$\Delta G_{m,pH} = \Delta G_{m,7} \pm n_e\ RT \ln 10^{(7 - pH)}$$

$$\Delta G_{m,pH} = -\ n\ F\ E_{m,pH}$$

where 'R' is the ideal gas constant (8.31451 J/mol K), 'T' is the standard temperature in Kelvin scale, 'n_e' is the number of protons consumed (negative sign) or produced (positive sign) during the reaction and 'n' the number of electrons for the reduction. For the previous reaction (5) this leads to:

$$\Delta G_{m,4} = -\ 154.4\ -\ 2 \times 8.31451 \times 10^{-3} \times 298.15 \times \ln 10^{(7-4)} = -188.6\ kJ/mol;$$

$$E_{m,4} = 978\ mV$$

$$\tfrac{1}{2}\ O_2 + 2\ e^- + 2\ H_P^+ \rightarrow H_2O \qquad E_{m,7} = 978\ mV,\ P_{O2} = 0.21\ atm \qquad (6)$$

Therefore, equation (6) accounts for the first half oxidoreductive couple with $E_{m,4}$ = 978 mV ($\Delta G_{m,4}$ = -188.6 kJ/mol) at P_{O2} = 0.21 atm. The second half reaction is described as follows.

The water-splitting component contains four manganese atoms. Subsequently, four sequential events are required to abstract four electrons from two molecules of water to yield O_2 (Renger and Wydrzynski, 1991). Finally, four protons (H_P^+) are released into the lumen (P-phase) due to the electron transfer. Hence, from one molecule of water, two protons will be produced consuming two quanta of photons at 680 nm. The total oxido-reductive scheme is given as follows:

$$P^+_{680} + e^- \rightarrow P_{680} \qquad E_{m,4} = 1\ 300\ mV$$

$$\tfrac{1}{2}\ O_2 + 2\ e^- + 2\ H_p^+ \rightarrow H_2O \qquad E_{m,4} = 978\ mV$$

As the first equation is more electropositive, it works in the reduction way while the second one works in oxidation. The stoichiometric ratios are determined by eliminating the number of electrons. The resulting equation is:

$$2\ P^{+}_{680} + H_2O \rightarrow 2\ P_{680} + 2\ H_P^{+} + ½\ O_2 \quad (7)$$

The value of free energy variation is:

$$\Delta G_{m,7} = - 2 \times 96.484 \times (1.3 - 0.8) = - 96.5 \text{ kJ/mol}$$

$$\Delta G_{m,4} = -2 \times 125.4 - (-188.6) = - 62.2 \text{ kJ/mol}$$

When totalising with light quanta uptake (equation 4), we eliminate P^{+}_{680}/P_{680} couple and then we obtain:

$$2\ h\nu_{680}: H_2O \rightarrow 2\ H_P^{+} + ½\ O_2 + 2e^{-} \quad (8)$$

$$\Delta G_{m,4} = - 2 \times 50.5 - 62.2 = -163.2 \text{ kJ/mol}$$

Therefore, the split of H_2O uses two quanta of light; equation (8) means that water reduction releases ½ O_2, two protons in lumen (H_P^{+}) and two electrons in the thylakoid membrane at a very low potential (- 163.2 / 2 F = - 850 mV). The two electrons follow the well-known Z-scheme as represented in Figure 3.3.

According to Figure 3.3, the electrons flow through a direct pathway via different steps inside the membrane. On excitation, either by the absorption of a photon or exciton transfer, P_{680}* rapidly transfers an electron to a nearby pheophytin *a* ($E_{m,7}$ = - 610 mV). The electron is then transferred to a tightly bound plastoquinone (PQ) at the Q_A site ($E_{m,7}$ = -150 mV) on the stroma side (N-phase) of the membrane. The electron is then transferred to an exchangeable plastoquinone located at the Q_B site (near P- phase) ($E_{m,7}$ = 100 mV, Nobel, 2009). Q_A and Q_B sites are similar to Q_P and Q_N sites of mitochondria which will be discussed later in paragraph 3.4.3.

The arrival of a second electron to the Q_B site with the uptake of two protons from the stroma produces plastoquinol, PQH_2. These different steps are characterised by the following oxido-reductive steps:

$$PQ + 2\ e^{-} + 2\ H^{+} \rightarrow PQH_2 \qquad E_{m,7} = 0 \text{ mV}, \quad \Delta G_{m,7} = 0$$

When this reaction involves protons from the stroma side of the membrane (pH = 7.5), we obtain:

$$\Delta G_{m,7.5} = \Delta G_{m,7} - 2\ RT \ln 10^{(7 - 7.5)}$$

$$= 0 - 2 \times 8.31451 \times 10^{-3} \times 298.15 \times \ln 10^{-0.5} = 5.7 \text{ kJ/mol}$$

$$E_{m,7.5} = - \Delta G_{m,4} / nF = 5.7/(2 \times 96.484) = - 30 \text{ mV}$$

Previous equation is therefore:

$$PQ + 2\ e^{-} + 2\ H_N^{+} \rightarrow PQH_2 \qquad E_{m,7.5} = -30 \text{ mV}, \ \Delta G_{m,7.5} = 5.7 \text{ kJ/mol} \quad (9)$$

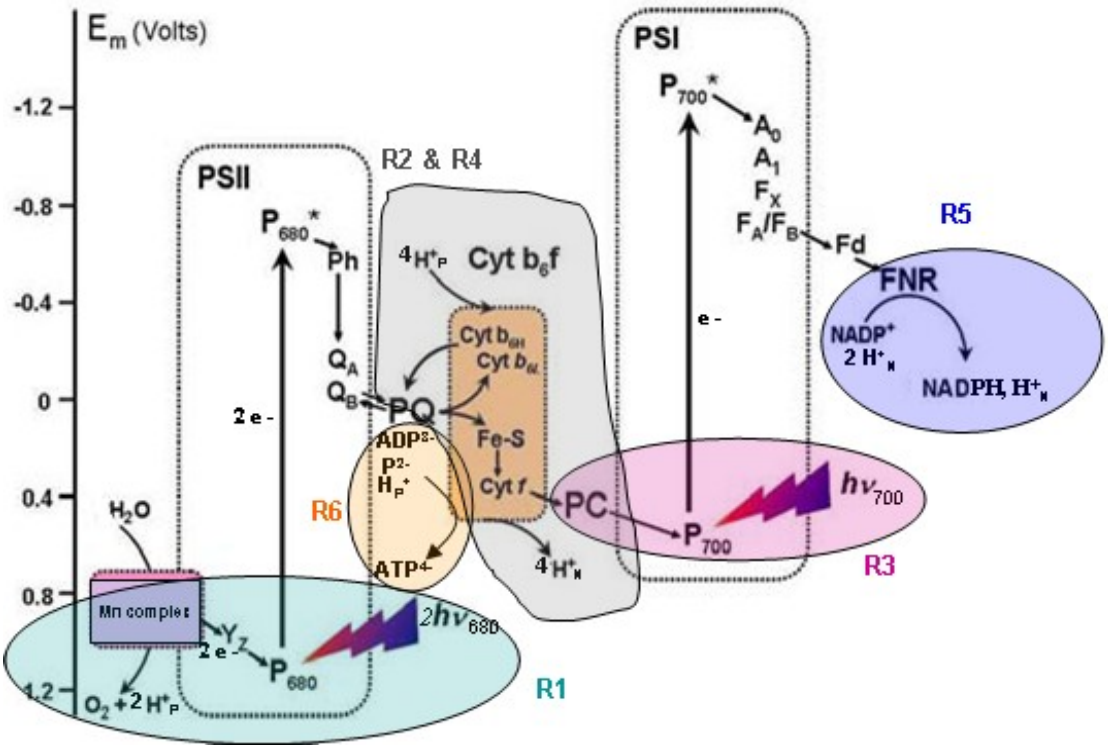

Figure 3.20: Z-scheme of photosynthesis Photosynthetic electron flow from H_2O to $NADP^+$. The relative redox potentials show that P_{680} and P_{700} are highly oxidising. Their excited forms (P_{680}* and P_{700}*) of the reaction centre pigments are highly reducing and located in the upper part of the diagram. Electrons are transferred from water, through Y_Z to reduce P_{680} $\bullet^+$. Further, P_{700} $\bullet^+$ is reduced by electrons from PSII, transferred via plastoquinol, through Cyt b6f complex and plastocyanin (PC). (Picture is adapted from Feyziyev, 2010).

No. Of Eqn	Metabolic steps:	$\Delta G_{m,7}$ (kJ/mol)	ΔG_{physio} (kJ/mol)	$E_{m,7}$ (mV)	$E_{m,4}$ (mV)	$E_{m,7.5}$ (mV)
1	$P_{680}^+ + e^- \rightarrow P_{680}$	-125.4	-125.4	1 300	1 300	
3	$h\nu_{680}$	175.9	175.9			
4	$h\nu_{680}$: $P_{680} \rightarrow P^+_{680} + e^-$	-50.5	-50.5			
5	$½ O_2 + 2 e^- + 2 H_P^+ \rightarrow H_2O$	-154.4	-188.6	800	978	
7	$2 P^+_{680} + H_2O \rightarrow 2 P_{680} + 2 H_P^+ + ½ O_2$	-96.5	-62.2			
8	2 $h\nu_{680}$: $H_2O \rightarrow 2 H_P^+ + ½ O_2 + 2e^-$		-163.2			
9	$PQ + 2 e^- + 2 H_N^+ \rightarrow PQH_2$	0	5.7	0		- 30
10	***Global:*** 2 $h\nu_{680}$: $H_2O + 2 H_N^+ + PQ \rightarrow PQH_2 + ½ O_2 + 2 H_P^+$		-157.5			

Table 3.8: Metabolic steps involved in photosystem II and plastoquinol pool of chloroplast thylakoids at physiological conditions pHN = 7.5 and pHP = 4

At least four electrons must be transferred to two molecules of plastoquinone in order to oxidise H_2O to molecular oxygen, O_2. Note that, here we used only two electrons. For every two electrons harvested from H_2O, one molecule of PQH_2 is formed extracting two protons from the stroma.

The two protons formed during the oxidation of water are released into the thylakoid lumen.

Adding (8) and (9) we obtain,

$$2\ h\nu_{680}: H_2O + 2\ H_N^+ + PQ \rightarrow PQH_2 + ½\ O_2 + 2\ H_P^+ \quad (10)$$

Free energy change is therefore possible at P-phase ($pH_P = 4$, $pH_N = 7.5$),

$$\Delta G_{physio} = -163.2 + 5.7 = -157.5\ kJ/mol$$

As the water oxidation happens at P-phase, the energy contributed by photosystem II at actual condition is -157.5 kJ/mol. The energy is sufficiently high so that the reaction occurs positively irreversible. For the oxidation of one water molecule, two protons from N-phase are translocated to the P-phase. Table 3.1 depicts all the necessary metabolic steps involved and the available free energy at different pH levels related to the photosystem II of chloroplast thylakoids.

At this step, we can summarise that PS II has splitted water molecule; it has translocated the proton, H^+ from N to P-phase and produced plastoquinol from plastoquinone. The next step concerns the recycling of plastoquinol.

3.2.3 Cytochrome *b6f* and plastocyanin

The cytochrome b_6f complex transfers electrons between two mobile redox carriers, plastoquinol (PQH_2) and a copper protein of the thylakoid lumen, plastocyanin (PC) while pumping two protons from the stroma into the thylakoid lumen. This complex is responsible for cyclic and non cyclic electron transfer through electron transport chain.

Continuing the reaction sequence, equation (9) is repeated;

$$PQ + 2\ e^- + 2\ H^+ \rightarrow PQH_2 \qquad E_{m,7} = 0\ mV;\ \Delta G_{m,7} = 0$$

There is a series of reactions associated with cytochrome *b6f* complex called Q-cycle analogous to mitochondrial Complex III, which will be described later. However, the net result is the uptake of two protons from the stroma side of the thylakoid membrane releasing four protons into the lumen. This is like adding two oxido-reductive couples of the same reaction, one occurring at N- phase (stroma equation 9) and one occurring at P-phase (lumen following equation 11):

On stroma side, we have:

$$PQ + 2\ e^- + 2\ H_N^+ \rightarrow PQH_2 \qquad E_{m,7.5} = -30\ mV,\ \Delta G_{m,7.5} = 5.7\ kJ/mol \qquad (9)$$

On lumen side, we have:

$$\Delta G_{m,4} = \Delta G_{m,7} - 2\ RT \ln 10^{(7-4)}$$

$$= 0 - 2 \times 8.31451 \times 10^{-3} \times 298.15 \times \ln 10^3 = -34.2\ kJ/mol$$

$$E_{m,4} = -\Delta G_{m,4} / n F = 34.2/(2 \times 96.484) = 177\ mV$$

So that:

$$PQ + 2\ e^- + 2\ H_P^+ \rightarrow PQH_2 \qquad E_{m,4} = 177\ mV,\ \Delta G_{m,4} = -34.2\ kJ/mol \qquad (11)$$

In fact, the previous reaction is not sufficiently electropositive to react with plastocyanin (see eqn. 13, $E_{m,7}$ = 370 mV). The cytochrome b_6f complex increases the potential by facilitating the transfer of two protons from N-phase to P-phase so that we have:

$$2\ H_P^+ \rightarrow 2\ H_N^+$$

$$\Delta G_{physio} = 2\ R\ T \ln 10^{(7-7.5-7+4)} = -2\ R\ T\ (7.5-4) \ln 10 = -40.0\ kJ/mol$$

By adding with equation 11, we obtain the following couple:

$$PQ + 2\ e^- + 4\ H_P^+ \rightarrow PQH_2 + 2\ H_N^+ \qquad (12)$$

$$\Delta G_{physio} = -34.2 + 2\ RT \ln 10^{(4-7.5)} = -74.2\ kJ/mol\ ;\ E_{m,\Delta pH} = 384\ mV$$

The redox potential of plastocyanin is higher than the normal half reaction of Cu^{2+}/Cu^+ ($E_{m,7}$ = 158 mV (Anderson *et al*., 1987)). The midpoint potential of plastocyanin is:

$$2\ Pc\ (Cu^{2+}) + 2\ e^- \rightarrow 2\ Pc\ (Cu^+) \qquad E_{m,7} = 370\ mV\ ,\ \Delta G_{m,7} = -71.4\ kJ/mol \qquad (13)$$

Combining the couples (12) and (13), in the way (12) - (13), we obtain:

$$PQH_2 + 2\ Pc\ (Cu^{2+}) + 2\ H_N^+ \rightarrow PQ + 2\ Pc\ (Cu^+) + 4\ H_P^+ \qquad (14)$$

$$\Delta G_{physio} = -74.2 - (-71.4) = -2.8\ kJ/mol$$

This process releases four protons to P-phase taking two protons from N-phase contributing to the electrochemical gradient (Figure 3.4). It must be noticed that this reaction proceeds at conditions close to equilibrium conditions. Conversely, the pH difference between lumen and stroma can be calculated at equilibrium, i.e. when $\Delta G \sim 0$.

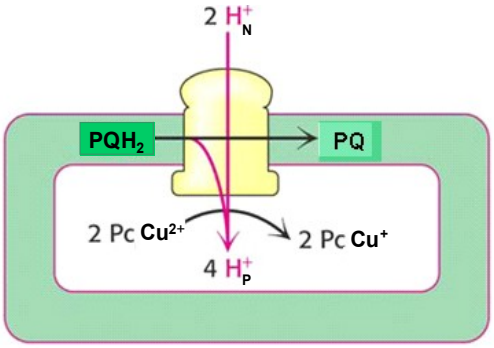

Figure 3.21 : Proton movement at Complex II

So,

$$-71.4 = -34.2 - 2\ RT \ln 10\ \Delta pH$$

$$\Delta pH = (71.4 - 34.2)/ 2\ RT \ln 10 = 3.25$$

It may be concluded that Q-cycle constituted of PQ and PQH_2 controls and maintains the H^+ balance near equilibrium. A similar mechanism will be explained in paragraph 3.4.3.

As the reaction proceeds at near equilibrium conditions, the reaction must be considered as reversible. Furthermore, it does not contribute energy for the electron transport. These values are summarised in Table 3.2.

Eqn	Metabolic steps involved:	$\Delta G_{m,7}$ (kJ/mol)	$\Delta G_{m,7.5}$ (kJ/mol)	$\Delta G_{m,4}$ (kJ/mol)	$E_{m,4}$ (mV)	$E_{m,7}$ (mV)
9	$PQ + 2\ e^- + 2\ H_N^+ \rightarrow PQH_2$	0	5.7			0
11	$PQ + 2\ e^- + 2\ H_P^+ \rightarrow PQH_2$			- 34.2	177	
12	$PQ + 2\ e^- + 4\ H_P^+ \rightarrow PQH_2 + 2\ H_N^+$	-74.2*				384*
13	$2\ Pc\ (Cu^{2+}) + 2\ e^- \rightarrow 2\ Pc\ (Cu^+)$	-71.4				370
14	***Global:*** $PQH_2 + 2\ Pc\ (Cu^{2+}) + 2\ H_N^+ \rightarrow PQ + 2\ Pc\ (Cu^+) + 4\ H_P^+$	-2.8*				

Table 3.9: Metabolic steps involved in plastoquinol and plastocyanin of chloroplast thylakoids. Values with * stands for physiological conditions $pH_N = 7.5$; $pH_P = 4$.

3.2.4 Photosystem I

Photosystem I is composed of a modified 'chlorophyll a' that absorbs light at a wavelength of 700 nm and transfers electrons to the next complex, ferredoxin NADP reductase. The concentration of P_{700} is small, only 0.25% of the total amount of chlorophyll in plants (Garrett and Grisham, 2000). The core of PS I contains about 40 molecules of chlorophyll a, several molecules of beta carotene, lipids, calcium, chlorine, four manganese, one iron, two molecules of plastoquinone, two molecules of pheophytin and a colorless form of chlorophyll a.

Absorbing one quantum of light, P_{700} ($E_{m,7}$ = 450 mV) is transformed into the strongest biological reducing agent known, P_{700}^+.

$$h\nu_{700}: P_{700} \rightarrow P_{700}^+ + e^- \qquad (15)$$

Free energy available for one quanta of photon at 700 nm (Berg *et al*., 2002) is calculated same as we have done for photosystem II.

$$h\nu_{700} = 170.9\ kJ/mol$$

P_{700}^+ is highly unstable and rapidly absorbs an electron. It could be said that at P-phase of the membrane, it appears to be a direct electron transfer from plastocyanin in order to recover P_{700}.

$$P_{700}^+ + e^- \rightarrow P_{700} \qquad E_{m,7} = 450 \text{ mV} \ , \Delta G_{m,7} = -43.4 \text{ kJ/mol} \qquad (16)$$

Taking the energy of photon, the energy for the first step in photosystem I is calculated:

$$\Delta G_{m,7} = -170.9 + 43.4 = -127.5 \text{ kJ/mol}$$

I.e. the available energy for the formation of P_{700}^+ by $h\nu_{700}$ is -127.5 kJ/mol:

$$h\nu_{700}: \ P_{700} \rightarrow P_{700}^+ + e^- \qquad E_{m,7} = 1\,320 \text{ mV}, \Delta G_{m,7} = -127.5 \text{ kJ/mol} \qquad (15)$$

The reduction of plastocyanin is then considered for reducing P_{700}^+ (eqn. 16),

$$Pc\ (Cu^{2+}) + e^- \rightarrow Pc\ (Cu^+) \qquad E_{m,7} = 370 \text{ mV} \ , \Delta G_{m,7} = -35.7 \text{ kJ/mol} \qquad (17)$$

The reduced plastocyanin, Pc (Cu^+) diffuses through the lumen and P_{700}^+ readily gains an electron coming from plastocyanin at lumen (P-phase) and reforms P_{700}.

Eqns. (16) + (17),

$$P_{700}^+ + Pc\ (Cu^+) \rightarrow Pc\ (Cu^{2+}) + P_{700} \qquad \Delta G_{m,7} = -7.7 \text{ kJ/mol} \qquad (18)$$

Combining eqns. (15) and (18):

$$h\nu_{700}: \ Pc\ (Cu^+) \rightarrow Pc\ (Cu^{2+}) + e^- \qquad \Delta G_{m,7} = -7.7 + -127.5 = -135.2 \text{ kJ/mol}$$

The electron liberated by the oxidation of P_{700} arrives on a chlorophyll molecule. Then, it passes to a phylloquinone (vitamin K1) and ultimately reaches a Fe-S centre, which serves as the electron donor to reduce the iron-sulphur ferredoxin in the stroma (N-phase).

$$Fd_{ox} + e^- \rightarrow Fd_{red} \qquad E_{m,7} = -450 \text{ mV}; \ \Delta G_{m,7} = 43.4 \text{ kJ/mol} \qquad (19)$$

Eqns. (19) + (17),

$$Pc\ (Cu^+) + Fd_{ox} \rightarrow Fd_{red} + Pc\ (Cu^{2+}) \qquad \Delta G_{m,7} = -79.1 \text{ kJ/mol} \qquad (20)$$

Finally when the eqn. resulted from (15) and (18) combines with (19),

$$h\nu_{700}: \ Pc\ (Cu^+) + Fd_{ox} \rightarrow Pc\ (Cu^{2+}) + Fd_{red} \qquad (21)$$

$$\Delta G_{m,7} = -135.2 + 43.4 = -91.9 \text{ kJ/mol}$$

Therefore, plastoquinone in PS I is reduced by ferredoxin. Ferredoxin is then re-oxidized via Q-cycle. One proposal is that there exists a ferredoxin plastoquinone-reductase or an NADP dehydrogenase (Joliot P. and Joliot A., 2002). It is found that the classical Q-cycle reaction mechanisms must be altered in the *b6f* complex and it has been proposed that a cyclic photophosphorylation follows (Cramer *et al*., 2005, 2006).

Combining eqns. (11) and (19):

$$PQ + 2\ e^- + 2\ H_P^+ \rightarrow PQH_2 \qquad E_{m,4} = 177\ mV;\quad \Delta G_{m,4} = -34.2\ kJ/mol \qquad (11)$$

$$Fd_{ox} + e^- \rightarrow Fd_{red} \qquad E_{m,7} = -450\ mV;\ \Delta G_{m,7} = 43.4\ kJ/mol \qquad (19)$$

So that:

$$2\ Fd_{red} + PQ + 2\ H_P^+ \rightarrow 2\ Fd_{ox} + PQH_2 \qquad \Delta G_{m,4} = -121.0\ kJ/mol \qquad (22)$$

This energy can be considered as the exact energy available for the Eqn. (22). This metabolic step is highly important in cyclic photophosphorylation. The summary of the metabolic reactions and energy are listed in Table 3.3.

Eqn	Metabolic equations	$\Delta G_{m,7}$ (kJ/mol)	$\Delta G_{m,4}$ (kJ/mol)	$E_{m,4}$ (mV)	$E_{m,7}$ (mV)
	$h\nu_{700}$	- 170.9			
15	$h\nu_{700}$: $P_{700} \rightarrow P_{700}^+ + e^-$	- 127.5			1 320
16	$P_{700}^+ + e^- \rightarrow P_{700}$	- 43.4			450
17	$Pc\ (Cu^{2+}) + e^- \rightarrow Pc\ (Cu^+)$	- 35.7			370
18	$P_{700}^+ + Pc\ (Cu^+) \rightarrow Pc\ (Cu^{2+}) + P_{700}$	- 7.7			
19	$Fd_{ox} + e- \rightarrow Fd_{red}$	43.4			-450
20	$Pc\ (Cu^+) + Fd_{ox} \rightarrow Fd_{red} + Pc\ (Cu^{2+})$	- 79.1			820
21	***Global:*** $h\nu_{700}$: $Pc\ (Cu^+) + Fd_{ox} \rightarrow Pc\ (Cu^{2+}) + Fd_{red}$	- 91.9*			
22	***Global:*** $2\ Fd_{red} + PQ + 2\ H_P^+ \rightarrow 2\ Fd_{ox} + PQH_2$	- 86.8	-121*	627	

Table 3.10 : Metabolic steps involved in photosystem I and plastocyanin of chloroplast thylakoids. Values with * stands for physiological conditions $pH_N = 7.5$; $pH_P = 4$.

3.2.5 Ferredoxin NADP reductase

Ferredoxin serves as a strong reductant; $NADP^+$ can accept two electrons in the form of a hydride. The mechanism proposed considers that this complex contains a tightly bound FAD which accepts the electrons one at a time from ferredoxin (Garrett and Grisham, 2000). The $FADH_2$ then transfers a hydride to $NADP^+$ to form NADPH, H_N^+. The mechanism is described as follows:

$$FAD + Fd_{red} + H_N^+ \rightarrow FADH^{\cdot} + Fd_{ox}$$

$$FADH^{\cdot} + Fd_{red} + H_N^+ \rightarrow Fd_{ox} + FADH_2$$

$$\underline{FADH_2 + NADP^+ \rightarrow FAD + NADPH,\ H_N^+}$$

$$2\ Fd_{red} + 2\ H_N^+ + NADP^+ \rightarrow 2\ Fd_{ox} + NADPH,\ H_N^+$$

The reaction takes place at the N-phase of the thylakoid membrane. The uptake of a proton by $NADP^+$ further contributes to the pH gradient across the thylakoid membrane. In terms of oxido-reductive mechanism, this can be written as follows:

$$2\ H_N^+ + 2\ e^- + NADP^+ \rightarrow NADPH, H_N^+ \quad E_{m,7} = -320\ mV;\ \Delta G_{m,7} = 61.7\ kJ/mol \qquad (23)$$

$$Fd_{ox} + e^- \rightarrow Fd_{red} \qquad E_{m,7} = -450\ mV;\ \Delta G_{m,7} = 43.4\ kJ/mol \qquad (19)$$

Eqns. (23) - 2 × (19),

$$2\ Fd_{red} + 2\ H_N^+ + NADP^+ \rightarrow 2\ Fd_{ox} + NADPH, H_N^+ \qquad (24)$$

$$\Delta G_{m,7} = -2 \times 43.4 + 61.7 = -25.1\ kJ/mol$$

$$\Delta G_{m,7.5} = -25.1 - 2\ RT \ln 10^{(7-7.5)} = -19.4\ kJ/mol$$

This energy is relatively small with the previously discussed complex. However, the reaction occurs in forward direction contributing to electrochemical gradient and ATP production. The important metabolic steps involved with this complex are given in the Table 3.4.

Eqn	Metabolic equations	$\Delta G_{m,7}$ (kJ/mol)	$\Delta G_{m,7.5}$ (kJ/mol)	$E_{m,7}$ (kJ/mol)	$E_{m,7.5}$ (kJ/mol)
19	$Fd_{ox} + e^- \rightarrow Fd_{red}$	43.4		- 450	
23	$2\ H_N^+ + 2e^- + NADP^+ \rightarrow NADPH, H_N^+$	61.7		- 320	
24	***Global:*** $2\ Fd_{red} + 2\ H_N^+ + NADP^+ \rightarrow 2\ Fd_{ox} + NADPH, H_N^+$	-25.1	-19.4*		100*

Table 3.11: Metabolic steps involved in ferredoxin NADP reductase of chloroplast thylakoids. Values with * stands for physiological conditions pHN = 7.5; pHP = 4

3.2.6 ATP synthase

The light-induced electron transport starts from PS II, and ends at CF_1CF_O ATP synthase, the enzyme for chloroplast ATP production. ATP synthase is located accessing a source of Pi^{2-} and ADP^{3-}. The proton motive force generated across the thylakoid membrane is used for the proton flow through the proton channel causing the rotation of ATP synthase and ATP production.

12 protons are taken through the proton channel for the complete rotation of ATP synthase followed by the release of 3-4 ATP, which means 3-4 protons per ATP is in need (Van Walraven *et al*., 1996; Yoshida *et al*., 2001). The mechanism is schemed in Figure 3.5.

ATP synthesis from ADP is energetically uphill without the driving force of electron potential gradient across the thylakoid membrane. The free energy available for ATP formation is known at standard conditions;

$$H_N^+ + ADP^{3-} + Pi^{2-} \rightarrow ATP^{4-} + H_2O \qquad \Delta G_{m,7} = 32.5 \text{ kJ/mol}; [Mg^{2+}] = 10^{-3} \qquad (25)$$

As ATP is produced at the N- phase,

$$\Delta G_{m,7.5} = 32.5 - RT \ln 10^{(7-7.5)} = 35.4 \text{ kJ/mol}$$

The free energy change for a pH gradient of 3.5 units for the proton movement (proton motive force of 200 mV) across the thylakoid membrane corresponds to -20 kJ/mol (Int. ref.4; Berg *et al*., 2002).

$$H_P^+ \rightarrow H_N^+ \qquad \Delta G_{physio} = RT \ln 10^{(4-7.5)} = -20 \text{ kJ/mol}$$

The light induced pH gradient is about 3.5 pH units. The transmembrane electrical potential ($\Delta\Psi$) is not a significant factor in the proton motive force of chloroplasts; because, the thylakoid membrane is permeable to chloride (Cl^-) and magnesium (Mg^{2+}) ions. Because of this permeability, the thylakoid lumen remains electrically neutral while the pH gradient is generated. The proton motive force across the thylakoid membrane is 200 mV, which drives ATP synthesis, nearly all of it is contributed by the pH gradient rather than the membrane potential. Considering that 3 protons are involved in both N and P- phases, the available free energy for the ATP production (26),

$$3\,H^+_P + H_N^+ + ADP^{3-} + Pi^{2-} \rightarrow 3\,H_N^+ + ATP^{4-} + H_2O \qquad (26)$$

$$\Delta G_{,physio} = -3 \times 20 + 35.4 = -24.5 \text{ kJ/mol}$$

Hence, it is concluded that without the proton movement across the thylakoid membrane ATP production is thermodynamically impossible. $\Delta G_{m,7.5}$ is negative, only when three protons from both N and P-phases are utilized (Table 3.5). The pH gradient between N and P-phases control and maintains the ATP release.

3.2.7 Equations for light reactions

From the studied photosynthetic complexes of light reactions, the six stoichiometric equations 10, 14, 21, 22, 24 and 26 (Table 3.6) summaries the steps of light energy conversion to chemical energy; this forms a small metabolic network of 16 metabolites. The metabolites are separated as exchangeables (outputs and inputs) and nonexchangeables (intermediates) according to the system-boundary concept (Figure 3.6).

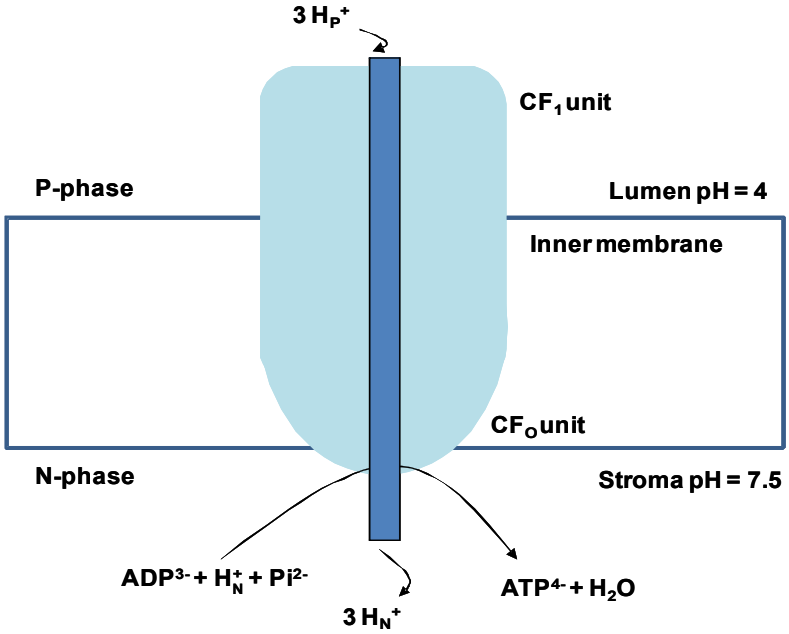

Figure 3.22: ATP synthesis in chloroplasts The CF1-part sticks into stroma, where dark reactions of photosynthesis (Calvin cycle) take place. The CF_O subunit spans the photosynthetic membrane and forms a proton channel through the membrane. CF_1 is composed of several different protein subunits. The top portion of the CF_1 subunit is composed of three ab-dimers that contain the catalytic sites for ATP synthesis.

Eqn	Metabolic equations	$\Delta G_{m,7}$ (kJ/mol)	ΔG_{physio} (kJ/mol)
25	$H_N^+ + ADP^{3-} + Pi^{2-} \rightarrow ATP^{4-} + H_2O$	32.5	35.4
26	***Global:*** $3\ H^+_P + H_N^+ + ADP^{3-} + Pi^{2-} \rightarrow 3\ H_N^+ + ATP^{4-} + H_2O$		- 24.5*

Table 3.12: Metabolic steps involved in chloroplast ATP synthase Values with * stands for physiological conditions pHN = 7.5; pHP = 4

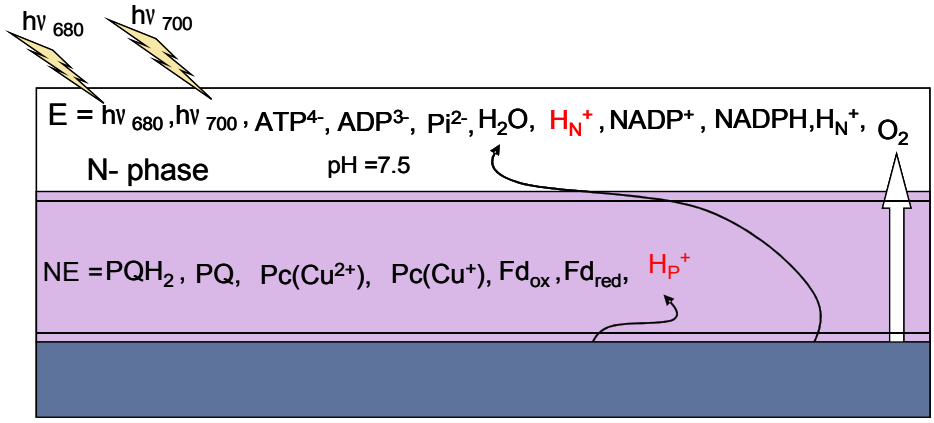

Figure 3.23: Separation of metabolites into non exchangeables and exchangeables for light reactions

In order to examine the topology of the two photosystems, the P-phase is supposed to be a closed one, while N-phase is an open system; N-phase contains a sequence of metabolisms (e.g. Calvin cycle, starch metabolism, lamellar protein synthesis etc (Garrett and Grisham, 2000). However, the energy molecules that are necessary to carry out those reactions produced directly into the N-phase so that the reactions can run at once the energy is available. The membrane which separate P and N-phases is assumed as an unchanged one; the oxygen molecule (O_2) formed at P-phase is diffused into the outside (exterior) of the system; the light energy of wave lengths 700 nm and 680 nm, photon 'hν' ($h\nu_{700}$ and $h\nu_{680}$), water (H_2O) and carbon dioxide (CO_2) are considered as inputs where the energy molecules like ATP^{4-} and NADPH H_N^+ are the outputs; ADP^{3-}, Pi^{2-} and $NADP^+$ are associated with the energy outputs. Hence, they are also considered together with the exchangeable group.

The molecules such as PQ, PQH_2, Pc (Cu^{2+}), Pc (Cu^+), Fd_{ox}, Fd_{red}, H_P^+, etc. are act as the intermediates for the production of outputs. The proton produced at N-phase, H_N^+ must be taken as output as it is related to the reduced molecule (NADPH, H_N^+) and the formation of ATP. However, H_P^+ is taken as an intermediate. During the ATP formation, three H_P^+ are used to rotate the ATP synthase at P-phase (as input) and three H_N^+ are produced at N-phase (as output) as in the Figure 3.5. Hence, we have 9 exchangeables and 7 nonexchangeables. Furthermore, exchangeables can be one of the three types: (1) the one producing and consuming within the system which also appear as a part of output or input indicated as 'E='; (2) output 'E+'; (3) input 'E-'. In this case, water being consumed and produced, it is an exchangeable, 'E='.

The metabolic equations for light reactions are listed and the stoichiometric matrix has been constructed as in Table 3.7. In the matrix representation, the reversible reactions are indicated with the number, '0' where irreversible reactions are '1'.

Reactions	Eqn	Protein complex involved	Metabolic equations	$\Delta G_{m,7}$ (kJ/mol)	$\Delta G_{m,7.5}$ (kJ/mol)	$\Delta G_{m,4}$ (kJ/mol)
R1	10	Photosystem II	2 $h\nu_{680}$: H_2O + 2 H_N^++ PQ → PQH_2 + ½ O_2 + 2 H_P^+		- 157.5*	
R2	14	Cytochrome b6f plastocyanin *non cyclic*	PQH_2 + 2 Pc (Cu^{2+}) + 2 H_N^+ ↔ PQ + 2 Pc (Cu^+) + 4 H_P^+	- 2.8	- 2.8*	
R3	21	Photosystem I	1 $h\nu_{700}$: Pc (Cu^+) + Fd_{ox} → Pc (Cu^{2+}) + Fd_{red}	- 91.9*		
R4	22	Cytochrome b6f Plastocyanin *cyclic*	PQ + 2 Fd_{red} + 2 H_P^+ → PQH_2 + 2 Fd_{ox}	- 86.8		- 121*
R5	24	Ferredoxin NADP reductase	2 Fd_{red} + 2 H_N^+ + $NADP^+$→ 2 Fd_{ox} + $NADPH,H_N^+$	- 25.1	-19.4*	
R6	26	ATP synthase	3 H_P^+ + H_N^+ + ADP^{3-} + Pi^{2-} → 3 H_N^+ + ATP^{4-} + H_2O		- 24.5*	

Table 3.13: Equations for light reactions. Values with * stands for physiological conditions $pH_N = 7.5$; $pH_P = 4$

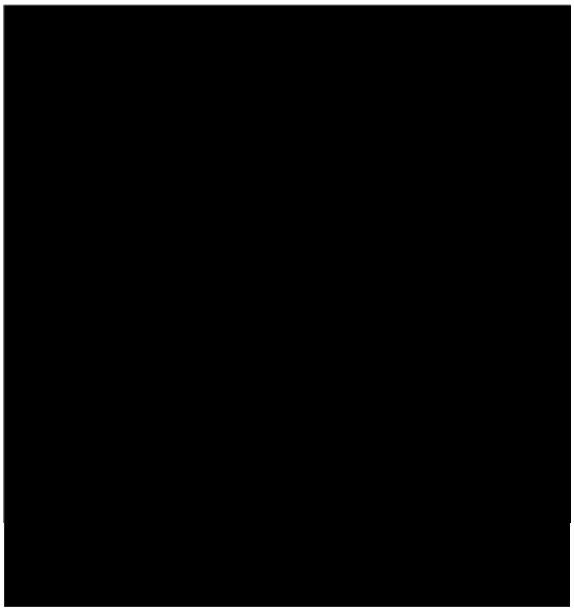

Table 3.14: Metabolic matrix for light reactions Exchangeables (E): $h\nu_{700}$, $h\nu_{680}$, O_2, H_2O, $NADP^+$, $NADPH,H_N^+$, ATP^{4-}, ADP^{3-}, Pi^{2-}, H_N^+; Non exchangeables, (NE): H_P^+, Fd_{red}, Fd_{ox}, Pc (Cu^+), Pc (Cu^{2+}), PQH_2, PQ. Abbreviations : $h\nu_{700}$ and $h\nu_{680}$ = photons at 700 nm and 680 nm respectively; O_2 = oxygen; H_2O = **water;** $NADPH,H_N^+$ = nicotinamide adenine dinucleotide phosphate ; $NADP^+$ = reduced nicotinamide adenine dinucleotide phosphate; ATP^{4-} = adenosine triphosphate; ADP^{3-} = adenosine diphosphate, energy molecule; Pi^{2-} = inorganic phosphate; **HN^+ and H_P^+** = protonated hydrogen at N and P phases; Fd_{red} = reduced ferredoxin; Fd_{ox} = oxidised ferredoxin; Pc (Cu^+) = reduced plastocyanin; Pc (Cu^{2+})= reduced plastocyanin; PQH_2 = plastoquinol; PQ =plastoquinone

3.3 Calvin cycle

The carbon assimilation reactions in plants (and other autotrophs) synthesise carbohydrates from atmospheric CO_2 by reducing at the expense of ATP and NADPH, H^+. This process takes place within the chloroplast stroma. Calvin cycle reactions (also known as dark reactions) are possible even in the absence of light. However, the regulation mechanisms have been described leading to inactivation of Calvin cycle enzymes in the absence of light. The assimilation of CO_2 occurs in three stages: carboxylation, reduction and regeneration. The first stage involves the incorporation of CO_2 and water into five-carbon acceptor: ribulose 1, 5-biphosphate ($RuBP^{4-}$) that is catalyzed by the enzyme ribulose 1, 5-biphosphate carboxylase or rubisco. Rubisco is one of the most crucial enzymes in the production of biomass from CO_2; it accounts almost 50% of the soluble proteins of the chloroplast. In the reduction phase, 3-phosphoglycerate (PGA^{3-}) is converted to glyceraldehyde 3-phosphate ($G3P^{2-}$). The regeneration phase contains a series of reactions that regenerate $RuBP^{4-}$ from $G3P^{2-}$.

Such experimentally determined metabolic reactions and metabolites of plant Calvin cycle are adapted from MetaCyc Encyclopedia of Metabolic Pathways (Table 3.8). In reality, only thirteen steps are involved in the Calvin cycle (R1 to R13). Anyhow, the steps R14 and R15 are necessary in order to produce one molecule of glucose, as glucose is necessarily produced in the chloroplast. Table 3.8 provides the standard free energies for reactions at standard conditions ($\Delta G_{m,7}$) and for physiological conditions (ΔG_{physio}).

The equation for calculating free energy,

$$\Delta G_{physio} = \Delta G_{m,7} + RT \ln \frac{products}{substrates}$$

Though $\Delta G_{m,7}$ is positive for a reaction, the cellular concentration of substrates and products are maintained in such a way that the actual free energy, ΔG_{physio} becomes negative (e.g. R2 of Table 3.8). Cells often drive a thermodynamically unfavourable reaction (where $\Delta G_{m,7}$ is positive) in the forward direction by coupling it to a highly exergonic reaction through a common intermediate. The metabolic matrix representing the Calvin cycle is given in Table 3.9.

Reaction	Metabolic equations	$\Delta G_{m,7}$ (kJ/mol)	ΔG_{physio} (kJ/mol)
R1	CO_2+ $RuBP^{4-}$ + H_2O → 2 $(PGA)^{3-}$ + 2 H_N^+	- 35.1	- 41
R2	PGA^{3-} + ATP^{4-}↔ $1,3BPGA^{4-}$+ ADP^{3-}	18	-6.7
R3	$1,3BPGA^{4-}$ + $NADPH,H_N^+$ ↔ $G3P^{2-}$ + $NADP^+$ + Pi^{2-}	-6.3	0
R4	$G3P^{2-}$ ↔ $DHAP^{2-}$	-7.5	-0.8
R5	$DHAP^{2-}$ + $G3P^{2-}$ ↔ FBP^{4-}	-23.4	-0.8
R6	FBP^{4-}+ H_2O→ $F6P^{2-}$+ Pi^{2-}	-14.2	-27.2
R7	$F6P^{2-}$+ $G3P^{2-}$ ↔ $E4P^{2-}$ + $Xu5P^{2-}$	6.3	-3.8
R8	$Ru5P^{2-}$ ↔ $Xu5P^{2-}$	0.8	-0.4
R9	$S7P^{2-}$ + $G3P^{2-}$ ↔ $Xu5P^{2-}$+ $R5P^{2-}$	0.4	-5.9
R10	$DHAP^{2-}$+ $E4P^{2-}$ ↔ SBP^{4-}	-21.8	-1.7
R11	SBP^{4-} + H_2O → $S7P^{2-}$+ Pi^{2-}	-14.2	-29.7
R12	$R5P^{2-}$ ↔ $Ru5P^{2-}$	2.1	-0.4
R13	$Ru5P^{2-}$ + ATP $^{4-}$ → $RuBP^{4-}$ + ADP^{3-} + H_N^+	-21.8	-15.9
R14	$F6P^{2-}$ ↔ $G6P^{2-}$	1.7	-2.9
R15	$G6P^{2-}$ + H_2O → Glucose + Pi^{2-}	-13.8	Negative

Table 3.15: Calvin cycle reactions Free energy values for metabolic reactions are taken from Bassham and Buchanan, 1982.

The metabolites are separated into exchangeables and non exchangeables; the input metabolites for the Calvin cycle system are CO_2 and H_2O with only one output glucose; in addition to this, energy molecules are also considered as exchangeables and the rest of the metabolites fall in the category of non exchangeables. As the proton at N-phase, H_N^+ is always associated with the NADPH, H_N^+ and ATP^{4-}, we need to treat it as an exchangeable just as we did in the previous system.

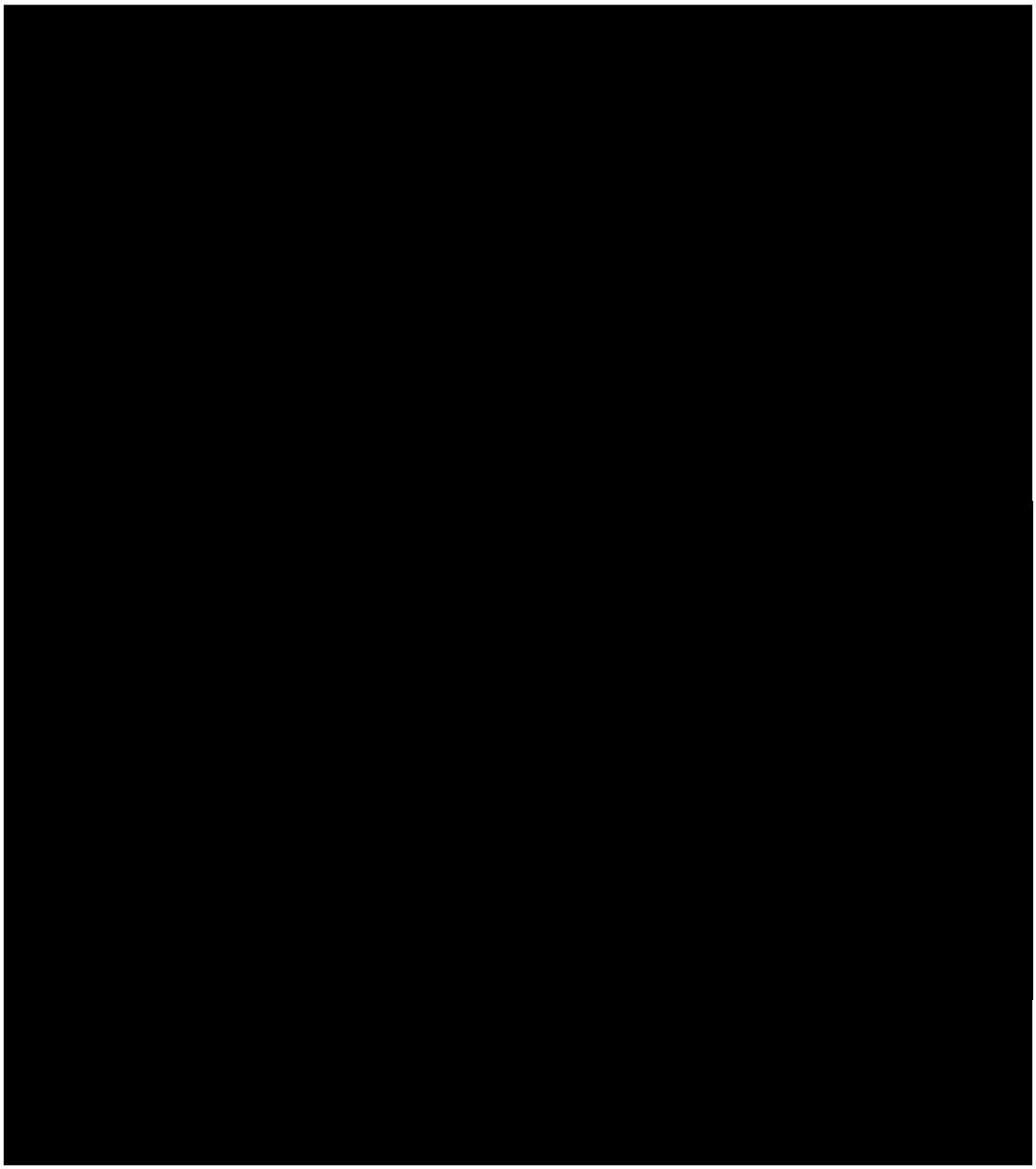

Table 3.16: Metabolic matrix for Calvin cycle reactions Exchangeables (E): H_2O; CO_2; Glucose; H_N^+; $NADP^+$; $NADPH,H_N^+$; ADP^{3-}; Pi^{2-}; $ATP^{4-;}$ Non exchangeables, (NE): PGA^{3-}; $RuBP^{4-}$; $Ru5P^{2-}$; $R5P^{2-}$; 1,3-$BPGA^{4-}$; $G3P^{2-}$; $DHAP^{2-}$; FBP^{4-}; $F6P^{2-}$; $E4P^{2-}$; $Xu5P^{2-}$; $G6P^{2-}$; $S7P^{2-}$ and SBP^{4-} Abbreviations : ADP^{3-} = adenosine diphosphate, energy molecule; ATP^{4-} = adenosine triphosphate; $DHAP^{2-}$ = **dihydroxyacetone phosphate;** 1, 3-$BPGA^{4-}$= **1, 3- diphosphate glycerate;** CO_2 = carbon dioxide ; $E4P^{2-}$ = **erythrose-4-phosphate;** $FADH_2$ = **reduced flavin adenine dinucleotide;** FBP^{4-} = **fructose 1, 6-biphosphate;** $F6P^{2-}$ = **fructose -6-biphosphate;** $G1P^{2-}$ = **glucose -1-phosphate;** $G6P^{2-}$ = **glucose 6-phosphate;** $G3P^{2-}$ = glyceraldehyde -3-phosphate ; H_2O = **water;** $\mathbf{H_N^+}$= protonated hydrogen at N-phase ; $NADPH,H_N^+$ = nicotinamide adenine dinucleotide phosphate ; $NADP^+$ = reduced nicotinamide adenine dinucleotide phosphate; O_2 = oxygen; PGA^{3-} = 3-phosphoglycerate; Pi^{2-} = inorganic phosphate; $RuBP^{4-}$ = **ribulose 1, 5-bisphosphate;** $R5P^{2-}$ = **ribose-5-phosphate;** $Ru5P^{2-}$ = ribulose-5-phosphate; SBP^{4-} = **sedoheptulose 1, 7-biphosphate;** $S7P^{2-}$ = **sedoheptulose-7-biphosphate;** $Xu5P^{2-}$ = **xylulose-5-phosphate**

3.4 Electron transport and oxidative phosphorylation

The metabolic processes associated with the electron transport and oxidative phosphorylation occurs in mitochondria; it fulfils the total cell energy requirements. Structurally, mitochondria are double-membraned organelle with an outer membrane and an inner membrane; between the two is the intermembrane space (Figure 3.7). The outer membrane is made up of large number of proteins called porins. The space enclosed by the inner membrane is called matrix. A large number of proteins named complexes I, II, III, IV and ATP synthase are situated in the inner membrane just like the electron transport chain (ETC) of chloroplast. The matrix contains highly concentrated mixture of enzymes (for the oxidation of pyruvate, fatty acids and the TCA cycle), ribosomes, mRNA, proteins, etc. The mitochondrial membrane also works as a channel for a variety of molecules, (but not all ions) to move in and out.

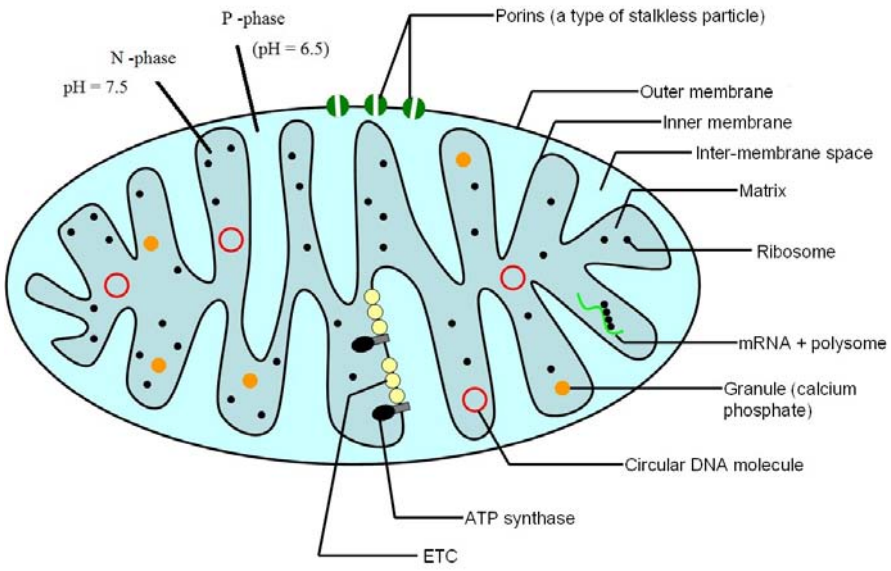

Figure 3.24: Structure of mitochondrion [Int. ref.3]

The proton concentration is less near to the matrix (N-phase) than that in the intermembrane space (P-phase). Principally, it must also be considered that in mitochondrial membrane the major part of the proton motive force is provided by the electrical potential difference between the two faces. It will be considered that the potential difference is 150 mV between the positive and negative phases.

3.4.1 Complex I

Complex I is known as NADH-UQ oxidoreductase. This promotes the transfer of two electrons from NADH to a lipid-soluble carrier called ubiquinone (UQ). The reduced product, ubiquinol (UQH_2) which resembles plastoquinol of thylakoid freely diffuses within the membrane. Complex I translocates four protons (H^+) across the membrane producing a proton gradient. The electrons get transferred as a part of several oxido-reduction reactions: NADH, H^+ is oxidized to NAD^+; then the electron passes through flavin, FMN reducing it to $FMNH_2$ and reach ubiquinone (UQ) via Fe-S clusters, reducing it to ubiquinol (UQH_2) in the matrix phase (Figure 3.8) (Garrett and Grisham, 2000; Nicholls and Ferguson, 1992).

There is a major role of UQ/UQH_2 as a carrier of reducing equivalents in the electron transport chain's I and II complexes towards complex III. The first couple to be considered is NADH, H^+ oxidation and UQ reduction.

$$NAD^+ + 2\ H^+ + 2e^- \rightarrow NADH,\ H^+ \qquad E_{m,7} = -\ 320\ mV;\ \Delta G_{m,7} = 61.7\ kJ/mol \qquad (27)$$

$$UQ + 2\ H^+ + 2e^- \rightarrow UQH_2 \qquad E_{m,7} = 60\ mV\ ;\ \Delta G_{m,7} = -11.6\ kJ/mol \qquad (28)$$

Eqn. (27) proceeds forward, while eqn. (28) proceeds backward. At standard conditions, the redox couple of the above reactions provide a potential difference of 380 mV and $\Delta G_{m,7}$ of -11.6 - 61.7 = - 73.3 kJ/mol. Considering the protons in the intermembrane space as 'H_P^+'(at P-phase) and matrix phase (N-phase) 'H_N^+', the reactions at N- phase for complex I can be written from eqns. (28) + (27) as follows:

$$NADH,H_N^+ + UQ + 2\ H_N^+ \rightarrow NAD^+ + UQH_2 + 2\ H_P^+ \qquad (29)$$

Without considering the proton transport at standard conditions, the energy per electron pair transported by complex I is, $\Delta G_{m,7} = -\ 2 \times 96.484 \times 0.38 = -\ 73.3$ kJ/mol.

However, this reaction takes place at N-phase (pH = 7.5) with a transport of two protons to P-phase (pH = 6.5).

Furthermore, considering the electrical potential difference: $E_P - E_N = \Delta\Psi = 150$ mV, the electrical potential of 150 mV affects the charges on both N and P-phases. It is considered that NAD^+, $NADH,H_N^+$ and H_N^+ are located at N-phase, so that:

$$\Delta G_{physio} = \Delta G_{m,7} + 2\ RT \ln 10^{(7 - pH_P)} - 3\ RT \ln 10^{(7 - pH_N)} + 2\ F\ E_P + F\ E_N - 3\ F\ E_N$$

$$= \Delta G_{m,7} + 2\ RT \ln 10\ [2\ (pH_N - pH_P) + (pH_N - 7)] + 2\ F\ (E_P - E_N)$$

$$= -73.3 + RT \ln 10\ [2\ (7.5 - 6.5) + (7.5 - 7)] + 2\ F\ \Delta\Psi$$

= -73.3 + 14.3 + 28.9 = - 30.1 kJ/mol

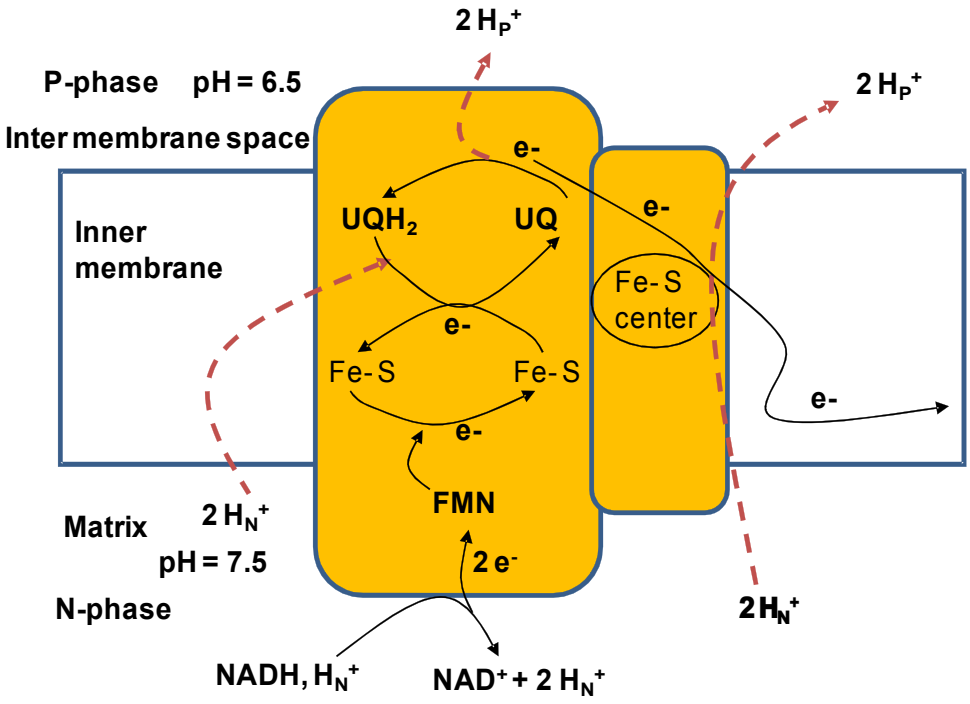

Figure 3.25: Electron transport pathway via Complex I Proton transport takes place from N-phase to P-phase (Adapted from Garrett and Grisham, 2000)

Eqn.	Metabolic equations	$\Delta G_{m,7}$ (kJ/mol)	ΔG_{physio} (kJ/mol)
27	$NAD^+ + 2\ H^+ + 2e^- \rightarrow NADH,\ H^+$	61.7	
28	$UQ + 2\ H^+ + 2e^- \rightarrow UQH_2$	-11.6	
29	$NADH,H_N^+ + UQ + 2\ H_N^+ \rightarrow NAD^+ + UQH_2 + 2\ H_P^+$	- 73.3	- 30.1
30	$2\ H_N^+ \rightarrow 2\ H_P^+$		40.4
31	***Global:*** $NADH,\ H_N^+ + UQ + 4\ H_N^+ \leftrightarrow NAD^+ + UQH_2 + 4\ H_P^+$		10.3

Table 3.17: Metabolic steps involved in Complex I

ΔG_{physio} of eqn. (29) represents the free energy change at physiological conditions; it accounts the location of charged species and pH differences between the two phases, N and P; at the same time, it does not account the concentration differences of other species.

Further, it is generally accepted that the NADH, H_N^+ oxidation is also coupled with the transfer of two additional protons against pH gradient so that the following equation must be taken into account:

$$2\ H_N^+ \rightarrow 2\ H_P^+ \qquad (30)$$

$\Delta G_{physio} = 2\ RT\ ln\ 10\ (pH_N - pH_P) + 2\ F\ \Delta\Psi = 11.4 + 28.9 = 40.4$ kJ/mol

This results to the global equation (31):

$$NADH,H_N^+ + UQ + 4\ H_N^+ \rightarrow NAD^+ + UQH_2 + 4\ H_P^+ \qquad (31)$$

The resulting ΔG_{physio} is positive and equal to 40.4 – 30.1 = + 10.3 kJ/mol.

The reaction is possible, only if $(NAD^+.UQH_2)$ / $(NADH, H_N^+.UQ)$ ratio is lower than 1 (ratio = 0.0157 for ΔG_{physio}= 0) and / or if a fractional number of H^+ transferred against electro-chemical potential is accepted: less than 4 and more than two. In any case, it appears that redox potential in matrix N-phase is strictly regulated at this level. Thus, at the end of these processes, 2 to 4 protons are translocated from N- phase to P-phase. The metabolic steps involved in this complex are shown in Table 3.10.

3.4.2 Complex II

Complex II is the succinate dehydrogenase complex. This is the only one complex directly related to the Krebs cycle; it catalyses the oxidation of succinate to fumarate. Consequently, the reaction rates associated with the Krebs cycle and complex II are not independent. The oxidation of $FADH_2$ takes place; the electrons are transferred to Fe-S centers and then to ubiquinone entering into the electron transport chain (Nicholls and Ferguson, 1992). It must be noticed that complex II is not connected to proton transfer (Figure 3.9).

The stoichiometric reaction is written as follows:

$$FAD + 2\ H_N^+ + 2e^- \rightarrow FADH_2 \qquad E_{m,7} = 30\ mV;\ \Delta G_{m,7} = -\ 5.8\ kJ/mol \qquad (32)$$

The complex II transfers two electrons from iron-sulfer (Fe-S) clusters to ubiquinone for ubiquinol production.

$$UQ + 2\ H_N^+ + 2e^- \rightarrow UQH_2 \qquad E_{m,7} = 60\ mV;\ \Delta G_{m,7} = -\ 11.6\ kJ/mol \qquad (33)$$

Coupling equations (33) and (32),

$$FADH_2 + UQ \rightarrow FAD + UQH_2 \qquad \Delta E_{m,7} = 30\ mV;\ \Delta G_{m,7} = -\ 5.8\ kJ/mol \qquad (34)$$

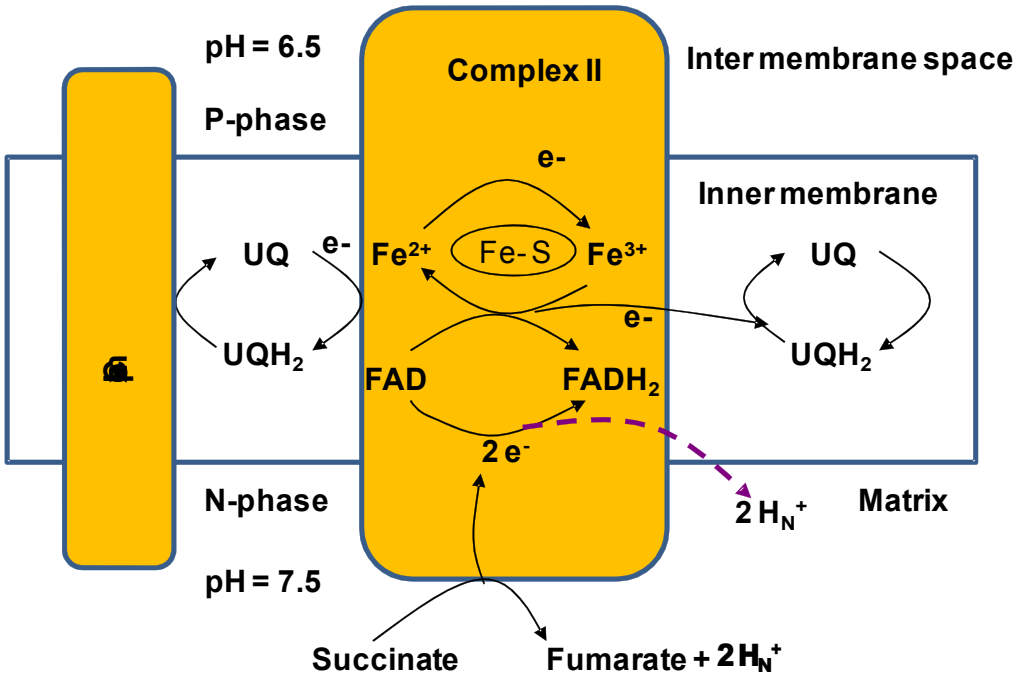

Figure 3.26: Electron transport pathway via Complex II. (Adapted from Garrett and Grisham, 2000)

Eqn.	Metabolic equations	$\Delta G_{m,7}$ (kJ/mol)	ΔG_{physio} (kJ/mol)	$E_{m,7}$
32	$FAD + 2\ H_N^+ + 2e^- \rightarrow FADH_2$	- 5.8		30
33	$UQ + 2\ H_N^+ + 2e^- \rightarrow UQH_2$	- 11.6		60
34	***Global:*** $FADH_2 + UQ \rightarrow FAD + UQH_2$	- 5.8	- 5.8	

Table 3.18: Metabolic steps involved in Complex II

The change in free energy is close to the equilibrium. Hence, it may be considered that the reaction is reversible. The energy is not sufficient to drive the transport of protons across the inner mitochondrial membrane. Hence, complex II does not act as proton pump. This is summarised in Table 3.11. Apparently, it operates as a regulation point of $FAD/FADH_2$ ratio.

3.4.3 Complex III

Complexes I and II globally produce UQH_2. The following steps concern UQH_2 recycling through a series of metabolic reactions called 'Q cycle'. This is almost same as mentioned before, when we described chloroplast light reactions; but, ubiquinone and ubiquinol bear the positions of plastoquinone and plastoquinol.

Globally, the oxidation of ubiquinol takes places at P-phase:

$$UQH_2 \rightarrow UQ + 2\ H_P^+ + 2\ e^-$$

At N-phase, the reduction of ubiquinone occurs:

$$UQ + 2\ H_N^+ + 2\ e^- \rightarrow UQH_2$$

According to the chemiosmotic theory, the free energy released during the mitochondrial electron transport is used in the active translocation of protons from N-phase to P-phase across the inner membrane. The mechanism is described in the following parapgraphs (Nicholls and Ferguson, 1992; Garrett and Grisham, 2000; Nobel, 2009).

Complex III contains two types of cytochromes (heme prosthetic group), named *b* and c_1. These carry electrons by the reduction and oxidation of an iron atom within the heme group. The iron atoms alternate the oxidation states between a reduced ferrous (+2) state and an oxidized ferric (+3) state during electron transport. Because of these processes, cytochrome b-c_1 complex (cytochrome *c* co-enzyme Q reductase) accepts electrons from ubiquinol and passes them on to cytochrome *c* through Q-cycle (Figures 3.10.1 and 3.10.2).

First part of the Q-cycle (at P-phase)

First Step at P-Phase

The function of cytochrome reductase is to catalyse the transfer of electrons from ubiquinol to cytochrome *c* and concomitantly pump protons across the inner mitochondrial membrane. Ubiquinone is always susceptible to be reduced to ubiquinol and vice versa.

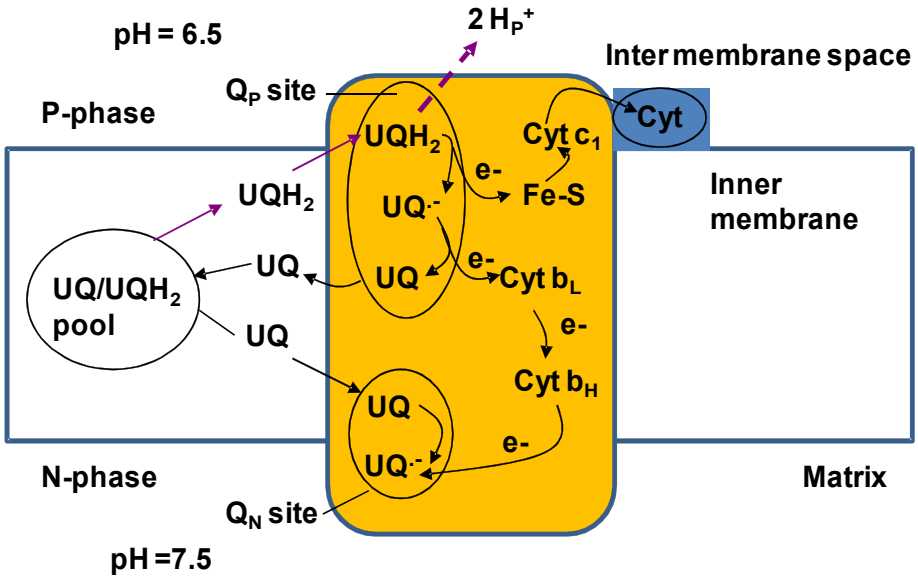

Figure 3.27.1 First part of Q-cycle of complex III. The electron transfer pathway following the oxidation of the first molecule of UQH_2 at the Q_p site near the cytosolic face of the membrane (P-phase). (Adapted from Garrett and Grisham, 2000)

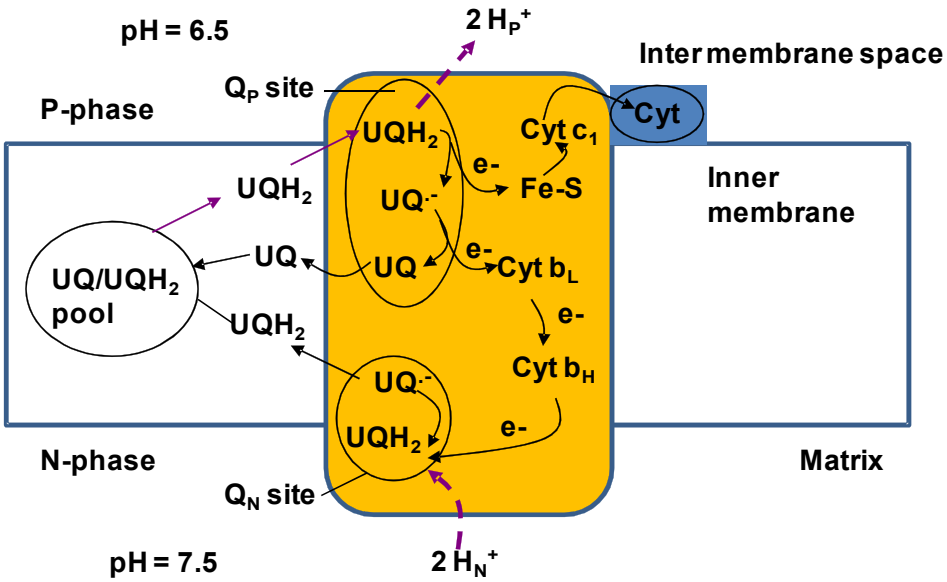

Figure 3.10.2: Second part of Q-cycle of complex III. Oxidation of a second molecule of UQH_2 (Adapted from Garrett and Grisham, 2000)

There are two couples to consider (Figure 3.10.1): Cyto Fe^{3+}/ Cyto Fe^{2+} and $UQ^{\cdot -}$/ UQH_2, where $UQ^{\cdot -}$ is the semiubiquinone radical.

$$\text{Cyto } Fe^{3+} + e^- \rightarrow \text{ Cyto } Fe^{2+} \qquad E_{m,7} = 235 \text{ mV}; \Delta G_{m,7} = -22.7 \text{ kJ/mol} \qquad (35)$$

$$UQ^{\cdot -} + 2\ H^+ + e^- \rightarrow UQH_2 \qquad E_{m,7} = 280 \text{ mV}; \Delta G_{m,7} = -27.0 \text{ kJ/mol} \qquad (36)$$

We write the resulting equation in the direction of Cyto Fe^{2+} oxidation.

$$UQ^{\cdot -} + 2\ H^+ + \text{Cyto } Fe^{2+} \rightarrow \text{Cyto } Fe^{3+} + UQH_2 \qquad \Delta G_{m,7} = -4.3 \text{ kJ/mol} \qquad (37)$$

As it takes place at P-phase, the free energy is calculated as follows:

$$\Delta G_{m,6.5} = \Delta G_{m,7} - 2\ RT \ln 10^{(7 - 6.5)} = -4.3 + -5.7 = -10.0 \text{ kJ/mol}$$

$$UQ^{\cdot -} + 2\ H_P^+ + \text{Cyto } Fe^{2+} \rightarrow \text{Cyto } Fe^{3+} + UQH_2 \qquad \Delta G_{m,6.5} = -10.0 \text{ kJ/mol} \qquad (38)$$

However, the concentration of semiubiquinone free radical ($UQ^{\cdot -}$) is very low compared to that of ubiquinol, principally due to the instability of $UQ^{\cdot -}$.

Considering $UQH_2/UQ^{\cdot -} = 10^4$, we obtain:

$$\Delta G_{physio} = \Delta G_{m,6.5} + RT \ln 10^4 = 12.8 \text{ kJ/mol}$$

Therefore, the previous reaction (38) most probably occurs in the reverse sense (UQH_2 oxidation).

$$\text{Cyto } Fe^{3+} + UQH_2 \rightarrow UQ^{\cdot -} + 2\ H_P^+ + \text{Cyto } Fe^{2+} \qquad (39)$$

More precisely, as soon as $UQH_2/UQ^{\cdot -} > 56$ the reaction proceeds as UQH_2 oxidation and this is what most probably takes place (Grammel and Ghosh, 2008).

For example, we can directly calculate ΔG from the standard potentials given in Eqns. (35) and (36) considering the concentration ratio ($UQH_2/UQ^{\cdot -}$) = 60 and at pH = pH_P = 6.5:

$$\Delta G = 96.484\ (0.28 - 0.235) - RT \ln (UQH_2/UQ^{\cdot -}) + 2\ RT\ (7 - pH_P) \ln 10$$

$$= 4.3 - RT \ln (60) + 2\ RT\ (7 - 6.5) \ln 10 = -0.1 \text{ kJ/mol}$$

In short, the minimum requirement is $\Delta G < 0$ for Eqn. (39) such that $UQH_2/UQ^{\cdot -}$ should be more than 60. Furthermore, UQH_2 oxidation (Eqn. 39) probably proceeds near equilibrium conditions.

In terms of mechanistic interpretation, from ubiquinol pool, ubiquinol diffuses through the bilipid layer to the 'ubiquinol binding site' situated near the P-phase, called 'Q_P site'. The electron transfer occurs in 2 steps: first, electron from ubiquinol is transferred to the Rieske protein (a Fe-S protein) which transfers the electron to cytochrome c1.

This process releases two protons to the P-phase along with the production of semi ubiquinone ($UQ^{\cdot-}$) which is highly unstable. Eqns. (35) + (36) represent the mechanism. The resulted Eqn. (39) globalises this first step.

Second Step at P-Phase

The second step involves $UQ^{\cdot-}$ oxidation following the oxido-reductions (Figure 3.10.1):

$$\text{Cyto } b_L + e^- \rightarrow \text{Cyto } b_L^- \qquad E_{m,7} = -100 \text{ mV}; \Delta G_{m,7} = 9.6 \text{ kJ/mol} \qquad (40)$$

where Cyto b_L is a heme of complex III.

$$UQ + e^- \rightarrow UQ^{\cdot-} \qquad E_{m,7} = -160 \text{ mV}; \Delta G_{m,7} = 15.4 \text{ kJ/mol} \qquad (41)$$

Eqns. (41) + (40) give,

$$\text{Cyto } b_L + UQ^{\cdot-} \rightarrow \text{Cyto } b_L^- + UQ \qquad \Delta G_{m,7} = -5.8 \text{ kJ/mol} \qquad (42)$$

Assuming the low concentration of $UQ^{\cdot-}$ (due to the instability), the negative ΔG can only be explained considering the products of Eqn. (42), Cyto b_L^- and UQ which remain very shortly at Q_P site. This is described in the next step.

Third Step from P-Phase to N-Phase

The produced ubiquinone diffuses away from the Q_P binding site.

The b_L heme ($E_{m,7} = -100$ mV) transfers its electron to the b_H heme ($E_{m,7} = 50$ mV) near to the N-phase.

$$\text{Cyto } b_H + e^- \rightarrow \text{Cyto } b_H^- \qquad E_{m,7} = 50 \text{ mV}; \Delta G_{m,7} = -4.8 \text{ kJ/mol} \qquad (43)$$

$$\text{Cyto } b_L + e^- \rightarrow \text{Cyto } b_L^- \qquad E_{m,7} = -100 \text{ mV}; \Delta G_{m,7} = 9.6 \text{ kJ/mol} \qquad (40)$$

Eqns. (40) + (43) give,

$$\text{Cyto } b_H + \text{Cyto } b_L^- \rightarrow \text{Cyto } b_H^- + \text{Cyto } b_L \qquad \Delta G_{m,7} = -14.5 \text{ kJ/mol} \qquad (44)$$

The transfer of electrons from b_L heme to b_H heme is accompanied by a electrical potential change of - 100 mV to 50 mV (Nicholls and Ferguson, 1992). This means that, if we consider equal concentrations of hemes, the thermodynamic equilibrium condition for Eqn. (44) obtains; if Cyto b_L^- is located at a place of potential + 100 mV and Cyto b_H^- at a place of potential - 50 mV, the membrane potential $\Delta\Psi$ will be close to 150 mV. In other words, if we consider that cytochrome concentrations are the same, the membrane potential is equal to the difference between the redox couples at thermodynamic equilibrium.

Conversely, it can be deduced that the membrane potential is regulated by the ratio of heme concentrations by reaction (44) which proceeds near equilibrium.

Second part of the Q-cycle (at N-phase)

First step at N-Phase

The next step concerns Cyto b_H^- oxidation at N-Phase. This involves the following couple:

$$\text{Cyto } b_H + e^- \rightarrow \text{Cyto } b_H^- \qquad E_{m,7} = 50 \text{ mV}; \quad \Delta G_{m,7} = -4.8 \text{ kJ/mol} \qquad (43)$$

$$UQ + e^- \rightarrow UQ^- \qquad E_{m,7} = -160 \text{ mV}; \ \Delta G_{m,7} = 15.4 \text{ kJ/mol} \qquad (41)$$

Eqns. (41) + (43) give,

$$UQ^- + \text{Cyto } b_H \rightarrow \text{Cyto } b_H^- + UQ \qquad \Delta G_{m,7} = -20.3 \text{ kJ/mol} \qquad (45)$$

Exactly same as involved in the first part of the Q-cycle, this reaction proceeds in the reverse direction though a negative $\Delta G_{m,7}$. More precisely, the equilibrium conditions are obtained, if $UQ/UQ^- >> 3640$, knowing that:

$$\Delta G = -20.3 + RT \ln (UQ^-/UQ) = -20.3 + 2.48 \ln (UQ^-/UQ)$$

Therefore, the concentration of ubiquinone must be at least 3600 times greater than that of free radical of semiubiquinone for considering that Eqn. (45) proceeds in the reverse direction such that,

$$\text{Cyto } b_H^- + UQ \leftrightarrow UQ^- + \text{Cyto } b_H \qquad \Delta G = 0 \qquad (46)$$

Second step at N-Phase

The reduction of ubiquinone takes place at N-phase taking a hydride from N- phase, while the reverse reaction (ubiquinol oxidation) takes place at P-phase. The electron is then transferred to a second molecule of ubiquinone at a binding site near the N-phase, called the Q_N binding site (Nicholls and Ferguson, 1992).

Following the same equation (39) as previously, this process again generates a free radical of semiubiquinone which remains firmly bound to the Q_N binding site.

The second part of the Q-cycle begins from Q_P site; one electron from ubiquinol (bound at Q_P) is transferred to the Rieske protein, which transfers it to cytochrome c1. This process releases two protons to the N-phase (Figure 3.10.2).

$$UQ^- + 2H^+ + e^- \rightarrow UQH_2 \qquad E_{m,7} = 280 \text{ mV}; \ \Delta G_{m,7} = -27.0 \text{ kJ/mol} \qquad (36)$$

The second electron is then transferred to the b_L heme to generate a second molecule of reoxidized ubiquinone.

$$\text{Cyto } b_H + e^- \rightarrow \text{Cyto } b_H^- \qquad E_{m,7} = 50 \text{ mV}; \ \Delta G_{m,7} = -4.8 \text{ kJ/mol} \qquad (43)$$

As the reaction occurs near N-Phase, H^+ is to be considered as H^+_N so that we obtain:

$$UQ^{\cdot -} + 2\ H_N^+ + \text{Cyto } b_H^- \rightarrow \text{Cyto } b_H + UQH_2 \qquad \Delta G_{m,7} = -22.2 \text{ kJ/mol} \tag{47}$$

Then, $\Delta G_{m,7.5}$ is calculated as follows:

$$\Delta G_{m,7.5} = \Delta G_{m,7} + RT \ln (UQH_2/UQ^{\cdot -}) - 2\ RT \ln 10^{(7-7.5)}$$
$$= -16.5 + RT \ln (UQH_2/UQ^{\cdot -})$$

In fact, this last reaction occurs at near equilibrium conditions considering UQH_2 is much more stable than $UQ^{\cdot -}$. More specifically, when $\Delta G_{m,7.5} = 0$, we have $(UQH_2/UQ^{\cdot -}) = 770$. This means, in order to occur a thermodynamically feasible reaction (of negative ΔG), the concentration of $UQH_2/UQ^{\cdot -}$ at pH 7.5 must be lower than 770.

Global functioning of Q-cycle

Globally, the Q cycle is summarised in Table 3.12. The first steps at P-phase occur two times and the neutral species UQ and UQH_2 belongs to the same UQ pool; eventually, the following equation is obtained:

$$2\ \text{Cyto } Fe^{3+} + UQH_2 + 2\ H_N^+ \rightarrow UQ + 4\ H_P^+ + 2\ \text{Cyto } Fe^{2+} \tag{48}$$

The free energy at pH 7, $\Delta G_{m,7}$ is calculated as follows:

$$\Delta G_{m,7} = 2\ (4.3 - 5.8 - 14.7) + 20.3 - 22.3 = -34.4 \text{ kJ/mol}$$

When accounting pH difference between two phases:

$$\Delta G = -34.4 + 4\ RT\ (7 - 6.5) \ln 10 - 2\ RT\ (7 - 7.5) \ln 10 = -17.3 \text{ kJ/mol}$$

When accounting electric potential difference:

$$\Delta G = -17.3 + 4\ F\ E_P + 2 \times 2\ F\ E_P - 2\ F\ E_N - 2 \times 3\ F\ E_P = -17.3 + 2\ F\ (E_P - E_N)$$
$$= -17.3 + 2\ F\ \Delta\Psi = +11.6 \text{ kJ/mol}$$

ΔG_{physio} is near equilibrium condition while accounting UQH_2/UQ ratio that must be at least equal to 110 for ensuring $\Delta G_{physio} = 0$. It is also possible to describe in more details the inequalities of Table 3.12. For that, it is necessary to distinguish semiubiquinone free radical at P-phase and at N-phase. Considering Table 3.12, we have the following inequalities:

$$\frac{UQH_2}{UQ_P^-} > 56 \qquad \frac{UQ}{UQ_P^-} < 10\, r_L$$

$$\frac{UQ}{UQ_N^-} > 3640\, r_H \qquad r_H\, \frac{UQH_2}{UQ_N^-} < 770$$

where $r_H = \dfrac{Cyto\ b_H}{Cyto\ b_H^-}$ and $r_L = \dfrac{Cyto\ b_L}{Cyto\ b_L^-}$ $\qquad r_H = r_L$

When using the last equation $r_H = r_L$ and considering that the electrochemical potentials of semiubiquinone on both phases are equal, we obtain:

$$\tilde{\mu}_{UQ_N^-} = -F E_N + RT \ln(UQ_N^-) + const.$$
$$\tilde{\mu}_{UQ_P^-} = -F E_P + RT \ln(UQ_P^-) + const.$$

so that:

$$\tilde{\mu}_{UQ_N^-} = \tilde{\mu}_{UQ_P^-}$$
$$\ln\left(\frac{UQ_P^-}{UQ_N^-}\right) = \frac{F(E_P - E_N)}{RT} = \frac{F\Delta\psi}{RT} = 5.84$$

This means that: $\frac{UQ_P^-}{UQ_N^-} = 343$

Then, solving the above system of inequalities leads to:

$$10.6\ r_H < \frac{UQ}{UQ_P^-} < 10\ r_L$$
$$56 < \frac{UQH_2}{UQ_P^-} < \frac{2.24}{r_H}$$
$$r_H < 0.04 \qquad r_L > 1.06\ r_H$$

We find that the equality between r_H and r_L hypothesis is quite satisfactory and furthermore, the value of r_H is around 0.04. Reducing again the above system leads to:

$$\frac{UQH_2}{UQ} > 130$$

This is quite consistent with the condition we have derived from the global equation in Table 3.12. In summary, it is very interesting to prove that Q-cycle is a sum of electrochemical equations that function at near equilibrium conditions, the global sum being itself near equilibrium. This also explains how the membrane potential, $\Delta\psi$ is controlled at a value near 150 mV with the ratios of Cytochromes b_L and b_H. This justifies a multilinear approach for considering the reaction rates. However, we do not exploit this approach for examining the kinetic behaviour of higher plant growth.

Eqn.	Metabolic equations	$\Delta G_{m,7}$ and ΔG_{physio} (kJ/mol)	Conditions for near equilibrium conditions : $\Delta G_{physio} = 0$	Number of occurrences in Q-cycle
39	Cyto Fe^{3+} + UQH_2 → $UQ^{\cdot -}$ + 2 H_P^+ + Cyto Fe^{2+}	+ 4.3 0	$UQH_2/UQ^{\cdot -}$ > 56 P-Phase: pH=6.5	2
42	Cyto b_L + $UQ^{\cdot -}$ → Cyto b_L^- + UQ	- 5.8 0	$UQ/UQ^{\cdot -}$ < 10 r_L P-Phase	2
44	Cyto b_H + Cyto b_L^- → Cyto b_H^- + Cyto b_L	- 14.5 0	$\Delta\psi \approx 150$ mV $r^L = r^H$	2
46	Cyto b_H^- + UQ → $UQ^{\cdot -}$ + Cyto b_H	+ 20.3 0	$UQ/UQ^{\cdot -}$ > 3640 r_H N-Phase	1
47	$UQ^{\cdot -}$ + 2 H_N^+ + Cyto b_H^- → Cyto b_H + UQH_2	- 22.2 0	r_H $UQH_2/UQ^{\cdot -}$ <770 N-Phase: pH=7.5	1
48	***Global:*** 2 Cyto Fe^{3+} + UQH_2 + 2 H_N^+ → UQ + 4 H_P^+ + 2 Cyto Fe^{2+}	- 34.4 0	UQH_2/UQ >110	

Table 3.19: Elementary mechanisms of Q cycle of Complex III: Values for near equilibrium conditions are given for ΔG=0. r_L is the ratio of Cyto b_L/ Cyto b_L^-. r_H is the ratio of Cyto b_H/ Cyto b_H^-

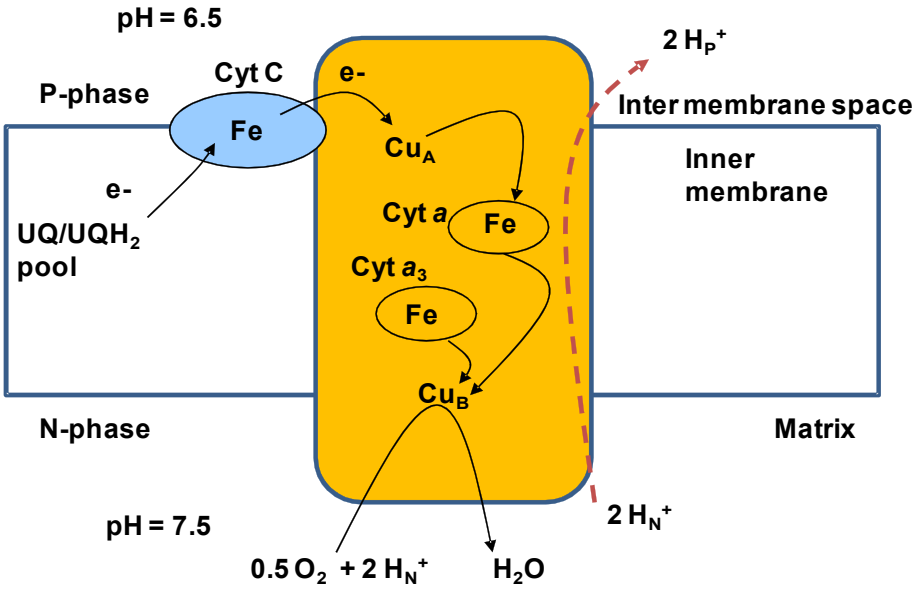

Figure 3.28: Mechanism for the reduction of oxygen at Complex IV Protons required for the reduction processes are taken from matrix side or P-phase.

3.4.4 Complex IV

Complex IV is known as cytochrome c oxidase, the protein located on the P-phase. It accepts electrons from cytochrome c given by complex III passes them to oxygen (Garrett and Grisham, 2000). The first step is again the reduction of heme:

$$\text{Cyto } Fe^{3+} + e^- \rightarrow \text{Cyto } Fe^{2+} \qquad E_{m,7} = 235 \text{ mV}; \Delta G_{m,7} = -22.7 \text{ kJ/mol} \qquad (35)$$

Four electrons are funnelled into O_2 to completely reduce it to H_2O and continuously pump protons from N-phase to the cytosolic side of the inner mitochondrial membrane, the P-phase.

Cytochrome c oxidase contains two heme centers (cytochrome a and cytochrome a_3) and two copper proteins in which the copper sites are Cu_A (near to P-phase) and Cu_B (near to N-phase). Cytochrome c transfers its electron to Cu_A (Figure 3.11). The oxidized cytochrome c dissociates. Cu_A then transfers the electron to cytochrome a. A second cytochrome c binds and transfers its electron to Cu_A which is subsequently transferred to 'cytochrome a' which in turn is transferred to cytochrome a_3. The binuclear metal center has two electrons bound allowing the binding of O_2 to binuclear center. The next step involves the uptake of two protons and the transfer of yet another electron through the same pathway which leads to cleavage of the O--O bond and the generation of a Fe^{4+} metal center. Then, the electron is transferred to form a hydroxide at the heme center which becomes protonated and dissociates as H_2O (Nicholls and Ferguson, 1992). We can summarise the metabolic processes of complex IV as follows,

$$\tfrac{1}{2} O_2 + 2 H_N^+ + 2e^- \rightarrow H_2O \quad E_{m,7} = 800 \text{ mV}; \quad P_{O2} = 0.21\text{atm} \quad \Delta G_{m,7} = -154.4 \text{ kJ/mol} \qquad (5)$$

This process takes place at pH=7.5, so that

$$\Delta G_{m,7.5} = \Delta G_{m,7} - 2 RT \ln 10^{(7 - 7.5)}$$

$$= -154.4 - 2 RT \ln 10^{-0.5} = -148.7 \text{ kJ/mol}$$

The two electrons released help to pump two more protons from N-phase to P-phase.

$$2 H_N^+ \rightarrow 2 H_P^+ \qquad \Delta G_1 = 11.4 \text{ kJ/mol} \qquad (49)$$

Even if ΔG is positive, when associating with Eqn. (47), it appears to be a feasible reaction:

$$\tfrac{1}{2} O_2 + 4 H_N^+ + 2e^- \rightarrow H_2O + 2 H_P^+ \qquad \Delta G = -137.3 \text{ kJ/mol} \qquad (50)$$

For the complex IV, the overall reaction can be written by adding (50) and (35),

$$\tfrac{1}{2} O_2 + 4 H_N^+ + 2 \text{ cyto } Fe^{2+} \rightarrow 2 \text{ cyto } Fe^{3+} + H_2O + 2 H_P^+ \qquad (51)$$

$$\Delta G_{physio} = -137.3 + 22.7 - 4 F E_N - 4 F E_P + 2 \times 3 F E_P + 2 F E_P$$

$$= -114.6 + 4 F (E_P - E_N) = -114.6 + 4 \times 96.484 \times 0.15 = -56.7 \text{ kJ/mol}$$

Eqn.	Metabolic equations	$\Delta G_{m,7}$ (kJ/mol)	$\Delta G_{m,7.5}$ (kJ/mol)	ΔG_{physio} (kJ/mol)	$E_{m,7}$ (mV)	$E_{m,7.5}$ (mV)
35	Cyto Fe^{3+} + e^{-} → Cyto Fe^{2+}	- 22.7			235	
5	½ O_2 + 2 H_N^+ + 2e^- → H_2O	-154.4	-148.7		800	770
50	½ O_2 + 4 H_N^+ + 2e^- → H_2O + 2 H_P^+			-108.3		
51	***Global:*** ½ O_2 + 4 H_N^+ + 2 cyto Fe^{2+} → 2 cyto Fe^{3+} + H_2O + 2 H_P^+			- 56.7		

Table 3.20: Metabolic steps involved in Complex IV

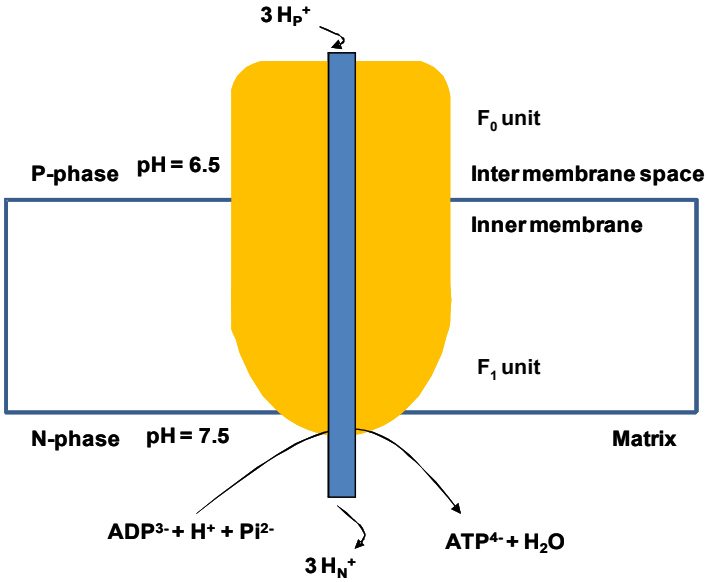

Figure 3.29: ATP synthesis in mitochondrion Flow of protons through ATP synathse turns the rotor and ATP released along with water. (Garrett and Grisham, 2000)

Eqn.	Metabolic equations	$\Delta G_{m,7}$ (kJ/mol)	$\Delta G_{m,7.5}$ (kJ/mol)	ΔG_{phy} (kJ/mol)
25	H_N^+ + ADP^{3-} + Pi^{2-} → ATP^{4-} + H_2O	32.5	35.4	
52	H_N^+ → H_P^+	- 34.5		
53	***Global:*** 3 H_P^+ + H_N^+ + ADP^{3-} + Pi^{2-} → 3 H_N^+ + ATP^{4-} + H_2O			- 68.1

Table 3.21: Metabolic steps in mitochondrial ATP synthase

3.4.5 Mitochondrial ATP synthesis

Electron flow and ATP synthesis are tightly coupled in the sense that, in normal mitochondria, neither occurs without the other. ATP synthesis takes place with the help of the enzyme called ATP synthase (or complex V) similar to that of chloroplast. It consists of two main complexes (F_0 unit and F_1 unit) as well as multiple protein sub units. The F_1 unit is towards the matrix phase (N-phase), while F_0 unit is towards P-phase, within the membrane (Figure 3.12). F_0 unit contains the proton channel of the complex. The developed proton gradient across the membrane helps to move protons through F_0 and as a result of this, the moving unit in the ATP synthase rotate in clockwise direction which finally release ATP^{4-}. The isotopic studies showed that about equal amounts of bound ATP^{4-} and ADP^{3-} are in equilibrium at the catalytic site, even in the absence of a proton gradient (Berg *et al*., 2002). Thus, we can conclude the role of proton gradient is to release ATP^{4-} from the synthase, not to produce really new ATP molecules.

The formation of one ATP^{4-} apparently requires the movement of four protons through the mitochondrial ATP synthase same as in the thylakoidal ATP synthase. ATP^{4-} is produced in the matrix, the N-phase; but, it is usually needed in the cell cytosol. Hence, the outer mitochondrial membrane is permeable to transport ATP^{4-}, ADP^{3-}, etc. Phosphate, which is used for the production of ATP^{4-} also enters to the matrix by H^+/Pi^{2-} symporter. ATP is transporting as ATP^{4-} while ADP as ADP^{3-}. The stoichiometry takes the form:

$$H_N^+ + ADP^{3-} + Pi^{2-} \rightarrow ATP^{4-} + H_2O \quad \Delta G_{m,7} = 32.5 \text{ kJ/mol} \quad (25)$$

Considering $pH_N = 7.5$, we obtain:

$$\Delta G_{m,7.5} = 32.5 - RT \ln 10^{(7-7.5)} = 35.4 \text{ kJ/mol}$$

Alongside, the proton translocation creates a pH gradient (ΔpH) of around 1 unit and a membrane potential, ΔΨ of 150 mV (Rehling *et al*., 2003). For ejection of one H^+ from the matrix, N-phase:

$$H_P^+ \rightarrow H_N^+ \qquad \Delta G = - RT \ln 10^{\Delta pH} - F\Delta\Psi = - 34.5 \text{ kJ/mol} \qquad (52)$$

So, the resulting equation for phosphorylation is:

$$3\ H_P^+ + H_N^+ + ADP^{3-} + Pi^{2-} \rightarrow 3\ H_N^+ + ATP^{4-} + H_2O \qquad (53)$$

$$\Delta G_{physio} = 3\times -34.5 + 35.4 = - 68.1 \text{ kJ/mol}$$

For each transmembrane process, the ΔpH and ΔΨ components may act either separately or together, depending on the enzyme structure and the balance of biological advantage.

Erreur : source de la référence non trouvée

Name of the protein complex	Eqn.	Reaction	Metabolic equations	ΔG_{physio} (kJ/mol)
Complex I	31	R1	$NADH,H_N^+ + UQ + 4\ H_N^+ \rightarrow NAD^+ + UQH_2 + 4\ H_P^+$	+ 10.3
Complex II	34	R2	$FADH_2 + UQ \leftrightarrow FAD + UQH_2$	- 5.8
Complex III	48	R3	$UQH_2 + 2$ cyto $Fe^{3+} + 2\ H_N^+ \leftrightarrow UQ + 4\ H_P^+ + 2$ cyto Fe^{2+}	0
Complex IV	51	R4	$½\ O_2 + 4\ H_N^+ + 2$ cyto $Fe^{2+} \rightarrow 2$ cyto $Fe^{3+} + H_2O + 2\ H_P^+$	- 56.7
ATP synthase	53	R5	$3\ H_P^+ + H_N^+ + ADP^{3-} + Pi^{2-} \rightarrow 3\ H_N^+ + ATP^{4-} + H_2O$	- 68.1

Table 3.22: Equations for mitochondrial electron transport and oxidative phosphorylation

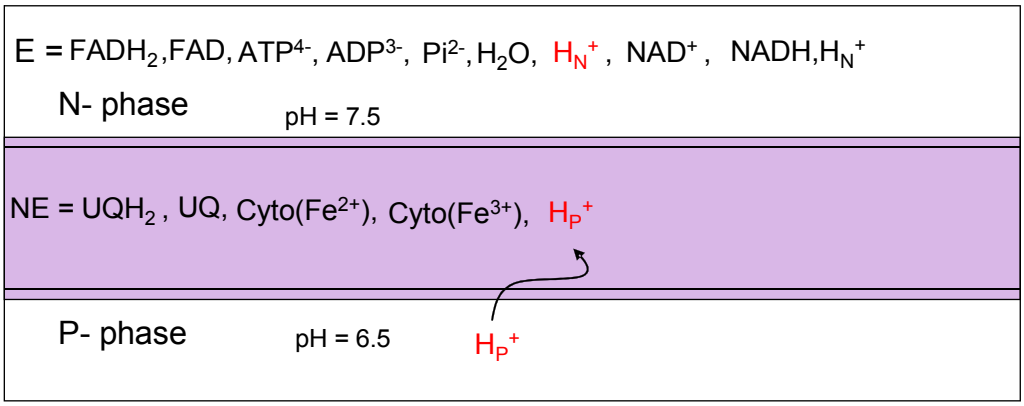

Figure 3.30: Separation of metabolites into non exchangeables and exchangeables for mitochondrial electron transport and oxidative phosphorylation

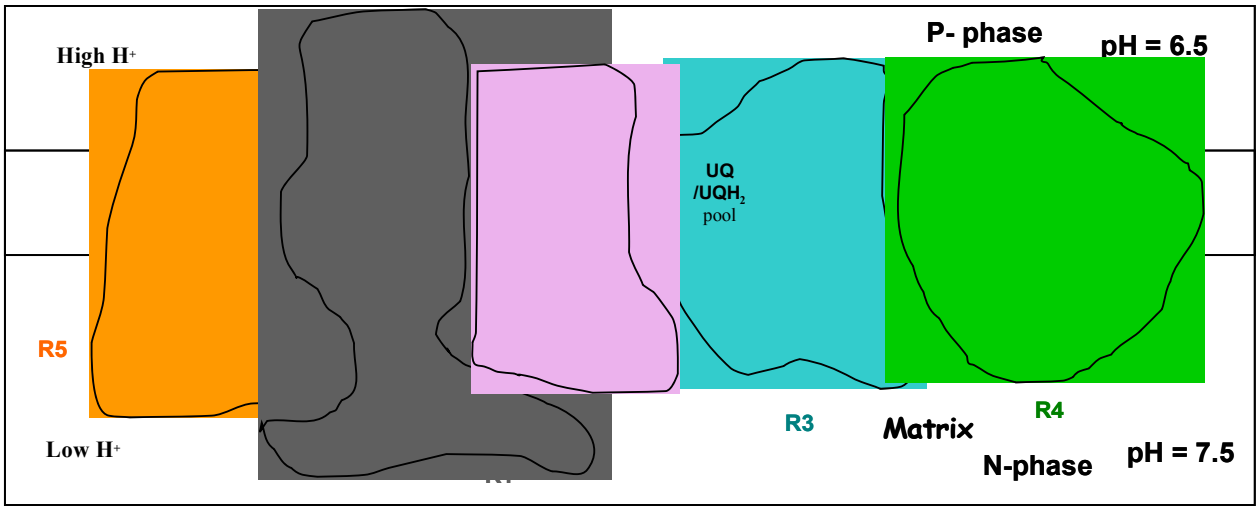

Figure 3.31: Metabolic reactions involved in mitochondrial electron transport and oxidative phosphorylation for ATP production

3.4.6 Equations for mitochondrial electron transport and oxidative phosphorylation

From the above mitochondrial complexes, the summarised equations (Table 3.15) form the backbone for oxidative phosphorylation metabolic network. There are 5 reactions in the network originally derived from the complexes situated in the mitochondrial membrane.

The metabolites are separated as 10 exchangeables and 5 nonexchangeables constituting 15 in total (Figure 3.13). Similar to light reaction network, P-phase is taken as a closed system; while N-phase is an open system, which contains a chain of metabolisms (e.g. TCA cycle, secondary metabolisms, etc.). The energy molecules (ATP^{4-} and NADH, H_N^+) are produced at N-phase; by which the sequential reactions (TCA cycle) can be favourably occurring at once as per the availability of energy. The membrane that separates P and N-phases is assumed as an unchanged one; the input substrates consumed at N-phase are oxygen molecule, ADP^{3-}, Pi^{2-}, NAD^+ and FAD; where the energy molecules ATP^{4-}, $FADH_2$, NADH, H_N^+ and water (H_2O) are the outputs. The inputs and outputs together come under the group exchangeables, E. The rest of the molecules such as UQ, UQH_2, Cyto(Fe^{2+}), Cyto(Fe^{3+}), H_P^+, etc. act as the intermediates (NE, non exchangeables) for the production of outputs. The proton produced at N-phase, H_N^+ must be taken as output as it is related to the reduced molecule NADH H_N^+, while H_P^+ is taken as intermediate as because of this movement proton gradient and thereby ATP formation can be achieved. Once, the metabolites are separated into E and NE, the stoichiometric matrix can be constructed as shown in Table 3.16.

Reactions		1	0	1	1	1
Directions		R1	R2	R3	R4	R5
$CytoFe^{2+}$	NE	0	0	2	-2	0
$CytoFe^{3+}$	NE	0	0	-2	2	0
UQ	NE	-1	-1	1	0	0
UQH_2	NE	1	1	-1	0	0
H_P^+	NE	4	0	4	2	-3
H_N^+	E=	-4	0	-2	-4	2
Pi^{2-}	E-	0	0	0	0	-1
ADP^{3-}	E-	0	0	0	0	-1
ATP^{4-}	E+	0	0	0	0	1
FAD	E+	0	1	0	0	0
$FADH_2$	E-	0	-1	0	0	0
NAD^+	E+	1	0	0	0	0
NADH, H_N+	E-	-1	0	0	0	0
H_2O	E+	0	0	0	1	1
O_2	E-	0	0	0	-0.5	0

Table 3.23: Metabolic matrix for mitochondrial electron transport and oxidative phosphorylation E = ATP^{4-}, ADP^{3-}, Pi^{2-}, $NADH,H_N^+$, NAD^+, H_2O, O_2, $FADH_2$, FAD; NE = UQ, UQH_2, Cyto(Fe^{2+}), Cyto(Fe^{3+}), H_P^+, Abbreviations: O_2 = oxygen; H_2O = **water;** $NADH,H_N^+$ = nicotinamide adenine dinucleotide; NAD^+ = oxidised nicotinamide adenine dinucleotide; FAD = flavin adenine dinucleotide ; $FADH_2$ = reduced flavin adenine dinucleotide; adenine dinucleotide; ATP^{4-} = adenosine triphosphate; ADP^{3-} = adenosine diphosphate; Pi^{2-} = inorganic phosphate; **H_N^+ and H_P^+** = protonated hydrogen at N and P phases; $CytoFe^{2+}$ = reduced iron of heme; $CytoFe^{2+}$ = oxidised iron of heme; UQH_2 = Ubiquinol; UQ = Ubiquinone

Reaction	Metabolic equations	$\Delta G_{m,7}$ (kJ/mol)	ΔG_{physio} (kJ/mol)
R1	$Oxaloacetate^{2-}$+ Acetyl CoA- + H_2O → $Citrate^{3-}$+ Coenzyme A + H_N^+	-31.4	Negative
R2	$Citrate^{3-}$ ↔ *cis*-$Aconitate^{3-}$ + H_2O	6.7	0
R3	*cis*-$Aconitate^{3-}$ + H_2O + H_N^+ ↔ D-$Isocitrate^{2-}$		
R4	D-$Isocitrate^{2-}$ + NAD^+ + H_N^+ → $NADH,H_N^+$ + 2-Ketoglutarate- + CO_2	-20.9	Negative
R5	2 -Ketoglutarate- + NAD^+ + CoenzymeA → Succinyl-CoA^- + $NADH,H_N^+$ + CO_2	-30	Negative
R6	Succinyl-CoA- + ADP^{3-} + P_i^{2-} ↔ $Succinate^{2-}$ + Coenzyme A + ATP^{4-}	-3.3	0
R7	$Fumarate^{2-}$ + H_2O ↔ $Malate^{2-}$	-3.8	0
R8	$Malate^{2-}$ + NAD^+ ↔ $Oxaloacetate^{2-}$ + $NADH,H_N^+$	29.7	0
R9	$Succinate^{2-}$ + FAD ↔ $FADH_2$ + $Fumarate^{2-}$	0.4	0

Table 3.24: Equations for Krebs cycle (Garrett and Grisham, 2000; Voet D. and Voet J.G, 2005)

3.5Krebs cycle

TCA cycle or Krebs cycle is responsible for the oxidation of respiratory substrates to drive ATP synthesis. It starts with the metabolite acetyl CoA, produced from pyruvate. As TCA cycle produces ATP from substrate (acetyl CoA), it is also known as substrate level phosphorylation. The enzymes required to carry out TCA cycle are situated inside the mitochondrial matrix (Figure 3.15). The metabolic reactions corresponding to TCA cycle are known and are taken from the database, MetaCyc (Table 3.17) to explain the network in the metabolic matrix given in Table 3.18. Some reactions are specified for plants, while some are common for all organisms; e.g. R6 and R9 are specific for plants. In plants, succinate formation is always accompanied with ADP^{3-}, ATP^{4-} and Pi^{2-}, not with $GDP^{3-}$and GTP^{4-}. Similarly in eukaryotes like plants, succinate is associated with fumarate through $FADH_2$ (Sweetlove *et al*., 2010); in some references, ubiquinol and ubiquinone are used instead of FAD and $FADH_2$ (MetaCyc).

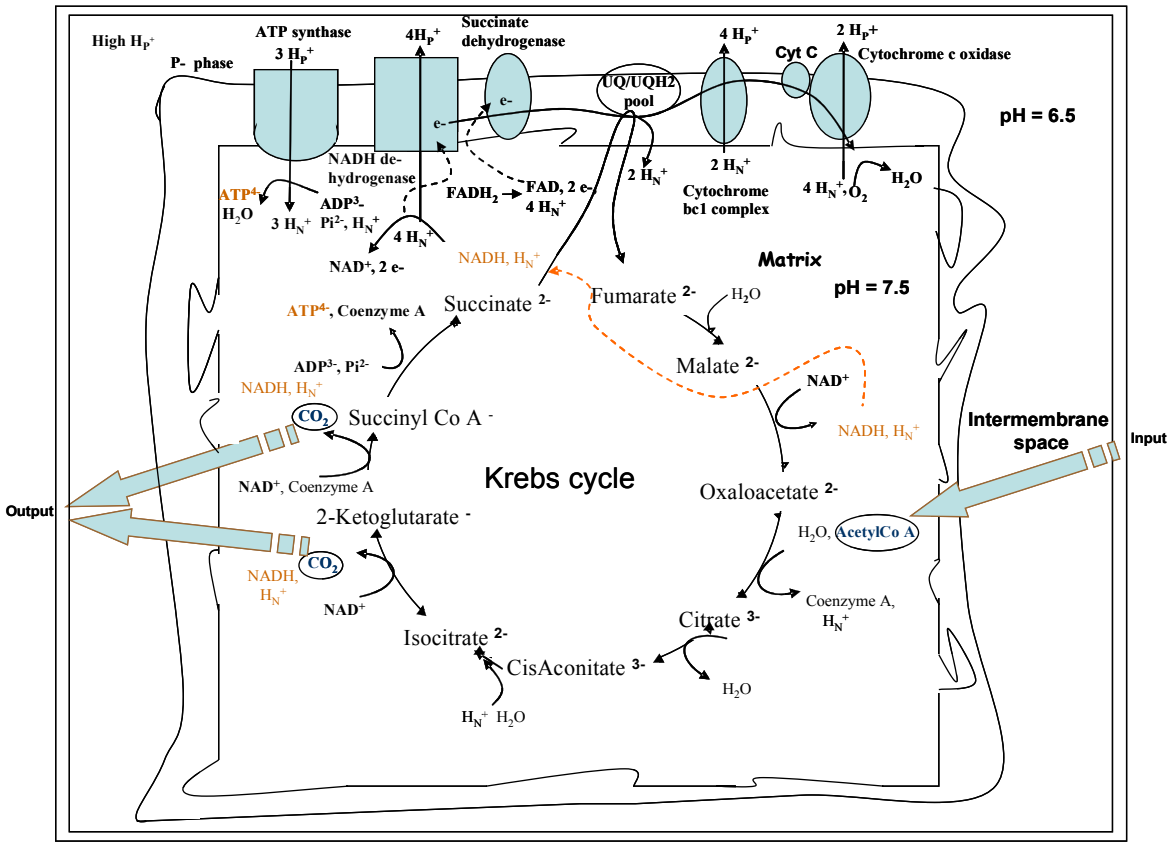

Figure 3.32: Electron transport, oxidative phosphorylation and Krebs cycle reactions

The metabolic system contains 21 metabolites and 9 reactions. The input and output metabolites involved are energy associated molecules FAD, $FADH_2$, NAD^+, $NADH,H_N^+$, ADP^{3-}, H_N^+, ATP^{4-} and Pi^{2-}; in addition to these, Acetyl Co A^-, Coenzyme A, CO_2, H_2O, etc. are also considered as exchangeables whilst the rest are nonexchangeables. Hence for this system, there are 12 exchangeables and 9 nonexchangeables.

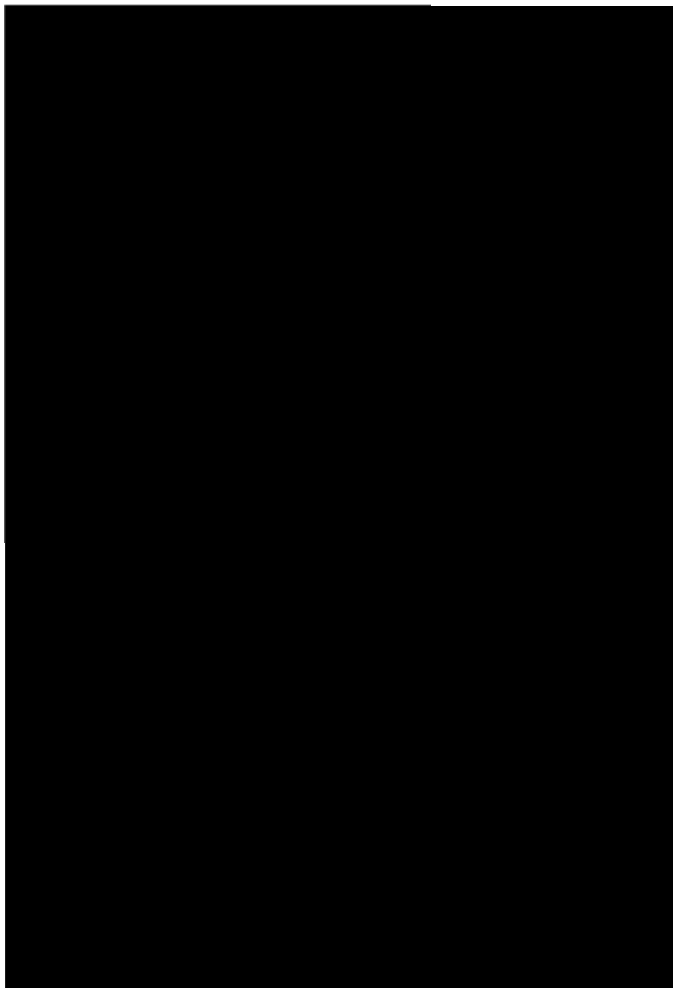

Table 3.25: Metabolic matrix for Krebs cycle E = FAD, $FADH_2$, NAD^+, $NADH,H_N^+$, H_2O, $AcetylCoA^-$, Coenzyme A, H_N^+, CO_2, ADP^{3-}, ATP^{4-} and Pi^{2-}; NE = $Oxaloacetate^{2-}$, $Citrate^{3-}$, $cis\text{-}Aconitate^{3-}$, $D\text{-}Isocitrate^{2-}$, 2–$Ketoglutarate^-$, $Succinyl\text{-}CoA^-$, $Succinate^{2-}$, $Malate^{2-}$, $Fumarate^{2-}$; Abbreviations: H_2O = water; $NADH,H_N^+$ = nicotinamide adenine dinucleotide; NAD^+ = oxidised nicotinamide adenine dinucleotide; FAD = flavin adenine dinucleotide ; $FADH_2$ = reduced flavin adenine dinucleotide; adenine dinucleotide; ATP^{4-} = adenosine triphosphate; ADP^{3-} = adenosine diphosphate; Pi^{2-} = inorganic phosphate; H_N^+ and H_P^+ = protonated hydrogen at N and P phases

3.6 Glycolysis

Glucose degradation by Embden Meyerhof Pathway - EMP involves 11 reactions and operates both under aerobic as well as anaerobic conditions. Under aerobic conditions, this pathway functions in conjunction with the TCA cycle in which the pyruvate generated through the EMP is oxidised to CO_2 and water. In plant leaves, as aerobic respiration takes place glycolysis combines with TCA and electron transport. But, in roots if oxygen lacks, anaerobic respiration performs (then, pyruvate is reduced to lactate or ethanol).

Energetically as a part of substrate level phosphorylation, glycolysis yields 2 moles of pyruvate per glucose. It also prepares the cell to derivate more energy in the form of ATP molecules. The formed pyruvate again changes into acetyl CoA which enters into the mitochondria for further metabolism. Here, we took the glycolysis metabolic network starting from glucose to acetyl CoA. The metabolic matrix for the glycolytic metabolic network is given in Table 3.20 and the equations are given in Table 3.19. The exchangeables and nonexchangeables of this sub system are separated. As inputs and outputs involve energy molecules, glucose, acetyl co A, coenzyme A, CO_2 and H_2O form exchangeables and the rest come under non exchangeables (See Table 3.20).

Reaction	Metabolic equations	$\Delta G_{m,7}$ (kJ/mol)	ΔG_{physio} (kJ/mol)
R1	Glucose + $ATP^{4-} \rightarrow G6P^{2-} + H_N^+ + ADP^{3-}$	-16.7	-27.2
R2	$G6P^{2-} \leftrightarrow F6P^{2-}$	1.67	-1.4
R3	$F6P^{2-} + ATP^{4-} \rightarrow FBP^{4-} + H_N^+ + ADP^{3-}$	-14.2	-25.9
R4	$FBP^{4-} \leftrightarrow DHAP^{2-} + G3P^{2-}$	23.9	-5.9
R5	$DHAP^{2-} \rightarrow G3P^{2-}$	7.56	Negative
R6	$3\ PGA^{3-} \leftrightarrow 2PGA^{3-}$	4.4	-0.6
R7	$2\ PGA^{3-} \leftrightarrow PEP^{3-} + H_2O$	1.8	-2.4
R8	$G3P^{2-} + Pi^{2-} + NAD^+ \rightarrow$ 1-3BPGA^{4-} + NADH, H_N^+	6.3	
R9	1-3BPGA^{4-} + $ADP^{3-} \rightarrow 3PGA^{3-} + ATP^{4-}$	-18.9	-16.7
R10	$PEP^{3-} + H_N^+ + ADP^{3-} \rightarrow$ pyruvate$^-$ + ATP^{4-}	-31.7	-13.9
R11	pyruvate- + CoA + $NAD^+ \rightarrow CO_2$ + AcCoA- + NADH,H_N^+		Negative

Table 3.26: Equations for glycolysis (Voet D. and Voet J.G, 2005)

Table 3.27: Metabolic matrix for glycolysis E = Coenzyme A ; Glucose ; NAD^+ ; NADH,H_N^+ ; Pi^{2-} ; ADP^{3-} ; ATP^{4-} ; CO_2 ; AcCoA$^-$; H_2O ; NE = $F6P^{2-}$; H_N^+; $G6P^{2-}$; FBP^{4-}; $DHAP^{2-}$; $G3P^{2-}$; $2PGA^{3-}$; $3PGA^{3-}$; PEP^{3-}; 1-3 $BPGA^{4-}$; pyruvate-; Abbreviations: H_2O = **water;** CO_2 = carbon dioxide; NADH,H_N^+ = nicotinamide adenine dinucleotide; NAD^+ = oxidised nicotinamide adenine dinucleotide; ATP^{4-} = adenosine triphosphate; ADP^{3-} = adenosine diphosphate; Pi^{2-} = inorganic phosphate; $\mathbf{H_N^+}$ = protonated hydrogen at N phase; PEP^{3-} = phosphoenol pyruvate; $DHAP^{2-}$ = **dihydroxyacetone phosphate;** 1, 3-$BPGA^{4-}$= **1, 3- diphosphate glycerate** FBP^{4-} = **fructose 1, 6-biphosphate;** $F6P^{2-}$ = **fructose -6-biphosphate;** $G6P^{2-}$ = **glucose 6-phosphate;** $G3P^{2-}$ = glyceraldehyde -3-phosphate ; $2PGA^{3-}$= 2-phosphoglycerate ; $3PGA^{3-}$ = 3-phosphoglycerate; AcCoA- = Acetyl Co A; CoA = Coenzyme A

3.7Elementary Flux Mode Analysis

The constructed metabolic network is subjected to analyse the topology using elementary flux mode analysis. The preliminarily analysis has been done successfully for the matrix network system in order to check the reaction stoichiometry, colinearity and cyclic relationship for the combination of metabolic reactions; there were no cyclic reactions to nullify the contribution of any metabolite. The verification has been carried out thoroughly considering that even a single perturbation may oppositely influence the system calculations and analysis. Hence for all systems, the preliminary checking has been carried out before performing the calculations, as it was unavoidable for having calculations.

3.7.1 Light reactions

As mentioned in chapter 2, the elementary flux modes are thermodynamically feasible pathways involved in a metabolic network. Therefore, the EFM analysis on any metabolic system provides the different possibilities of metabolic pathways and reactions hidden in the system. Figure 3.16 shows the metabolic inputs and outputs involved in the system.

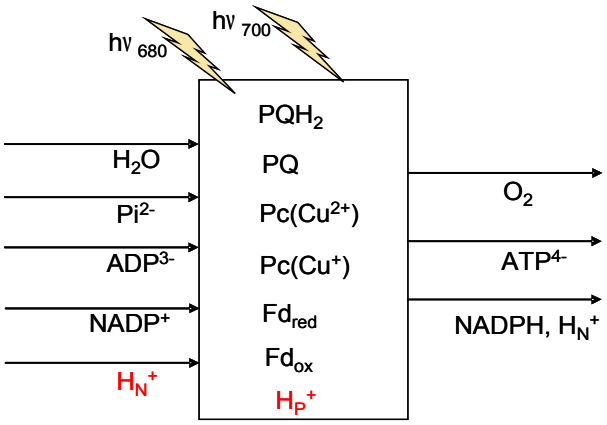

Figure 3.33 : System with inputs and outputs

When the light reaction metabolic network has been subjected to elementary flux mode analysis using METATOOL 5.1, two elementary flux modes are obtained:

EFM 1: $3\ h\nu_{700} + H^{+}_{N} + ADP^{3-} + Pi^{2-} \rightarrow ATP^{4-} + H_2O$

EFM 2: $2\ h\nu_{680} + 2\ h\nu_{700} + 2\ H^{+}_{N} + NADP^{+} + 2\ ADP^{3-} + 2\ Pi^{2-} \rightarrow$

$2\ ATP^{4-} + H_2O + NADPH,H^{+}_{N} + ½\ O_2$

These are actually the results of two different pathways for the light energy conversion - cyclic and non cyclic modes of photophosphorylation. The two modes were first discovered in 1954 by Arnon and co-workers (Arnon *et al.*, 1954). The same pathway we observed (which is given above), when the light reactions network was analysed for EFM analysis.

The reactions involved in EFMs are:

EFM 1 - R2 R3 R4 R6 (cyclic)

EFM 2 - R1 R2 R3 R5 R6 (noncyclic)

Thus, the resulted flux modes provide the mathematical explanative forms of cyclic and noncyclic photophosphorylation metabolic pathways. Though both are distinguished by differences in their electron transfer pathways, these are finally coupled to ATP synthesis and therefore considered alternative mechanisms of photophosphorylation.

Cyclic photophosphorylation produces only ATP whilst non cyclic produces both ATP and NADPH, H^+_N. Cyclic phosphorylation follows a cyclic electron flow through the complexes situated in the thylakoid membrane. Absorbing one quanta of energy, the electron travels through PS I, ferredoxin, plastoquinone, cytochrome b6f and plastocyanin and then finally, the electron is sent back to photosystem I (Follow the pathway, R2 R3 R4 R6 from Figure 3.3).

The transport chain produces a proton-motive force, pumping H^+ ions across the membrane and produces a concentration gradient that can be used to power ATP synthase. Therefore, this results in the ATP production. The first elementary flux mode (EFM 1) involving the equations R2 R3 R4 R6 produce ATP as per the equation given below:

$$3\ h\nu_{700} + H^+_N + ADP^{3-} + Pi^{2-} \rightarrow ATP^{4-} + H_2O$$

The energy for cyclic pathway is calculated ΔG = - 485.9 kJ/mol (using the combination responsible for EFM and the free energy values at physiological conditions given in Table 3.6.). The cyclic electron flow produces only ATP, neither O_2 nor $NADPH/H^+$. Three photons of wavelength at 700 nm are necessary to produce one ATP.

The second elementary flux mode (EFM 2), R1 R2 R3 R5 R6 corresponds to the noncyclic electron flow as given below.

$$2\ h\nu_{680} + 2\ h\nu_{700} + 2\ H^+_N + NADP^+ + 2\ ADP^{3-} + 2\ Pi^{2-} \rightarrow$$
$$2\ ATP^{4-} + H_2O + NADPH,H^+_N + \tfrac{1}{2}\ O_2$$

For this process, calculated ΔG = -365.2 kJ/mol.

Total energy due to eight photons of wave length = $2 \times (2 \times 170.9 + 2 \times 175.9) = 1387$ kJ/mol

Eight photon of wavelength (four at 680 nm and four at 700 nm) with a total energy of about 1387 kJ/mol is necessary for the formation of four ATP, two $NADPH,H^+_N$ and one O_2 molecule.

The change in free energy, $\Delta G = -365.2 \times 2 - (-1387.2) = 656.8$ kJ/mol.

Thus, the coefficient of photosynthesis $\eta_{max} = 656.8/1387 \sim 0.47$.

Almost similar values are reported which says, 8 photons are necessary for the production of one molecule of oxygen (Jorgensen and Svirezhev, 2004). EFM 2 shows the same fact; it also emphasizes the importance of non cylic photophosphorylation.

Plants are forced to create ATP via cyclic and noncyclic pathways and maintain NADPH, H^+_N in the right proportion for the light-independent reactions. The maximal rate of cyclic photophosphorylation is less than 5% of the rate of noncyclic photophosphorylation (Garrett and Grisham, 2000). One of the reasons for this may be due to the small concentration of P_{700} (0.25% of the total amount of chlorophyll) in plants. However, the complex cytochrome *b6f* uses the energy of electrons from not only PSII, but also PSI to create more ATP and thereby maintains the production of NADPH, H^+_N.

Noncyclic photophosphorylation occurs as a result of noncyclic electron flow in the order of the photosynthetic pigments situated (metabolic pathway - R1 R2 R3 R5 R6 from Table 3.6 and Figure 3.3). The two electrons originating in the H_2O/O_2 couple with a redox potential of 780 mV are moved to the redox level of -320 mV reducing one mole of $NADP^+$/NADPH, H^+_N couple. The movement of electrons from 780 mV to -320 mV requires considerable free energy which explains why the relative large amount of energy supplied by the light wavelength of 680 nm (Energy = 175.9 kJ/mol) and 700 nm (Energy = 170.9 kJ/mol) is needed.

The resulted two elementary modes reduce the light reaction metabolic network which can be used for future implementations and coupling with dark reactions in the plant model. Moreover, this study reflects the importance of EFM studies in metabolic network analysis without entering into the details of kinetic factors, genetical experiments and such type of complex and tedious studies. This will be more explained while we study the same system using metabolic flux analysis (MFA).

In the case of small sub systems, the number of EFMs helps to understand the number of degrees of freedom. The number of degrees of freedom provides the necessary and minimum number of experimental data in order to establish a black box model. When metabolic information is used in the model, the degree of freedom reduces. If one understands the various degrees of freedom that exist for a system, the model flexibility and accuracy can be

predicted. The better understanding of the metabolic processes of the system is substantial in this aspect.

3.7.2 Calvin cycle

Similar to the light reaction system, the EFM analysis on Calvin cycle provided a simple and feasible elementary flux mode pathway connecting all equations of the system (from R1 to R15).

The obtained EFM is,

$$12\ NADPH,H_N^+ + 12\ H_2O + 6\ CO_2 + 18\ ATP^{4-} \rightarrow 12\ NADP^+ + 1Glucose + 18\ H_N^+ + 18\ ADP^{3-} + 18\ Pi^{2-}$$

Figure 3.17 shows the inputs and output metabolites involved in the metabolic system.

The energy for the above reaction, $\Delta G \sim$ -150 kJ/mol. This is calcuated using the energy provided for the metabolic reactions participated (Table 3.8). In fact, this is the minimal independent pathway, more elementary modes can be observed, (i) if we add more reactions concerning other metabolic processes or (ii) if we consider more exchangeables as nonexchangeables.

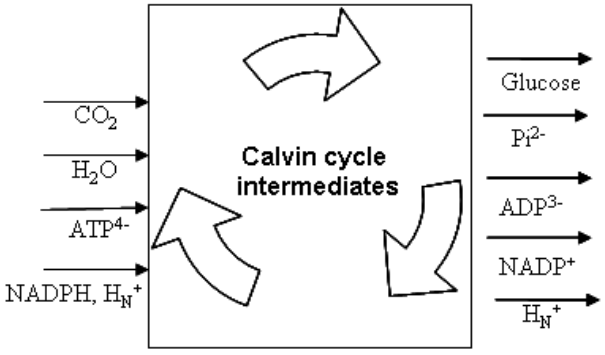

Figure 3.34: System with inputs and outputs

In an earlier study, Poolman *et al*. (2004) found a number of elementary modes for the formation of starch, starting from $RuBP^{4-}$. However, the flux mode we found cannot be subdivided into further modes; but, it can be used for coupling with EFMs of light reactions or similar type of metabolic networks requiring photosynthetic energy.

Nevertheless, the obtained elementary mode for Calvin cycle cannot exist alone as the metabolites participated are not independent elements; without reacting with the available energy in chloroplast stroma, it is not capable of producing neither glucose nor triose phosphate.

3.7.3 Electron transport and oxidative phosphorylation

Two elementary modes were determined when the constructed metabolic network has been subjected to the elementary flux mode analysis. The different pathways for ATP formation in plant cells: one linked with $NADH,H_N^+$ and the other with $FADH_2$.

These are the backbones of the mitochondrial energetic pathways. Electron flow and ATP synthesis are so tightly coupled in the sense that, in normal mitochondria, neither occurs without the other. Two electrons are transferred down the chain per oxygen atom reduced; the P/O ratio reflects the ratio of ATPs synthesised per pair of electrons consumed.

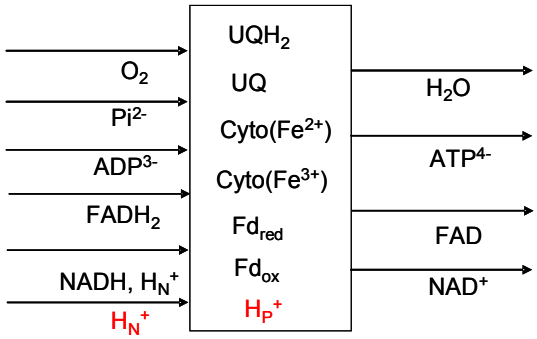

Figure 3.35: Mitochondrial electron transport and oxidative phosphorylation system with inputs and outputs

It is reported that the P/O ratio is 3 or close to 2.5 for $NADH,H_N^+$ oxidation and 2 or close to 1.5 for $FADH_2$ oxidation (Rich, 2003; Hinkle *et al*., 1991). These ratios are largely confirmed in plant mitochondria (Smith, 1977). The oxidation pathways discovered by them is given by the resulted EFMs.

They are:

EFM 1

$$3.33\ H_N^+ + 3.33\ ADP^{3-} + 3.33\ Pi^{2-} + ½\ O_2 + NADH,H_N^+ \rightarrow NAD^+ + 3.33\ ATP^{4-} + 4.33\ H_2O$$

EFM 2

$$2\ H_N^+ + 2\ ADP^{3-} + 2\ Pi^{2-} + ½\ O_2 + FADH_2 \rightarrow FAD + 2\ ATP^{4-} + 3\ H_2O$$

These two EFMs describe the possible and experimentally determined pathways starting from $NADH,H_N^+$ and $FADH_2$. The first elementary flux mode is formed as a result of reactions - R1 R3 R4 R5 (See Figure 3.14); it is produced as a combination of 3 R1 + 3 R3 + 3 R4 + 10 R5 which gives enormous energy (ΔG = -1165.8 kJ/mol). The existence of two respiratory pathways, both transporting electrons to oxygen in higher plant mitochondria raises the question how the partitioning of electrons between the two pathways is regulated. It is actually regulated by cytochrome and ubiquinone pool (Carbo *et al*., 1995). Nevertheless,

the pumping of electrons across the inner membrane causes a concentration gradient across the membrane. By diffusion, the hydrogen ions travel back into the matrix to reach the equilibrium condition. This causes the ATP formation.

Metabolic systems	Resulting EFMs
Light reactions	1. $3\ h\nu_{700} + H^+_N + ADP^{3-} + Pi^{2-} \rightarrow ATP^{4-} + H_2O$ 2. $2\ h\nu_{700} + 2\ h\nu_{680} + 2H^+_N + NADP^+ + 2\ ADP^{3-} + 2\ Pi^{2-} \rightarrow 2\ ATP^{4-} + H_2O + NADPH, H_N^+ + ½\ O_2$
Calvin cycle	1. $12\ NADPH, H_N^+ + 12\ H_2O + 6\ CO_2 + 18\ ATP^{4-} \rightarrow 18\ ADP^{3-} + 18\ Pi^{2-} + 12\ NADP^+ + Glucose + 18\ H_N^+$
Oxidative phosphorylation	1. $3.33\ H^+_N + 3.33\ ADP^{3-} + 3.33\ Pi^{2-} + ½\ O_2 + NADH, H^+_N \rightarrow NAD^+ + 3.33\ ATP^{4-} + 4.33\ H_2O$ 2. $2\ H_N^+ + 2\ ADP^{3-} + 2\ Pi^{2-} + ½\ O_2 + FADH_2 \rightarrow FAD + 2\ ATP^{4-} + 3\ H_2O$
Krebs cycle	1. $2\ H_N^+ + 2\ H_2O + ADP^{3-} + Pi^{2-} + Acetyl\ CoA^- + FAD + 3\ NAD^+ \rightarrow 3\ NADH, H_N^+ + FADH_2 + 2\ CO_2 + ATP^{4-} +$ Coenzyme A
Glycolysis	1. $Glucose + 4\ NAD^+ + 2\ ADP^{3-} + 2\ Pi^{2-} + 2\ CoA \rightarrow 2\ ATP^{4-} + 2\ AcCoA^- + 2\ H_2O + 2\ CO_2 + 4\ NADH, H_N^+$

Table 3.28: Obtained elementary flux modes for subsystems of central carbon metabolism

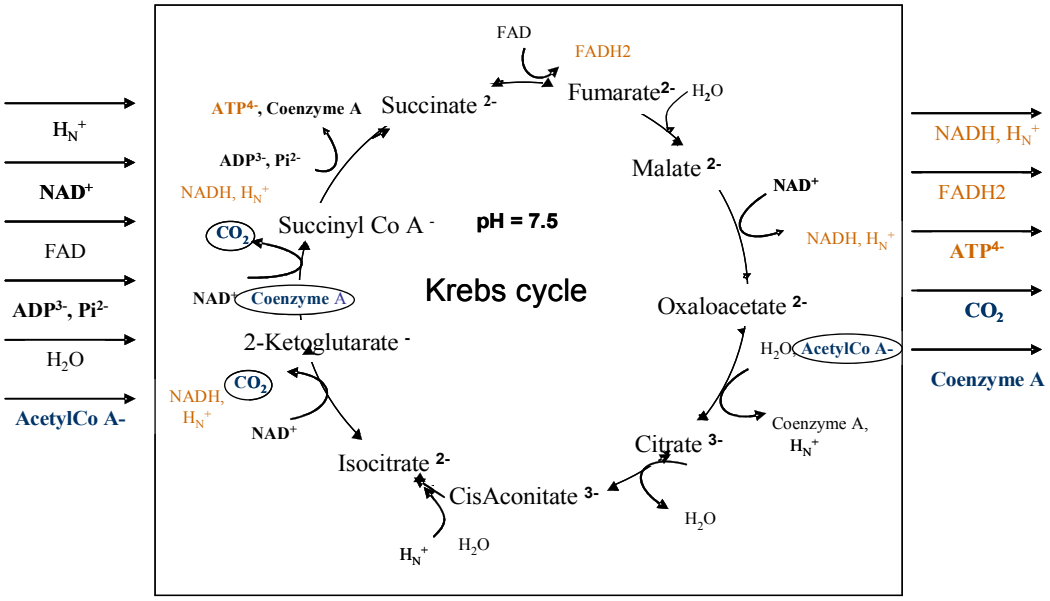

Figure 3.36: Krebs cycle system with inputs and outputs

The second elementary mode (R2 R3 R4 R5) using $FADH_2$ also produces ATP. The combination responsible for EFM 2 is R2 + R3 + R4 + 2 R5, ΔG = -230.2 kJ/mol. $FADH_2$ accounts only 2 ATPs. It reacts with ubiquinone instead of FMN; thus, the proton pumping does not use electrons. Therefore, $FADH_2$ contributes less to the proton gradient than $NADH,H_N^+$; it provides enough power for the production of two ATPs rather than three as $NADH,H_N^+$ does. Obviously, both two respiratory pathways are essential even for the maintenance of high photosynthetic rates at saturating light (Smith, 1977). Agreeing the classical studies of oxidative phosphorylation, the two resulted elementary modes reveal the true metabolic pathways for the ATP formation: $NADH,H_N^+$ gives 3.33 and $FADH_2$ gives only 2 ATPs. In this way, EFM analysis reduced the network of 5 stoichiometric metabolic equations into two.

3.7.4 Krebs cycle

Similar to the Calvin cycle system, we found only one elementary mode for Krebs cycle. The resulted elementary flux mode is the shortest possible thermodynamically feasible pathway for Krebs cycle (Figure 3.19). The metabolic pathway associated with the following EFM involves a series of reactions, from R1 to R9.

$$2\ H_N^+ + ADP^{3-} + Pi^{2-} + \text{Acetyl Co } A^- + 2\ H_2O + FAD + 3\ NAD^+ \rightarrow$$
$$3\ NADH,H_N^+ + FADH_2 + 2\ CO_2 + ATP^{4-} + \text{Coenzyme A}$$

The input of acetyl CoA allows the TCA cycle to maintain a cyclic flux in which the levels of all intermeadiates of the cycle remain constant. In plants, acetyl CoA is usually derived from the products of glycolysis. The pyruvate is either imported directly from the cytosol, or is synthesised from cytosolic phosphoenolpyruvate (PEP). The main benefit of TCA cycle is the generation of more ATP and reducing equivalents in order to carry out the metabolic functions, oxidative phosphorylation. But, sometimes the whole TCA cycle will not occur, as the organisation of TCA cycle in plants is highly dependent on the metabolic and biochemical demands of the cell. This will be discussed later (paragraph 3.9.3.2).

3.7.5 Glycolysis

The number of elementary flux mode for glycolysis network is found to be one. The system is tightly fixed. The resulted EFM equation for glycolysis constituted by 11 reactions is,

$$\text{Glucose} + 4\ NAD^+ + 2\ ADP^{3-} + 2\ Pi^{2-} + 2\ \text{CoA} \rightarrow 2\ ATP^{4-} + 2\ H_2O + 4\ NADH,H_N^+ +$$
$$2\ \text{AcCoA-} + 2\ CO_2$$

2 ATP is produced per glucose as a consequence of glycolysis. The reducing equivalent, NADH, H_N^+ produced by glycolysis cannot cross the mitochondrial inner membrane. Therefore, glycolysis is one of the factors to control the concentration levels of NADH, H_N^+ and NADPH,H_N^+ in cell cytosol. The simple and basic pathway of glycolysis has a high versatility, as most of the metabolic equations have free energy values near to equilibrium.

3.8 Metabolic flux analysis

3.8.1 Light reactions

According to the experimental data reported by Nissen (Nissen *et al*., 1997), metabolic flux analysis is validated in terms of predictability and accuracy with precise measurements of the specific consumption rates of the substrates and the production rates of the products. For metabolic flux analysis, the program detected one degree of freedom; hence, two independent flux values were fixed. As we did not measure metabolite's rate of production/consumption for light reactions using radio active techniques or any other methods/experiments, we have assumed the production rates of ATP^{4-} and NADPH,H^+_N: ATP^{4-} = 300 μ mol s^{-1}, NADPH,H^+_N = 100 μ mol s^{-1}. The estimated intracellular fluxes are shown in Figure 3.20 (See, R6 = 300 μ mol s^{-1} and R5 = 100 μ mol s^{-1} Figure 3.20 (a)). All fluxes are positive for reversible as well as irreversible reactions, thus not violating thermodynamic or biochemical constraint. The flux distribution reflects the existence of two elementary modes of cyclic and noncyclic photophosphorylation, superimposed on each other. EFM and MFA results are correlated in such a way that knowing the EFMs of a system, the exact behaviour in terms of exchangeables (output/input) can be interpreted. Taking the EFMs corresponding to cyclic and noncyclic photophosphorylation, the flux distribution shown in Figure 3.20 (a) is explained as a sum of 100 EFM 1 + 100 EFM 2 (as NADPH,H_N^+ = 100 μ mol s^{-1} and ATP^{4-} = 300 μ mol s^{-1}), see Table 3.22. But, Figure 3.20 (b) is resulted because of 100 EFM 2 (NADPH,H_N^+ = 100 μ mol s^{-1} and ATP^{4-} = 200 μ mol s^{-1}); i.e. EFM 1 is absent in Figure 3.20 (b) due to the low ATP^{4-} production rate. The rate assumptions provided for the Figures 3.20 (a) and (b) automatically determine/fix which EFM should have given more priority. The exchangeable metabolites follow the ratios of metabolites involved in the EFMs or we can say that the metabolic flux distribution reflects the involved EFMs.

Further, the photophosphorylation ratio P/$2e^-$ (J_{ATP}/J_{NADP} = 300/100 = 3) is calculated. In the absence of cyclic reactions, P/2e- will be less than 3. If the ratio of ATP: NADPH, H^+_N is not

3:1; e.g. if ATP^{4-} is fixed as 200 μ mol s^{-1} where NADPH, H^{+}_{N} = 100 μ mol s^{-1} (Figure 3.6(b)), R4 is close to zero, i.e. $P/2e^{-} = 2$.

The existence of PSI cyclic photophosphorylation activity is a great requirement for the subsequent CO_2 fixation in chloroplasts. In order to maintain the necessary balance between ATP and NADPH, H^{+}_{N} for CO_2 fixation activity, PSI cyclic electron flow accounts a mechanism by which the chloroplast regulates cyclic and noncyclic electron transport. It is reported that this mechanism is closely related to the ferredoxin and plastoquinone/plastoquinol complex with restriction of electron flow from PSII to PQ (Arnon and Chain, 1975). This is explained here mathematically, when the equation R4 ($PQ + 2\ Fd_{red} + 2\ H_P^{+} \rightarrow PQH_2 + 2\ Fd_{ox}$) which regulates the system became zero. Moreover, the addition of NADPH, H^{+}_{N} to isolated thylakoids in the presence of ferredoxin stimulates cyclic photophosphorylation (Arnon and Chain, 1975; Ravenel *et al*., 1994) and the NADPH,H^{+}_{N} /$NADP^{+}$ ratio has been proposed to regulate the partitioning of electrons between the cyclic and noncyclic pathways at the level of ferredoxin (Arnon and Chain, 1975).

The existence of two electron transfer pathways leads to a novel explanation of the regulation of cyclic and noncyclic electron transport to optimize the ratio of ATP and NADPH, H_N^{+} *in vivo*. The $P/2e^{-}$ ratio never falls significantly below 1.5 in the case of light reactions. Studies have been carried out regarding the possible contribution of cyclic phosphorylation to non-cyclicphosphorylation; it is suggested that not more than 10% of the total phosphorylation could be due to cyclic phosphorylation (Reeves and Hall, 1973). This means, 90% of the photophosphorylation is due to non cylic electron flow. This is applicable while considering *in vivo* biomass production.

Additionally it is noted that, water releases as a result of light reactions, if and only if cyclic reactions are absent. As this is not the case, inside the cell, the produced water molecule might be used for other reactions (e.g. Calvin cycle uses one molecule of water); furthermore, cell cytoplasm is aqueous. The overall reactions indicate the overall stoichiometry in terms of the external metabolites; this is very helpful in determining optimal yields. The metabolic flux distribution values for the metabolites of photosynthetic systems are shown in Table 3.22.

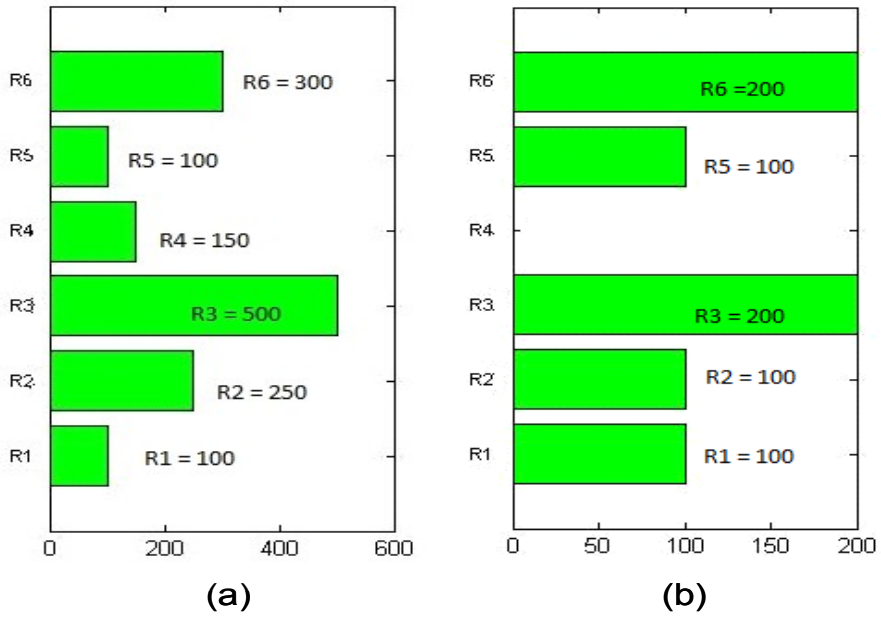

Figure 3.37: Metabolic flux distribution for light reactions

(a): $NADPH,H^{+}_{N}$ = 100 µ $mols^{-1}$ and ATP^{4-} = 300 µ mol s^{-1} (b): $NADPH,H^{+}_{N}$ = 100 µ mol s^{-1} and ATP^{4-} = 200 µ mol s^{-1}

Studied systems	Light reactions (µ mol s^{-1})	Calvin cycle (µ mol s^{-1})
Exchangeables fixed	ATP^{4-} = 300 $NADPH,H_N^+$ = 100	Glucose = 100
Production/ consumption rates for exchangeables	$h\nu_{680}$ = -200 $h\nu_{700}$ = -500 H_2O = 200 $NADP^+$ = -100 ADP^{3-} = -300 Pi^{2-} = -300 H_N^+ = -300 O_2 = 50	$NADPH,H_N^+$ = -1200 $NADP^+$ = 1200 H_2O = -1200 ADP^{3-} = 1800 ATP^{4-} = -1800 Pi^{2-} = 1800 H_N^+ = 1800 CO_2 = -600

Table 3.29: Metabolic flux distributions for photosynthesis

3.8.2 Calvin cycle

In order to analyse MFA, it was required to provide one of the output/input production or consumption values from the exchangeables listed, as the system detected zero degree of freedom. Hence, when we fixed the glucose production = 100 μ mol s^{-1}, we found the metabolic flux distributions as shown in the Figure 3.21. The flux distribution of Calvin cycle reactions can also be explained in terms of EFM of Calvin cycle (100 times of Calvin cycle EFM, since glucose = 100 μ mol s^{-1}); see the rates of exchangeable metabolites from Table 3.22.

In Figure 3.21, the equation R8 ($Ru5P^{2-} \leftrightarrow Xu5P^{2-}$) is having negative value of about -400 μ mol s^{-1} which means it goes in the reverse direction; it can proceed the direction so, as the particular reaction is thermodynamically reversible, $\Delta G \sim 0$. Also, the carbon fixation by $RuBP^{4-}$ occurs 6 times greater than that of glucose production. The energy consuming reactions are R2, R3 and R13. From these, P/2e- ratio is calculated as 1.5 ($J_{ATP}{}^{4-}/J_{NADPH,HN}{}^{+}$), which is considered and confirmed as true value by recent experiments (Kramer *et al*., 1999). The metabolic flux distributions in terms of exchangeables are given in Table 3.22. From the table, one molecule of glucose production needs 18 ATP^{4-} and 12 $NADPH,H_N{}^{+}$, exactly matching with the classical studies.

The most interesting thing is, even though we are not considering enzymatic effects, the metabolic system mathematically works and predicts physiological yields closely matching with the experimental results. We agree the importance of enzymes like RuBisCO which catalyses the carboxylation of RuBP ($CO_2 + RuBP^{4-} + H_2O \rightarrow 2\ (PGA)^{3-} + 2\ H_N{}^{+}$) during Calvin cycle reactions. In fact, it is the most abundant protein in plant leaves accounting 50% of the soluble leaf protein. But, these kinds of information are not necessary in order to analyse the metabolic network using neither MFA nor EFM analyses.

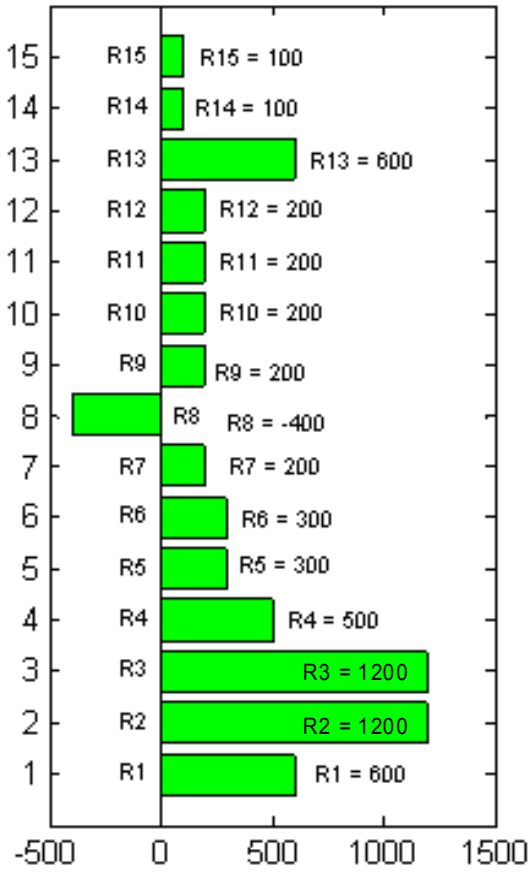

Figure 3.38: Metabolic flux distribution for Calvin cycle reactions Glucose = 100μ mols-1

3.8.3 Electron transport and oxidative phosphorylation

For mitochondrial electron transport system, two metabolite consumption/production rates are fixed to obtain the possible flux distributions shown in Figure 3.22. The flux distribution figures express the presence of two various elementary modes at different conditions.

The P/O ratio may be lower when oxidative phosphorylation reactions are coupled to other reactions (e.g. Krebs' cycle), or if, any of the reactions are blocked by inhibitors or due to climatic stress. When the rate of use of ATP is relatively low, the rate of electron transfer decreases and when demand for ATP increases, the electron transfer rate also increases.

By fixing various values for P/O ratio, we have studied the connections with other reactions/or complexes involved in the electron transport and oxidative phosphorylation similar to the studies previously done for light reactions. We considered four situations for mitochondrial phosphorylation, P/O ratio: (a) $FADH_2 = 2$ and NADH, $H_N^+ = 3.33$; (b) $FADH_2 = 2$, NADH, $H_N^+ = 0$; (c) $FADH_2 = 0$, NADH, $H_N^+ = 3.33$ (d) $FADH_2 = 0$, NADH,$H_N^+ = 1$. The

condition (a) is normal, while (b), (c) and (d) are abnormal and the cell survival rarely happens. The metabolites are fixed as follows and the metabolic flux distributions are shown in Figure 3.22:

(a) ATP^{4-} = 533 μ mol s^{-1} and $FADH_2$ = -100 μ mol s^{-1}

This is the normal physiological cell condition according to almost all theories (including our results). All fluxes are positive for reversible as well as irreversible reactions without violating any thermodynamic or biochemical constraint. Figure 3.22 (a) is formed as a result of two EFMs of mitochondrial electron transport of Table 3.21 (100 EFM 1 + 100 EFM 2, since the rates are fixed as ATP^{4-} = 533 μ mol s^{-1} and $FADH_2$ = -100 μ mol s^{-1}). The reactions R3 and R4 representing metabolic processes at cytochrome/ubiquinone and water formation proceed at similar rates (200 μ mol s^{-1}). Further, R1 ~100 μ mol s^{-1} which means NADH, H_N^+ = -100 μ mol s^{-1}; it produces ATP^{4-} at the rate of 333 μ mol s^{-1}; again, $FADH_2$ = -100 μ mol s^{-1} which produces ATP^{4-} at the rate of 200 μ mol s^{-1}. I.e. in total, ATP^{4-} production = 533 μ mol s^{-1}

(b) $FADH_2$ = -100 μ mol s^{-1} and ATP^{4-} = 200 μ mol s^{-1}

Figure 3.22 (b) is obtained because of 100 times of EFM 2 (Table 3.21), since the rates are fixed as ATP^{4-} = 200 μ mol s^{-1} and $FADH_2$ = -100 μ mol s^{-1}. Hence, EFM 1 (associated with NADH, H_N^+ oxidation) does not occur due to the low rate values we fixed for the system. In fact, this is the condition when P/O ratio is lower than the usual circumstances; the metabolic flux distribution shows R1 = 0, which means NADH, H_N^+ = 0; the phosphorylation occurs only because of $FADH_2$. Eqn. R1 is associated with ubiquinone/ubiquinol and complex I (NADH- dehydrogenase):

$$UQ + NADH,H_N^+ + 4\ H_N^+ \rightarrow UQH_2 + 4\ H_P^+ + NAD^+$$

Just a while ago, it is reported that similar condition happens, only if rotenone (a toxic chemical) inhibits the transfer of electrons from iron-sulfur centers of mitochondrial complex I to ubiquinone, interfering the ATP production (Moller, 2001). In the same way, rotenone can influence the mitochondrial life of insects and kill them; hence, a light dusting of it on the plant leaves protects the plants for several days.

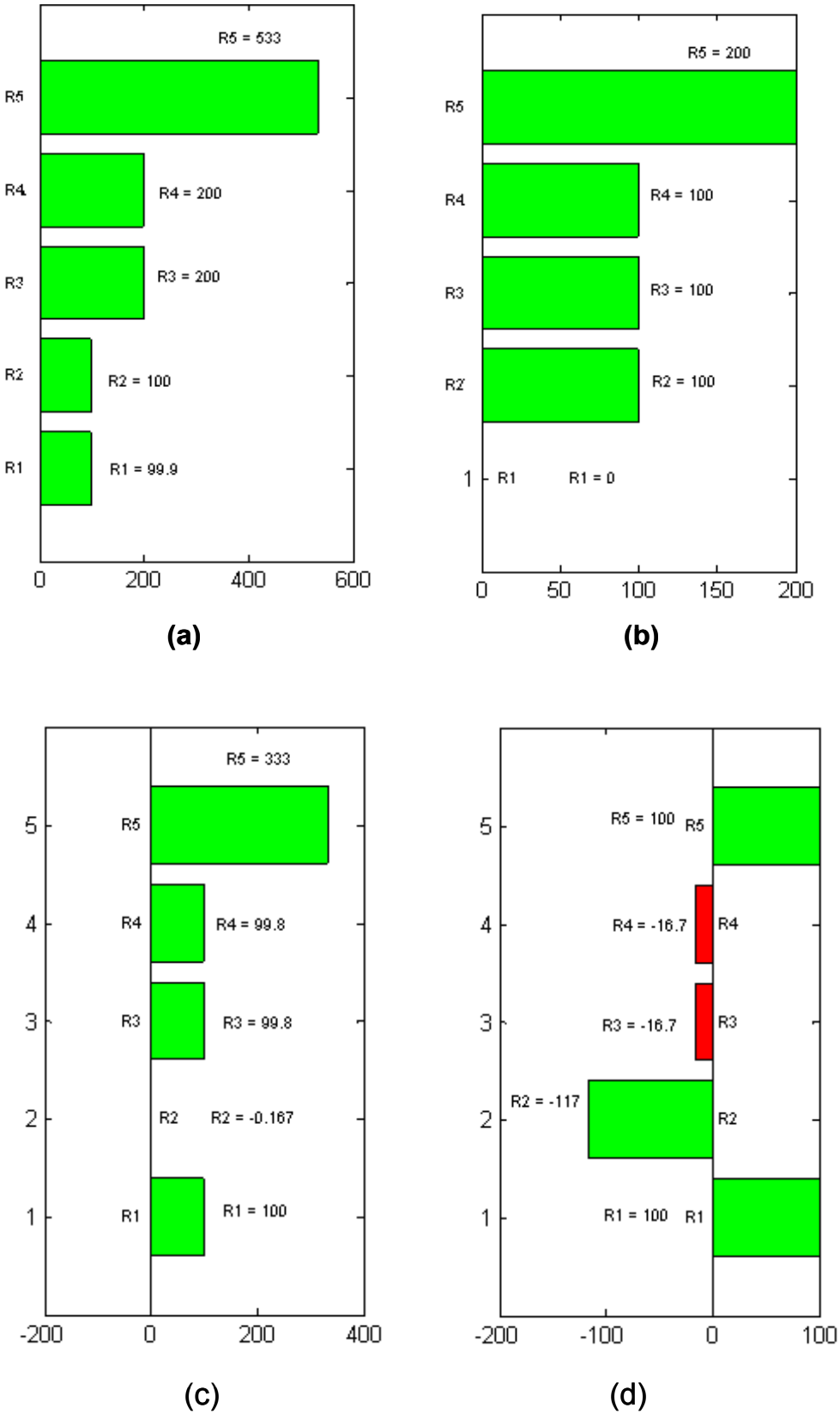

Figure 3.39: Various possibilities of oxidative phosphorylation in mitochondria

(c) $\underline{NADH,H_N^+ = -100\ \mu mol\ s^{-1} \text{ and } ATP^{4-} = 333\ \mu mol\ s^{-1}}$

This condition happens when P/O ratio is lower than the previous case; the metabolic flux graph gives R2 = 0, i.e. $FADH_2 = 0$, the condition where $FADH_2$ oxidation does not occur. In that case, phosphorylation occurs only due to NADH, H_N^+. This condition can make severe challenges for the survival of a cell. The flux distribution Figure 3.22 (c) shows the presence of only one EFM (EFM 1) associated with NADH, H_N^+ oxidation.

(d) $\underline{NADH,H_N^+ = -100\ \mu mol\ S^{-1} \text{ and } ATP^{4-} = 100\ \mu mol\ S^{-1}}$

This situation stands for very low P/O ratio. Neither of the two EFMs involved in the system (EFM 1 and EFM 2) do not precede well due to the rate values we provided. Hence in Figure 3.22 (c), the reactions R2, R3 and R4 are occurring in the negative direction. It is possible for R2 and R3 to be in reverse direction; but, it seems impossible for R4. However in such a case, the transmembrane potential is certainly affected so that the calculations done in paragraph 3.4.4 might be reconsidered. This would clearly call for a variable stoichiometry analysis considering that the ΔG already calculated at nominal conditions does not remain valid as soon as Q-cycle is no longer functioning in a "normal" way.

R2 $FADH_2 + UQ \leftrightarrow FAD + UQH_2$

R3 $UQH_2 + 2 \text{ cyto } Fe^{3+} + 2\ H_N^+ \rightarrow UQ + 4\ H_P^+ + 2 \text{ cyto } Fe^{2+}$

R4 $\frac{1}{2}\ O_2 + 4\ H_N^+ + 2 \text{ cyto } Fe^{2+} \rightarrow 2 \text{ cyto } Fe^{3+} + H_2O + 2\ H_P^+$

Nevertheless, inhibitors like 'antimycin A' can create such a situation in mitochondria. Antimycin A binds to the Q site of cytochrome c reductase, thereby inhibiting the oxidation of ubiquinol in the electron transport chain of oxidative phosphorylation (Moller, 2001). Moller studied very well this phenomenon; the inhibition of this reaction disrupts the formation of the proton gradient across the inner membrane. The production of ATP is subsequently inhibited, as protons are unable to flow through the ATP synthase complex (Moller, 2001).

Further, uncouplers of oxidative phosphorylation inhibit the coupling between electron transport and phosphorylation reactions and thus inhibit ATP synthesis without affecting respiratory chain and ATP synthase (Terada, 1990). In the presence of an uncoupling agent (though it is relatively low), the P/O ratios drop; but, the cell can compensate this by increasing the rate of electron flow; ATP levels can be kept relatively normal (Emerson *et al*., 1944). At high levels of an uncoupler, the P/O ratios approach zero and the cell cannot maintain ATP levels. This condition may occur *in vivo*, if cell consumes an uncoupler like ethanol. In such cases, alcohol directly affects mitochondria (Fukumura *et al*., 2003). When the possibility of a bypass of complex I via rotenone-insensitive pathway and other inhibitory

possibilities are taken into account, the ATP yield can vary from zero to three per NADH, H^+ oxidation which may lead serious diseases. Thus, the worst condition may occur due to the effect of uncouplers on mitochondria explaining the metabolic condition of drunkers. However, mitochondrial diseases are rare, because the defects in the respiratory chain are incompatible with life and affected embryos rarely survive to birth (Garrett and Grisham, 2000). Thus, MFA acts as a platform to study and understand the relative ATP production differences in cellular level and how the complexes are involved in the electron transport of respiratory chain without conducting any experiments.

On a methodological point of view, this clearly shows that EFM brings useful topological information, considering a set of hypotheses concerning reversibility of reactions. When this set does not remain valid, only MFA can bring further useful and interesting information.

3.8.4 Krebs cycle

The Krebs cycle provides intermediates for numerous biosynthetic processes in the cell. It is always found oxidative phosphorylation couples to the mitochondrial electron transport chain via succinate. However, here we consider the reactions involved only in Krebs cycle. The metabolic flux map is shown in Figure 3.23 obtained by fixing Coenzyme A production as 100 μ mol s^{-1}; it seems that all reactions happen at the same rate.

The P/O quotient, the measure of the coupling between electron flow and phosphorylation may vary depending on the extent of coupling between oxidation and ATP synthesis; if the membranes are leaky to protons (uncoupled), or if the protons are used for the processes other than ATP synthesis (e.g. for ion transport), then the measured P/O ratio will be less than the maximal one (Harris, 1995).

3.8.5 Glycolysis

While analysing metabolic flux analysis for glycolysis, the program detected zero degree of freedom; hence one flux (input or output) value was fixed for the calculation. We assumed the glucose consumption as 100 μ mol s^{-1}. The estimated intracellular fluxes are shown in the graph (Figure 3.23). The flux distribution reflects exactly the existence of only one elementary flux mode. All fluxes are positive for reversible as well as irreversible reactions, thus not violating thermodynamical or biochemical constraint. The metabolic flux distributions for respiratory components are listed in Table 3.24 in terms of exchangeables.

Recent evidence from labelling studies and metabolic network models suggest that the organisation of carboxylic acid metabolism in plants is highly dependent on the metabolic and physiological demands of the cell (Sweetlove *et al*., 2010).

For all the 5 metabolic sub systems considered here, the constructed elementary modes are irreversible and indecomposable (Table 3.21) which clearly demonstrate the metabolic flux distributions for each system under study (Table 3.22 and 3.24). Table 3.23 depicts all metabolites (exchangeable and non exchangeables) involved in each sub system of central carbon metabolism.

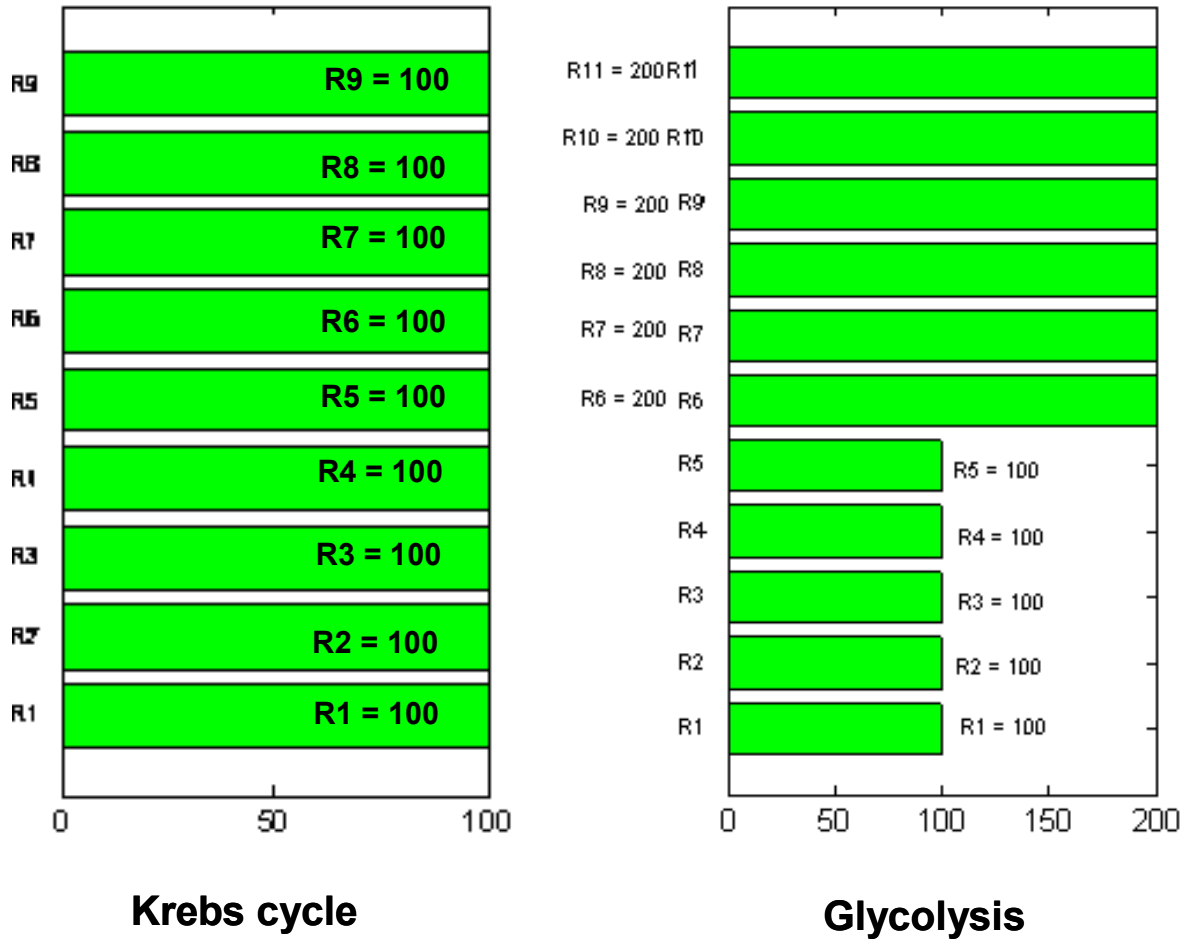

Figure 3.40: Metabolic flux distributions for Krebs cycle and Glycolysis

Light reactions		Calvin cycle			
NE	**E**	**NE**		**E**	
$Pc\ (Cu^{+})$ $Pc\ (Cu^{2+})$ Fd_{ox} Fd_{red} PQH_2 PQ H_P^+	$h\nu_{700}$ $h\nu_{680}$ O_2 H_2O H^+_N $NADP^+$ $NADPH,H_N^+$ ATP^{4-} ADP^{3-} Pi^{2-}	$RuBP^{4-}$ PGA^{3-} $1\text{-}3BPGA^{4}$ $G3P^{2-}$ $DHAP^{2-}$ $Ru5P^{2-}$ $R5P^{2-}$	FBP^{4-} $F6P^{2-}$ $G6P^{2-}$ $E4P^{2-}$ $Xu5P^{2-}$ SBP^{4-} $S7P^{2-}$	O_2 H_2O CO_2 Glucose $NADP^+$ $NADPH,H_N^+$ ATP^{4-} ADP^{3-} Pi^{2-} H_N^+	
Oxidative phosphorylation		Krebs cycle		Glycolysis	
NE	**E**	**NE**	**E**	**NE**	**E**
H^+_P UQ UQH_2 cyto Fe^{3+} cyto Fe^{2+}	H^+_N H_2O O_2 FAD $FADH_2$ NAD^+ $NADH,H^+_N$ ATP^{4-} ADP^{3-} Pi^{2-}	$Oxaloacetate^{2-}$ $Citrate^{3-}$ *cis*-$Aconitate^{3-}$ $D\text{-}Isocitrate^{3-}$ 2- $Ketoglutarate^{2-}$ Succinyl- CoA- $Succinate^{2-}$ $Fumarate^{2-}$ $Malate^{2-}$	H^+_N H_2O CO_2 Coenzyme A Acetyl CoA- ATP^{4-} ADP^{3-} Pi^{2-} FAD $FADH_2$ NAD^+ $NADH,H_N^+$	Pyruvate- FBP^{4-} $F6P^{2-}$ $G6P^{2-}$ $2PGA^{3-}$ $3PGA^{3-}$ PEP^{3-} $1\text{-}3BPGA^{4}$ $G3P^{2-}$ $DHAP^{2-}$ H_N^+	Glucose H_2O $NADH,H^+_N$ NAD^+ ATP^{4-} ADP^{3-} Pi^{2-} CO_2 Co A AcCoA-

Table 3.30: Metabolites involved in each sub system NE: non exchangeables; E: exchangeables

Studied systems	Oxidative phosphorylation	Krebs cycle	Glycolysis
Exchangeables fixed	$FADH_2$ = -100 ATP^{4-} = 533	CoenzymeA = 100	Glucose = -100
Production/ consumption rates for exchangeables	H_N^+ = -533 O_2 = -100 H_2O = 733 ADP^{3-} = -533 Pi^{2-} = -533 $NADH,H^+_N$ = -100 NAD^+ = 100 FAD = 100	H_N^+ = -200 H_2O = -200 CO_2 = 200 ADP^{3-} = -100 Pi^{2-} = -100 ATP^{4-} = 100 AcetylCoA- = -100 $FADH_2$ = 100 FAD = -100 $NADH,H^+_N$ = 300 NAD^+ = -300	CoA = -200 AcCoA- = 200 H_2O = 200 $NADH,H^+_N$ = 400 NAD^+ = -400 ATP^{4-} = 200 ADP^{3-} = -200 Pi^{2-} = -200 CO_2 = 200

Table 3.31: Metabolic flux distributions for respiratory system

3.9 The unique tuning of Photosynthesis and respiration

Without any doubt, it can be said that photosynthesis and respiration altogether control plant activities; both processes are inevitable for the plant growth and survival. It is always convenient to couple the reactions that are necessarily operated together such as Calvin cycle and light reactions; same for all the three respiratory sub systems of respiration, i.e. electron transport followed by oxidative phosphorylation, Krebs cycle of mitochondria and glycolysis of cell cytosol reflecting the *in vivo* plant central carbon metabolic system. The perfect tuning of photosynthesis and respiration are represented and studied in the following sections.

3.9.1 The energy model construction

3.9.1.1 Light reactions with Calvin cycle

Calvin cycle plays a complementary role and always associated with light reactions of photosynthesis, as they are the source of energy available for photosynthesis. In cellular structural level, the ATP synthesis happens in such a way that the metabolites of Calvin cycle can utilize ATP, at once it is produced as shown in Figure 3.24. Two possibilities are there to study the coupling.

Method 1: Using the entire reactions

In this method, we have just coupled the reactions of light reactions (Table 3.6) and Calvin cycle (Table 3.8). The entire reactions are again given in the Table 3.25. The matrix constructed is given in Table 3.26. The system of light reactions coupling with Calvin cycle has 21 reactions and 33 metabolites on which 10 are exchangeables. The exchangeables and nonexchangeables corresponding to light reactions and Calvin cycle remain the same for the coupling too, except for the energy molecules: NADPH, H_N^+ and $NADP^+$.

Reaction	Metabolic equations	ΔG_{physio} (kJ/mol)
R1	$2\ h\nu_{680}: H_2O + 2\ H_N^+ + PQ \rightarrow PQH_2 + ½\ O_2 + 2\ H_P^+$	-129
R2	$PQH_2 + 2\ Pc\ (Cu^{2+}) + 2\ H_N^+ \leftrightarrow PQ + 2\ Pc\ (Cu^+) + 4\ H_P^+$	-2.8
R3	$1\ h\nu_{700}: Pc\ (Cu^+) + Fd_{ox} \rightarrow Pc\ (Cu^{2+}) + Fd_{red}$	-91.9
R4	$PQ + 2\ Fd_{red} + 2\ H_P^+ \rightarrow PQH_2 + 2\ Fd_{ox}$	-121
R5	$2\ Fd_{red} + 2\ H_N^+ + NADP^+ \rightarrow 2\ Fd_{ox} + NADPH,H_N^+$	-19.4
R6	$3\ H_P^+ + H_N^+ + ADP^{3-} + Pi^{2-} \rightarrow 3\ H_N^+ + ATP^{4-} + H_2O$	-24.5
R7	$CO_2 + RuBP^{4-} + H_2O \rightarrow 2\ (PGA)^{3-} + 2\ H_N^+$	-41
R8	$PGA^{3-} + ATP^{4-} \leftrightarrow 1,3BPGA^{4-} + ADP^{3-}$	-6.7
R9	$1,3BPGA^{4-} + NADPH,H_N^+ \leftrightarrow G3P^{2-} + NADP^+ + Pi^{2-}$	0
R10	$G3P^{2-} \leftrightarrow DHAP^{2-}$	-0.8
R11	$DHAP^{2-} + G3P^{2-} \leftrightarrow FBP^{4-}$	-0.8
R12	$FBP^{4-} + H_2O \rightarrow F6P^{2-} + Pi^{2-}$	-27.2
R13	$F6P^{2-} + G3P^{2-} \leftrightarrow E4P^{2-} + Xu5P^{2-}$	-3.8
R14	$Ru5P^{2-} \leftrightarrow Xu5P^{2-}$	-0.4
R15	$S7P^{2-} + G3P^{2-} \leftrightarrow Xu5P^{2-} + R5P^{2-}$	-5.9
R16	$DHAP^{2-} + E4P^{2-} \leftrightarrow SBP^{4-}$	-1.7
R17	$SBP^{4-} + H_2O \rightarrow S7P^{2-} + Pi^{2-}$	-29.7
R18	$R5P^{2-} \leftrightarrow Ru5P^{2-}$	-0.4
R19	$Ru5P^{2-} + ATP^{4-} \rightarrow RuBP^{4-} + ADP^{3-} + H_N^+$	-15.9
R20	$F6P^{2-} \leftrightarrow G6P^{2-}$	-2.9
R21	$G6P^{2-} + H_2O \rightarrow Glucose + Pi$	Negative

Table 3.32: Metabolic equations for photosynthesis (Method 1)

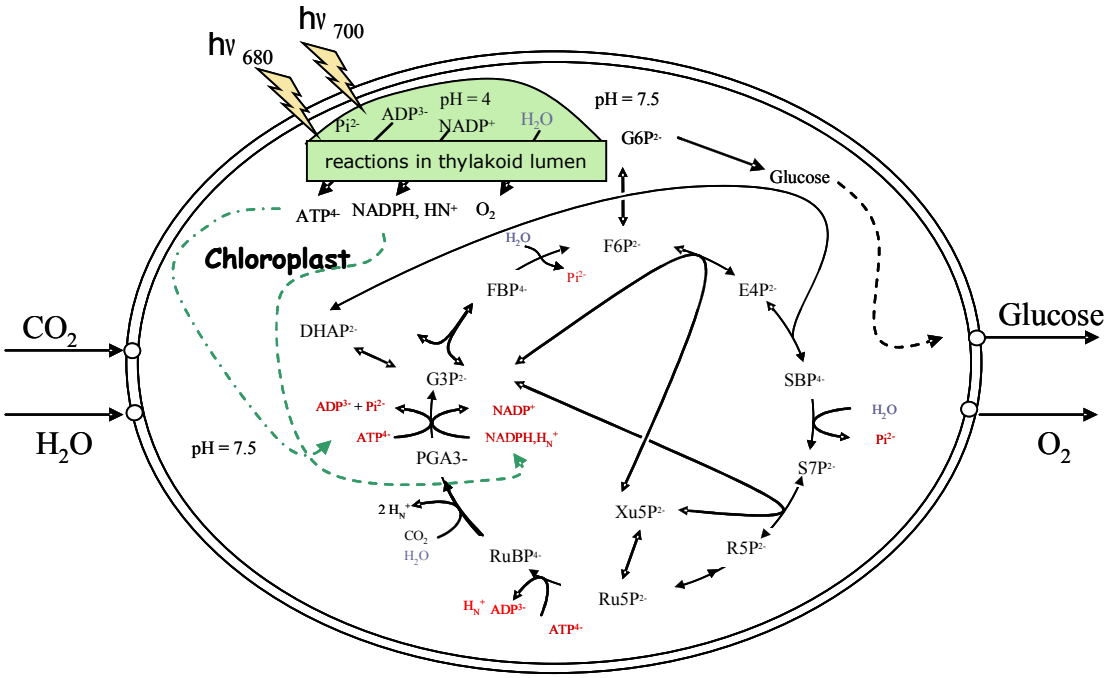

Figure 3.41: Metabolites involved in photosynthesis

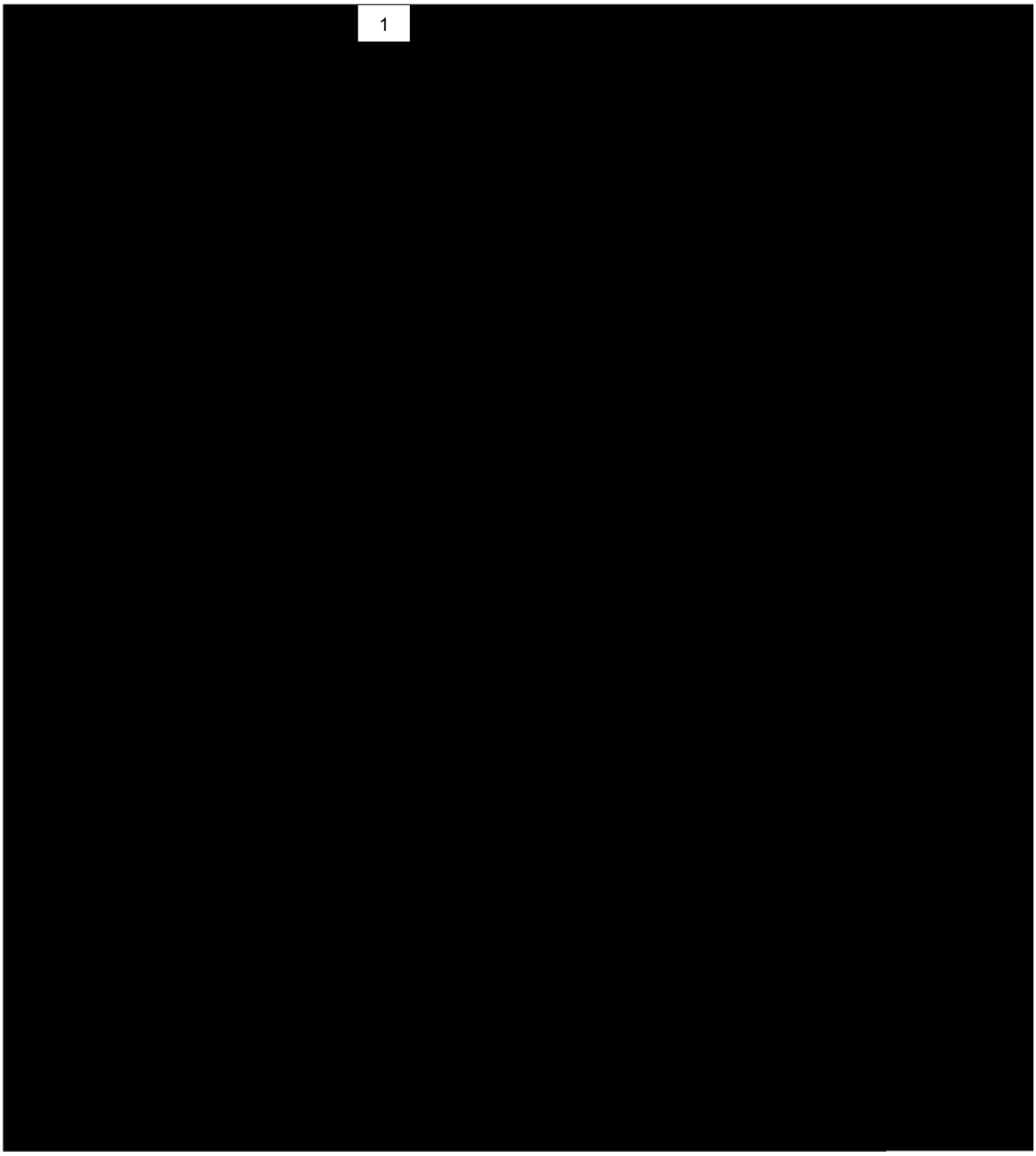

Table 3.33: Metabolic matrix for photosynthesis (Method 1) E = $h\nu_{700}$, $h\nu_{680}$, ATP^{4-}, ADP^{3-}, Pi^{2-}, H_N^+, H_2O, CO_2, Glucose, O_2 ; NE = PGA^{3-}; $RuBP^{4-}$; $Ru5P^{2-}$; $R5P^{2-}$; 1,3-$BPGA^{4-}$; $G3P^{2-}$; $DHAP^{2-}$; FBP^{4-}; $F6P^{2-}$; $E4P^{2-}$; $Xu5P^{2-}$; $G6P^{2-}$; $S7P^{2-}$; SBP^{4-}; PQ; PQH_2; Pc (Cu^{2+}); Pc(Cu^+); Fd $_{ox}$; Fd $_{red}$; H_P^+; $NADPH,H_N^+$; $NADP^+$; Abbreviations : $h\nu_{700}$ and $h\nu_{680}$ = photons at 700 nm and 680 nm respectively; O_2 = oxygen; H_2O = **water;** $NADPH,H_N^+$ = nicotinamide adenine dinucleotide phosphate ; $NADP^+$ = reduced nicotinamide adenine dinucleotide phosphate; ATP^{4-} = adenosine triphosphate; ADP^{3-} = adenosine diphosphate, energy molecule; Pi^{2-} = inorganic phosphate; **H_N^+ and H_P^+** = protonated hydrogen at N and P phases; Fd $_{ed}$ = reduced ferredoxin; Fd $_{ox}$ = oxidised ferredoxin; Pc (Cu^+) = reduced plastocyanin; Pc (Cu^{2+})= reduced plastocyanin; PQH_2 = plastoquinol; PQ =plastoquinone; $DHAP^{2-}$ = **dihydroxyacetone phosphate;** 1, 3-$BPGA^{4-}$= **1, 3- diphosphate glycerate;** CO_2 = carbon dioxide ; $E4P^{2-}$ = **erythrose-4-phosphate;** $FADH_2$ = **reduced flavin adenine dinucleotide;** FBP^{4-} = **fructose 1, 6-biphosphate;** $F6P^{2-}$ = **fructose -6-biphosphate;** $G1P^{2-}$ = **glucose -1-phosphate;** $G6P^{2-}$ = **glucose 6-phosphate;** $G3P^{2-}$ = glyceraldehyde -3-phosphate ; $NADPH,H_N^+$ = nicotinamide adenine dinucleotide phosphate ; $NADP^+$ = reduced nicotinamide adenine dinucleotide phosphate; PGA^{3-} = 3-phosphoglycerate; $RuBP^{4-}$ = **ribulose 1, 5-bisphosphate;** $R5P^{2-}$ = **ribose-5-phosphate;** $Ru5P^{2-}$ = ribulose-5-phosphate; SBP^{4-} = **sedoheptulose 1, 7-biphosphate;** $S7P^{2-}$ = **sedoheptulose-7-biphosphate;** $Xu5P^{2-}$ = **xylulose-5-phosphate**

Method 2: using the obtained EFMs

We have seen that light reactions subsystem has 2 EFMs revealing cyclic and noncyclic photophosphorylation pathways. Besides, Calvin cycle system has only one EFM.

Subsequently, in the coupling dealing the EFMs of both systems involve only 3 equations, which stand for 21 reactions of light reactions (6) and Calvin cycle (15) subsystems; in other words, these 3 EFMs are equivalent to the 21 reactions of Table 3.28. As the inputs and outputs come under the group 'exchangeables', they are taken the same as in the previous system. Then only two energy molecules NADPH, H_N^+; $NADP^+$ are remaining, which fall under non exchangeable group. The matrix representing the metabolic network constituted of three EFMs is given in the Table 3.27. The energy of each EFM is taken from the paragraphs 3.7.1 and 3.7.2.

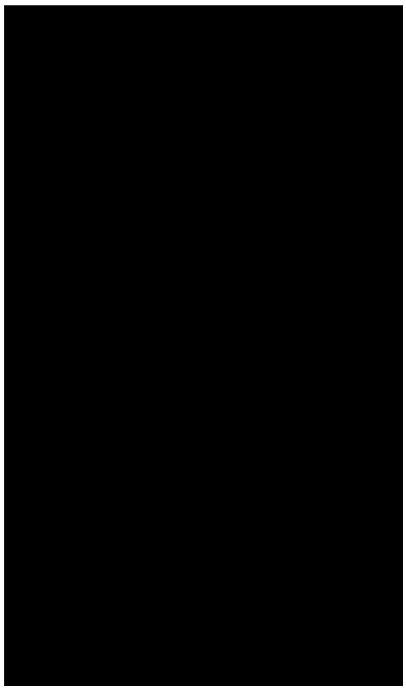

Table 3.34: Metabolic matrix for photosynthesis (Method 2) E = $h\nu_{700}$, $h\nu_{680}$, ATP^{4-}, ADP^{3-}, Pi^{2-}, H_N^+, H_2O, CO_2, Glucose, O2; NE = NADPH, H_N^+; $NADP^+$

		Metabolic equations	ΔG_{physio} (kJ/mol)
Light reactions	R1	$3\ h\nu_{700} + H_N^+ + ADP^{3-} + Pi^{2-} \rightarrow ATP^{4-} + H_2O$	-485.9
	R2	$2\ h\nu_{680} + 2\ h\nu_{700} + 2\ H_N^+ + NADP^+ + 2\ ADP^{3-} + 2\ Pi^{2-} \rightarrow 2\ ATP^{4-} + H_2O + NADPH,H_N^+ + ½\ O_2$	-365.2
Calvin cycle	R3	$12\ NADPH,H_N^+ + 12\ H_2O + 6\ CO_2 + 18\ ATP^{4-} \rightarrow 12\ NADP^+ + Glucose + 18\ H_N^+ + 18\ ADP^{3-} + 18\ Pi^{2-}$	~ -150

Table 3.35: Metabolic equations for photosynthesis (Method 2)

3.9.1.2 Mitochondrial reactions with Glycolysis

Here, we have coupled the reactions occurs in mitochondria with cytosolic glycolysis. These two processes are closely related and combinely know as cellular respiration. Similar to the previous methods 1 and 2, we couple these three sub systems in two ways.

Method 1: Using the entire reactions

Respiration reactions involve 5 reactions of electron transport and oxidative phosphorylation, 9 reactions of Krebs cycle and 11 reactions of glycolysis. Thus altogether, there are 25 reactions as in Table 3.29. The metabolites are separated into exchangeables and non exchangeables. The metabolic matrix is given in Table 3.30.

Reaction	Metabolic equations	ΔG_{physio} (kJ/mol)
R1	Glucose + $ATP^{4-} \rightarrow G6P^{2-} + H_N^+ + ADP^{3-}$	-27.2
R2	$G6P^{2-} \leftrightarrow F6P^{2-}$	-1.4
R3	$F6P^{2-} + ATP^{4-} \rightarrow FBP^{4-} + H_N^+ + ADP^{3-}$	-25.9
R4	$FBP^{4-} \leftrightarrow DHAP^{2-} + G3P^{2-}$	-5.9
R5	$DHAP^{2-} \rightarrow G3P^{2-}$	Negative
R6	$3\ PGA^{3-} \leftrightarrow 2PGA^{3-}$	-0.6
R7	$2\ PGA^{3-} \leftrightarrow PEP^{3-} + H_2O$	-2.4
R8	$G3P^{2-} + Pi^{2-} + NAD^+ \rightarrow 1\text{-}3BPGA^{4-} + NADH, H_N^+$	
R9	$1\text{-}3BPGA^{4-} + ADP^{3-} \rightarrow 3PGA^{3-} + ATP^{4-}$	-16.7
R10	$PEP^{3-} + H_N^+ + ADP^{3-} \rightarrow pyruvate^- + ATP^{4-}$	-13.9
R11	$pyruvate^- + CoA + NAD^+ \rightarrow CO_2 + AcCoA^- + NADH,H_N^+$	
R12	$NADH,H_N^+ + UQ + 4\ H_N^+ \rightarrow NAD^+ + UQH_2 + 4\ H_P^+$	-70.5
R13	$FADH_2 + UQ \leftrightarrow FAD + UQH_2$	-2.9
R14	$UQH_2 + 2$ cyto $Fe^{3+} + 2\ H_N^+ \rightarrow UQ + 4\ H_P^+ + 2$ cyto Fe^{2+}	-11.7
R15	$½\ O_2 + 4\ H_N^+ + 2$ cyto $Fe^{2+} \rightarrow 2$ cyto $Fe^{3+} + H_2O + 2\ H_P^+$	-79.4
R16	$3\ H_P^+ + H_N^+ + ADP^{3-} + Pi^{2-} \rightarrow 3\ H_N^+ + ATP^{4-} + H_2O$	-68.1
R17	$Oxaloacetate^{2-} +$ Acetyl CoA- $+ H_2O \rightarrow Citrate^{3-} +$ Coenzyme A $+ H_N^+$	Negative
R18	$Citrate^{3-} \leftrightarrow$ *cis*-$Aconitate^{3-} + H_2O$	0
R19	*cis*-$Aconitate^{3-} + H_2O + H_N^+ \leftrightarrow$ D-$Isocitrate^{2-}$	
R20	D-$Isocitrate^{2-} + NAD^+ + H_N^+ \rightarrow NADH,H_N^+ +$ 2-Ketoglutarate- $+ CO_2$	Negative
R21	2 -Ketoglutarate- $+ NAD^+ +$ CoenzymeA $\rightarrow$ Succinyl-$CoA^- + NADH,H_N^+ + CO_2$	Negative
R22	Succinyl-CoA- $+ ADP^{3-} + P_i^{2-} \leftrightarrow Succinate^{2-} +$ Coenzyme A $+ ATP^{4-}$	0
R23	$Fumarate^{2-} + H_2O \leftrightarrow Malate^{2-}$	0
R24	$Malate^{2-} + NAD^+ \leftrightarrow Oxaloacetate^{2-} + NADH,H_N^+$	0
R25	$Succinate^{2-} + FAD \leftrightarrow FADH_2 + Fumarate^{2-}$	0

Table 3.36: Metabolic equations for respiration (Method 1)

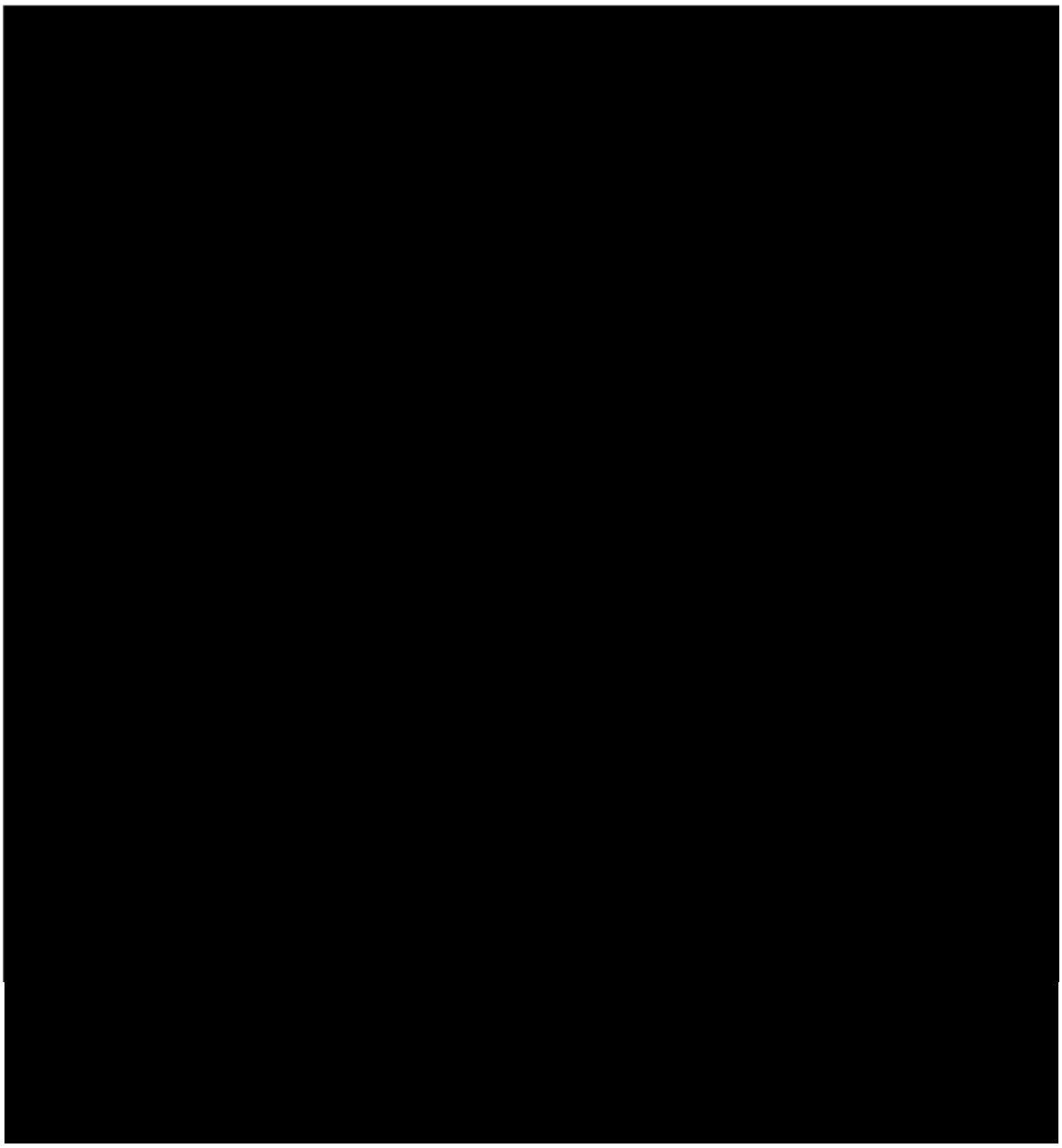

Table 3.37 : Metabolic matrix for respiration (Method 1) E = $NADH,H_N^+$; NAD^+, H_N^+; O_2; H_2O; CO_2; ADP^{3-}; Pi^{2-}; ATP^{4-}; Glucose; NE = UQ, UQH_2, Cyto(Fe^{2+}), Cyto(Fe^{3+}), H_P^+, Fd_{ox}, Fd_{red} $Oxaloacetate^{2-}$, $Citrate^{3-}$, *cis*-$Aconitate^{3-}$, D-$Isocitrate^{2-}$, 2-Ketoglutarate-, Succinyl-CoA^-, $Succinate^{2-}$, $Malate^{2-}$, $Fumarate^{2-}$, $F6P^{2-}$; $G6P^{2-}$; FBP^{4-}; $DHAP^{2-}$; $G3P^{2-}$; $2PGA^{3-}$; $3PGA^{3-}$; PEP^{3-}; 1-3 $BPGA^{4-}$; pyruvate- Coenzyme A ; Acetyl CoA^-; Abbreviations : H_2O = **water;** CO_2 = carbon dioxide; $NADH,H_N^+$ = nicotinamide adenine dinucleotide; NAD^+ = oxidised nicotinamide adenine dinucleotide; ATP^{4-} = adenosine triphosphate; ADP^{3-} = adenosine diphosphate; Pi^{2-} = inorganic phosphate; $2PGA^{3-}$= 2-phosphoglycerate ; PEP^{3-} = phosphoenol pyruvate; $DHAP^{2-}$ = **dihydroxyacetone phosphate;** 1, 3-$BPGA^{4-}$= **1, 3- diphosphate glycerate** FBP^{4-} = **fructose 1, 6-biphosphate;** $F6P^{2-}$ = **fructose -6-biphosphate;** $G6P^{2-}$ = **glucose 6-phosphate;** $G3P^{2-}$ = glyceraldehyde -3-phosphate ; 3 PGA^{3-} = 3-phosphoglycerate; O_2 = oxygen; FAD = flavin adenine dinucleotide ; $FADH_2$ = reduced flavin adenine dinucleotide; **H_N^+ and H_P^+** = protonated hydrogen at N and P phases; Cyto(Fe^{2+}) = reduced iron of heme; Cyto(Fe^{2+}) = oxidised iron of heme; UQH_2 = Ubiquinol; UQ = Ubiquinone

Method 2: Using the obtained EFMs

The elementary flux mode for glycolysis and Krebs cycle gave one for each sub system, where oxidative phosphorylation has two EFMs. Hence in total, 4 EFMs (given in Table 3.31) stand for 25 reactions of respiration system. The matrix with 4 EFMs is created (Table 3.32) by separating metabolites into exchangeables and nonexchangeables. Exchangeables are the same metabolites, we classified for method 1. Only 4 metabolites act as non exchangeables: FAD, $FADH_2$, Coenzyme A and Acetyl CoA^-.

Oxidative phosphorylation	R1	$2\ H^+_N + 2\ ADP^{3-} + 2\ Pi^{2-} + ½\ O_2 + FADH_2 \rightarrow FAD + 2\ ATP^{4-} + 3\ H_2O$
	R2	$3.33\ H^+_N + 3.33\ ADP^{3-} + 3.33\ Pi^{2-} + ½\ O_2 + NADH,H^+_N \rightarrow NAD^+ + 3.33\ ATP^{4-} + 4.33\ H_2O$
Krebs cycle	R3	$2\ H^+_N + 2\ H_2O + ADP^{3-} + Pi^{2-} + \text{Acetyl CoA-} + FAD + 3\ NAD^+ \rightarrow 3\ NADH,H^+_N + FADH_2 + 2\ CO_2 + ATP^{4-} + \text{Coenzyme A}$
Glycolysis	R4	$\text{Glucose} + 4\ NAD^+ + 2\ ADP^{3-} + 2\ Pi^{2-} + 2\ CoA \rightarrow 2\ ATP^{4-} + 2\ \text{Acetyl } CoA^- + 2\ H_2O + 2\ CO_2 + 4\ NADH,H^+_N$

Table 3.38: Metabolic equations for respiration (Method 2)

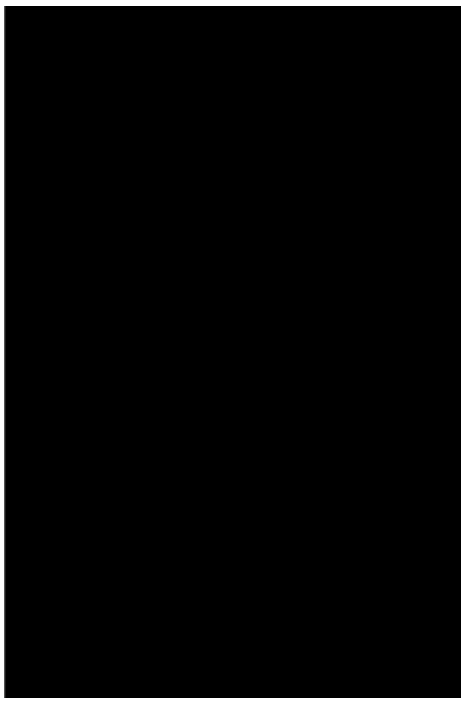

Table 3.39: Metabolic matrix for respiration (Method 2) E = $NADH,H^+_N$; NAD^+, H^+_N; O_2; H_2O; CO_2; ADP^{3-}; Pi^{2-}; ATP^{4-}; Glucose; NE = FAD, $FADH_2$, Coenzyme A, Acetyl CoA^-

3.9.2 Elementary flux mode analysis

The coupled systems obtained for photosynthesis and respiration (using method 1 and 2) are subjected to analyse the network topology and intracellular fluxes using elementary flux mode analysis and metabolic flux analysis similar to what we have done for each small sub system of photosynthesis and respiration.

3.9.2.1 Light reactions with Calvin cycle

EFM analysis was performed on the coupled systems representing *in vivo* photosynthesis obtained using method 1 and method 2. With respect to EFM analysis on the systems, Method 1 and 2 should give the same EFMs. As expected, two elementary modes were calculated by both of the systems which were similar: one corresponds to the production of energy, ATP^{4-} via cyclic photophosphorylation (EFM 1) and one for the production of a molecule of glucose (EFM 2) maintaining the classical photosynthetic stoichiometry along with the number of quanta of light and extra energy (ATP^{4-}). This extra energy is used for other *in vivo* cellular metabolic functions.

<u>EFM 1</u>

In the case of first system (method 1), EFM 1 shown below is resulted due to the four equations R2 R3 R4 R6 listed in Table 3.25:

$$3\ h\nu_{700} + H^{+}_{N} + ADP^{3-} + Pi^{2-} \rightarrow ATP^{4-} + H_2O \qquad \Delta G_{physio} = -485.9\ kJ/mol$$

This is the same EFM, we have found for the cyclic photophosphorylation.

When we analysed the second system (i.e. method 2), the same EFM is resulted; it was because of R1 of Table 3.28. Remember that, R1 of the second system itself is an EFM, which originally resulted from light reactions.

<u>EFM 2</u>

In the case of first system (method 1), EFM 2 is resulted from 20 equations (from R1 to R21, excluding the reaction, R4 of Table 3.25). There may have a question: why R4 is excluded from the metabolic pathway; the answer will get when we analyze MFA which will be described in the paragraph 3.9.3.1.

EFM 2 is;

$$24\ h\nu_{700} + 24\ h\nu_{680} + 6\ CO2 + 6\ H_N^{+} + 6\ ADP^{3-} + 6\ Pi^{2-} \rightarrow Glucose + 6\ O_2 + 6\ ATP^{4-}$$

$$\Delta G_{physio} = -\ 4532.4\ kJ/mol\ (from\ Table\ 3.25)$$

Again, the same EFM is observed when we have done the EFM calculations on the second system (method 2), as a result of R2 and R3 of Table 3.28; this means, both the coupling results give the same topology as expected.

Moreover, the two resulted EFMs support the already known global equations. For one molecule of oxygen production, it is discovered that 8 photons are necessary (Jorgensen and Svirezhev, 2004). We have obtained the same from the resulted EFM equation. Our results also suggest that for the production of either glucose or oxygen, cyclic photophosphorylation is not necessary, although it is important for the metabolite level maintenance. This is confirmed by experiments (Reeves and Hall, 1973) and will be explained while analysing MFA. Photosynthesis provides more energy than which is required for one molecule of glucose production. The extra ATP produced from EFM 2 and EFM 1 will be utilized for other cell requirements like metabolite transports or anabolic processes in cellular level. The coupling of light reactions with Calvin cycle provided two elementary modes revealing the strong influences of two photosystems and the quantity of light (photons) in photosynthesis. The elementary mode which constitutes the reactions is a linear pathway without any branch points so that all intermediates between CO_2 and glucose are lumped to give the global equations like a black box metabolic model of photosynthesis.

3.9.2.2 Mitochondrial reactions with Glycolysis

Essentially, respiration system is also analysed to calculate the elementary flux modes. The systems of respiration created via method 1 and method 2 provided 3 EFMs with considerable energy; as expected, the EFMs obtained from both methods were found similar.

EFM 1

$O_2 + 2\ NADH,H_N^+ + 6.64\ ADP^{3-} + 6.64\ Pi^{2-} + 6.64\ H_N^+ \rightarrow 8.64\ H_2O + 2\ NAD^+ + 6.64\ ATP^{4-}$

Method 1 gave EFM 1 as a combination of 4 equations, R12 R14 R15 R16 (Table 3.29); it was originally given by mitochondrial electron transport and oxidative phosphorylation. The second system (method 2) also supported the same result, as the system itself was built by EFM originally came from mitochondrial electron transport and oxidative phosphorylation (See Table 3.31).

EFM 2

$10\ NAD^+ + O_2 + Glucose + 8\ ADP^{3-} + 8\ Pi^{2-} + 4\ H_N^+ \rightarrow 10\ NADH,H_N^+ + 4\ H_2O + 6\ CO_2 + 8\ ATP^{4-}$

Method 1 gave EFM 2 as a combination of 24 equations, R1 to R25 excluding R12 (Table 3.29); one molecule of glucose decomposes into CO_2 and energy (ATP^{4-} and NADH, H_N^+). The second system (method 2) also favoured EFM 2 due to the combination of equations R1, R3 and R4 (See Table 3.31). It means that respiration can occur without the oxidation of NADH, H_N^+. Therefore, this may be referred as partial respiration.

EFM 3

$$6\ O_2 + \text{Glucose} + 41.3\ ADP^{3-} + 41.3\ Pi^{2-} + 41.3\ H_N^+ \rightarrow 47.3\ H_2O + 6\ CO_2 + 41.3\ ATP^{4-}$$

Method 1 gave EFM 3 as a combination of 25 equations, R1 to R25 of Table 3.29; one molecule of glucose decomposes into CO_2 and tremendous energy, ATP^{4-}. It is because of the complete oxidation of NADH,H_N^+. The second system (method 2) also favoured EFM 3 due to the combination of entire equations R1, R2, R3 and R4 of Table 3.31.

The three EFMs offer three possibilities. EFM 1 gave energy without the decomposition of glucose and EFM 2 and 3 gives energy along with the decomposition of glucose; but the amount of energy is highly varied. Obviously, all these pathways are depending on the energy demand; partial respiration and full respiration are controlled by many physiological and biochemical factors. From Table 3.29, the energies associated with each EFM cannot be calculated as the exact free energies of all reactions at physiological conditions are not available.

3.9.3 Metabolic Flux Analysis

3.9.3.1 Light reactions with Calvin cycle

The estimated fluxes are shown in Figure 3.25, where the fluxes for glucose = 100 μ mol s^{-1} and CO_2 = -600 μ mol s^{-1}. In Figure 3.25 (a), all fluxes are positive except R4 and R14; R14 is negative, but indicated in green colour, which means it can go in the reverse direction (see the free energy given in Table 3.25). Besides, the negative value of R4 marked in red colour shows that it cannot precede so. From MFA analysis of light reactions (paragraph 3.8.1), we have already seen that equation R4 has very important role in controlling cyclic photophosphorylation by maintaining P/2e- ratio.

Also, in Figure 3.25 (b), R1 is zero, but from MFA flux distribution from the Table 3.33, it is found that equal amounts of photons are absorbed by the system, but, R1 became zero; it explains the absence of EFM 1 (EFM responsible for cyclic reaction), which is the exact *in vivo* metabolism in cellular level. For the production of glucose, cyclic reactions are not

required. Recent studies support this flux distribution: non-cyclic photophosphorylation is enough for Calvin cycle *in vivo* as it produces sufficient ATP and $NADPH,H_N^+$ (Reeves and Hall, 1973). This is the reason why equal amounts of photons are absorbed. Since, only non cyclic photophosphorylation is proceeding, the ratio of photons at 680 and 700 nm are found equal which is quite normal.

While in the case of Figure (a), it could be said that in order to balance the metabolic network, P/2e- ratio and to avoid cyclic photophosphorylation R4 occurs in the negative direction to control the system (Reeves and Hall, 1973). Precisely, enough ATP is made by the non cyclic electron transfer chain to carry out stoichiometric CO_2 fixation and the role of cyclic electron transfer is reduced. But under stress conditions, it may dramatically change (Fork and Herbert, 1993).

Certainly, the reaction R4 may occur positively at normal conditions; this is because, inside the chloroplast, numerous types of reactions happen and in cellular metabolism, there is a big demand for energy molecule, ATP^{4-}. Even then, in the case of glucose production since such a big amount of energy is not necessary, R4 appeared to be negative. Usually, cyclic reactions are also necessary to maintain the cell's whole functions. Here, the photophosphorylation ratio, P/2e- is calculated as 1.33 (from Figure (a)), which has been accepted for many years. However nowadays, our result, the P/2e- ratio obtained from Calvin cycle alone (1.5) (paragraph 3.8.2) is widely accepted as true value (Kramer *et al*., 1999). As 1.33 is not the normal case, if cyclic photophosphorylation happens, our results are exactly matching with the experimental true value.

Studied systems	Light reactions + Calvin cycle using method 1 (μ mol S^{-1})	Light reactions + Calvin cycle using method 2 (μ mol S^{-1})
Exchangeables fixed	Glucose = 100 CO_2 = -600	Glucose = 100 CO_2 = -600
Production/ consumption rates for exchangeables	$h\nu_{680}$ = -2400 $h\nu_{700}$ =-41.4 H_2O = -786 O_2 = 600 ADP^{3-} = 186 ATP^{4-} = -186 Pi^{2-} = 186 H_N^+ = 186	$h\nu_{680}$ = -2400 $h\nu_{700}$ =-2400 H_2O = 0 O_2 = 600 ADP^{3-} = -600 ATP^{4-} = 600 Pi^{2-} =-600 H_N^+ = -600

Table 3.40: Metabolic flux distribution for photosynthesis

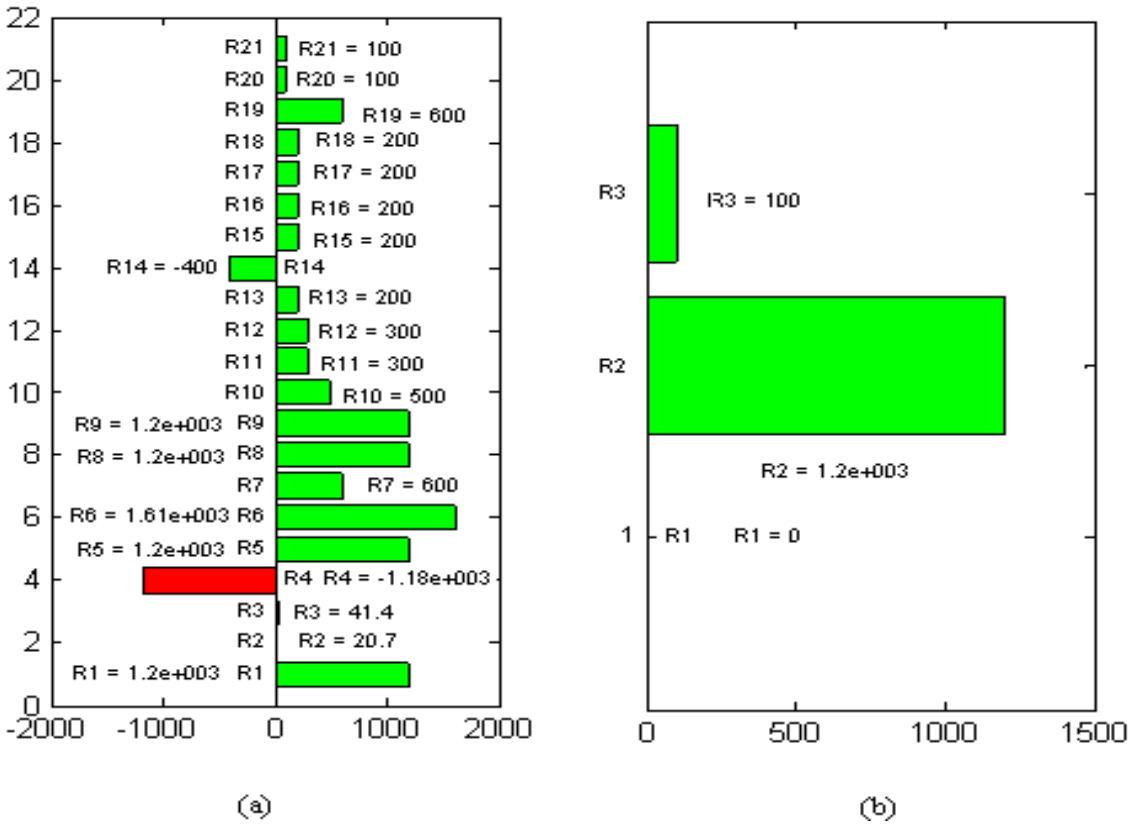

Figure 3.42: Flux distributions for photosynthesis: (a) method 1 (b) method 2

Glucose = 100 μ mol s^{-1} and CO_2 = -600 μ mol s^{-1}

3.9.3.2 Mitochondrial reactions with Glycolysis

The estimated fluxes are shown in Figure 3.26, where the fluxes for glucose = -200 μ mol s^{-1} and O_2 = -300 μ mol s^{-1}. In Figure, all fluxes are positive, although some reactions are zeroes. The flux distribution showed in Figure 3.26 (a) represents a condition which is perfect for a cell where glucose and oxygen are fixed as, glucose = -200 μ mol s^{-1} and O_2 = -300 μ mol s^{-1}. Here, enormous energy is produced both in the form of $NADH,H_N^+$ and ATP^{4-}. The third elementary flux mode, EFM 3 is using here in order to produce such a big amount of energy and hence complete glucose decomposition occurs. But, Figure 3.26 (b) use EFM 2 instead of EFM 3, therefore R12 becomes zero and this is why in EFM 2, R12 was absent. R12 corresponds to the reaction originated from electron transport and oxidative phosphorylation, which associated with ubiquinone/ubiquinol pool and $NADH,H_N^+$; the complex I, NADH dehydrogenase is supposed to be one of the main reasons, if ATP production appears to be low (Moller, 2001). Almost similar facts are found in Figure 3.26 (c) and (d). Analogous to Figure 3.26 (a), (c) is also a perfect situation, where an ideal organism can have. If we verify the metabolic flux distributions given in Table 3.34, the resulting energy can be seen as exactly same for both the methods.

In Figure 3.26 (d), R2 = 0; R2 again corresponds to the reaction associated with $NADH,H_N^+$. Hence, we can conclude that, if there is no need of much energy; first of all, the system has a tendency to suppress the reaction associated with the complex I, accurately matching with the *invivo* condition; however, sometimes the related deficiencies of NAD^+/ $NADH,H_N^+$ cause problems (Moller, 2001). Mitochondria regulate the redox balance in the cell which makes an integral part of a flexible metabolic system in the photosynthetic cell like leaf cell (Gardestrom and Lernmark, 1995). There is a substantial reduction in decarboxylation of TCA cycle intermediates takes place during respiration in the presence of light. At normal situation, a leaf would probably be some mixture between a total and partial TCA cycle in most metabolic conditions. However, all these are important to override disturbances caused by the changing environment, which plants are adapted to (Gardestrom and Lernmark, 1995).

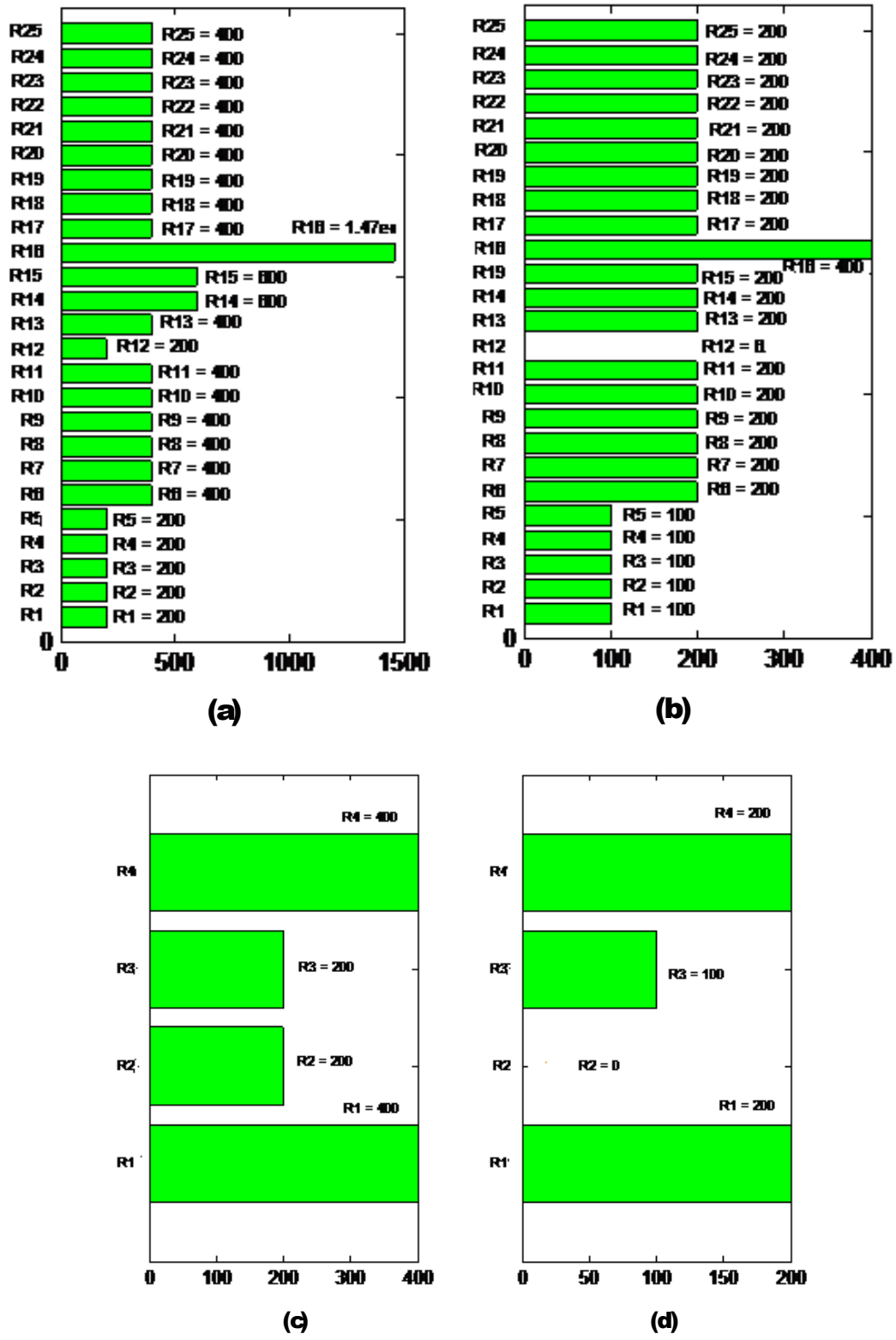

Figure 3.43: Flux distribution for respiration: i) method 1: (a) Glucose = -200 μ mol s^{-1}, O_2 = -300 μ mol s^{-1} (b) Glucose = -100 μ mol s^{-1}, O_2 = -100 μ mol s^{-1}; ii) method 2 (c) Glucose = -200 μ mol s^{-1}, O_2 = -300 μ mol s^{-1}(d) Glucose = -100 μ mol s^{-1},O_2 = -100 μ mol s^{-1}

Nevertheless, the EFM and MFA are interesting and relatively easy tools to study the relevant metabolic pathways. It needs some input/output fluxes to calculate the intracellular rates without perturbing any bioprocesses. However, understanding the topology by EFM analysis, we assumed and studied the rates which cause the metabolical limitations without conducting any experiments which is a very tough and tedious process. The interesting fact is our results could explain the *in vivo* observations done by earlier studies.

Studied systems	Glycolysis + mitochondrial reactions using method1 (μ mol s^{-1})	Glycolysis + mitochondrial reactions using method 2 (μ mol s^{-1})
Exchangeables fixed	Glucose = -200 O_2 = -300	Glucose = -200 O_2 = -300
Production/ consumption rates for exchangeables	$NADH,H_N^+$ = 1800 NAD^+ = -1800 H_2O = 1670 ADP^{3-} = -2270 ATP^{4-} = 2270 Pi^{2-} = -2270 H_N^+ = -2270 CO_2 = 1200	$NADH,H_N^+$ = 1800 NAD^+ = -1800 H_2O = 1670 ADP^{3-} = -2270 ATP^{4-} = 2270 Pi^{2-} = -2270 H_N^+ = -2270 CO_2 = 1200
Exchangeables fixed	Glucose = -100 O_2 = -100	Glucose = -100 O_2 = -100
Production/ consumption rates for exchangeables	$NADH,H_N^+$ = 1000 NAD^+ = -1000 H_2O = 400 ADP^{3-} = -800 ATP^{4-} = 800 Pi^{2-} = -800 H_N^+ = -800 CO_2 = 600	$NADH,H_N^+$ = 1000 NAD^+ = -1000 H_2O = 400 ADP^{3-} = -800 ATP^{4-} = 800 Pi^{2-} = -800 H_N^+ = -800 CO_2 = 600

Table 3.41: Metabolic flux distributions for respiration

3.10Conclusion

Plant metabolic network is very complex as it involves a large number of reactions and metabolites. In addition to this, complex metabolic topography and compartmental separation at the organ and organelle levels increase the demand to focus on relatively small and simple metabolic systems which control and regulate plant metabolic pathways. Quite reasonably, as central metabolism is the major metabolic pathway, without none can survive, it captures all

attention. The case study involving a compartmentalised stoichiometric model of plant metabolism separate various enzymes which regulate the transport and metabolites that interconnect the entire plant metabolic network. The metabolic networks of photosynthesis and respiration were studied and analysed. The obtained results are trustworthy and satisfying with the already existing experimental values and clearly explain regulating complexes and reactions without entering into the keen details of genetic and kinetic studies. This work is still in the initial stages of development for the entire plant growth modelling, but holds future promise for other organ and developmental sub models. In order to achieve that, more studies in the specialized isotopic techniques may be needed to measure the carbon fluxes in organ level, as the calculation of material and isotopic balance for the entire system is not often possible.

3.11Main outcomes of Chapter 3

- Two levels of metabolism are needed to analyse: first level is for energy metabolism (central carbon metabolism) while second level stands for global reactions producing biomass from basic constituents.
- In the cell level, the process of photosynthesis and respiration are studied separately to establish the energy model; each complex involved in light reaction and mitochondrial electron transport processes are studied providing thermodynamic constraints while analysing MFA and EFM. The present approach was completely detailed mechanisms of energy transducing processes.
- The directions of reactions involved in Calvin cycle reactions, Krebs cycle and glycolysis processes are issued from literature data.
- Satisfying *in vivo* results are found while analysing small metabolic networks as well as the coupled metabolic networks using EFM and MFA techniques.
- The study of central carbon metabolism provided the link between physical parameters and biochemical parameters (light energy to chemical energy).
- Importantly, EFM analysis associated with detailed energetics analyses of chloroplast and mitochondrion reveals that the mathematical analyses supported by convex algebra permits to recover the main pathways such as cyclic and noncyclic phosphorylation pathways and NAD^+ and FAD producing pathways.

Chapter 4 Metabolic model for lettuce leaves – Results and discussion

4.1 Introduction

Leaf metabolic model - the metabolic model for leaves is the primary step to achieve the entire biochemical process plant model, which we developed as per the general design of the whole plant growth model. A minimum knowledge of plant leaf metabolism is necessary for the construction of leaf metabolic model. Leaf metabolism involves several types of metabolism other than the central carbon metabolism which may create network complexity, and this complexity increases with the increase in number of participating reactions. In addition, in order to produce one metabolite in an *in vivo* metabolic pathway, there may have lots of possibilities, copying of which makes difficulties in the calculation of metabolic system/model. Therefore, the most possible/observed relevant pathways are accounted while constructing leaf metabolic network.

The purpose of this chapter is to apply leaf metabolic model in the case of lettuce (*Lactuca sativa*) leaves; the model validation is necessary in any type of models and it is important, as it is one of the primary steps of any general plant metabolic model. We agree that only leaf metabolic model is not sufficient to validate the growth of lettuce; nevertheless, as the main part of lettuce plant itself are leaves constituting almost 75% of plant biomass, an approximate validation is achievable. Consequently, the reactions that may happen in lettuce leaves were chosen for the model construction. The aim is to compare and verify the leaf metabolic model of lettuce (*Lactuca sativa*) leaves using the experimental data found from USDA reference [Int. ref. 6] and chambers of Guelph university, where the same type of lettuce grown in Controlled Environment Systems Research Facility (CESRF); it shows the need of various levels of measurements for more accurate biochemical plant growth predictions.

4.2 Leaf metabolic model for lettuce

In day time, due to photosynthesis, carbon enters through leaf stomata and assimilates in chloroplasts as sugar phosphates (glyceradehyde-3-phosphates or G3P), starch, etc. The metabolite G3P enters into the cell cytoplasm and using this as substrate, sucrose sugar forms. Usually in all plants, the carbon fixed by photosynthesis accumulates as starch in chloroplasts, which remobilized at night to support metabolism and growth via respiration. Lettuce plants are exceptional in this context; they do not contain starch (Int. ref. 6); so, by the time being we do not account starch for leaf model.

Like every biomass composition of plant leaves, lettuce contains proteins, carbohydrates, lipids and fatty acids in higher amounts, while nucleic acids and chlorophylls are found relatively very low compared to the rest of the biomass components. Subsequently, protein, lipid, fatty acid metabolisms are considered in addition to the central carbon metabolic pathways, the synthesis and maintenance of which require considerable energy. In the absence of proteins, growth and maintenance of organs stop and thus, it represents the rate limiting step for potential growth rate. The rate of protein synthesis depends on genomic level (both the rate of transcription and translation of the genetic information) and also on the amino acid supply for the growth of the polypeptide chain.

Knowing the entire leaf metabolism, the main fuelling reactions of the cells associated with the plant metabolism are rerouted in such a way as to channel the main carbon flux into the biosynthetic pathway required for final product synthesis- biomass. To achieve, or at least approach, one must know how carbon partitioning occurs between the fuelling reactions, biomass and product (though input carbon = output carbon); i.e. for leaf metabolic model, the leaf biomass composition as well as the input/output carbon measurements are primarily required. This necessitates the development of means to determine the partitioning of carbon flux between the fundamental biosynthetic pathways (Vallino and Stephanopoulos, 1990).

Similar to the metabolic flux analysis studies on central carbon metabolic pathways described in chapter 3, the carbon flux of each reaction in the leaf network can be calculated knowing the extracellular data, mainly in terms of CO_2 uptake/O_2 release. For that, it was required to represent the leaf cellular metabolism in a matrix form. It is quite obvious that not all biosynthetic reactions have been incorporated. Thousands of reactions are there, to include all would be impractical. Therefore, one of the preliminary steps in the development of the model was to extract those reactions that represent the major carbon fluxes; most of them were available in the literature or data bases like KEGG and MetaCyc.

4.2.1 Model construction

To construct a simplified network for leaf metabolism, the main fuelling and metabolite-generating bioreactions, such as light reactions, mitochondrial electron transport reactions, Calvin cycle reactions, Embden-Meyerhof-Parnas pathway, Pentose phosphate pathway and Krebs or tricarboxylic acid (TCA) cycle were assembled. Some of the reactions involving biomass component synthesis and maintenance requirements were expressed as lumped reactions as explained in chapter 3; for example, the equations for energy metabolism (light

reactions and mitochondrial electron transport oxidative phosphorylation) obtained as a result of EFM/MFA analysis form the first four equations (R1, R2, R3 and R4) of the metabolic model:

R1. $1\ ADP + 1\ Pi + 3\ h\nu_{700} \rightarrow 1\ ATP + 1\ H_2O$

R2. $2\ ADP + 1\ NADP^+ + 2\ Pi + 2\ h\nu_{700} + 2\ h\nu_{680} \rightarrow 2\ ATP + 1\ NADPH, H^+ + 0.5\ O_2 + 1\ H_2O$

R3. $2\ ADP + 2\ Pi + 1\ FADH_2 + 0.5\ O_2 \rightarrow 2\ ATP + 1\ FAD + 3\ H_2O$

R4. $3\ ADP + 1\ NADH, H^+ + 3\ Pi + 0.5\ O_2 \rightarrow 3\ ATP + 1\ NAD^+ + 4\ H_2O$

The energy molecule, ATP is considered as an intermediate in the stoichiometric matrix. According to Vallino and Stephanopoulos, a reaction is included to dissipate excess ATP and to account maintenance and futile cycles (Vallino and Stephanopoulos, 1990). To maintain a steady state approximation for ATP, this excess is removed by the conversion of ATP into ADP.

R35. $1\ PPi + 1\ H_2O \leftrightarrow 2\ Pi$

R36. $1\ AMP + 1\ ATP \leftrightarrow 2\ ADP$

R37. $1\ NAD^+ + 1\ NADPH \leftrightarrow 1\ NADH + 1\ NADP^+$

Finally, to minimize the network dimension of the system, the metabolites involved at branch points of the biosynthetic pathways are considered. For example, there are several metabolites between aspartyl semialdehyde and lysine; however, due to steady state assumption, all of them need not to be taken into account, as they comprise a non-branching sequence of reactions of which proceed at same rates. At the same time, the lumping reactions of Calvin cycle, glycolysis, TCA cycle, etc. were taken carefully; lumping surely makes the metabolic network a reduced one. But, sometimes it may create problems for finding substrate metabolites for additional metabolic pathways such as protein, fatty acid, lipid metabolism, etc. For example, if we summarise most of the reactions in terms of the building block, ‘glucose’, the entire metabolic pathway will not run properly; the unavailability of simple molecules such as G3P, PEP, G6P, F6P, acetate, pyruvate, etc. in the system may block the matrix calculations of the entire system; in fact, the matrix representation and calculation stands for the exact *in vivo* physiological conditions. It should be noted that the same happens in the case of almost all organisms; however we say, glucose as building block, it does not directly participate in all types of metabolic reactions. Usually, when there is a need, it breaks into simple molecules (G3P, PEP, G6P, F6P, acetate, pyruvate) and becomes available for all other constructive metabolic pathways. It might be seen that the removal of metabolites like

G3P may cause ‘network traffic jam’ in the system analysis. Because of the same reason, Calvin cycle, glycolysis and TCA cycle reactions are kept as exactly same, without repeating the equations.

Further, proteins are made up of various types of amino acids. Consequently, amino acids are produced in the very beginning of protein synthesis. A number of amino acids are partly synthesized in the mitochondria (Jones and Fink, 1981), and it is assumed that the intermediates of these reactions can be transported across the inner mitochondrial membrane. If it is in the order, G3P → sucrose → glucose → pyruvate, the metabolite pyruvate is necessary for cysteine production which is transported across the mitochondria. Also, there are lots of possibilities to produce pyruvate (other than the way suggested), as most of the reactions are reversible and highly depending on the cellular pH; different metabolic pathways would be possible/accessible in the cellular level according to the environmental stress conditions. Nevertheless, we have considered the most occurring pathway for the same.

Additionally, tetrahydrofolate (THF) and its derivatives, collectively termed folates related to the synthesis of nucleic acids, e.g. purines, thymidylate (anyhow, we did not account nucleic acids in our model, as the contribution is small), triglycerides and amino acids like methionine, glycine and serine were taken into account. The precursors of THF are synthesized in the cell cytosol and plastids (Linka and Weber, 2010). Further, additional metabolic pathways were added for each amino acid production and to balance the production and consumption of their precursors.

Equations for macromolecules

The equations for the production of protein (using amino acids), lipids and fats (constituting brassicasterol and triglycerides) and other carbohydrates (involving sugars, disaccharides, fibers, etc.) were added to the system. This has been done taking the reference (Int. ref. 6) due to the unavailability of biomass composition from lettuce plants (*Lactuca sativa*) grown in the controlled chambers. As per [Int. ref. 6], the fresh biomass contains 95% of water. The biomass components involved are calculated for 1 g of dry biomass as in Table 4.1.

Biomass components	Composition as per the reference for 1 g of dry biomass (g)	Composition for 1g of dry biomass (g) (recalculated for normalisation)	Biomass component percentage (%)
Protein	0.276	0.3228	32.28
Triglycerides	0.022	0.0257	2.57
Brassicasterol	0.008	0.0093	0.94
Fibers	0.28	0.327	32.75
Sugars	0.269	0.3146	31.46
Biomass (Total)	0.855	1	100
Ash	0.13	-	-
Total	0.985	-	-

Table 4.42: Available biomass composition (Int. ref. 6)

The reference does not provide any information about chlorophylls, DNA, RNA, etc. From other literatures, they are found to be very small compared to the rest of the components. For example, RNA content is approximately 0.001g, while chlorophyll content is 1.8×10^{-6} g (Int. ref. 7; Fontes *et al*., 1997). Without accounting ash (Ca^{2+}, Mg^{2+}, Fe^{2+}, K^{+}, etc.), the sum of all nutrients do not give 1 g of biomass in total; hence, the second column of Table 4.1 is meant for the biomass composition which we used for our metabolic network model. Additionally, the amounts of amino acids for protein (Table 4.2), saturated, unsaturated, polyunsaturated fatty acids, for lipid formation (Table 4.3) and sucrose, glucose, fructose for sugars (Table 4.4), etc. were taken from the same reference.

4.2.1.1 Protein production

There are 20 amino acids present in proteins. The precise amino acid content and the sequence of those amino acids, of a specific protein is determined by the sequence of the bases in the gene that encodes that protein. The chemical properties of the amino acids of proteins determine the biological activity of the protein. Protein production is assumed as a result of poly condensation process of amino acids. The amino acid present in 1 g of dry biomass was taken from [Int. ref. 6]; but, as the composition of the important amino acids, asparagine and glutamine (both play major roles in metabolism) were absent, we have taken them into account by some approximations as given below:

Total protein content in 1g of dry biomass = 0.276 g

Total amino acid content in 1g of dry biomass = 0.226 g

So, total amount of glutamine and asparagine in 1 g of dry biomass = 0.276 - 0.226 = 0.05 g

The approximate ratio between glutamine and asparagine was assumed (Giannino *et al*., 2008) which gave a total amino acid content of 0.276 g (third column of Table 4.2).

Then, if 'N' number of amino acids present in one mole of protein, (N-1) mole of water releases:

$$N \text{ amino acids} \rightarrow \text{protein} + (N-1)\ H_2O$$

Taking this concept, calculations were made (Table 4.2), to know the moles of amino acids (aa) needed for one mole of protein production ($CH_{1.57}O_{0.356}N_{0.2835}S_{0.005}$).

Then, $N_1\ aa_1 + N_2\ aa_2 + N_3\ aa_3 + ... \rightarrow$ protein + $(N_1 + N_2 + N_3 + ...)\ H_2O$

0.0126 Alanine + 0.0119 valine + 0.0128 isoleucine + 0.00989 threonine + 0.00734 asparagine + 0.0114 lysine + 0.0214 aspartate + 0.0259 glutamine + 0.00226 methionine + 0.0251 glutamate + 0.0119 leucine + 0.00744 serine + 0.0014 cystine + 0.0157 glycine + 0.00826 proline + 0.00802 arginine + 0.00102 tryptophan + 0.00324 tyrosine + 0.00618 phenylalanine + 0.00287 histidine → 1 Protein + 0.20668 H_2O

Protein components (Amino acids)	Mass of amino acids in 1 g of dry biomass (g)	Mass of amino acids in 1 g of dry biomass (g) after adding asn & glu	Molar mass of amino acids (g/mol)	Moles of amino acids/g of protein	Amino acids /C of protein (in mol)
alanine	0.0132	0.0132	89	0.0005	0.0126
valine	0.0165	0.0165	117	0.0005	0.0119
isoleucine	0.0198	0.0198	131	0.0005	0.0128
threonine	0.01398	0.01398	119	0.0004	0.00989
asparagine	**-**	**0.0115**	132	0.0003	0.00734
lysine	0.0198	0.0198	146	0.00049	0.0114
aspartate	0.0337	0.0337	133	0.0009	0.0214
glutamine	-	0.0444	145	0.0011	0.0259
methionine	0.004	0.004	149	0.00009	0.00226
glutamate	**-**	**0.0436**	147	0.0010	0.0251
leucine	0.0185	0.0185	131	0.0005	0.0119
serine	0.009	0.009	105	0.0003	0.00744
cystine	0.004	0.004	240	0.00006	0.0014
glycine	0.0139	0.0139	75	0.00067	0.0157
proline	0.0112	0.0112	115	0.0003	0.00826
arginine	0.0165	0.0165	174	0.0003	0.00802
tryptophan	0.0019	0.0019	165	0.00004	0.00102
tyrosine	0.0078	0.0078	204	0.00013	0.00324
phenylalanine	0.0132	0.0132	181	0.00027	0.00618
histidine	0.0053	0.0053	155	0.0001	0.00287
Total	**0.226**	**0.276**			
water					0.20668

Table 4.43: Available amino acid composition [Int. ref. 6](asn = asparagine; glu = glutamate)

4.2.1.2 Lipid production

Additionally, lipid (triglyceride) formation is considered; it is always associated with unsaturated, saturated, polyunsaturated fats and glycerol. Similar to protein formation, it releases water as per the following equation.

α unsaturated fats + β saturated fats + γ polyunsaturated fats + ∂ glycerol → triglyceride + 3 ∂ H_2O, where ∂ = α + β + γ

Triglyceride components	Composition as per the reference 1 g of dry biomass (g)	Composition for 1g of triglyceride (g)	Molecular formula	Components / C of triglycerides (in mol)
Unsaturated fats	0.001	0.0455	$CH_{1.847}O_{0.0962}$	0.0226
Saturated fats	0.004	0.182	$CH_{1.97}O_{0.0999}$	0.0895
Polyunsaturated fats	0.017	0.773	$CH_{1.66}O_{0.097}$	0.39
Triglycerides	0.022	1	$CH_{1.201}O_{0.0488}$	1
Brassicasterol	0.0094	-	$CH_{1.64}O_{0.036}$	-

Table 4.44: Available lipid component composition [Int. ref. 6]

The sum of moles of unsaturated, saturated, polyunsaturated fats from Table 4.3 gives the number of moles of water involved.

0.0226 unsaturated fats + 0.0895 saturated fats + 0.39 polyunsaturated fats + 0.167 glycerol → triglyceride + 0.5013 H_2O

Usually, brassicasterol is associated with lipids; but, like most other macromolecules, it is not a polymerised product.

0.6429 G3P + 0.0357 S-ade-methionine + 0.4643 NAD+ + 0.357 O_2 → 0.0357 S-ad-homocysteine + 0.4643 NADH, H^+ + 0.6429 Pi + 1 brassicasterol + 0.9643 CO_2 + 0.0357 H_2O

4.2.1.3 Carbohydrate (sugars and fibers) production

Sugars

In lettuce biomass, sugars involve in the mainly in the form of glucose, fructose and sucrose. As the amount of sucrose was not listed in the Int. ref. 6, an approximation is taken (total sugar content - glucose + fructose = sucrose) as shown in the Table 4.4.

Components of sugars	Composition as per the reference 1 g of dry biomass (g)	Composition in 1g of sugars (g)	Components / C of sugars (in mol)
glucose	0.0854	0.2715	0.032
fructose	0.0994	0.3159	0.037
sucrose	0.1298	0.4159	0.0487
Total sugars	0.3146	1	1
Fibers	0.327	-	-

Table 4.45: Available carbohydrate composition Int. ref. 6

From Table 4.4, the production of one mole of sugars ($CH_{1.9}O_{0.9548}$) corresponds to:

0.032 glucose + 0.0373 fructose + 0.049 sucrose → 1 sugars

Fibers

Fiber production needs energy in the form of ATP; the formation is almost same as starch, so the equation was taken from the reference (Cogne, 2003).

0.167 G6P + 0.167 ATP → 0.167 PPi + 0.167 ADP + 1 fibers; where the molecular formula of fibers is $CH_{1.67}O_{0.835}$

Further from Table 4.5, for one mole of leaf biomass constituting protein, lipids (brassicasterol and triglycerides) and carbohydrates (sugars and fibers) with respect to Int. ref. 6 is,

0.3518 Protein + 0.0469 Triglycerides + 0.0168 Brassicasterol + 0.3089 Fibers + 0.2757 Sugars → Biomass

Biomass components	moles /g of dry weight	Molecular formula (CHONS)	Moles per C mol of biomass
Protein	0.01379	$CH_{1.57}O_{0.356}N_{0.2835}S_{0.005}$	0.3518
Triglycerides	0.0018	$CH_{1.201}O_{0.0488}$	0.0469
Brassicasterol	0.00065	$CH_{1.64}O_{0.036}$	0.0168
Fibers	0.0121	$CH_{1.67}O_{0.835}$	0.3089
Sugars	0.0108	$CH_{1.9}O_{0.9548}$	0.2757
Biomass	0.0392 (Total)	$CH_{1.674}O_{0.6469}N_{0.099}S_{0.0018}$	1.0000 (Total)

Table 4.46: Molar biomass composition

With all of the above information and stoichiometric equations (given in Table 4.6), a reliable metabolic network for leaves was constructed as in Figure 4.1 and 4.2. Figure 4.1 stands for central carbon metabolism involving energy metabolism occurring at different cell compartments (choloroplast, cytosol, mitochondria, etc.); it produces sugars and fibers contributing biomass production. Figure 4.2 describes the pathways for lipid and protein production. The leaf metabolic model is constituted of 107 reactions and 118 metabolites.

From various literatures, 59 reactions were taken as reversible. The metabolites like HNO_3, CO_2, H_2O, $h\nu_{700}$, $h\nu_{680}$, H_2S were assumed as inputs where biomass and O_2 as outputs; thereby, 8 exchangeable metabolites (E) and 110 non exchangeable metabolites (NE) were defined.

Equations used for leaf metabolic model network

1.	Central carbon metabolism (Bioenergetics):
	(a) Light reactions
[1]	1 ADP + 1 Pi + 3 $h\nu_{700}$ → 1 ATP + 1 H_2O
[2]	2 ADP + 1 $NADP^+$ + 2 Pi + 2 $h\nu_{700}$ + 2 $h\nu_{680}$ → 2 ATP + 1 NADPH, H^+ + 0.5 O_2 + 1 H_2O
	(b) Mitochondrial phosphorylation
[3]	2 ADP + 2 Pi + 1 $FADH_2$ + 0.5 O_2 → 2 ATP + 1 FAD + 3 H_2O
[4]	3.33 ADP + 1 NADH, H^+ + 3.33 Pi + + 0.5 O_2 → 3.33 ATP + 1 NAD^+ + 4.33 H_2O
2.	Nitrogen fixation
[5]	4 NADPH, H^+ + 1 HNO_3 → 4 $NADP^+$ + 1 NH_3 + 3 H_2O
3.	Carbon fixation
	(a) Calvin cycle
[6]	1 RuBP + 1 CO_2 + 1 H_2O → 2 3PGA
[7]	1 3PGA + 1 ATP ↔ 1 1-3BPGA + 1 ADP
[8]	1 1-3BPGA + 1 NADPH, H^+ ↔ 1 G3P + 1 $NADP^+$ + 1 Pi
[9]	1 G3P ↔ 1 DHAP
[10]	1 G3P + 1 DHAP ↔ 1 FBP
[11]	1 FBP + 1 H_2O → 1 F6P + 1 Pi
[12]	1 G3P + 1 F6P ↔ 1 E4P + 1 Xu5P
[13]	1 Ru5P ↔ 1 Xu5P
[14]	1 R5P + 1 Xu5P ↔ 1 G3P + 1 S7P
[15]	1 DHAP + 1 E4P ↔ 1 SBP
[16]	1 SBP + 1 H_2O → 1 S7P + 1 Pi
[17]	1 R5P ↔ 1 Ru5P
[18]	1 ATP + 1 Ru5P → 1 RuBP + 1 ADP
[19]	1 F6P ↔1 G6P
[20]	1 G6P + 1 H_2O → 1 glucose + 1 Pi
	(b) ***Pentose phosphate pathway***
[21]	1 G3P + 1 S7P ↔ 1 F6P + 1 E4P
4.	Respiration
	(a) Glycolysis
[22]	1 glucose + 1 ATP → 1 G6P + 1 ADP
[23]	1 F6P + 1 ATP → 1 FBP + 1 ADP
[24]	1 3PGA ↔ 1 2PGA
[25]	1 2PGA ↔ 1 PEP + 1 H_2O
[26]	1 PEP + 1 ADP → 1 pyruvate + 1 ATP
	(b) ***Krebs cycle***
[27]	1 coenzymeA + 1 pyruvate + 1 NAD^+ → 1 acetylcoA + 1 NADH, H^+ + 1 CO_2
[28]	1 oxaloacetate + 1 acetylcoA + 1 H_2O → 1 coenzymeA + 1 citrate
[29]	1 citrate ↔ 1 cisaconitate + 1 H_2O
[30]	1 cisaconitate + 1 H_2O ↔ 1 isocitrate
[31]	1 isocitrate + 1 NAD^+ → 1 oxoglutarate + 1 NADH, H^+ + 1 CO_2
[32]	1 coenzymeA + 1 oxoglutarate + 1 NAD^+ ↔ 1 Succinyl-CoA + 1 NADH, H^+ + 1 CO_2
[33]	1 fumarate + 1 H_2O ↔ 1 malate
[34]	1 NAD^+ + 1 malate ↔ 1 oxaloacetate + 1 NADH, H^+

[35] 1 Succinate + 1 FAD ↔ 1 fumarate + 1 $FADH_2$
5. Energy Balancing reactions
[36] 1 PPi + 1 H_2O ↔ 2 Pi
[37] 1 AMP + 1 ATP ↔ 2 ADP
[38] 1 NAD^+ + 1 NADPH ↔ 1 NADH + 1 $NADP^+$
6. Connecting reactions
[39] 2 pyruvate + 1 NADPH, H^+ → 1 2-oxoisovalerate + 1 $NADP^+$ + 1 CO_2 + 1 H_2O
[40] 1 PEP + 1 CO_2 + 1 H_2O ↔ 1 oxaloacetate + 1 Pi
[41] 1 R5P + 1 ATP ↔ 1 RBP + 1 ADP
[42] 1 NADPH, H^+ + 1 CO_2 ↔ 1 $NADP^+$ + 1 formate
[43] 1 acetylcoA + 1 formate ↔ 1 coenzymeA + 1 pyruvate
[44] 1 coenzymeA + 1 acetate + 1 ATP ↔ 1 acetylcoA + 1 PPi + 1 AMP
[45] 1 coenzymeA + 1 acetate ↔ 1 acetylcoA + 1 H_2O
7. Carbohydrate production
[46] 1 glucose ↔ 1 fructose
[47] 1 fructose + 1 UDP-glucose ↔ 1 sucrose + 1 UDP
[48] 1 UMP + 1 G1P ↔ 1 UDP-glucose + 1 H_2O
[49] 1 G6P ↔ 1 G1P
[50] 1 UDP + 1 H_2O ↔ 1 Pi + 1 UMP
[51] 0.032 glucose + 0.037 fructose + 0.0487 sucrose → 1 sugars
[52] 0.167 G6P + 0.167 ATP → 0.167 PPi + 0.167 ADP + 1 fibers
8. Protein production
[53] 1 aspartate + 1 NH_3 ↔ 1 asparagine + 1 H_2O
[54] 1 ATP + 1 homoserine + 1 H_2O ↔ 1 threonine + 1 ADP + 1 Pi
[55] 1 pyruvate + 1 glutamate + 1 2-oxobutanoate + 1 NADPH, H^+ ↔ 1 isoleucine + 1 oxoglutarate + 1 $NADP^+$ + 1 CO_2 + 1 H_2O
[56] 1 glutamate + 1 2-oxoisovalerate → 1 valine + 1 oxoglutarate
[57] 1 pyruvate + 1 glutamate → 1 alanine + 1 oxoglutarate
[58] 1 acetylcoA + 1 glutamate + 1 2-oxoisovalerate + 1 NAD^+ + 1 H_2O →1 coenzymeA + 1 oxoglutarate + 1 leucine + 1 NADH, H^+ + 1 CO_2
[59] 1 homocysteine + 1 serine ↔ 1 2-oxobutanoate + 1 cysteine + 1 NH_3
[60] 2 cysteine + 1 NAD^+ ↔ 1 cystine + 1 NADH, H^+
[61] 1 THF + 1 glycine + 1 NAD^+ ↔ 1 CH2=THF + 1 NADH, H^+ + 1 NH_3 + 1 CO_2
[62] 1 oxoglutarate + 1 glutamine + 1 NADH + 1 H^+ → 2 glutamate + 1 NAD^+
[63] 1 glutamate + 1 ATP + 1 NADPH, H^+ → 1 glutamate- γ -semialdehyde + 1 ADP + 1 $NADP^+$ + 1 Pi
[64] 1 glutamate-γ-semialdehyde → 1 1-pyrroline-5-carboxylate + 1 H_2O
[65] 1 1-pyrroline-5-carboxylate + 1 NADPH, H^+ → 1 proline + 1 $NADP^+$
[66] 1 glutamate + 1 glutamate- γ -semialdehyde ↔ 1 oxoglutarate + 1 ornithine
[67] 1 ornithine + 1 NH_3 + 1 CO_2 ↔ 1 citrulline + 1 H_2O
[68] 1 aspartate + 1 ATP + 1 citrulline ↔ 1 fumarate + 1 arginine + 1 PPi + 1 AMP
[69] 2 PEP + 1 E4P + 1 ATP + 1 NADPH, H^+ → 1 chorismate + 1 ADP + 1 $NADP^+$ + 4 Pi
[70] 1 glutamate + 1 4-hydroxyphenylpyruvate ↔ 1 oxoglutarate + 1 tyrosine
[71] 1 chorismate + 1 $NADP^+$ ↔ 1 4-hydroxyphenylpyruvate + 1 NADPH, H^+ + 1 CO_2
[72] 1 glutamate + 1 phenylpyruvate → 1 oxoglutarate + 1 phenylalanine
[73] 1 glutamine + 1 serine + 1 chorismate + 1 5p-ribosyl-1-pp → G3P + 1 oxaloacetate + 1 glutamate + 1 tryptophan + 1 PPi + 2 H_2O
[74] 1 RBP + 1 Pi ↔ 1 5p-ribosyl-1-pp + 1 H_2O
[75] 1 Succinyl-CoA + 1 pyruvate + 1 aspartate + 1 glutamate + 1 ATP + 2 NADPH, H^+ → 1 Succinate + 1 coenzymeA + 1 lysine + 1 oxoglutarate + 1 ADP + 2 $NADP^+$ + 1 Pi + 1 CO_2
[76] 1 aspartate + 1 ATP + 1 NADPH, H^+ ↔ 1 aspartate-semialdehyde + 1 ADP + 1 $NADP^+$ + 1 Pi
[77] 1 aspartate-semialdehyde + 1 NADH, H^+ ↔ 1 NAD^+ + 1 homoserine

[78]	1 G6P + 3 ATP + 2 $NADP^+$ + 3 NH_3 → 1 histidine + 3 ADP + 2 NADPH, H^+ + 4 Pi
[79]	1 chorismate ↔ 1 phenylpyruvate + 1 CO_2 + 1 H_2O
[80]	1 glutamate + 1 ATP + 1 NH_3 ↔ 1 glutamine + 1 ADP + 1 Pi
[81]	1 oxaloacetate + 1 glutamate ↔ 1 aspartate + 1 oxoglutarate
[82]	1 Succinyl-CoA + 1 homoserine ↔ 1 coenzymeA + 1 succinylhomoserine
[83]	1 succinylhomoserine + 1 H_2S ↔ 1 Succinate + 1 homocysteine
[84]	1 pyruvate + 1 NH_3 + 1 H_2S ↔ 1 cysteine + 1 H_2O
[85]	1 2-oxobutanoate + 1 NH_3 + 1 H_2S ↔ 1 homocysteine + 1 H_2O
[86]	1 homocysteine + 1 CH3THF→ 1 methionine + 1 THF
[87]	0.0126 Alanine + 0.0119 valine + 0.0128 isoleucine + 0.00989 threonine + 0.00734 asparagine + 0.0114 lysine + 0.0214 aspartate + 0.0259 glutamine + 0.00226 methionine + 0.0251 glutamate + 0.0119 leucine + 0.00744 serine + 0.0014 cystine + 0.0157 glycine + 0.00826 proline + 0.00802 arginine + 0.00102 tryptophan + 0.00324 tyrosine + 0.00618 phenylalanine + 0.00287 histidine → 1 Protein + 0.20668 H_2O
9.	Lipid production
[88]	1 THF + 1 ATP + 1 formate ↔ 1 10-formylTHF + 1 ADP + 1 Pi
[89]	1 10-formylTHF ↔ 1 methenylTHF + 1 H_2O
[90]	1 methenylTHF + 1 NADH, H^+ → 1 CH_2=THF + 1 NAD^+
[91]	1 CH_2=THF + 1 NADH, H^+ ↔ 1 CH_3THF + 1 NAD^+
[92]	1 DHAP + 1 NADPH, H^+ → 1 glycerol3P + 1 $NADP^+$
[93]	1 glycerol3P + 1 ADP ↔ 1 ATP + 1 glycerol
[94]	1 palmitate + 1 $NADP^+$ → 1 palmitoleate + 1 NADPH, H^+
[95]	1 oleate + 1 $NADP^+$ → 1 linoleate + 1 NADPH, H^+
[96]	1 linoleate + 1 $NADP^+$→ 1 g-linolenate + 1 NADPH, H^+
[98]	1 acetylcoA + 1 CO_2 → 1 malonylcoA
[99]	1 stearate + 1 $NADP^+$ → 1 oleate + 1 NADPH, H^+
[100]	1 palmitate + 2 NADPH, H^+ + 1 malonylcoA → 1 stearate + 1 coenzymeA + 2 $NADP^+$ + 1 CO_2 + 1 H_2O
[101]	1 S-ad-homocysteine + 1 methionine ↔ 1 S-ade-methionine + 1 homocysteine
[102]	0.6429 G3P + 0.0357 S-ade-methionine + 0.4643 NAD^+ + 0.357 O_2 → 0.0357 S-ad-homocysteine + 0.4643 NADH, H^+ + 0.6429 Pi + 1 brassicasterol + 0.9643 CO_2 + 0.0357 H_2O
[103]	0.0428 stearate + 0.0143 palmitate → 1 saturated-fats + 0.0143 H_2O
[104]	0.0192 palmitoleate + 0.0385 oleate → 1 unsaturated-fats + 0.0192 H_2O
[105]	0.0138 linoleate + 0.0416 g-linolenate → 1 polyunsaturated-fats + 0.0138 H_2O
[106]	0.0895 saturated-fats + 0.0226 unsaturated-fats + 0.39 polyunsaturated-fats + 0.167 glycerol → 1 triglycerides + 0.5013 H_2O
10.	Biomass production
[107]	0.0469 triglycerides + 0.01678 brassicasterol + 0.3518 Protein + 0.3089 fibers + 0.2756 sugars → 1 biomass

Table 4.6 : Stoichiometric equations used for leaf biochemical model

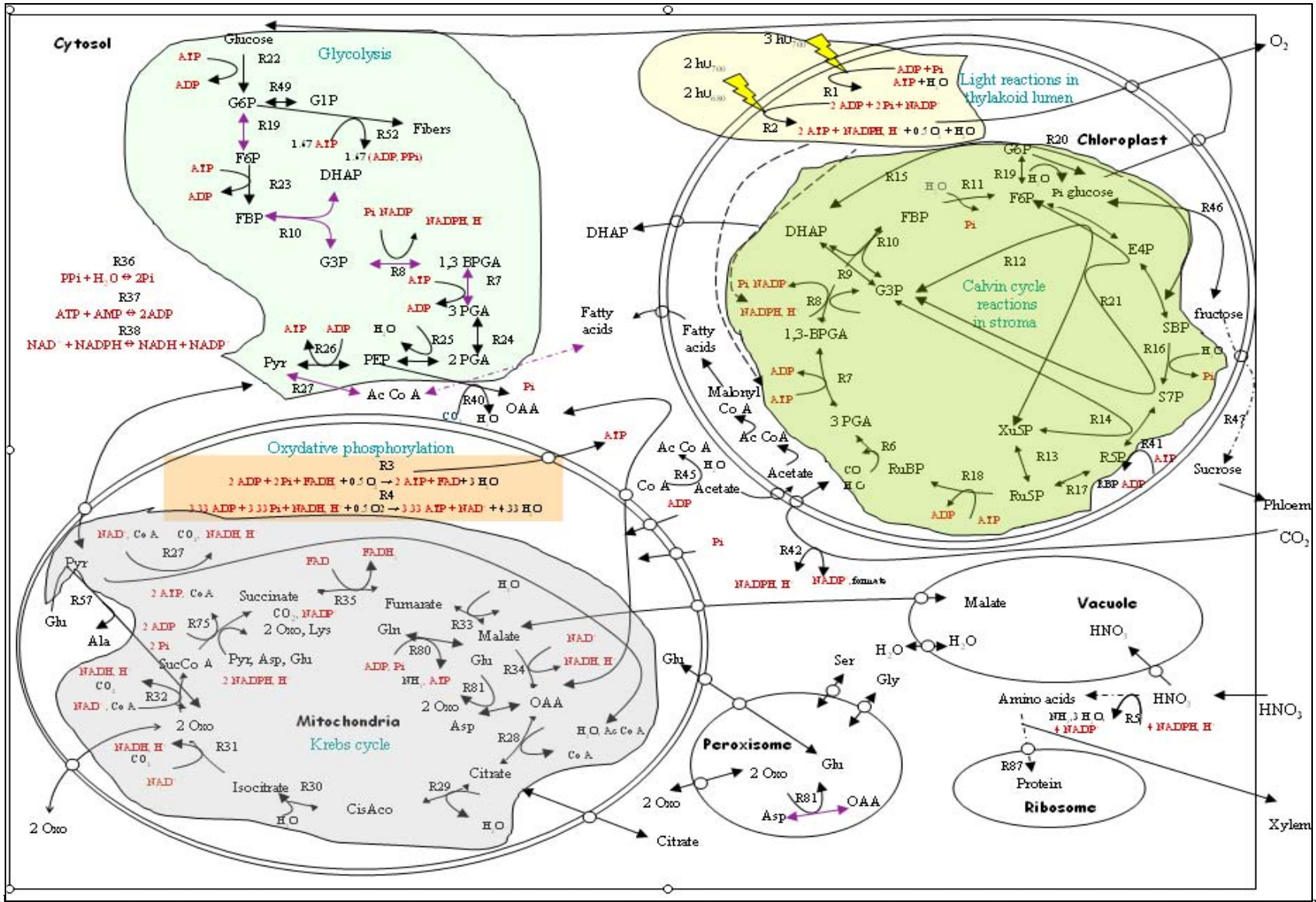

Figure 4.44: Metabolic network model involving central carbon metabolism in different cell compartments: chloroplast (Calvin cycle), mitochondria (Krebs cycle), cytosol (Glycolysis), peroxisome, ribosome and vacuole. Violet colour -repeating reactions, red colour- energetic reactions, yellow colour- light energy

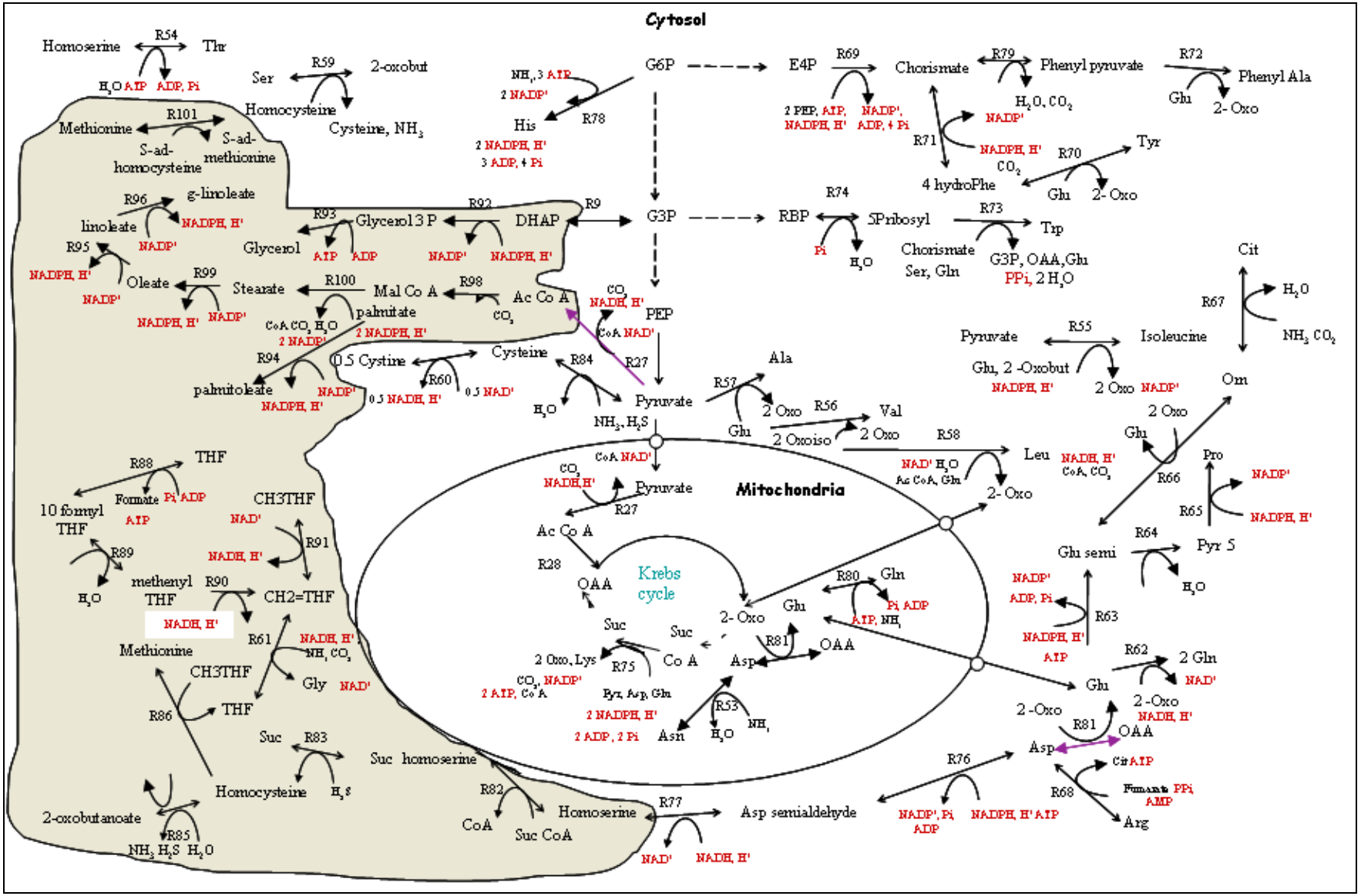

Figure 4.45: Leaf metabolic network for protein and lipid production

4.2.2 Results and Discussion

The preliminary analysis was carried out to check the stoichiometry of all participating reactions. It revealed 4 sets of cyclic reactions, all of them involved the energy components such as ATP, ADP, Pi, NADH, H^+/NADPH, H^+, etc.

They are schemed in Figure 4.3 revealing their cyclic nature and described below as 4 relations:

Relation: 1 (involving 4 reactions) [1 R27 -1 R38 + 1 R42 + 1 R43 = 0]

[R27] 1 coenzymeA + 1 pyruvate + 1 NAD^+→1 acetylcoA + 1 NADH + 1 H^+ +1 CO_2

[R38] 1 NAD^+ + 1 NADPH ↔1 NADH + 1 $NADP^+$

[R42] 1 NADPH + 1 H^+ + 1 CO_2 ↔ 1 $NADP^+$ + 1 formate

[R43] 1 acetylcoA + 1 formate ↔ 1 coenzymeA + 1 pyruvate

Relation: 2 (involving 5 reactions) [-1 R10 -1 R11 + 1 R15 + 1 R16 + 1 R21 = 0]

[R10] 1 G3P + 1 DHAP ↔ 1 FBP

[R11] 1 FBP + 1 H_2O → 1 F6P + 1 Pi

[R15] 1 DHAP + 1 E4P↔1 SBP

[R16] 1 SBP + 1 H_2O → 1 S7P + 1 Pi

[R21] 1 G3P + 1 S7P ↔ 1 F6P + 1 E4P

Relation: 3 (involving 6 reactions) [1R20 + 1 R22 -0.5 R36 -0.5 R37 -0.5 R44 + 0.5 R45 =0]

[R20] 1 G6P + 1 H_2O → 1 glucose + 1 Pi

[R22] 1 glucose + 1 ATP →1 G6P + 1 ADP

[R36] 1 PPi + 1 H_2O ↔ 2 Pi

[R37] 1 AMP + 1 ATP ↔ 2 ADP

[R44] 1 coenzymeA + 1 acetate + 1 ATP↔ 1 acetylcoA + 1 PPi + 1 AMP

[R45] 1 coenzymeA + 1 acetate ↔ 1 acetylcoA + 1 H_2O

Relation: 4 (involving 6 reactions) [1R11 + 1R23 -0.5 R36 -0.5 R37 -0.5 R44 + 0.5 R45 = 0]

[R11] 1 FBP + 1 H_2O → 1 F6P + 1 Pi

[R23] 1 F6P + 1 ATP→1 FBP + 1 ADP

[R36] 1 PPi + 1 H_2O ↔ 2 Pi

[R37] 1 AMP + 1 ATP ↔ 2 ADP

[R44] 1 coenzymeA + 1 acetate + 1 ATP ↔ 1 acetylcoA + 1 PPi + 1 AMP

[R45] 1 coenzymeA + 1 acetate ↔ 1 acetylcoA + 1 H_2O

However, elementary flux mode calculations do not be perturbed as a result of cyclic reactions, while metabolic flux analysis does. But, MFA overcome this, when the constraints

are applied in terms of relations for the equations involved in the cyclic reactions which will be explained later.

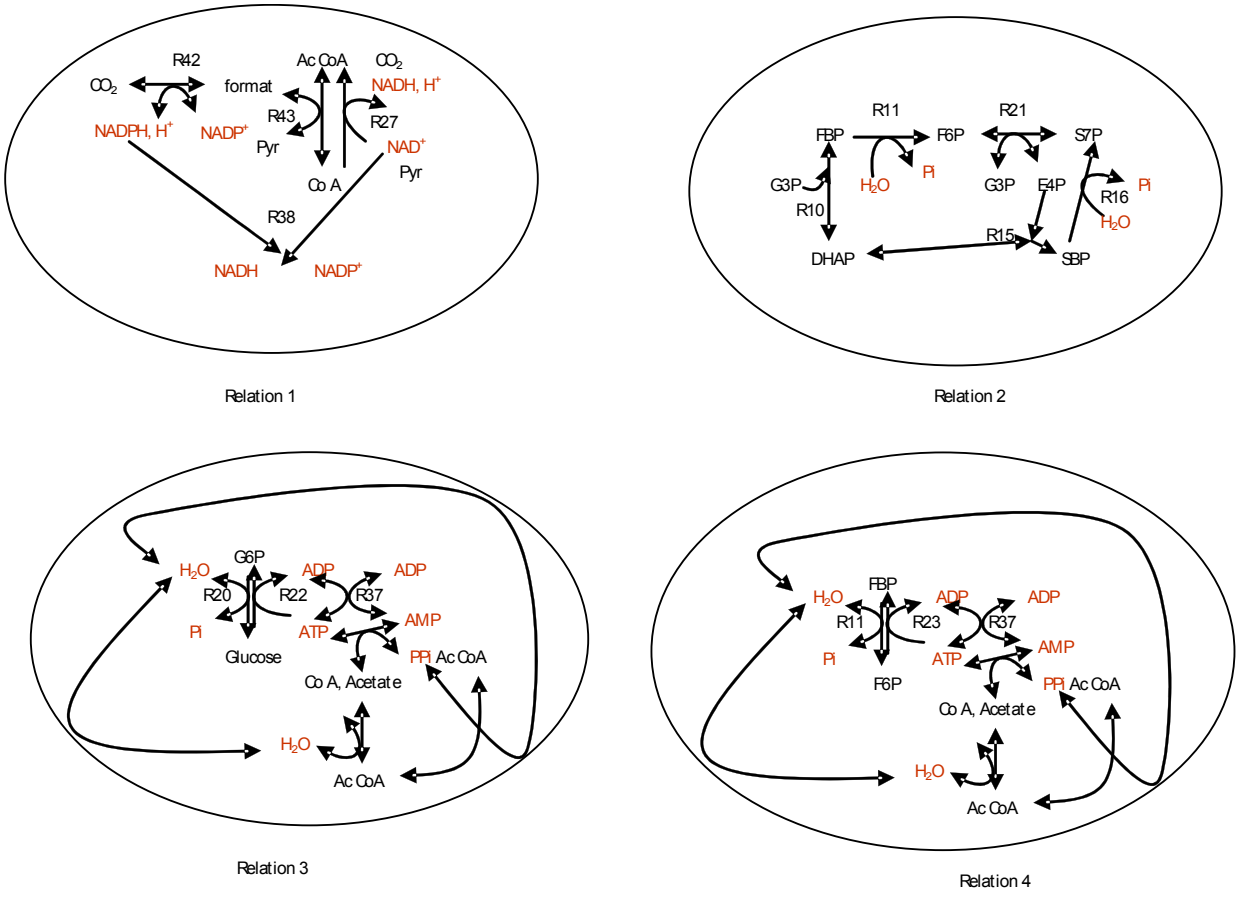

Figure 4.46: Cyclic reactions involved in the leaf metabolic network

4.2.2.1 Elementary flux mode analysis

Elementary flux mode analysis provided a way to systematically identify sets of relevant pathways of leaf metabolic network (Schuster *et al*., 1999, 2002; Trinh, 2009). They are the simplest (steady-state) flux distribution and metabolic routes that a metabolic network can show. The elementary flux modes for the leaf network were calculated using METATOOL 5.1 (von Kamp and Schuster, 2006; Klamt *et al*., 2005; Pfeiffer *et al*., 1999; Schuster *et al*., 2000; Urbanczik and Wagner, 2005).

There were 202 EFMs in total, in which 186 EFMs were strictly linked to biomass production; this large number of EFMs illustrates the complexity of the high level connections within the network. However, we have classified these EFMs into 4 main groups based on the nature of inputs and outputs. The first 2 groups of EFM pathways involve the pathways

utilising cyclic and noncyclic photophosphorylation of light energy. The third group of EFMs shows relatively small, but possible futile pathways. They are not directly linked to energy metabolism, but related to the energy metabolites like phosphate, Pi and maintain the metabolic network. Fourth group stands for biomass production; 186 EFMs of 4^{th} group reveals 186 possibilities to obtain the leaf biomass. This is the case, where we consider thermodynamic (reversibility/irreversibility) constraints; in the absence of these constraints, the metabolic network provided 1632 EFMs in which almost 1500 pathways account biomass production.

However, Group [1] contains 4 EFMs: EFM 1, EFM 2, EFM 3 and EFM 4 in the list of elementary flux obtained (see below); same for Group [2] and [3]. Group [4] contains 186 EFMs involving biomass production and it was difficult to express, as each EFM contains hundreds of equations; therefore, the EFMs involved are given in the appendix. 3.

Group [1] contains 4 EFMs = [1 2 3 4] involving cyclic photophosphorylation

Group [2] contains 8 EFMs = [5 6 7 8 9 10 11 12] involving noncyclic photophosphorylation

Group [3] contains 4 EFMs = [13 14 15 16] involving futile cycles

The stoichiometric contributions of each reaction involved in the first three groups are given in Table 4.6. In the table, as Group [3] is formed as a result of cyclic reactions, the relations along with stoichiometris are mentioned, while the stoichiometries involved for Group [4] is not shown as it was complicated to calculate.

Group 1	Stoichiometries involved (Cyclic)	Energy inputs
1	2 R1 + 2 R20 + 2 R22	-6 hv_{700}
2	2 R1 + 2 R11 + 2 R23	-6 hv_{700}
3	2 R1 + 1 R36 + 1 R37 + 1 R44 - 1 R45	-1 hv_{700}
4	2 R1 - 2 R10 + 2 R15 +2 R16 + 2 R21 + 2 R23	-6 hv_{700}
Group 2	**Stoichiometries involved (Non cyclic)**	**Energy inputs**
5	0.375 R2 + 0.375 R4 + 2 R20 + 2 R22 + 0.375 R38	-0.75 hv_{700} -0.75 hv_{680}
6	0.375 R2 + 0.375 R4 + 2 R11 + 2 R23 + 0.375 R38	-0.75 hv_{700} -0.75 hv_{680}
7	1.5 R2 + 1.5 R4 + 2 R36 + 2 R37 + 1.5 R38 + R44 + R45	-3 hv_{700} -3 hv_{680}
8	0.375 R2 + 0.375 R4 +2 R20 + 2 R22 + 0.375 R27 + 0.375 R42 + 0.375 R43	-0.75 hv_{700} -0.75 hv_{680}
9	0.375 R2 + 0.375 R4 + 2 R11+ 2 R23 +0.375 R27 + 0.375 R42 + 0.375 R43	-0.75 hv_{700} -0.75 hv_{680}
10	0.375 R2 + 0.375 R4 – 2 R10 + 2 R15 + 2 R16 + 2 R21 + 2 R23 + 0.375 R38	-0.75 hv_{700} -0.75 hv_{680}
11	1 R2 + 1 R4 + 1 R27 + 5.33 R36 + 5.33 R37 + 1 R42 + 1 R43 + 5.33 R44 -5.33 R45	-2 hv_{700} -2 hv_{680}
12	0.375 R2 +0.375 R4 -2 R10 + 2 R15 + 2 R16 + 2 R21 + 2 R23 + 0.375 R27 + 0.375 R42 + 0.375 R43	-0.75 hv_{700} -0.75 hv_{680}
Group 3	**Stoichiometries involved (Futile pathways)**	**Not directly linked to energy**
13	1 R27 -1 R38 + 1 R42 + 1R43 = 0	Relation 1
14	1 R11 + 1 R23 – 0.5 R36 – 0.5 R37 – 0.5 R44 + 0.5 R45 = 0	Relation 4
15	1 R20 + 1 R22 – 0.5 R36 – 0.5 R37 – 0.5 R44 + 0.5 R45 = 0	Relation 3
16	1 R10 - 1R15 -1 R16 -1 R21 – 1 R23 + 0.5 R36 + 0.5 R37 + 0.5 R44 -0.5 R45 = 0	Relation 2 + 4

Table 4.47 : Stoichiometries involved in different groups of EFMs '-'sign indicates the energy consumption. The relations for Group [3] are found from paragraph 4.2.2

4.2.2.2 Metabolic flux analysis

While analysing flux distribution of leaf metabolic network, 4 degrees of freedom were detected. Furthermore, the preliminary analysis has shown 4 cyclic reactions without the breaking of which (the cyclic effect) could give wrong results, as they are associated with the energy metabolites like phosphates.

It is reported that cyclic photophosphorylation happens only 10% compared to non cyclic photophosphorylation (Reeves and Hall, 2003). From this knowledge, we have applied a constraint which correlates cyclic (R1) and non cyclic photophosphorylation (R2) of the metabolic network: 1 R2 - 9 R1 = 0.

Similarly, the ATP production ratios associated with $FADH_2$ and NADH, H^+ of mitochondrial oxidative phosphorylation was also linked: 3 R3 -2 R4 = 0.

These constraints in terms of energy metabolites make much difference in the flux distribution which automatically break the effects of cyclic reactions (as they associated with the energy

molecules); in addition, the usage of these constraints eliminates four degrees of freedom. Thus, as a matter of fact, P/O ratio and P/2e- ratio were fixed. Hence, only one experimental value in terms of input or output is needed in order to predict the biomass output.

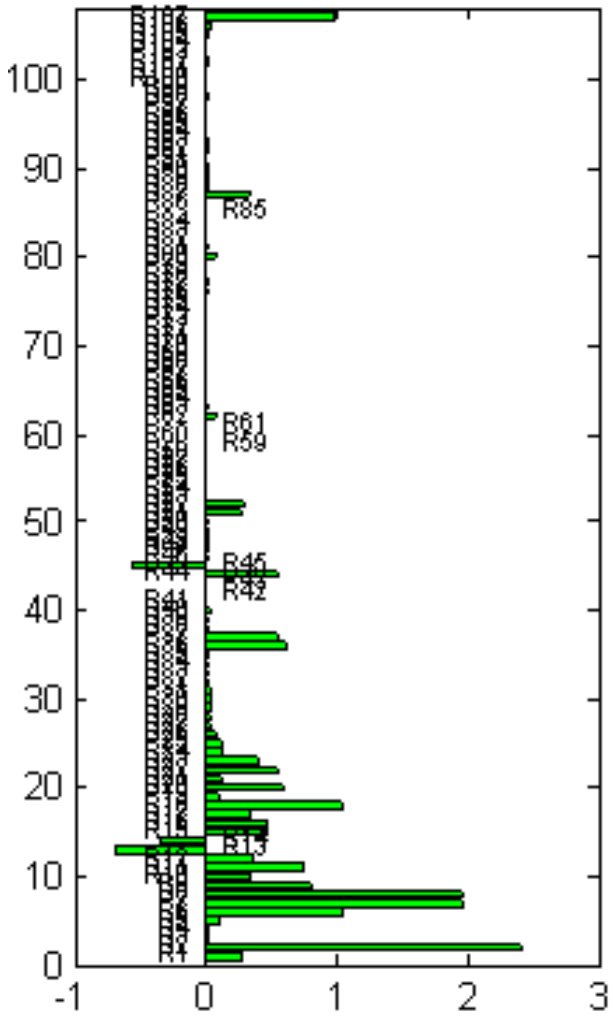

Figure 4.47: Flux distribution for leaf model

For example, if 0.978 mole of CO_2 is used as an input for the entire culture of lettuce plants, the amount of other exchangeable metabolites (the required amounts of light energy, nutrients, etc.) involved can be predicted along with the flux distribution (Figure 4.4) as shown below:

$h\nu_{700}$ = -5.64 µmol/S; $h\nu_{680}$ = -4.84 µmol/S; H_2S = -0.00175 µmol/S;

HNO_3 = -0.0975 µmol/S; O_2 = 1.19 µmol/S; H_2O = -0.769 µmol/S;

Biomass = 0.978 µmol/S, where Biomass = $C\ H_{1.67}\ O_{0.6469}\ N_{0.099}\ S_{0.0018}$.

Flux distribution values for reactions participated in the leaf model are given in the appendix 4. From Figure 4.4, we can see that the reactions are not thermodynamically violating and

hence, satisfying the normal behaviour of leaf metabolic network. In the same way, the leaf metabolic model can be validated by comparing it with the available experimental data.

4.3 Comparison and verification with the experimental data

Very few experimental data were available to validate the leaf metabolic model of lettuce. The percentage of the biomass components varies according to the plant species and the environmental condition where it grows. The leaf biomass composition was necessary to predict the *in vivo* flux distribution of lettuce leaves. Due to the unavailability of plant composition of lettuce grown in controlled environments, the plant composition was taken from Int. ref. 6 as mentioned before. As the cellular composition changes with the environmental conditions, it was important to consider the differences in input output metabolite (nutrient) fluxes along with the biomass composition. However, using Int. ref. 6, the following stoichiometric equation was proposed to describe the model after the application of constraints in the forms of P/2e- and P/O ratios.

If one mole of CO_2 is consumed by the plant of dry biomass, $C\ H_{1.67}\ O_{0.6469}\ N_{0.099}\ S_{0.0018}$:

$0.0017\ H_2S + 0.797\ H_2O + 0.097\ HNO_3 + 5.83\ h\upsilon_{700} + 5\ h\upsilon_{680} + CO_2 \rightarrow \text{Biomass} + 1.22\ O_2$,

where molecular weight of biomass = 25.47 g/mol.

From the equation, 11 photons (in μmol) are required to produce one mole of dry biomass while 9 photons are necessary to produce one mole of oxygen; it matches with the earlier studies (Jorgensen and Svirezhev, 2004) which say the requirements: 10-12 photons for the fixation of CO_2 in biomass and 8-10 photons for O_2 formation (Tredici, 2010). It is because of, what we have applied as the first constraint for the flux distribution (knowing the relative ratio of cyclic and non cyclic photophosphorylation).

Without applying the constraints itself, the EFM analysis already revealed the metabolically possible pathways involved in the biomass production, excluding the cyclic photophosphorylation reaction, R1 (see the EFM pathway for biomass production from appendix 3); besides, oxygen production depends on the noncyclic photophosphorylation, R2.

Nevertheless, the above metabolic equation for biomass production reveals the importance of cyclic photophosphorylation. The whole photons absorbed by the plants cannot be directly used for biomass. Some of them wasted as heat or fluorescence; for example, the small pathways such as the EFMs of group [1, 2 and 3] (Table 4.6). Due to the energy costs in maintenance processes like concentration gradients across the cell wall, futile cycles, transport

costs, etc., the energy consumption and production metabolites (ATP, NADPH/NADH) were assumed as non exchangeables and that is why, the above equation for biomass production does not account energy.

4.3.1 Global estimation considering final experimental data

From experiments of lettuce grown in controlled environment, the experimental data, average dry biomass weights for initial and final stages of one plant are collected.

Initial weight of the plant after seedling (in dry weight) = 1.5 g

Final weight at the end of the culture (in dry weight) = 24.9 g

Biomass production at the end of the culture = 24.9 -1.5 = 23.4 g

From the Guelph chamber measurements where the lettuce grown, the carbon and nitrogen consumed per plant for the entire experimental culture were:

Total carbon consumed per plant (as measured) = 0.978 mol

Total nitrogen consumed per plant (as measured) = 0.069 mol

According to the model performance, if 0.978 mol of CO_2 is used as an input, 0.978 C mol of biomass will be getting as output respecting the stoichiometric balance ($C H_{1.67} O_{0.6469} N_{0.099} S_{0.0018}$). But, as the experimental biomass composition was not available, it was difficult to validate the metabolic model very well. However, the first validation has been done using Int. ref. 6,

Total biomass (in moles) at the end of the culture = 23.4g ~ 0.918 mol (instead of 0.978 mol), since the molecular weight of the biomass is 25.47 g/mol.

Thus, differences in carbon and nitrogen contents in the biomass predictions have been clearly observed; thus, the predicted values were found to be relatively higher than that of the experimental values.

The third column of Table 4.7 indicates the model predictions: if CO_2 accumulation (0.978 moles) per plant for the entire culture is used as the input, according to the model predictions, 0.0975 moles of nitrate is necessary (as per biomass stoichiometry) which is relatively higher than what observed from experimental data 0.069 moles. If the biomass production at the end of the culture (23.4/25.47 = 0.918 moles) is used as input for the metabolic model (fourth column), nitrate accumulation in biomass must be 0.0915 moles, far from the experimental nitrogen accumulation. Thus, obviously the biomass composition details of leaves grown in

controlled chambers along with the rest of the experimental data are needed for accurate model validations.

No.	Exchangeables	Stoichiometric coefficients when CO_2 measured value as input is fixed (in mole)	Stoichiometric coefficients when biomass measured value as output is fixed (in mole)
1	Oxygen release	+1.19	+1.12
2	H_2S accum	-0.0018	-0.0017
3	H_2O accum	-0.769	-0.722
4	NO_3 accum	**-0.0975**	**-0.0915**
5	Photon (light energy) used 1. $h\nu_{680}$ 2. $h\nu_{700}$	 -4.84 -5.64	 -4.54 -5.3
6	Biomass	+0.978	**+0.918**
7	CO_2 accum	**-0.978**	-0.918

Table 4.48: Model predictions. '+ sign' indicates output components while '– sign' indicates input components 1) if CO_2 accumulation in the biomass is used as an input 2) if Biomass production is used as an input

From the dry biomass experiments, the carbon and nitrogen contents are listed.

C content in the final dry biomass = 0.7467 mole

N content in the final dry biomass = 0.0665 mole

Oxygen produced during the entire culture from the chamber experiments = 0.7679 mole

Using these experimental data and model predictions of Table 4.7, yields were calculated as in Table 4.8.

No.	Yield substrate/biomass	(predicted) mole of substrate/mole of carbon in biomass	(experimental) mole of substrate/mole of carbon in biomass
1	Oxygen release	1.22	1.028
2	NO_3 uptake	0.099	0.089

Table 4.49: Experimental and predicted yields

4.3.2 Time course analysis of mass balanced data

The amounts of nitrogen and carbon accumulation in the biomass with respect to time during lettuce growth culture were calculated from the supplied and disappeared CO_2 in the gas level of the closed chamber where lettuce has grown; hence, the carbon (input) accumulated in the biomass or used by the plant have been calculated. But, as we targeted to build leaf metabolic model, it was not possible to get the values only for leaves. Hence, we assumed that the lettuce leaves represent 75% of total biomass where root represent the rest (Table 4.10). The amount of nitrate accumulated in the plant is also indicated in the table, knowing the supplied and disappeared nitrate levels in the hydroponics solution of the lettuce culture. Hence, the model was expected to validate the biomass production and nitrogen accumulation (outputs), when we imply the carbon consumed/accumulated in the leaves (input).

I.e. carbon accumulation (input) → nitrogen accumulation in the biomass (output) + Biomass (output)

For this validation, it was required to imply the exact dry biomass composition of lettuce into the metabolic model, the same which has grown in the closed and controlled chambers. However, as we said earlier, we have taken it from Int. ref. 6. Using the carbon input (experimental value) in the model, the exact biomass and nitrogen accumulated in the biomass were predicted (Table 4.9).

Time (days)	Expt Carbon accu (mol)	Expt Nitrogen accu (mol)	Expt dry wt biomass (g)	Expt dry wt biomass (mol)	Predicted biomass (mol)	Predicted biomass (g)	Predicted Nitrogen accu (mol)
16/06/2004	0.0569	No data	1.125	0.044	0.0563	1.43	0.0054
23/06/2004	0.0998	0.0067	No data	No data	0.0998	2.54	0.0096

30/06/2004	0.2498	0.0165	No data	No data	0.2498	6.36	0.024
07/07/2004	0.428	0.0293	No data	No data	0.428	10.88	0.041
14/07/2004	0.585	0.0413	No data	No data	0.585	14.89	0.0561
21/07/2004	0.759	0.051	18.675	0.733	0.758	19.29	0.0726

Table 4.50 : Experimental and predicted data comparison

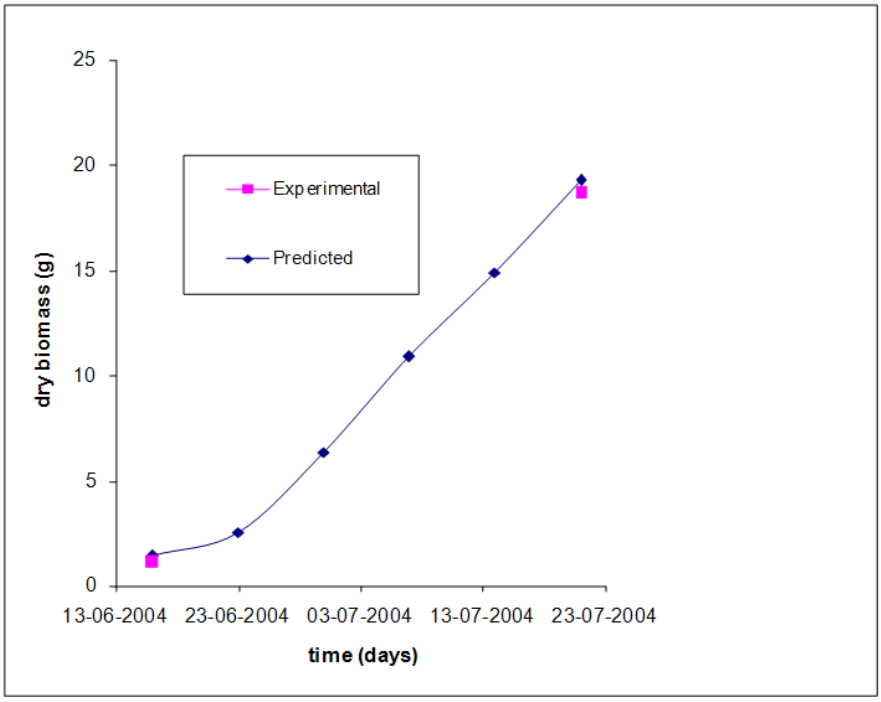

Figure 4.48 : Comparing predicted and experimental biomass

The experimental and the predicted biomass values are increasing in the same manner with time (Figure 4.5). The predicted final biomass value is very close to the experimental value.

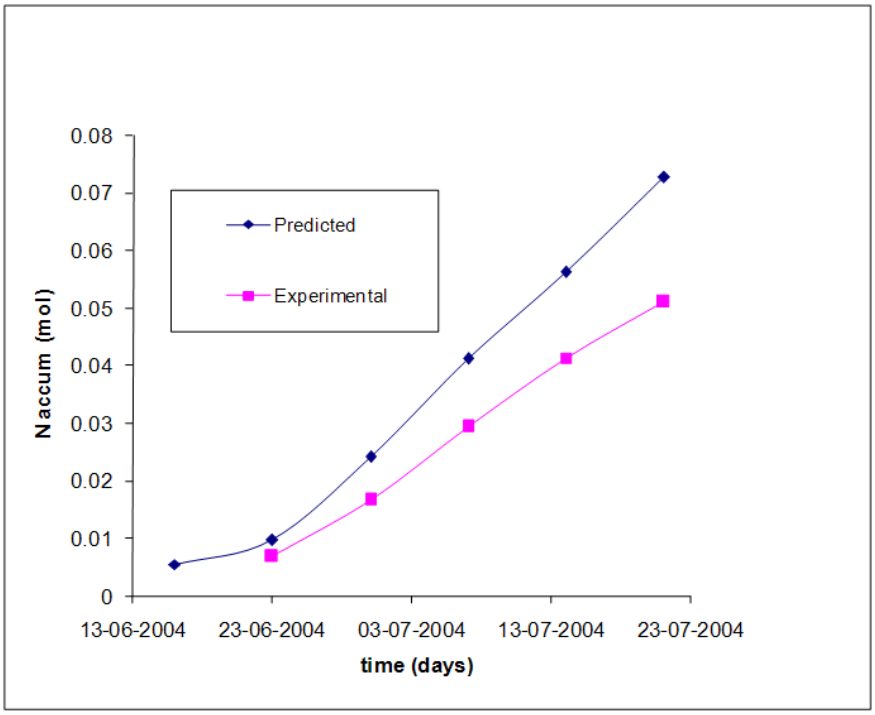

Figure 4.49 : Comparing predicted and experimental nitrogen amount in the biomass

The predicted and experimental nitrogen accumulation in the biomass was not found exactly matching (Figure 4.6). The disagreement may be probably due to the following reasons:

- The equation that is used (Int. ref. 6) for the biomass composition may be violating with the actual biomass composition of lettuce grown in Guelph experimental chambers. We do not know where and in what environmental condition they were grown.
- Due to the absence of stem and root models in the metabolic network: we have taken only an approximation- 75% of the dry biomass represents leaf biomass.
- Usually, the nutrients like nitrate enters root cells from the hydroponics culture solution is either reduced to ammonium for amino acid synthesis in the root cell and exported to the shoot as amino acids, or transported directly to the shoot as nitrate. Export from root to shoot occurs in the xylem stream. Nitrate transported to the shoot is converted to ammonium and then amino acids in chloroplasts. In most plants, the main transported amino acids are glutamine and asparagines; their composition we used for the model was also an approximation. Moreover, nitrogen assimilation is regulated at many levels and at many stages in the growth process.

- The difference in water contents of fresh biomass: the lettuce grown in controlled chambers were found 93% of it contains water, while the biomass composition equation that used in the model assumes 95%.

Nevertheless, the results obtained can be considered as the first step of the biochemical model, since, in the case of lettuce, the leaves predominate both in the biochemical model and in the edible biomass level.

4.4 General propositions for more accurate metabolic model validation

For general metabolic model, similar to leaf model, separate metabolic models for different organs are some of the minimum requirements. In addition to this, the biomass compositional changes during each growth phase can also be taken into account (if possible), it may help, if someone has keen interest to predict at a particular point of growth or period of time what happens or what can be happened, what may be the exact situation, etc. in terms of growth, quality and composition of food. However, depending on the plant physiology and morphology, these requirements can vary slightly.

Further essential demands are from dry biomass experiments:

- Biomass composition- the exact biomass composition along with protein, lipid, chlorophyll, carbohydrate, nucleic acids, etc.
- For stem model, xylem and phloem composition and for root model, root composition is required.
- Differentiate the plant composition for leaf, root, stem, fruit, etc. so that it can be applied for each specific organ metabolic model, if required. This could be coupled later after understanding the rest of the metabolical and physical mechanisms depending on which type of plant is needed to be modelled.

Up to a great extent, plant growth rate depends on the biomass rate regulated by the rates of substrate uptake. Strong correlations exist between growth rate, whole plant canopy, photosynthetic, respiration and transpiration rates. Therefore, along with the above mentioned requirements, the experimental data that we have used for our model validation (i.e. the rate and quantity of input and output metabolites) are also needed.

4.5 Conclusion

For the first step of the plant biochemical model, leaf metabolic model is established and compared with lettuce plants grown in controlled chambers of Guelph University. Taking the carbon accumulation amount in the biomass as input, the metabolic model predicted the quantity of biomass; it is compared with the actual biomass obtained at the end of the culture. The graphs plotted for the predicted biomass and experimental biomass were found matching. But, the predicted values and experimental values of nitrogen accumulation in the biomass were not so much satisfying; in fact, the predicted values were much higher than the measured values. The possible reasons are explained. More experimental values are required in terms of biomass composition, nitrogen accumulation in biomass, oxygen release and carbon source transport/concentration in each organ level to achieve the whole biochemical modeling, including root model and stem model. However, agreeing the data limitations we had, the results found were satisfying and promising for the first attempt of leaf metabolic model. Moreover, the model also calculates metabolic fluxes and other interesting features like hormone signaling which are hidden in the large EFMs of biomass production pathways and makes certainly far predictive method for metabolic studies and modeling for other areas of biology. For the designed general plant growth model, this model enabled us to couple and validate the biochemical perturbations and energy exchange with respect to physical limitations (e.g. light availability), thus provided, the link between matter and energy exchange laws of the physical mechanisms in addition to the biomass growth and composition exploration.

For MELiSSA loop target, taking our first attempt as an example, the complete biochemical model when it will be developed and coupled to establish the overall model of higher plant growth, the biochemical model will play a major role as it can predict not only the final biomass, but also, the time-course level of plant growth, the required inputs for the plant growth, in terms of light energy consumption, amount of CO_2, nutrients, etc. connecting with the physical mechanisms of plant growth factors. Hence, along with all these, the biomass and oxygen production for the crew can be predicted, knowing by which the fluxes from other compartments of MELiSSA loop can be controlled and managed.

4.6 Main outcomes of Chapter 4

- The first level modelling described in chapter 3 allowed, the second level modelling of metabolism.

- The leaf metabolic model was constructed for lettuce leaves; hence, in addition to the central carbon metabolism, protein, lipid and carbohydrate formations were added.
- The constructed leaf metabolic network was analysed; EFM and MFA gave possible pathways and flux distribution for biomass production.
- Using the data from Guelph experiments (CESRF) and USDA [Int. ref. 6], the mass balanced leaf model was compared and data reconciliation has been done.
- Variation is found for experimental and model prediction regarding nitrogen accumulation in biomass. The possible reasons for this deviation and general propositions for more accurate metabolic model validation are suggested.

Conclusion and perspectives

Conclusion and perspectives

The initial objective of this thesis was to construct a general biochemical model for plant growth containing different sub models for plant organs, in order to connect it with the designed plant growth model of MELiSSA loop concept. From various modelling methodologies, appropriate metabolic techniques which use mass balance and steady state approaches were selected, satisfying preliminary MELiSSA loop model concept of any continuous system. Then, there were two levels of metabolism to be modelled: central carbon metabolism and the secondary metabolism relating global reactions producing biomass from basic constituents.

One challenge that became immediately apparent in the initial stages of this study was associated with the localisation of metabolites, thermodynamics, the physiological condition, etc. in specific compartments within the plant cell. That was solved using recent studies found from various literatures. The case study involving a compartmentalised stoichiometric model of plant metabolism may provide new insights to other plant biologists. The analysis showed the secrets hidden under different compartments: the analysis in central carbon metabolism, the study using EFM and MFA techniques revealed the importance of thermodynamic constraints in the energy metabolism model. Without the usage of constraints, the EFM as well as MFA analysis on the network system under consideration will give wrong result. Therefore, the biochemical knowledge of complexes and at what physiological condition they are involved, etc. in a metabolic system must be known. Luckily, most of the metabolic pathways were already known (e.g. Calvin cycle, Krebs cycle), and the rest are probably on the way. Assuming various physiological conditions in the energy level (ATP^{4-}, $NADH/H^{+}$, $NADPH/H^{+}$), the metabolic flux analysis successfully predicted which complexes could be affected, if there is a lack of energy in the cell level; also at normal conditions, what will be the proportional rate of reactions. The proportional rates are predicted from the EFM results; also it provided the thermodynamically and metabolically feasible pathways, if we subject to analyse a system of stoichiometric metabolic equations in the form of matrices. It describes how our method has been fruitfully employed to model the metabolism in various compartments. Depending on the direction of reactions in terms of reversibility or irreversibility we provide, the metabolic analysis result will change.

As a preliminary step of the initial aim of our thesis, the leaf model is successfully constructed for lettuce plant leaves. The constructed leaf model is applicable only for lettuce plants, as the

biomass composition, including protein, lipid and carbohydrate formation for lettuce leaves were included in the model. Usually, leaf model alone is not sufficient for model validation, as the biochemical model, which itself is a sub model in the designed plant growth model for MELiSSA loop. It is incomplete due to the absence of stem and root models, and by the time being, it was not possible to build them due to the absence of available data.

Directions for the future

- The metabolic methods used for the modelling or small network studies can be used for purposes (e.g. medicinal) other than plant modelling and experimental validations. It can provide promising results. This can also make more interesting, if isotopic labelling can be done, at least in the case of simple network studies.
- The modelling approach for the plant model can be attained once root and stem metabolic models are available, and knowing the carbon source contents in organ level to connect all of the three models (in the case of lettuce). So, isotopic label studies are necessary in order to connect leaf and root sub models.
- For other type of plants having storage organ at roots or branches will have different morphology and the biochemical model will be different, although the central carbon metabolism will be the same.
- It is necessary to study and develop each and every plant model separately, those are aimed to cultivate in the controlled chambers of MELiSSA loop.
- Though our model is aimed for plants grown in life support system, the same type of models can be used in the area of agriculture, where plants grow in greenhouses.

The main conclusion of this thesis is that, though higher plant growth modelling was found difficult at the very beginning, the theories hidden in the metabolism along with recent metabolic techniques/studies helped to establish the leaf metabolic model. The results were found satisfying and promising for the first step of plant biochemical model, even though we had data limitations. Also, the EFM results showed that the metabolic knowledge with thermodynamical directions can aid in predicting the metabolic routes of biomass product, the technique described here can be used more generically as it enlightens metabolic studies and modeling for other areas of biology. Any attempt to construct a stoichiometric model of eukaryotic system, particularly higher plants may not be complete, if this property has not been well addressed. Among the large number of publically available metabolic techniques, our approach may significantly contribute to the identification of new pathways in many different eukaryotic systems.

For the designed general plant growth model, this model enable to couple and validate the plant biochemical perturbations and energy exchange with respect to physical limitations (e.g. light availability), thus it links matter and energy exchange laws of the physical mechanisms in addition to the biomass growth and composition exploration. Considering MELiSSA loop, when the complete biochemical model will be coupled to the designed model of higher plant growth, the biochemical model will play a major role, as it can connect directly to the prediction of plant growth requirement factors (light energy consumption, amount of CO_2, nutrients, etc.) as well as human requirement factors (CO_2 release, biomass and oxygen consumption), knowing by which the fluxes from other compartments of MELiSSA loop can be controlled and managed. Thus, the approach we used for this thesis along with the designed model for plant growth surely fulfil our target of controlling and predicting plant growth for human survival during long term space missions. Further, the modelling concept can be used for the agricultural purposes, as greenhouses are very common in industrial levels.

References

References

Aalto T., Vesala T., Mattila T., Simbierowicz P. & Hari P. (1999), A Three-dimensional Stomatal CO_2 Exchange Model Including Gaseous Phase and Leaf Mesophyll Separated by Irregular Interface, *J Theo Biol* **196**, 115–128.

Affourtit C., Krab K., & Moore, A.L. (2001), Control of plant mitochondrial respiration. *Biochim Biophys Acta* **1504**, 58-69.

Anderson G.P., Sanderson D.G., Lee C.H., Durell S., Anderson L.B. & Gross E.L. (1987), The effect of ethylenediamine chemical modification of plastocyanin on the rate of cytochrome f oxidation and P-700^+ reduction. *Biochim Biophys Acta* **894**, 386–98.

Allen M. T., Prusinkiewicz P. & DeJong T. M. (2005), Using L-systems for modeling source-sink interactions, architecture and physiology of growing trees: the L-PEACH model. *New Phyto* **166**, 869–880.

Arnon D.I., Allen M.B. & Whatley F.R. (1954), Photosynthesis by isolated chloroplasts. *Nat* **174**, 394-406.

Arnon D.I. & Chain R.K. (1975), Regulation of ferredoxin-catalyzed photosynthetic phosphorylations. *PNAS* USA **72**, 4961-4965.

Asner G. P. & Wessman C. A. (1997), Scaling PAR absorption from the leaf to landscape level in spatially heterogenous ecosystems, *Eco Mod* **103**, 81–97.

Atkins C.A., Pate J.S. & McNeil D.L. (1980), Phloem loading and metabolism of xylem-borne amino compounds in fruiting shoots of a legume. *J Exp Bot* **31**, 1509–1520.

Atwell B.J., Kriedemann P.E. & Turnbull C.G.N. (1999), Plants in action: adaptation in nature, performance in cultivation. *In* Woodrow I.E (Ed.), *Carbon dioxide assimilation and respiration*, 54-60, Macmillian publishers, PTY LTD, Australia.

Bailey J.E. (1998), Mathematical modeling and analysis in biochemical engineering: past accomplishments and future opportunities. *Biotechnol Prog* **14**, 8-20.

Bailey J.E. (2001), Complex biology with no parameters. *Nat Biotechnol* **19**, 503-504.

Balakrishnan A. C. (2010), *Stoichiometric modelling of plant metabolic networks*, Ph.D. thesis, Oxford Brookes University.

Bassham J. A. & Buchanan B. B. (1982), Carbon dioxide pathways in plant and bacteria, Vol **2** *In.* Govindjee (Ed.), *Photosynthesis: development carbon metabolism and plant productivity*, 141-189, Academic press, New York.

Berg J.M., Tymoczko J.L. & Stryer L. (2002) Biochemistry. 5th ed. Chapters 18 & 19, New York: W H Freeman http://www.ncbi.nlm.nih.gov/books/NBK21208/, http://www.ncbi.nlm.nih.gov/books/NBK21191/, consulted on 26/11/2010

Bertheloot J., Andrieu B., Fournier C. & Martre P. (2008), A process-based model to simulate nitrogen distribution in wheat (*Triticum aestivum*) during grain-filling. *Func Plant Biol* **35**, 781–796.

Bertin N., Martre P., Génard M., Quilot B. & Salon C. (2010), Under what circumstances can process-based simulation models link genotype to phenotype for complex traits? Casestudy of fruit and grain quality traits. *J Exp Bot* **61**, 955–967.

Beurton M.-A., Beauvoit B., Monier A., Vallée F., Dieuaide N. M. & Colombié S. (2011), Comparison between elementary flux modes analysis and 13C-metabolic fluxes measured in bacterial and plant cells. *BMC Syst Biol* **5**, 95-108.

Blasius B., Beck F. & Lüttge U. (1998), Oscillatory model of Crassulacean acid metabolism: Structural analysis and stability boundaries with a discrete hysteresis switch. *Plant, Cell & Environ* **21**, 775–784.

Blasius B., Neff R., Beck F. & Lüttge U. (1999), Oscillatory model of crassulacean acid metabolism with a dynamic hysteresis switch. *Proc Royal Soc B Biological Sciences*. **266**, 93-101.

Boote K. J., Jones J. W. & Hoogenboom G. (1998), Simulation of crop growth: CROPGRO model, *In* Peart R. M. & Curry R. B. (Eds), *Agricultural Systems Modeling and Simulation*, Marcel Decker, 651-693, New York.

Boulard T., Mermier M., Fargues J., Smits N., Rougier M. & Roy J. C. (2002), Tomato leaf boundary layer climate: implications for microbiological whitefly control in greenhouses. *Agric and Forest Meteorol* **110**, 159–176.

Bouman B. A. M., Keulen H. van, Laar H. H. and van Rabbinge R. (1996), The 'School of de Wit' Crop Growth Simulation Models: A Pedigree and Historical Overview. *Agri Sys* **52**, 171–198.

Brisson N., Launay M., Mary B. & Beaudoin N. (Eds.) (2008), *Conceptual Basis, Formalisations and Parameterization of the Stics Crop Model*, Quae editions Versailles, 304.

Calik P., Calik G., Takac S, & Ozdamar T.H. (1999), Metabolic flux analysis for serine alkaline protease fermentation by Bacillus licheniformis in a defined medium: effects of the oxygen transfer rate. *Biotechnol Bioeng* **64**, 151-167.

Carbo M.R., Berry J. A.., Dan Y., Larry G., Robinson S. A., Lennon A. M. & Siedow J. N. (1995), Electron Partitioning between the Cytochrome and Alternative Pathways in Plant Mitochondria *Plant Physiol* **109**, 829-837.

Cassimeris L., Lingappa V. R. & Plopper G. (2011), *Lewin's Cells*, 2nd edition, Jones and Bartlett publishers, LLC. Massachusetts, 1056.

Chance B. (1943), The kinetics of the enzyme-substrate compound of peroxidase. *J Biol Chem* **151**, 553–577.

Chelle M. & Andrieu B. (1998), The nested radiosity model for the distribution of light within plant canopies. *Eco Modl* **111**, 75–91.

Chen L., Wang R. & Zhang X. (2009), Biomolecular networks: methods and applications in systems biology, In. *Metabolic networks: Analysis, reconstruction and application*, 281-298, John Wiley and Sons, New Jersey, USA.

Christy A. L. & Ferrier J. M. (1973), A Mathematical Treatment of Munch's Pressure-Flow Hypothesis of Phloem Translocation. *Plant Physio* **52**, 531–538.

Clarke B.L. (1981), Complete set of steady states for the general stoichiometric dynamical system *J Chem Phy* **75**, 4970-4979.

Cogne G. (2003), *Conception, mise en œuvre et modélisation d'un photo bioréacteur à membrane pour l'étude du comportement de la cyanobactérie Arthrospira platensis en microgravité*, Ph.D. thesis, Laboratoire de Génie Chimique et Biochimique, Université Blaise Pascal.

Collatz G.J., Ribas-Carbo M. & Berry J.A. (1992), Coupled Photosynthesis-Stomatal Conductance Model for Leaves of C4 Plants. *Aus J Plant Physio* **19**, 519 - 538.

Covert M.W., Schilling C.H., Famili I., Edwards J.S., Goryanin I.I., Selkov E., Palsson B.O.. (2001), Metabolic modeling of microbial strains in silico. *Trends Biochem Sci* **26**, 179–186.

Cournède P.H., Kang M.Z., Mathieu A., Barczi J.F., Yan H.P., Hu B.G. & de Reffye P. (2006), Structural Factorization of Plants to Compute their Functional and Architectural Growth. *Sim* **82**, 427–438.

Cramer W.A., Yan J., Zhang H., Kurisu G. & Smith J.L. (2005), Structure of the cytochrome b6f complex: new prosthetic groups, Q-space, and the 'hors d'oeuvres hypothesis' for assembly of the complex.. *Photosynth Res* **85**, 133–143.

Cramer W.A., Zhang H., Yan J., Kurisu G. & Smith J.L. (2006), Transmembrane traffic in the cytochrome b6f complex. *Annu Rev Biochem* **75**, 769–90.

Curien G., Ravanel S. & Dumas R. (2003), A kinetic model of the branch-point between the methionine and threonine biosynthesis pathways in *Arabidopsis thaliana*. *Eur J Biochem* **270**, 4615–4627.

Curien G., Bastien O., R-Genthon M., C-Bowden A., Cádenas M.L. & Dumas R. (2009), Understanding the regulation of aspartate metabolism using a model based on measured kinetic parameters. *Mol Syst Biol* **5,** 271.

Daae E.B., Dunnill P. Mitsky T.A., Padgette S.R., Taylor N.B., Valentin H.E. & Gruys K.J. (1999), Metabolic modeling as a tool for evaluating polyhydroxyalkanoate copolymer production in plants. *Metab Eng* **1**, 243-254.

Dandekar T., Schuster S., Snel B., Huynen M. & Bork P. (1999). Pathway alignment: Application to the comparative analysis of glycolytic enzymes. *Biochem J* **343**, 115-124.

Da Silva D., Favreau R., Auzmendi I. & DeJong T. M. (2011), Linking water stress effects on carbon partitioning by introducing a xylem circuit into L-PEACH. *Annals of Botany* **108**, 1135–1146.

De Graaf A.A., Striegel K., Wittig R.M., Laufer B., Schmitz G., Wiechert W., Sprenger G.A. & Sahm H. (1999), Metabolic state of Zymomonas mobilis in glucose-, fructose-, and xylose-fed continuous cultures as analysed by 13C- and 31P-NMR spectroscopy. *Arch Microbiol* **171**, 371-385

De Noronha P.P., Nielsen J. & Bazin M.J. (1996), Pathway kinetics and metabolic control analysis of a high-yielding strain of Penicillium chrysogenum during fed batch cultivations. *Biotechnol Bioeng* **52**, 631.

De Reffye P., Heuvelink E., Barthélémy D. and Cournède P.-H. (2008), Plant Growth Models, *In* Jorgensen S. E. and Fath B. D. (Ed), *Encyclopedia of Ecology* vol. **4**, 2824-2837, Elsevier, Oxford.

Dewar R. C. (2002), The Ball–Berry–Leuning and Tardieu–Davies stomatal models: synthesis and extension within a spatially aggregated picture of guard cell function. *Plant, Cell and Environ* **25**, 1383–1398.

Dussap C.-G. (2005), Projet BRUME: Base de données et calcul de flux métaboliques, Réseau Français de Metabolomoque et Fluxomique, 1-2 Décembre, Toulouse.

Dussap C.-G., Frisch C., Creuly C., Cornet J.F. & Poughon L. (2005), *Bioregenerative life support basic development – Appendix 1: Fundamental R&D for MELiSSA engineering development*, Contract no. 19304/05/NL/CP, 74.

Edwards J.S. & Palsson B.O. (1999), Systems properties of the Haemophilus influenzae Rd metabolic genotype. *J Biol Chem* **274**, 17410-17416.

Edwards J.S. & Palsson B.O. (2000 a), The *Escherichia coli* MG1655 *in silico* metabolic genotype: its definition, characteristics and capabilities. *PNAS* **97**, 5528-5533.

Edwards J.S., Ibarra R.U., & Palsson B.O. (2001), *In silico* predictions of *Escherichia coli* metabolic capabilities are consistent with experimental data. *Nat Biotechnol* **19**, 125-130.

Edwards J.S., Covert M. & Palsson B., (2002), Metabolic modelling of microbes: the flux-balance approach *Environ Microbiol* **4**,133-140.

Emerson R.L., Stauffer J.F. & Umbreit W.W. (1944), Relationships between phosphorylation and photosynthesis in Chlorella. *Am J Botany* **31**, 107–120.

Emes (1991), Compartmentation of plant metabolism in non-photosynthetic tissues, SEB Seminar Series 42, *In* Beevers H. (Ed.), *Metabolic compartmentation in plant cells,* 1-20, Cambridge University Press, UK.

Evers J. B., Vos J., Fournier C., Andrieu B., Chelle M. & Struik P. C. (2005), Towards a generic architectural model of tillering in Gramineae, as exemplified by spring wheat (Triticum aestivum). *New Phyto* **166**, 801–812.

Famili I., Forster J., Nielsen J., & Palsson B.O. (2003), Saccharomyces cerevisiae phenotypes can be predicted by using constraint-based analysis of a genome-scale reconstructed metabolic network. *Proc Natl Acad Sci U S A* **100**, 13134-13139.

Farquhar G.D., von Caemmerer S., & Berry J. A. (1980), A biochemical model of photosynthetic CO_2 assimilation in leaves of C3 species. *Planta* **149**, 78-90.

Farquhar G.D., von Caemmerer S., & Berry J.A. (2001), Models of photosynthesis. *Plant Physiol* **125**, 42-45.

Feist A.M., Scholten J.C., Palsson B.O., Brockman F.J., & Ideker T. (2006), Modeling methanogenesis with a genome-scale metabolic reconstruction of Methanosarcina barkeri. *Mol Syst Biol* **2**.

Feist A.M. Henry C.S., Reed J.L., Krummenacker M., Joyce A.R., Karp P.D., Broadbelt L.J., Hatzimanikatis V. & Palsson B.O. (2007), A genome-scale metabolic reconstruction for *Escherichia coli* K-12 MG1655 that accounts for 1260 ORFs and thermodynamic information. *Mol Syst Biol* **3**, 121

Fernie A.R., Geigenberger, P., & Stitt, M. (2005), Flux an important, but neglected, component of functional genomics. *Curr Opin Plant Biol* **8**, 174-182.

Fernie A.R., Aharoni A., Willmitzer L., Stitt M., Tohge T., Kopka J., Carroll A.J., Saito K., Fraser P.D., DeLuca V. (2011), Recommendations for reporting metabolite data. *Plant Cell* **23**, 2477-2482.

Feyziyev Y. M. (2010), Oxygenic photosynthesis, *Proc ANAS (Biol Sc),* **65**, 71-82.

Fiscus E. L. & Kramer P. J. (1975), General model for osmotic and pressure-induced flow in plant roots. *PNAS* **72**, 3114–3118.

Follstad B.D., Balcarcel R.R., Stephanopoulos G., & Wang D.I.C. (1999), Metabolic flux analysis of hybridoma continuous culture steady state multiplicity. *Biotechnol Bioeng* **63**, 675-683.

Fontes P. C. R., Pereira P. R. G. & Conde R. M. (1997), Critical chlorophyll, total nitrogen, and nitrate - nitrogen in leaves associated to maximum lettuce yield. *J Plant Nutri* **20**, 1061-1068.

Fournier C. & Andrieu B. (1998), A 3D Architectural and Process-based Model of Maize Development. *Ann Bot* **81**, 233–250.

Fournier C. & Andrieu B. (1999), ADEL-maize: an L-system based model for the integration of growth processes from the organ to the canopy. Application to regulation of morphogenesis by light availability. *Agro* **19**, 313–327.

Fridlyand L.E. (1998), Independent changes of ATP/ADP or delta pH could cause oscillations in photosynthesis. *J Theor Biol* **193**, 739–741.

Fridlyand L.E., Backhausen J.E. & Scheibe R. (1998), Flux control of the malate valve in leaf cells. *Arch Biochem Biophys* **349**, 290-298.

Fridlyand L.E. & Scheibe R. (1999), Regulation of the Calvin cycle for CO_2 fixation as an example for general control mechanisms in metabolic cycles. *Biosys* **51**, 79-93.

Fridlyand L.E. & Scheibe R. (2000), Regulation in metabolic systems under homeostatic flux control. *Arch Biochem Biophys* **374**, 198-206.

Fukumura A., Tsutsumi M., Tsuchishima M. & Takase S. (2003), Correlation Between Adenosine Triphosphate Content and Apoptosis in Liver of Rats Treated With Alcohol, *Alcohol Clin Exp Res* **27,**12S- 15S.

Gabrielle B., Denoroy P., Gosse G., Justes E. & Andersen M. N. (1998), Development and evaluation of a CERES-type model for winter oilseed rape. *Field Crops Research* **57**, 95–111.

Gagneur J. & Klamt S. (2004) Computation of elementary modes: a unifying framework and the new binary approach. *BMC bioinform* **5**,175.

Gao J., Gorenflo V.M., Scharer J.M., & Budman H.M. (2007), Dynamic metabolic modeling for a MAB bioprocess. *Biotechnol Prog* **23**, 168-181.

Gardestrom P. & Lernmark U. (1995), The contribution of mitochondria to energetic metabolism in photosynthetic cells. *J Bioenerg Biomembr* **27**, 415-421.

Garfinkel D. & Hess B. (1964),Metabolic Control Mechanisms. Vii.A Detailed Computer Model of the Glycolytic Pathway in Ascites Cells. *J Biol Chem* **239**, 971-983.

Garrett R. & Grisham C.M. (2000), *Biochimie*, 2nd ed, (translated, De Boeck Université, Paris), 1254 p.

Gayen K. & Venkatesh K. V. (2006), Analysis of optimal phenotypic space using elementary modes as applied to *Corynebacterium glutamicum*. *BMC Bioinform* **7**, 445.

Ghannoum O., Siebke K., von Caemmerer S. & Conroy J. P. (1998), The photosynthesis of young Panicum C4 leaves is not C3-like. *Plant Cell Environ* **21**, 1121–1131.

Giannino D., Nicolodi C., Testone G., Frugis G., Pace E., Santamaria P., Guardasole M. & Mariotti D. (2008), The over expression of asparagines synthetase A from *E. Coli* affects the nitrogen status in leaves of lettuce (*Lactuca Sativa L.*) and enhances vegetative growth. *Euphytica* **162**, 11–22.

Giersch C. (2000), Mathematical modelling of metabolism. *Cur Opi Plant Biol* **3**, 249–253.

Gimmler H. (1977), Photophosphorylation *in vivo*. *In* A Trebst & M Avron (Eds.), *Encyclopedia of Plant Physiology*, New Series, Vol 5. 448-472, Springer-Verlag, Berlin, Germany.

Gombert A.K. & Nielsen J. (2000), Mathematical modelling of metabolism. *Curr Opin Biotechnol* **11**, 180-186.

Goodwin B.C. (1963), *Temporal organization in cells, a dynamic theory of cellular control processes*. Academic Press, New York, USA. 163 p.

Goryanin I., Hodgman T.C., & Selkov E. (1999), Mathematical simulation and analysis of cellular metabolism and regulation. *Bioinfor* **15**, 749-758.

Govaerts Y. M. (1996), *A Model of Light Scattering in Three-Dimensional Plant Canopies: a Monte Carlo Ray Tracing Approach*, Ph.D. Thesis, Institute for Remote Sensing Applications, UCL, Belgium.

Grammel H. & Ghosh R. (2008), Redox state dynamics of ubiquinone-10 imply cooperative regulation of photosynthetic membrane expression in *Rhodospirillum rubrum*, *J Bacteriol* **190**, 4912-4921.

Gross L.J., Kirschbaum M. U. F. & Pearcy R. W. (1991), A dynamic model of photosynthesis in varying light taking account of stomatal conductance, C3-cycle intermediates, photorespiration and Rubisco activation. *Plant Cell Environ* **14**, 881–893.

He D.X. & Edwards G. E. (1996), Estimation of diffusive resistance of bundle sheath cells to CO_2 from modeling of C4 photosynthesis. *Photosynth Res*, **49**, 195–208.

Heinrich R. & Schuster S. (1996), *The Regulation of Cellular Systems,* Chapman and Hall, New York, USA, 372 p.

Heldt H.W. & Flugge U.I. (1987), Subcellular transport of metabolites in plant cells, Vol. **12**. *In* D.D. Davis (Ed), *The Biochemistry of Plants*, 49-85, Academic Press, New York, USA.

Heldt H. W. & Heldt F. (2005), Plant biochemistry 3rd ed, Elsvier Academic press, San diego, USA, 630 p.

Henton S. M., Greaves A. J., Piller G. J. and Minchin P. E. H. (2002), Revisiting the Münch pressure-flow hypothesis for long-distance transport of carbohydrates: modelling the dynamics of solute transport inside a semipermeable tube. *J Exp Bot* **53 (373)**, 1411–1419.

Hibberd J.M. & Quick W.P. (2002), Characteristics of C-4 photosynthesis in stems and petioles of C-3 flowering plants. *Nature* **415** (6870), 451-454.

Himmelblau D. M. (Ed.) (1967), *Basic Principles and Calculations in Chemical Engineering,* 2nd ed, Prentice-Hall, Englewood, Cliffs, New Jersey, 483 p.

Holms W.H. (1986), The central metabolic pathways of *Escherichia coli*: relationship between flux and control at a branch point, efficiency of conversion to biomass, and excretion of acetate. *Curr Top Cell Regul* **28**, 69–105.

Hopmans J.W. & Bristow K.L. (2002), Current capabilities and future needs of root water and nutrient uptake modelling, *Adv Agro* **77**, 104–175.

Hua Q., Yang C. & Shimizu K. (1999), Metabolic flux analysis for efficient pyruvate fermentation using vitamin-auxotrophic yeast of Torulopsis glabrata. *J Biosci Bioeng* **87**, 206-213.

Ishii N., Robert M., Nakayama Y., Kanai A., & Tomita M. (2004), Toward large-scale modeling of the microbial cell for computer simulation. *J Biotech* **113**, 281-294.

Jamshidi N. & Palsson B.O. (2008), Formulating genome-scale kinetic models in the post-genome era. *Mol Syst Biol* **4**, 171.

Jarvis P. G. & McNaughton K. G. (1986), Stomatal Control of Transpiration: Scaling Up from Leaf to Region, *Adv Eco Res* **15**, 1–49.

Jeong H., Tombor B., Albert R., Oltvai Z.N. & Barabási A.L. (2000), The large-scale organization of metabolic networks. *Nat* **407**, 651-654.

Jenks M. A. & Bebeli P. J. (2011), Breeding for Fruit Quality, *In*. H.C. Passam, I. C. Karapanos and A.A. Alexopoulos, (Eds.) *The Biological basis of Fruit quality*, John Wiley & Sons, Ames, UK.

Jones E. W. & Fink G. R. (1981), Regulation of amino acid and nucleotide biosynthesis in yeast. *In.* J. R. Broach and. E. W Jones (Eds). *The Molecular Biology of the Yeast*

Saccharomyces: Metabolism and Gene Expression, 181- 299, Cold Spring Harbor Laboratory, Cold Spring Harbor, New York, USA.

Joliot P. & Joliot A. (2002), Cyclic electron transfer in plant leaf. *PNAS* **99**, 10209-10214.

Jorgensen S.E & Svirezhev YM (Eds) (2004), Towards a thermodynamic theory for Ecological systems 1st (ed), *In Stability in mathematics, thermodynamics and ecology,* 127-129, Elsevier Ltd, Netherlands.

Junker B. H. & Schreiber F., (2008) *Analysis of biological networks* John Wiley & Sons, New Jersey. USA, 368 p.

Kacser H. & Burns J.A. (1973), The control of flux. *Symp Soc Exp Biol* **27**, 65-104.

Kaiser H. (2009), The relation between stomatal aperture and gas exchange under consideration of pore geometry and diffusional resistance in the mesophyll. *Plant, Cell and Environ* **32**, 1091–1098.

Kaitala V. Hari P, Vapaavuori E. & Salminen R. (1982), A dynamic model for photosynthesis. *Ann Bot* **50**, 385–396.

Katoh S. & Yoshida F. (Eds) (2009), Biochemical engineering: a textbook for engineers, chemists and biologists*, Introduction: material balance and energy balance* 8-10, Wiley-VCH, Weinheim, Germany.

Kauffman K.J., Prakash, P. & Edwards J.S. (2003), Advances in flux balance analysis. *Curr Opin Biotechnol* **14**, 491-496.

Kepes F. (2007), Biological networks- Complex systems and Interdisciplinary Science Vol **3**, *In* D.A. Fell (Ed.) *Metabolic networks*,World Scientific Publishing Co Pt Ltd, Singapore, 163-197 p.

Ketsaa S, Uthairatanakij A & Prayurawong A. (2001), Senescence of diploid and tetraploid cut inflorescences of Dendrobium Caesar, *Scientia Horticutlurae* **91**, 133-141.

Klamt S. & Stelling J. (2002), Combinatorial complexity of pathway analysis in metabolic networks. *Mol Biol Rep* **29**, 233–236.

Klamt S., Gagneur J. & von Kamp A. (2005), Algorithmic approaches for computing elementary modes in large biochemical reaction networks. *IEE Proceedings Systems Bio* **152**, 249-255.

Klebs G. (1906), Uber kunstliche Metamorphosem, 115 p, (Abh Natur Ges Halle xxv), Stuttgart.

Kolek J. & Kozinka V. (1992), Physiology of the plant root system, *In* M. Luxova and M. Ciamporova, *Root sturucture*, 82-86, Kluwer Academic Publishers, Boston, USA.

Krab K. (1995), Kinetic and regulatory aspects of the function of the alternative oxidase in plant respiration. *J Bioenerg Biomembr* **27** (4), 387-396.

Kramer D.M., Sacksteder C.A. & Cruz J.A. (1999), How acidic is the lumen? *Photosynth Res* **60**, 151–163.

Kuepfer L. (2010), Towards whole-body systems physiology. *Mol Syst Biol* **6**, 409.

Kwak J.M., Mäser P., & Schroeder J.I. (2008), The clickable guard cell, version II: Interactive model of guard cell signal transduction mechanisms and pathway. *In*.(Eds.) R. Last, C. Chang, I. Graham, O. Leyser, R. McClung & C. Weinig, *The Arabidopsis Book*, American Society of Plant Biologists, Rockville, 1-17.

Lambers H., Chapin III F. S. & Pons T. L. (Eds.) (2008), *Plant physiological Ecology*, 2nd edition Springer, USA, 604 p.

Laisk A (1973), Mathematical model of photosynthesis and photorespiration: reversible phosphoribulokinase reaction. *Biophy* **18**, 679-684.

Laisk A., Eichelmann H., Oja V., Eatherall A. & Walker D. A. (1989), A Mathematical Model of the Carbon Metabolism in Photosynthesis. Difficulties in Explaining Oscillations by Fructose 2,6-Bisphosphate Regulation. *Proc R Soc Lond B* **237**, 389– 415.

Latowski D., Burda K. & Strzalka K. (2000), A mathematical model describing kinetics of conversion of violaxanthin to zeaxanthin via intermediate antheraxanthin by the xanthophyll cycle enzyme violaxanthin de-epoxidase. *J Theor Biol* **206**, 507–514.

Lens F., Sperry J. S., Christman M.A., Choat B., Rabaey D. & Jansen S. (2011), Testing hypotheses that link wood anatomy to cavitation resistance and hydraulic conductivity in the genus Acer. *New Phytol* **190**, 709-723.

Leuning R. (1995), A critical appraisal of a combined stomatal-photosynthesis model for C3 plants, *Plant, Cell and Environ* **18**, 339–355.

Liao J. C., Hou S.-Y. & Chao Y.P. (1996), Pathway analysis, engineering and physiological considerations for redirecting central metabolism. *Biotechnol Bioeng* **52**, 129-140.

Liedvogel B. (1986). Acetyl-CoA and isopentenylpyrophosphate as lipid precursors in plant cells: Biosynthesis and compartmentation. *J Plant Physiol* **124**, 211–222.

Linka N. & Weber A.P.M. (2010), Intracellular Metabolite Transporters in Plants. *Mol Plant,* **3**, 21–53.

Llaneras F. & Pico J. (2007), An interval approach for dealing with flux distributions and elementary modes activity patterns. *J Theor Biol* **246**, 290-308.

Llaneras F. & Pico J. (2008), Stoichiometric modelling of cell metabolism. *J Biosci Bioeng* **105**, 1-11.

Luscombe N.M, Babu M.M., Yu. H, Snyder M, Teichmann S.A. & Gerstein M. (2004), Genomic analysis of requlatory network dynamics reveals large topological changes. *Nature* **431**, 308-312.

Masakapalli S.K., Le Lay P., Huddleston J.E., Pollock N.L., Kruger N.J. & Ratcliffe R.G. (2010), Subcellular flux analysis of central metabolism in a heterotrophic Arabidopsis cell suspension using steady-state stable isotope labeling. *Plant Physiol* **152**, 602–619.

McNeil S.D., Nuccio M.L., Rhodes D., Shachar-Hill Y. & Hanson A.D. (2000), Radiotracer and computer modeling evidence that phospho-base methylation is the main route of choline synthesis in tobacco. *Plant Physiol* **123**, 371-380.

Mendes P. (1997), Biochemistry by numbers: simulation of biochemical pathways with Gepasi 3. *Trends Biochem Sci* **22**, 361-363.

Mendes P. & Kell D. (1998), Non-linear optimization of biochemical pathways: applications to metabolic engineering and parameter estimation. *Bioinform* **14**, 869-883.

Mettler I.J. & Beevers H. (1980), Oxidation of NADH in glyoxysomes by a malate-aspartate shuttle. *Plant Physiol* **66**, 555-560.

Milner P.C. (1964), The possible mechanisms of complex reactions involving consecutive steps. *J Electrochem Soc* **111**, 228-232.

Milstein J. & Bremermann H.J. (1979), Parameter identification of the Calvin photosynthesis cycle. *J Math Biol* **7**, 99–116.

Mohr H. & Schopfer P. (Eds.) (1995), Plant physiology, *Ripening and germination of reproductive and distributive organs*, Springer-Verlag, Berlin 416 p.

Mollenhauer & Morre (Eds.), (2009), The Golgi Apparatus: The First 100 Years, *The function in the flow differentiation of membranes*, Springer, New York, 94-100 p.

Moller I. M. (2001), Plant mitochondria and oxidative stress: Electron Transport, NADPH Turnover, and Metabolism of Reactive Oxygen Species, *Annu Rev Plant Physiol Plant Mol Biol* **52**, 561–91.

Monteith J. L. (1981), Evaporation and surface temperature. *Quart J Roy Met Soc* **107**, 1–27.

Morgan J.A. & Rhodes D. (2002), Mathematical Modeling of Plant Metabolic Pathways. *Meta Eng* **4**, 80–89.

Neff R., Blasius B., Beck F. & Lüttge U. (1998), Thermodynamics and energetics of the tonoplast membrane operating as a hysteresis switch in an oscillatory model of Crassulacean acid metabolism. *J Membr Biol* **165**, 37-43.

Nicholls D. G. & Ferguson S.J. (Eds.) (1992), *Bioenergetics 2*, Academic press, Sandiego, California, 42-204.

Nielsen J. (2003), It is all about metabolic fluxes. *J Bacteriol* **185**, 7031-7035.

Nissen T., Schulze U., Nielsen J. &Villadsen J. (1997), Flux distributions in anaerobic, glucose-limited continuous cultures of Saccharomyces cerevisiae. *Microbiology* **143**, 203–218.

Nobel P.S. (2009), 4th ed, Physicochemical and environmental plant physiology, *Photochemistry of photosynthesis and Bioenergetics*, 229-317, Academic press publications, UK.

Nuccio M.L., McNeil S. D., Ziemak M. J., Hanson A. D., Jain R. K., Selvaraj G. (2000), Choline import into chloroplasts limits glycine betaine synthesis in tobacco: Analysis of plants engineered with a chloroplastic or a cytosolic pathway. . *Metab Eng* **2**, 300–311.

Nungesser D., Kluge M., Tolle H. and Oppelt W. (1984), A dynamic computer model of the metabolic and regulatory processes in Crassulacean acid metabolism. *Planta* **162**, 204–214.

Nuno J.C., S´anchez-Valdenebro I., P´erez-Iratxeta C., Mel´endez-Hevia E. & Montero F. (1997), Network organization of cell metabolism: monosaccharide interconversion. *Biochem J* **324**, 103–111.

Olivier B.G., Rohwer J.M. & Hofmeyr J.H.S. (2005), Modelling cellular systems with PySCeS. *Bioinformatics* **21**, 560-561.

Palsson B. (2000), The challenges of *in silico* biology. *Nat Biotechnol* **18**, 1147-1150.

Papin J.A., Price N.D., Edwards J.S., Palsson B.O. (2002 a), The genome-scale metabolic extreme pathway structure in *Haemophilus influenzae* shows significant network redundancy. *J Theor Biol* **215**, 67–82.

Papin J.A, Price N.D., Palsson B.O. (2002 b), Extreme pathway lengths and reaction participation in genome-scale metabolic networks. *Genome Res* **12**, 1889–1900.

Papin J.A., Price N.D., Wiback S.J., Fell D.A., & Palsson B.O. (2003), Metabolic pathways in the post-genome era. *Trends Biochem Sci* **28**, 250-258.

Papin J.A., Stelling J., Price N.D., Klamt S., Schuster S. & Palsson B.O. (2004), Comparison of network-based pathway analysis methods. *Trends Biotechnol* **22**, 400-405.

Park S. H., Elless M. P., Park J., Jenkins A., Lim W., Chambers E. & Hirschi K. D. (2009) Sensory analysis of calcium biofortified lettuce. *J Plant Biotech* **7**, 106–117.

Hézard P. (2010), *Higher plant growth modelling for life support systems: global model design and simulation of mass and energy transfers at the plant level*, Ph.D. Thesis, Institut Pascal axe Génie des Procédés, Energétique et Biosystèmes, Université Blaise Pascal.

Pearcy R.W., Gross L. J. and He D. (1997), An improved dynamic model of photosynthesis for estimation of carbon gain in sunfleck light regimes. *Plant, Cell & Environment* **20**, 411–424.

Pessarakli M. (2005), Handbook of Plant and Crop Physiology, 2nd (ed), *In* Miranda et al., (Eds), *Phloem transport of solutes in crop plants*, 461- 474, Taylor and Francis e-library Marcell Dekker, Inc, New York. USA.

Pettersson G. & Pettersson R.U. (1988), A mathematical model of the Calvin photosynthesis cycle. *Eur J Biochem* **175**, 661-672.

Pettersson G. (1997), Control properties of the Calvin photosynthesis cycle at physiological carbondioxide concentrations. *Biochimica et Biophysica Acta (BBA) - Bioenerg* **1322**, 173–182.

Pfeiffer T., Sánchez-Valdenebro I., Nuño J. C., Montero F. & Schuster S. (1999), METATOOL: For Studying Metabolic Networks. *Bioinform* **15**, 251-257.

Pilarski J. (1994), Diffusion of carbon dioxide through the cork and stomata in lilac. *Acta Physiol Plant* **16**, 137-140.

Polle A. (2001), Dissecting the Superoxide Dismutase-Ascorbate-Glutathione-Pathway in Chloroplasts by Metabolic Modeling. Computer Simulations as a Step towards Flux Analysis. *Plant Physiol* **126**, 445-462.

Porter J. R. & Lawlor D.W. (1991). Plant Growth: Interactions with nutrition and environment. In. (Eds.) R. A. Leigh and R. Storey, *Nutrient compartmentation in cells and its relevance to the nutrition of the whole plant,* SEB Seminar Series 43, Cambridge University Press, New York, 15-18.

Poolman M.G., Fell D.A., & Thomas S. (2000), Modelling photosynthesis and its control. *J Exp Bot* **51** Spec No, 319-328.

Poolman M.G., Fell D.A. &Raines C.A. (2003), Elementary modes analysis of photosynthate metabolism in the chloroplast stroma. *Eur J Biochem* **270**, 430-9.

Poolman M. G., Assmus H. E. & Fell D. A. (2004), Applications of metabolic modelling to plant metabolism *J Exp Bot* **55**, 1177-1186.

Poolman MG. (2006), ScrumPy: metabolic modelling with Python. *Syst Biol (Stevenage)* **153**, 375-8.

Poolman M.G., Miguet L., Sweetlove L.J. &. Fell D. A. (2009), Genome-scale metabolic model of Arabidopsis and some of its properties. *Plant Physiol* **151**, 1570–1581.

Poorter H, Remkes C &Lambers H (1990), Carbon and nitrogen economy of 24 wild species differing in relative growth rate. *Plant Physiol* **94**, 621-627.

Preiss J. (1988), Biosynthesis of starch and its regulation. In. Preiss J. (Ed), *The Biochemistry of Plants*, **14**. Academic Press, San Diego, 181-254.

Price A. L., Patterson N. J., Plenge R.M., Weinblatt M. E., Shadick N. A. & Reich D. (2006), Principal components analysis corrects for stratification in genome-wide association studies. *Nat Gene* **38**, 904 – 909.

Price N.D., Papin J.A., Schilling C.H., & Palsson B.O. (2003), Genome-scale microbial in silico models: the constraints-based approach. *Trends Biotechnol* **21**, 162-169.

Price N.D., Reed J.L. & Palsson B.O. (2004), Genome-scale models of microbial cells: evaluating the consequences of constraints. *Nat Rev Microbiol* **2**, 886–897.

Priesack E. & Gayler S. (2009), Agricultural Crop Models: Concepts of Resource Acquisition and Assimilate Partitioning, *In* U. Lüttge et al. (Eds.), *Progress in Botany* **70**, 195–222, Springer-Verlag Berlin.

Provost A. & Blastin G. (2004), Dynamic metabolic modelling under the balanced growth condition. *J Proc Cont* **14,** 717–728.

Provost A., (2006), *Metabolic design of dynamic bioreaction models*, Ph.D. thesis, Université Catholique de Louvain, Louvain-la-Neuve.

Raman K. & Chandra, N. (2009), Flux balance analysis of biological systems: applications and challenges. *Brief Bioinform* **10** (4), 435-449.

Rappaport F., Guergova-Kuras M., Nixon P.J., Diner B.A. & Lavergne J. (2002), Kinetics and pathways of charge recombination in photosystem II. *Biochem* **41**, 8518-8527.

Ravenel J., Peltier G & Havaux M. (1994), The cyclic electron pathways around photosystem I in Chlamydomonas reinhardtii as determined in vivo by photoacoustic measurements of energy storage *Planta,* **193**, 251-259.

Reder C. (1988), Metabolic control theory: a structural approach. *J Theor Biol* **135**, 175-201.

Reeves S.G. & Hall D.O. (1973), The stoichiometry (ATP/2e− ratio) of non-cyclic photophosphorylation in isolated spinach chloroplasts, Biochimica et Biophysica Acta (BBA) – *Bioenerg* **314**, 66-78.

Rehling P., Model K., Brandner K., Kovermann P., Sickmann A., Meyer H.E., ühlbrandt W., Wagner R., Truscott K.N. & Pfanner N. (2003), Protein insertion into the mitochondrial inner membrane by a twin-pore translocase. *Sc* **299**, 1747–1751.

Renger G. & Wydrzynski T. (1991), The role of manganese in photosynthetic water oxidation *Biol Metals* **4**, 73-80.

Rice S.A. (2009), Advances in Chemical Physics Vol.**142,** *In*. (Eds.), R. Steuer & B. H. Junker *Computational Models of Metabolism Stability and Regulation in Metabolic Networks Advances in Chemical Physics*, John Wiley & Sons, New Jesrey, 105-121.

Rich P.R. (2003), The molecular machinery of Keilin's respiratory chain. *Biochem Soc Trans* **31** (6), 1095–1105.

Robards A.W. (1975), Plasmodesmata. *Ann Rev Plant Physiol* **26**, 13-29.

Roose T. (2000), *Mathematical Model of Plant Nutrient Uptake*, Ph.D Thesis, University of Oxford.

Rohwer J.M. & Botha F.C. (2001), Analysis of sucrose accumulation in the sugar cane culm on the basis of in vitro kinetic data. *Biochem J* **358**, 437–445.

Sauro H.M. (1993), SCAMP: a general-purpose simulator and metabolic control analysis program. *Comput Appl Biosci* **9**, 441-450.

Sauro H. M. & Ingalls B. (2004), Conservation analysis in biochemical networks computational issues for software writers. *Biophys Chem* **109**, 1-15.

Sauro H.J. (2000), A system for interactive metabolic analysis. In: Hofmeyr J-H.S. et al. editors. Animating the Cellular Map. Proceedings of the 9th International Meeting on BioThermoKinetics. South Africa: Stellenbosch University Press, 221–228.

Savageau M.A., Voit E.O., & Irvine D.H. (1987), Biochemical systems theory and metabolic control theory: 1. Fundamental similarities and differences. *Mat Biosci* **86**, 127–145.

Savageau M.A. (1992), Dominance according to metabolic control analysis: major achievement or house of cards? *J Theor Biol* **154**, 131-136.

Schellenberger J. & Palsson BØ. (2009), Use of randomized sampling for analysis of metabolic networks. *J Biol Chemi* **284**, 5457-61.

Schilling C.H., Schuster S., Palsson B.O., & Heinrich R. (1999), Metabolic pathway analysis: basic concepts and scientific applications in the post-genomic era. *Biotechnol Prog* **15**, 296-303.

Schilling C.H. & Palsson B.O. (2000), Assessment of the metabolic capabilities of Haemophilus influenzae Rd through a genome-scale pathway analysis. *J Theor Biol* **203**, 249-283.

Schilling C.H., Covert M.W., Famili I., Church G.M., Edwards J.S. & Palsson B.O. (2002), Genome-scale metabolic model of Helicobacter pylori 26695. *J Bacteriol* **184**, 4582-4593.

Schroeder J.I., Kwak J.M., & Allen G.J. (2001), Guard cell abscisic acid signalling and engineering drought hardiness in plants. *Nature* **410**, 327-330.

Schuster S. & Hilgetag C. (1994), On elementary flux modes in biochemical reaction systems at steady state. *J Biol Syst* **2**, 165-182.

Schuster S., Hilgetag C., Woods J. H. & Fell D. A. (1996), *Elementary Modes of Functioning in Biochemical Networks*. *In*. R. Cuthbertson, M. Holcombe & R. Paton (Eds.), *Computation in Cellular and Molecular Biological Systems*, World Scientific, Singapore.

Schuster S., Dandekar T. & Fell D.A. (1999), Detection of elementary flux modes in biochemical networks: A promising tool for pathway analysis and metabolic engineering. *Trends Biotech* **17**, 53-60.

Schuster S., Fell D.A., & Dandekar T. (2000), A general definition of metabolic pathways useful for systematic organization and analysis of complex metabolic networks. *Nat Biotechnol* **18**, 326-332.

Schuster S., Hilgetag C., Woods J.H. & Fell D.A. (2002), Reaction routes in biochemical reaction systems: algebraic properties, validated calculation procedure and example from nucleotide metabolism. *J Math Biol* **45**, 153-181.

Schwartz J.M. & Kanehisa M. (2006), Quantitative elementary mode analysis of metabolic pathways: The example of yeast glycolysis, *BMC Bioinfrom* **7**, 186.

Schwarz R., P. von Kamp Musch A., Engels B., Schirmer H., Schuster S. & Dandekar T. (2005), YANA - a software tool for analyzing flux modes, gene-expression and enzyme activities, *BMC Bioinform* **6**, 135.

Schwender J., Ohlrogge J.B. & Shachar-Hill Y. (2003), A flux model of glycolysis and the oxidative pentosephosphate pathway in developing Brassica napus embryos. *J Biol Chem* **278**, 29442-29453.

Schwender J., Goffman F., Ohlrogge J.B., & Shachar-Hill Y. (2004 a), Rubisco without the Calvin cycle improves the carbon efficiency of developing green seeds. *Nature* **432**, 779-782.

Schwender J., Ohlrogge J., & Shachar-Hill Y. (2004 b), Understanding flux in plant metabolic networks. *Curr Opin Plant Biol,* **7**, 309–317.

Schwender J. (2009), *Plant metabolic networks*, Springer, New York, USA, 331 p.

Shi H., Nikawa J., & Shimizu K. (1999), Effect of modifying metabolic network on poly-3-hydroxybutyrate biosynthesis in recombinant *Escherichia coli*. *J Biosci Bioeng* **87**, 666-677.

Sielewiesiuk J. & Gruszecki W.I. (1991), A simple model describing the kinetics of the xanthophyll cycle. *Biophys Chem* **41**, 125-129.

Slepchenko B.M., Schaff J.C., Macara I., & Loew L.M. (2003), Quantitative cell biology with the Virtual Cell. *Trends Cell Biol* **13**, 570-576.

Smith H. (1977), The molecular Biology of Plant cells Vol. **14**, *In*. N. K. Boardman and D. C. Lee (Eds.), *Chrloroplast structure and photosynthesis, Plant mitochondria*, 91- 135, University of California Press, Blackwell Scientific Publications, California, USA.

Stephanopoulos G. & Vallino J.J. (1991), Network rigidity and metabolic engineering in metabolite overproduction. *Sci* **252**, 1675-1681.

Stephanopoulos G., Aristidou A. A. & Nielsen J. (1998), *Metabolic Engineering: Principles and Methodologies*, Academic Press, San Diego, USA.

Stephanopoulos G. (1999), Metabolic fluxes and metabolic engineering. *Meta Eng* **1,** 1-11.

Stoermer H., Seith B., Hanemann U., Georger E., Rennenberg H. (1997), Nitrogen distribution in younge Norway spruce (Picea abies trees as affected by pedospheric nitrogen supply. *Physiol Plant* **101**, 764-769.

Strange K. (2004), Cellular volume homeostasis. *Adv Physiol Educ* **28**, 155-159.

Sweetlove L.J., Beard K.F.M., Nunes-Nesi A., Fernie A.R. & Ratcliffe R.G. (2010), Not just a circle: flux modes in the plant TCA cycle. *Trends Plant Sci* **15,** 462–470.

Taiz L & Zeiger E. (Eds.) (1998), *plant physiology* 2nd edition, Sinauer Associates, Sunderland, MA, USA, 525 p.

Terada H., (1990), Uncouplers of oxidative phosphorylation. *Environ health Perspect* **87,** 213-218.

Theilgaard, H. & Nielsen, J. (1999), Metabolic control analysis of the penicillin biosynthetic pathway: the influence of the LLD-ACV: bisACV ratio on the flux control. *Antonie Van Leeuwenhoek* **75**, 145-154.

Thomas S., Mooney P.J., Burrell M.M., & Fell D.A. (1997), Metabolic Control Analysis of glycolysis in tuber tissue of potato (Solanum tuberosum): explanation for the low control coefficient of phosphofructokinase over respiratory flux. *Biochem J* **322**, 119-127.

Thornley J.H.M. (1974), Light Fluctuations and Photosynthesis. *Ann Bot.* **38**, 363-373.

Tredici M.R. (2004), Mass production of microalgae: photobioreactors. In: Richmond A (ed) *Handbook of microalgal culture biotechnology and applied phycology*. Blackwell Science, Oxford, 273–280 p.

Trinh C.T., Wlaschin A. & Srienc F. (2009), Elementary mode analysis: a useful metabolic pathway analysis tool for characterizing cellular metabolism. *App Microbiol Biotechnol* **81**, 813-826.

Tuzet A., Perrier A. & Leuning R. (2003), A coupled model of stomatal conductance, photosynthesis and transpiration. *Plant, Cell and Environ* **26**, 1097–1116.

Tyree M. T. (1997), The Cohesion–Tension theory of sap ascent: current controversies. *J Exp Bot* **48**, 1753–1765.

Ulrich (1970). Organic acids. In: Hulme, A.C. (Ed.), *The Biochemistry of Fruits and their Products*, Vol **1**. Academic Press, New York, 89–118.

Ulrich L.,Wolfram B., Burkhard B. & Dennis F. (2012). Progress in Botany, **73**, *In.* (C. Herschbach et al. Eds), *Long distance transport and plant internal cycling of N and S compounds*, 177-179, Springer-Verlag, Berlin, Germany.

Urbanczik R. & Wagner C. (2005), An improved algorithm for stoichiometric network analysis: theory and applications. *Bioinform* **21**, 1203-1210.

Van Noort V., Snel B. & Huynen M. A. (2004), The yeast coexpression network has a small World, Scale free architecture and can be explained by a simple model *EMBO Rep* **5,** 280-284.

Van Walraven H.S., Strotmann H., Schwarz O. & Rumberg B. (1996). The H+/ATP coupling ratio of the ATP synthase from thiol-modulated chloroplasts and two cyanobacterial strains is four. *FEBS Lett* **379**, 309–13.

Varma A. & Palsson B.O. (1994), Stoichiometric flux balance models quantitatively predict growth and metabolic by-product secretion in wild-type *Escherichia-Coli* W3110. *Appl Environ Microbiol* **60**, 3724–3731.

Vallino J.J. & Stephanopoulos G. (1990), Flux determination in cellular bioreaction networks: applications to lysine fermentations, S.K. Sikdar, M. Bier and P. Todd (Eds.), Frontiers in Bioprocessing, 205-219, CRC Press, FL, USA.

Voet D. and Voet J.G. (2005), Biochimie, 2nd (Ed), Translated version *In*. De Boeck Université, *Le cycle de l'acide citrique*, 581-768, Bruxelles.

Von Caemmerer S. (2000), *Biochemical Models of Leaf Photosynthesis*, CSIRO Publishing, Victoria, Australia, 165 p.

Von Kamp & Schuster S. (2006), Metatool 5.0: fast and flexible elementary modes analysis. *Bioinform* **22**, 1930-1931.

Wang Y.-P. & Leuning R. (1998), A two-leaf model for canopy conductance, photosynthesis and partitioning of available energy I: Model description and comparison with a multi-layered model, *Agric Forest Meteorol* **91**, 89–111.

Waisel Y., A. Eshel & U. Kafkafi (Eds.) (2002), *Plant Roots: The Hidden Half.* 3rd edition, Marcel Dekker, INC. New York.

Walz D. & Caplan S.R. (1988), Energy coupling and thermokinetic balancing in enzyme kinetics. *Cell Biophys* **12**, 13–28.

Wheeler D.S., Wong H.R. & Shanley T.P. (2008), Resuscitation and Stabilization of the Critically Ill Child*, In.* A. Abboud, J. Raake and D. S. Wheeler (Eds.), *Supplemental oxygen and Bag valve mask ventialtion* 32, Springer, London.

Wiback S.J., Mahadevan R., & Palsson B.O. (2003), Reconstructing metabolic flux vectors from extreme pathways: Defining the alpha spectrucm *J Theo Bio* **224**, 313-324.

Wiback S.J, Mahadevan R. & Palsson B.O. (2004), Using metabolic flux data to further constrain the metabolic solution space and predict internal flux patterns: the *Escherichia coli* spectrum. *Biotech and bioeng* **86**, 317-331.

Wiechert W. (2002), Modeling and simulation: tools for metabolic engineering. *J Biotechnol* **94**, 37-63.

Wiechert W. & Takors R. (2004), Validation of metabolic models: Concepts, tools, and problems. *In* B. N. Kholodenko & H. V. Westerhoff (eds.), *Metabolic Engineering in the Post Genomic Era*, 277-320, Horizon Bioscience,Wymondham, UK.

Winter H., Robinson D. & Heldt H.W. (1994) Subcellular volumes and metabolite concentrations in spinach leaves. *Planta* **193**, 530-535.

Williams T.C.R., Miguet L., Masakapalli S.K., Kruger N J., Sweetlove L. J. & Ratcliffe R. G. (2008), Metabolic Network Fluxes in Heterotrophic Arabidopsis Cells: Stability of the Flux Distribution under Different Oxygenation Conditions. *Plant Physi* **148**, 704-718.

Wittmann C. & de Graaf A (2005), *Metabolic flux analysis in Corynebacterium glutamicum.* In Eggeling L., Bott M. (Eds), Handbook of *Corynebacterium glutamicum* CRC press, USA.

Xu L. & Baldocchi D. D. (2003), Seasonal trends in photosynthetic parameters and stomatal conductance of blue oak (*Quercus douglasii*) under prolonged summer drought and high temperature, *Tree Physiol* **23**, 865–877.

Yan H.-P., Kang M. Z., de Reffye P. & Dingkuhn M. (2004), A Dynamic, Architectural Plant Model Simulating Resource-dependent Growth. *Annals of Botany* **93**, 591–602.

Yang Y.T., Bennett G.N. & San K.Y. (1999), Effect of inactivation of nuo and ackA-pta on redistribution of metabolic fluxes in *Escherichia coli*. *Biotechnol Bioeng* **65**, 291-297.

Yoshida M., Muneyuki E. & Hisabori T. (2001), ATP synthase—a marvellous rotary engine of the cell. *Nat Rev Mol Cell Biol* **2**, 669–677.

Yoshida S. & Eguchi H. (1994), Environmental analysis of aerial O_2 transport through leaves for root respiration in relation to water uptake in cucumber plants (*Cucumis sativus L.*) in 02-deficient nutrient solution. *Exp Bot* **45**, 187-192.

Yugi K. & Tomita M. (2004), A general computational model of mitochondrial metabolism in a whole organelle scale. *Bioinform* **20**, 1795-1796.

Zavala M. A. (2004), Integration of drought tolerance mechanisms in Mediterranean sclerophylls: a functional interpretation of leaf gas exchange simulators. *Eco Mod* **176**, 211–226.

Zhu X.G., de Sturler E. & Long S.P. (2007), Optimizing the distribution of resources between enzymes of carbon metabolism can dramatically increase photosynthetic rate: a numerical simulation using an evolutionary algorithm. *Plant Physiol* **145**, 513–526.

Zhu X.-G., Long S.P. & Ort D.R. (2008), What is the maximum efficiency with which photosynthesis can convert solar energy into biomass? *Trends Biotech* **19**, 153-159.

Zimmer, W., Brüggemann, N., Emeis, S., Giersch, C. & Lehning, A., Steinbrecher, R., & Schnitzler, J.P. (2000), Process-based modelling of isoprene emission by oak leaves. *Plant Cell Environ* **23**, 585–595.

References from internet

[Int. ref. 1.] Cliff notes: root zones

http://www.cliffsnotes.com/study_guide/Root-Zones.topicArticleId-23791,articleId-23669.html, consulted on 29/8/2010

[Int. ref. 2.] Darling D. Encyclopedia of Science, Phloem

http://www.daviddarling.info/encyclopedia/P/phloem.html, consulted on 29/8/2009

[Int. ref. 3.] Hope medical group, mitochondria

http://hopestemcell.com/treatment/stem-cell-treatments/mitochondria, consulted on 5/4/2012

[Int. ref. 4.] Miesfeld F. (2008), Lecture 29, Photophosphorylation Key Concepts - Overview of photosynthesis and carbon fixation

http://www.biochem.arizona.edu/miesfeld/Miesfeld-Fall2008Lecs/Lec29-Fall08/Lec29-F08-Handout.pdf, consulted on 29/4/2011

[Int. ref. 5.] Koning R. E. (1994), Lettuce Seed Germination Introduction. Plant Physiology Information

http://plantphys.info/organismal/labaids/lettucegerm/, consulted on 29/4/2011

[Int. ref. 6.] USDA, National Nutrient Database for Standard Reference, Release 18, (2005)

http://healthrecipes.com/lettuce.htm, consulted on 29/8/2010

[Int. ref. 7.] Usermanual of Macherey-Nagel, Total RNA isolation from plant, NucleoSpin RNA plant, February, 2011/Rev.06, Printed in Germany.

http://www.mnnet.com/Portals/8/attachments/Redakteure_Bio/Protocols/RNA%20and%20mRNA/UM_TotalRNAPlant.pdf, consulted on 29/4/2011

Appendices

a. List of URLs used

For the construction of leaf metabolic network, familiar metabolic reactions and pathways for plants such as Calvin cycle, glycolysis, Krebs cycle, pentose phosphate pathway, carbohydrate metabolism, amino acid metabolism, lipid metabolism, etc. are adapted from biological data bases, AraCyc, KEGG, MetaCyc and PlantCyc. Most of the metabolites were in the reduced or charged form.

AraCyc	http://www.arabidopsis.org/biocyc/index.jsp, consulted on 10/6/2009
KEGG	http://www.genome.jp/kegg/kegg1.html, consulted on 25/4/2009
MetaCyc	http://metacyc.org/ consulted on 12/7/2009
PlantCyc	http://www.plantcyc.org/, consulted on 29/8/2009

b. List of metabolites used in the leaf metabolic model

The below listed metabolites can be found from Table 4.6.

10-formylTHF	10-Formyltetrahydrofolate
1-3BPGA	1,3- bisphospho-D-glycerate
2PGA	2-phospho-D-glycerate
3PGA	3-phospho-D-glycerate
5p-ribosyl-1-pp	5-phospho-alpha-d-ribosyl 1-pyrophosphate
AcCoA	Acetyl-CoA
ADP	Adenosine diphosphate
AMP	Adenosine monophosphate
ATP	Adenosine-triphosphate
CH2=THF	Methyltetrahydrofolate
CH3THF	5-formyl-tetrahydrofolate
cisaconitate	Cis aconitate
CO_2	Carbon dioxide
DHAP	Dihydroxyacetone phosphate
E4P	D-erythrose-4-phosphate
F6P	D-fructose-6-phosphate
FAD	Flavine adenine dinucleotide (oxidised form)
$FADH_2$	Flavine adenine dinucleotide (reduced form)
FBP	D-fructose-1,6-bisphosphate
G1P	D-glucose 1-phosphate
G3P	Glyceraldehyde-3-phosphate
G6P	D-glucose 6-phosphate
g-linolenate	Gamma-linolenate
glycerol3P	Glycerol 3-phosphate
H^+	Hydrogen ion
H_2O	Water
H_2S	Hydrogen sulphide
HNO_3	Nitrate
$h\nu_{680}$	Photon of light at 680 nm
$h\nu_{700}$	Photon of light at 700 nm
malate	L-malate
methenylTHF	5,10-methenyltetrahydrofolate
NAD^+	Nicotinamide adenine dinucleotide
NADH, H^+	Nicotinamide adenine dinucleotide (reduced form)
$NADP^+$	Nicotinamide adenine dinucleotide phosphate

$NADPH, H^+$	Nicotinamide adenine dinucleotide phosphate (reduced form)
NH_3	Ammonia
O_2	Dioxygen (molecular oxygen)
oxoglutarate	2-oxoglutarate or 2-ketoglutarate
PEP	Phosphoenolpyruvate
Pi	Inorganic phosphate
PPi	Pyrophosphate
R5P	Alpha-D-ribose 5-phosphate
RBP	Ribose 1,5-bisphosphate
Ru5P	D-ribulose 5-phosphate
RuBP	D-ribulose 1,5-bisphosphate
S7P	Sedoheptulose 7-phosphate
S-ade-methionine	S-Adenosyl-L-methionine
S-ad-homocysteine	S-Adenosyl-L-homocysteine
SBP	Sedoheptulose-1,7-bisphosphate
THF	Tetrahydrofolate
UDP	Uridine-diphosphate
UDP-glucose	Uridine 5'-(trihydrogen diphosphate) alpha-D-glucopyranosyl ester
UMP	Uridine-monophosphate
Xu5P	D-xylulose 5-phosphate

c. Elementary flux modes

Obtained Elementary flux modes

EFMs are given in the order of serial number (of EFMs), thermodynamic direction, number of reactions involved in each EFM, original reactions involved in the EFM, mass balanced equation, etc.

1. Energy metabolism involving cyclic photophosphorylation

1,0,3, R1 R20 R22, -6 * hv700

2,0,3, R1 R11 R23, -6 * hv700

3,0,5, R1 R36 R37 R44 R45, -1 * hv700

4,0,6, R1 R10 R15 R16 R21 R23, -6 * hv700

2. Energy metabolism involving noncyclic photophosphorylation

5,0,5, R2 R4 R20 R22 R38, -0.75047 * hv700 -0.75047 * hv680

6,0,5, R2 R4 R11 R23 R38, -0.75047 * hv700 -0.75047 * hv680

7,0,7, R2 R4 R36 R37 R38 R44 R45, -3 * hv700 -3 * hv680

8,0,7, R2 R4 R20 R22 R27 R42 R43, -0.75047 * hv700 -0.75047 * hv680

9,0,7, R2 R4 R11 R23 R27 R42 R43, -0.75047 * hv700 -0.75047 * hv680

10,0,8, R2 R4 R10 R15 R16 R21 R23 R38, -0.75047 * hv700 -0.75047 * hv680

11,0,9, R2 R4 R27 R36 R37 R42 R43 R44 R45, -2 * hv700 -2 * hv680

12,0,10, R2 R4 R10 R15 R16 R21 R23 R27 R42 R43, -0.75047 * hv700 -0.75047 * hv680

3. Futile pathways

13,0,4, R27 R38 R42 R43,

14,0,6, R11 R23 R36 R37 R44 R45,

15,0,6, R20 R22 R36 R37 R44 R45,

16,0,9, R10 R15 R16 R21 R23 R36 R37 R44 R45,

4. Biomass production pathways

17,0,100, R2 R3 R5 R6 R7 R8 R9 R12 R13 R14 R15 R16 R17 R18 R19 R20 R21 R24 R25 R26 R28 R29 R30 R31 R32 R33 R34 R35 R36 R37 R38 R39 R40 R41 R42 R43 R44 R45 R46 R47 R48 R49 R50 R51 R52 R53 R54 R55 R56 R57 R58 R59 R60 R61 R62 R63 R64 R65 R66 R67 R68 R69 R70 R71 R72 R73 R74 R75 R76 R77 R78 R79 R80 R81 R82 R83 R84 R85 R86 R87 R88 R89 R90 R91 R92 R93 R94 R95 R96 R97 R98 R99 R100 R101 R102 R103 R104 R105 R106 R107, -6.0447 * hv700 -6.0447 * hv680 -0.0022055 * H2S -0.12256 * HNO3 -1.2293 * CO2 1.4981 * O2 -0.96619 * H2O 1.2293 * biomass

18,0,100, R2 R3 R5 R6 R7 R8 R9 R10 R11 R12 R13 R14 R17 R18 R19 R20 R21 R24 R25 R26 R28 R29 R30 R31 R32 R33 R34 R35 R36 R37 R38 R39 R40 R41 R42 R43 R44 R45 R46 R47 R48 R49 R50 R51 R52 R53 R54 R55 R56 R57 R58 R59 R60 R61 R62 R63 R64 R65 R66 R67 R68 R69 R70 R71 R72 R73 R74 R75 R76 R77 R78 R79 R80 R81 R82 R83 R84 R85 R86 R87 R88 R89 R90 R91 R92 R93 R94 R95 R96 R97 R98 R99 R100 R101 R102 R103 R104 R105 R106 R107, -3 * hv700 -3 * hv680 -0.0010946 * H2S -0.060825 * HNO3 -0.61011 * CO2 0.7435 * O2 -0.47952 * H2O 0.61008 * biomass
19,0,100, R2 R3 R5 R6 R7 R8 R9 R12 R13 R14 R15 R16 R17 R18 R19 R20 R21 R24 R25 R26 R27 R28 R29 R30 R31 R32 R33 R34 R35 R36 R37 R38 R39 R40 R41 R43 R44 R45 R46 R47 R48 R49 R50 R51 R52 R53 R54 R55 R56 R57 R58 R59 R60 R61 R62 R63 R64 R65 R66 R67 R68 R69 R70 R71 R72 R73 R74 R75 R76 R77 R78 R79 R80 R81 R82 R83 R84 R85 R86 R87 R88 R89 R90 R91 R92 R93 R94 R95 R96 R97 R98 R99 R100 R101 R102 R103 R104 R105 R106 R107, -117.0719 * hv700 -117.0719 * hv680 -0.042715 * H2S -2.3736 * HNO3 -23.8089 * CO2 29.0144 * O2 -18.7127 * H2O 23.8077 * biomass
20,0,100, R2 R3 R5 R6 R7 R8 R9 R10 R11 R12 R13 R14 R17 R18 R19 R20 R21 R24 R25 R26 R27 R28 R29 R30 R31 R32 R33 R34 R35 R36 R37 R38 R39 R40 R41 R43 R44 R45 R46 R47 R48 R49 R50 R51 R52 R53 R54 R55 R56 R57 R58 R59 R60 R61 R62 R63 R64 R65 R66 R67 R68 R69 R70 R71 R72 R73 R74 R75 R76 R77 R78 R79 R80 R81 R82 R83 R84 R85 R86 R87 R88 R89 R90 R91 R92 R93 R94 R95 R96 R97 R98 R99 R100 R101 R102 R103 R104 R105 R106 R107, -117.0719 * hv700 -117.0719 * hv680 -0.042715 * H2S -2.3736 * HNO3 -23.8089 * CO2 29.0144 * O2 -18.7127 * H2O 23.8077 * biomass
21,0,100, R2 R3 R5 R6 R7 R8 R9 R12 R13 R14 R15 R16 R17 R18 R19 R20 R21 R24 R25 R26 R27 R28 R29 R30 R31 R32 R33 R34 R35 R36 R37 R38 R39 R40 R41 R42 R44 R45 R46 R47 R48 R49 R50 R51 R52 R53 R54 R55 R56 R57 R58 R59 R60 R61 R62 R63 R64 R65 R66 R67 R68 R69 R70 R71 R72 R73 R74 R75 R76 R77 R78 R79 R80 R81 R82 R83 R84 R85 R86 R87 R88 R89 R90 R91 R92 R93 R94 R95 R96 R97 R98 R99 R100 R101 R102 R103 R104 R105 R106 R107, -100.489 * hv700 -100.489 * hv680 -0.036665 * H2S -2.0374 * HNO3 -20.4364 * CO2 24.9046 * O2 -16.0621 * H2O 20.4354 * biomass
22,0,100, R2 R3 R5 R6 R7 R8 R9 R10 R11 R12 R13 R14 R17 R18 R19 R20 R21 R24 R25 R26 R27 R28 R29 R30 R31 R32 R33 R34 R35 R36 R37 R38 R39 R40 R41 R42 R44 R45 R46 R47 R48 R49 R50 R51 R52 R53 R54 R55 R56 R57 R58 R59 R60 R61 R62 R63 R64 R65 R66 R67 R68 R69 R70 R71 R72 R73 R74 R75 R76 R77 R78 R79 R80 R81 R82 R83 R84 R85 R86 R87 R88 R89 R90 R91 R92 R93 R94 R95 R96 R97 R98 R99 R100 R101 R102

R103 R104 R105 R106 R107, -100.489 * hv700 -100.489 * hv680 -0.036665 * H2S -2.0374 * HNO3 -20.4364 * CO2 24.9046 * O2 -16.0621 * H2O 20.4354 * biomass
23,0,100, R2 R3 R4 R5 R6 R7 R8 R9 R12 R13 R14 R15 R16 R17 R18 R19 R20 R21 R24 R25 R26 R27 R28 R29 R30 R31 R32 R33 R34 R35 R36 R37 R39 R40 R41 R42 R44 R45 R46 R47 R48 R49 R50 R51 R52 R53 R54 R55 R56 R57 R58 R59 R60 R61 R62 R63 R64 R65 R66 R67 R68 R69 R70 R71 R72 R73 R74 R75 R76 R77 R78 R79 R80 R81 R82 R83 R84 R85 R86 R87 R88 R89 R90 R91 R92 R93 R94 R95 R96 R97 R98 R99 R100 R101 R102 R103 R104 R105 R106 R107, -302.3506 * hv700 -302.3506 * hv680 -0.10959 * H2S -6.0896 * HNO3 -61.0822 * CO2 74.437 * O2 -48.0079 * H2O 61.0792 * biomass
24,0,100, R2 R3 R4 R5 R6 R7 R8 R9 R12 R13 R14 R15 R16 R17 R18 R19 R20 R21 R24 R25 R26 R27 R28 R29 R30 R31 R32 R33 R34 R35 R36 R37 R39 R40 R41 R43 R44 R45 R46 R47 R48 R49 R50 R51 R52 R53 R54 R55 R56 R57 R58 R59 R60 R61 R62 R63 R64 R65 R66 R67 R68 R69 R70 R71 R72 R73 R74 R75 R76 R77 R78 R79 R80 R81 R82 R83 R84 R85 R86 R87 R88 R89 R90 R91 R92 R93 R94 R95 R96 R97 R98 R99 R100 R101 R102 R103 R104 R105 R106 R107, -522.8696 * hv700 -522.8696 * hv680 -0.19005 * H2S -10.5606 * HNO3 -105.9292 * CO2 129.0891 * O2 -83.2556 * H2O 105.9239 * biomass
25,0,100, R2 R3 R5 R6 R7 R8 R9 R12 R13 R14 R15 R16 R17 R18 R19 R20 R21 R24 R25 R26 R27 R28 R29 R30 R31 R32 R33 R34 R35 R36 R37 R39 R40 R41 R42 R43 R44 R45 R46 R47 R48 R49 R50 R51 R52 R53 R54 R55 R56 R57 R58 R59 R60 R61 R62 R63 R64 R65 R66 R67 R68 R69 R70 R71 R72 R73 R74 R75 R76 R77 R78 R79 R80 R81 R82 R83 R84 R85 R86 R87 R88 R89 R90 R91 R92 R93 R94 R95 R96 R97 R98 R99 R100 R101 R102 R103 R104 R105 R106 R107, -151.0142 * hv700 -151.0142 * hv680 -0.0551 * H2S -3.0618 * HNO3 -30.7117 * CO2 37.4264 * O2 -24.1381 * H2O 30.7102 * biomass
26,0,100, R2 R3 R4 R5 R6 R7 R8 R9 R10 R11 R12 R13 R14 R17 R18 R19 R20 R21 R24 R25 R26 R27 R28 R29 R30 R31 R32 R33 R34 R35 R36 R37 R39 R40 R41 R42 R44 R45 R46 R47 R48 R49 R50 R51 R52 R53 R54 R55 R56 R57 R58 R59 R60 R61 R62 R63 R64 R65 R66 R67 R68 R69 R70 R71 R72 R73 R74 R75 R76 R77 R78 R79 R80 R81 R82 R83 R84 R85 R86 R87 R88 R89 R90 R91 R92 R93 R94 R95 R96 R97 R98 R99 R100 R101 R102 R103 R104 R105 R106 R107, -302.3506 * hv700 -302.3506 * hv680 -0.10959 * H2S -6.0896 * HNO3 -61.0822 * CO2 74.437 * O2 -48.0079 * H2O 61.0792 * biomass
27,0,100, R2 R3 R4 R5 R6 R7 R8 R9 R10 R11 R12 R13 R14 R17 R18 R19 R20 R21 R24 R25 R26 R27 R28 R29 R30 R31 R32 R33 R34 R35 R36 R37 R39 R40 R41 R43 R44 R45 R46 R47 R48 R49 R50 R51 R52 R53 R54 R55 R56 R57 R58 R59 R60 R61 R62 R63 R64 R65 R66 R67 R68 R69 R70 R71 R72 R73 R74 R75 R76 R77 R78 R79 R80 R81 R82 R83

R84 R85 R86 R87 R88 R89 R90 R91 R92 R93 R94 R95 R96 R97 R98 R99 R100 R101 R102 R103 R104 R105 R106 R107, -522.8696 * hv700 -522.8696 * hv680 -0.19005 * H2S -10.5606 * HNO3 -105.9292 * CO2 129.0891 * O2 -83.2556 * H2O 105.9239 * biomass

28,0,100, R2 R3 R5 R6 R7 R8 R9 R10 R11 R12 R13 R14 R17 R18 R19 R20 R21 R24 R25 R26 R27 R28 R29 R30 R31 R32 R33 R34 R35 R36 R37 R39 R40 R41 R42 R43 R44 R45 R46 R47 R48 R49 R50 R51 R52 R53 R54 R55 R56 R57 R58 R59 R60 R61 R62 R63 R64 R65 R66 R67 R68 R69 R70 R71 R72 R73 R74 R75 R76 R77 R78 R79 R80 R81 R82 R83 R84 R85 R86 R87 R88 R89 R90 R91 R92 R93 R94 R95 R96 R97 R98 R99 R100 R101 R102 R103 R104 R105 R106 R107, -151.0142 * hv700 -151.0142 * hv680 -0.0551 * H2S -3.0618 * HNO3 -30.7117 * CO2 37.4264 * O2 -24.1381 * H2O 30.7102 * biomass

29,0,100, R2 R3 R4 R5 R6 R7 R8 R9 R12 R13 R14 R15 R16 R17 R18 R19 R20 R21 R22 R24 R25 R26 R27 R28 R29 R30 R31 R32 R33 R34 R35 R37 R39 R40 R41 R42 R44 R45 R46 R47 R48 R49 R50 R51 R52 R53 R54 R55 R56 R57 R58 R59 R60 R61 R62 R63 R64 R65 R66 R67 R68 R69 R70 R71 R72 R73 R74 R75 R76 R77 R78 R79 R80 R81 R82 R83 R84 R85 R86 R87 R88 R89 R90 R91 R92 R93 R94 R95 R96 R97 R98 R99 R100 R101 R102 R103 R104 R105 R106 R107, -5.0289 * hv700 -5.0289 * hv680 -0.0018227 * H2S -0.10129 * HNO3 -1.016 * CO2 1.2381 * O2 -0.7985 * H2O 1.0159 * biomass

30,0,100, R2 R3 R4 R5 R6 R7 R8 R9 R12 R13 R14 R15 R16 R17 R18 R19 R20 R21 R22 R24 R25 R26 R27 R28 R29 R30 R31 R32 R33 R34 R35 R37 R39 R40 R41 R43 R44 R45 R46 R47 R48 R49 R50 R51 R52 R53 R54 R55 R56 R57 R58 R59 R60 R61 R62 R63 R64 R65 R66 R67 R68 R69 R70 R71 R72 R73 R74 R75 R76 R77 R78 R79 R80 R81 R82 R83 R84 R85 R86 R87 R88 R89 R90 R91 R92 R93 R94 R95 R96 R97 R98 R99 R100 R101 R102 R103 R104 R105 R106 R107, -5.1107 * hv700 -5.1107 * hv680 -0.0018576 * H2S -0.10322 * HNO3 -1.0354 * CO2 1.2618 * O2 -0.81377 * H2O 1.0353 * biomass

31,0,100, R2 R3 R5 R6 R7 R8 R9 R12 R13 R14 R15 R16 R17 R18 R19 R20 R21 R22 R24 R25 R26 R27 R28 R29 R30 R31 R32 R33 R34 R35 R37 R39 R40 R41 R42 R43 R44 R45 R46 R47 R48 R49 R50 R51 R52 R53 R54 R55 R56 R57 R58 R59 R60 R61 R62 R63 R64 R65 R66 R67 R68 R69 R70 R71 R72 R73 R74 R75 R76 R77 R78 R79 R80 R81 R82 R83 R84 R85 R86 R87 R88 R89 R90 R91 R92 R93 R94 R95 R96 R97 R98 R99 R100 R101 R102 R103 R104 R105 R106 R107, -5.2273 * hv700 -5.2273 * hv680 -0.0019073 * H2S -0.10598 * HNO3 -1.0631 * CO2 1.2955 * O2 -0.83553 * H2O 1.063 * biomass

32,0,100, R2 R3 R5 R6 R7 R8 R9 R12 R13 R14 R15 R16 R17 R18 R19 R20 R21 R22 R24 R25 R26 R27 R28 R29 R30 R31 R32 R33 R34 R35 R37 R38 R39 R40 R41 R42 R44 R45 R46 R47 R48 R49 R50 R51 R52 R53 R54 R55 R56 R57 R58 R59 R60 R61 R62 R63 R64

R65 R66 R67 R68 R69 R70 R71 R72 R73 R74 R75 R76 R77 R78 R79 R80 R81 R82 R83 R84 R85 R86 R87 R88 R89 R90 R91 R92 R93 R94 R95 R96 R97 R98 R99 R100 R101 R102 R103 R104 R105 R106 R107, -5.2273 * hv700 -5.2273 * hv680 -0.0019073 * H2S -0.10598 * HNO3 -1.0631 * CO2 1.2955 * O2 -0.83553 * H2O 1.063 * biomass
33,0,100, R2 R3 R5 R6 R7 R8 R9 R12 R13 R14 R15 R16 R17 R18 R19 R20 R21 R22 R24 R25 R26 R27 R28 R29 R30 R31 R32 R33 R34 R35 R37 R38 R39 R40 R41 R43 R44 R45 R46 R47 R48 R49 R50 R51 R52 R53 R54 R55 R56 R57 R58 R59 R60 R61 R62 R63 R64 R65 R66 R67 R68 R69 R70 R71 R72 R73 R74 R75 R76 R77 R78 R79 R80 R81 R82 R83 R84 R85 R86 R87 R88 R89 R90 R91 R92 R93 R94 R95 R96 R97 R98 R99 R100 R101 R102 R103 R104 R105 R106 R107, -5.2273 * hv700 -5.2273 * hv680 -0.0019073 * H2S -0.10598 * HNO3 -1.0631 * CO2 1.2955 * O2 -0.83553 * H2O 1.063 * biomass
34,0,100, R2 R3 R5 R6 R7 R8 R9 R12 R13 R14 R15 R16 R17 R18 R19 R20 R21 R22 R24 R25 R26 R28 R29 R30 R31 R32 R33 R34 R35 R37 R38 R39 R40 R41 R42 R43 R44 R45 R46 R47 R48 R49 R50 R51 R52 R53 R54 R55 R56 R57 R58 R59 R60 R61 R62 R63 R64 R65 R66 R67 R68 R69 R70 R71 R72 R73 R74 R75 R76 R77 R78 R79 R80 R81 R82 R83 R84 R85 R86 R87 R88 R89 R90 R91 R92 R93 R94 R95 R96 R97 R98 R99 R100 R101 R102 R103 R104 R105 R106 R107, -5.2273 * hv700 -5.2273 * hv680 -0.0019073 * H2S -0.10598 * HNO3 -1.0631 * CO2 1.2955 * O2 -0.83553 * H2O 1.063 * biomass
35,0,100, R2 R3 R4 R5 R6 R7 R8 R9 R10 R11 R12 R13 R14 R17 R18 R19 R20 R21 R22 R24 R25 R26 R27 R28 R29 R30 R31 R32 R33 R34 R35 R37 R39 R40 R41 R42 R44 R45 R46 R47 R48 R49 R50 R51 R52 R53 R54 R55 R56 R57 R58 R59 R60 R61 R62 R63 R64 R65 R66 R67 R68 R69 R70 R71 R72 R73 R74 R75 R76 R77 R78 R79 R80 R81 R82 R83 R84 R85 R86 R87 R88 R89 R90 R91 R92 R93 R94 R95 R96 R97 R98 R99 R100 R101 R102 R103 R104 R105 R106 R107, -5.0289 * hv700 -5.0289 * hv680 -0.0018227 * H2S -0.10129 * HNO3 -1.016 * CO2 1.2381 * O2 -0.7985 * H2O 1.0159 * biomass
36,0,100, R2 R3 R4 R5 R6 R7 R8 R9 R10 R11 R12 R13 R14 R17 R18 R19 R20 R21 R22 R24 R25 R26 R27 R28 R29 R30 R31 R32 R33 R34 R35 R37 R39 R40 R41 R43 R44 R45 R46 R47 R48 R49 R50 R51 R52 R53 R54 R55 R56 R57 R58 R59 R60 R61 R62 R63 R64 R65 R66 R67 R68 R69 R70 R71 R72 R73 R74 R75 R76 R77 R78 R79 R80 R81 R82 R83 R84 R85 R86 R87 R88 R89 R90 R91 R92 R93 R94 R95 R96 R97 R98 R99 R100 R101 R102 R103 R104 R105 R106 R107, -5.1107 * hv700 -5.1107 * hv680 -0.0018576 * H2S -0.10322 * HNO3 -1.0354 * CO2 1.2618 * O2 -0.81377 * H2O 1.0353 * biomass
37,0,100, R2 R3 R4 R5 R6 R7 R8 R9 R10 R11 R12 R13 R14 R17 R18 R19 R20 R21 R23 R24 R25 R26 R27 R28 R29 R30 R31 R32 R33 R34 R35 R37 R39 R40 R41 R42 R44 R45

R46 R47 R48 R49 R50 R51 R52 R53 R54 R55 R56 R57 R58 R59 R60 R61 R62 R63 R64 R65 R66 R67 R68 R69 R70 R71 R72 R73 R74 R75 R76 R77 R78 R79 R80 R81 R82 R83 R84 R85 R86 R87 R88 R89 R90 R91 R92 R93 R94 R95 R96 R97 R98 R99 R100 R101 R102 R103 R104 R105 R106 R107, -5.0289 * hv700 -5.0289 * hv680 -0.0018227 * H2S -0.10129 * HNO3 -1.016 * CO2 1.2381 * O2 -0.7985 * H2O 1.0159 * biomass

38,0,100, R2 R3 R4 R5 R6 R7 R8 R9 R10 R11 R12 R13 R14 R17 R18 R19 R20 R21 R23 R24 R25 R26 R27 R28 R29 R30 R31 R32 R33 R34 R35 R37 R39 R40 R41 R43 R44 R45 R46 R47 R48 R49 R50 R51 R52 R53 R54 R55 R56 R57 R58 R59 R60 R61 R62 R63 R64 R65 R66 R67 R68 R69 R70 R71 R72 R73 R74 R75 R76 R77 R78 R79 R80 R81 R82 R83 R84 R85 R86 R87 R88 R89 R90 R91 R92 R93 R94 R95 R96 R97 R98 R99 R100 R101 R102 R103 R104 R105 R106 R107, -5.1107 * hv700 -5.1107 * hv680 -0.0018576 * H2S -0.10322 * HNO3 -1.0354 * CO2 1.2618 * O2 -0.81377 * H2O 1.0353 * biomass

39,0,100, R2 R3 R5 R6 R7 R8 R9 R10 R11 R12 R13 R14 R17 R18 R19 R20 R21 R22 R24 R25 R26 R27 R28 R29 R30 R31 R32 R33 R34 R35 R37 R39 R40 R41 R42 R43 R44 R45 R46 R47 R48 R49 R50 R51 R52 R53 R54 R55 R56 R57 R58 R59 R60 R61 R62 R63 R64 R65 R66 R67 R68 R69 R70 R71 R72 R73 R74 R75 R76 R77 R78 R79 R80 R81 R82 R83 R84 R85 R86 R87 R88 R89 R90 R91 R92 R93 R94 R95 R96 R97 R98 R99 R100 R101 R102 R103 R104 R105 R106 R107, -5.2273 * hv700 -5.2273 * hv680 -0.0019073 * H2S -0.10598 * HNO3 -1.0631 * CO2 1.2955 * O2 -0.83553 * H2O 1.063 * biomass

40,0,100, R2 R3 R5 R6 R7 R8 R9 R10 R11 R12 R13 R14 R17 R18 R19 R20 R21 R22 R24 R25 R26 R27 R28 R29 R30 R31 R32 R33 R34 R35 R37 R38 R39 R40 R41 R42 R44 R45 R46 R47 R48 R49 R50 R51 R52 R53 R54 R55 R56 R57 R58 R59 R60 R61 R62 R63 R64 R65 R66 R67 R68 R69 R70 R71 R72 R73 R74 R75 R76 R77 R78 R79 R80 R81 R82 R83 R84 R85 R86 R87 R88 R89 R90 R91 R92 R93 R94 R95 R96 R97 R98 R99 R100 R101 R102 R103 R104 R105 R106 R107, -5.2273 * hv700 -5.2273 * hv680 -0.0019073 * H2S -0.10598 * HNO3 -1.0631 * CO2 1.2955 * O2 -0.83553 * H2O 1.063 * biomass

41,0,100, R2 R3 R5 R6 R7 R8 R9 R10 R11 R12 R13 R14 R17 R18 R19 R20 R21 R22 R24 R25 R26 R27 R28 R29 R30 R31 R32 R33 R34 R35 R37 R38 R39 R40 R41 R43 R44 R45 R46 R47 R48 R49 R50 R51 R52 R53 R54 R55 R56 R57 R58 R59 R60 R61 R62 R63 R64 R65 R66 R67 R68 R69 R70 R71 R72 R73 R74 R75 R76 R77 R78 R79 R80 R81 R82 R83 R84 R85 R86 R87 R88 R89 R90 R91 R92 R93 R94 R95 R96 R97 R98 R99 R100 R101 R102 R103 R104 R105 R106 R107, -5.2273 * hv700 -5.2273 * hv680 -0.0019073 * H2S -0.10598 * HNO3 -1.0631 * CO2 1.2955 * O2 -0.83553 * H2O 1.063 * biomass

42,0,100, R2 R3 R5 R6 R7 R8 R9 R10 R11 R12 R13 R14 R17 R18 R19 R20 R21 R22 R24 R25 R26 R28 R29 R30 R31 R32 R33 R34 R35 R37 R38 R39 R40 R41 R42 R43 R44 R45 R46 R47 R48 R49 R50 R51 R52 R53 R54 R55 R56 R57 R58 R59 R60 R61 R62 R63 R64 R65 R66 R67 R68 R69 R70 R71 R72 R73 R74 R75 R76 R77 R78 R79 R80 R81 R82 R83 R84 R85 R86 R87 R88 R89 R90 R91 R92 R93 R94 R95 R96 R97 R98 R99 R100 R101 R102 R103 R104 R105 R106 R107, -5.2273 * hv700 -5.2273 * hv680 -0.0019073 * H2S -0.10598 * HNO3 -1.0631 * CO2 1.2955 * O2 -0.83553 * H2O 1.063 * biomass
43,0,100, R2 R3 R5 R6 R7 R8 R9 R10 R11 R12 R13 R14 R17 R18 R19 R20 R21 R23 R24 R25 R26 R27 R28 R29 R30 R31 R32 R33 R34 R35 R37 R39 R40 R41 R42 R43 R44 R45 R46 R47 R48 R49 R50 R51 R52 R53 R54 R55 R56 R57 R58 R59 R60 R61 R62 R63 R64 R65 R66 R67 R68 R69 R70 R71 R72 R73 R74 R75 R76 R77 R78 R79 R80 R81 R82 R83 R84 R85 R86 R87 R88 R89 R90 R91 R92 R93 R94 R95 R96 R97 R98 R99 R100 R101 R102 R103 R104 R105 R106 R107, -5.2273 * hv700 -5.2273 * hv680 -0.0019073 * H2S -0.10598 * HNO3 -1.0631 * CO2 1.2955 * O2 -0.83553 * H2O 1.063 * biomass
44,0,100, R2 R3 R5 R6 R7 R8 R9 R10 R11 R12 R13 R14 R17 R18 R19 R20 R21 R23 R24 R25 R26 R27 R28 R29 R30 R31 R32 R33 R34 R35 R37 R38 R39 R40 R41 R42 R44 R45 R46 R47 R48 R49 R50 R51 R52 R53 R54 R55 R56 R57 R58 R59 R60 R61 R62 R63 R64 R65 R66 R67 R68 R69 R70 R71 R72 R73 R74 R75 R76 R77 R78 R79 R80 R81 R82 R83 R84 R85 R86 R87 R88 R89 R90 R91 R92 R93 R94 R95 R96 R97 R98 R99 R100 R101 R102 R103 R104 R105 R106 R107, -5.2273 * hv700 -5.2273 * hv680 -0.0019073 * H2S -0.10598 * HNO3 -1.0631 * CO2 1.2955 * O2 -0.83553 * H2O 1.063 * biomass
45,0,100, R2 R3 R5 R6 R7 R8 R9 R10 R11 R12 R13 R14 R17 R18 R19 R20 R21 R23 R24 R25 R26 R27 R28 R29 R30 R31 R32 R33 R34 R35 R37 R38 R39 R40 R41 R43 R44 R45 R46 R47 R48 R49 R50 R51 R52 R53 R54 R55 R56 R57 R58 R59 R60 R61 R62 R63 R64 R65 R66 R67 R68 R69 R70 R71 R72 R73 R74 R75 R76 R77 R78 R79 R80 R81 R82 R83 R84 R85 R86 R87 R88 R89 R90 R91 R92 R93 R94 R95 R96 R97 R98 R99 R100 R101 R102 R103 R104 R105 R106 R107, -5.2273 * hv700 -5.2273 * hv680 -0.0019073 * H2S -0.10598 * HNO3 -1.0631 * CO2 1.2955 * O2 -0.83553 * H2O 1.063 * biomass
46,0,100, R2 R3 R5 R6 R7 R8 R9 R10 R11 R12 R13 R14 R17 R18 R19 R20 R21 R23 R24 R25 R26 R28 R29 R30 R31 R32 R33 R34 R35 R37 R38 R39 R40 R41 R42 R43 R44 R45 R46 R47 R48 R49 R50 R51 R52 R53 R54 R55 R56 R57 R58 R59 R60 R61 R62 R63 R64 R65 R66 R67 R68 R69 R70 R71 R72 R73 R74 R75 R76 R77 R78 R79 R80 R81 R82 R83 R84 R85 R86 R87 R88 R89 R90 R91 R92 R93 R94 R95 R96 R97 R98 R99 R100 R101 R102

R103 R104 R105 R106 R107, -5.2273 * hv700 -5.2273 * hv680 -0.0019073 * H2S -0.10598 * HNO3 -1.0631 * CO2 1.2955 * O2 -0.83553 * H2O 1.063 * biomass
47,0,100, R2 R3 R4 R5 R6 R7 R8 R9 R12 R13 R14 R15 R16 R17 R18 R19 R20 R21 R22 R24 R25 R26 R27 R28 R29 R30 R31 R32 R33 R34 R35 R36 R39 R40 R41 R42 R44 R45 R46 R47 R48 R49 R50 R51 R52 R53 R54 R55 R56 R57 R58 R59 R60 R61 R62 R63 R64 R65 R66 R67 R68 R69 R70 R71 R72 R73 R74 R75 R76 R77 R78 R79 R80 R81 R82 R83 R84 R85 R86 R87 R88 R89 R90 R91 R92 R93 R94 R95 R96 R97 R98 R99 R100 R101 R102 R103 R104 R105 R106 R107, -5.309 * hv700 -5.309 * hv680 -0.0019243 * H2S -0.10693 * HNO3 -1.0726 * CO2 1.307 * O2 -0.84298 * H2O 1.0725 * biomass
48,0,100, R2 R3 R4 R5 R6 R7 R8 R9 R12 R13 R14 R15 R16 R17 R18 R19 R20 R21 R22 R24 R25 R26 R27 R28 R29 R30 R31 R32 R33 R34 R35 R36 R39 R40 R41 R43 R44 R45 R46 R47 R48 R49 R50 R51 R52 R53 R54 R55 R56 R57 R58 R59 R60 R61 R62 R63 R64 R65 R66 R67 R68 R69 R70 R71 R72 R73 R74 R75 R76 R77 R78 R79 R80 R81 R82 R83 R84 R85 R86 R87 R88 R89 R90 R91 R92 R93 R94 R95 R96 R97 R98 R99 R100 R101 R102 R103 R104 R105 R106 R107, -5.4011 * hv700 -5.4011 * hv680 -0.0019631 * H2S -0.10909 * HNO3 -1.0942 * CO2 1.3335 * O2 -0.86002 * H2O 1.0942 * biomass
49,0,100, R2 R3 R5 R6 R7 R8 R9 R12 R13 R14 R15 R16 R17 R18 R19 R20 R21 R22 R24 R25 R26 R27 R28 R29 R30 R31 R32 R33 R34 R35 R36 R39 R40 R41 R42 R43 R44 R45 R46 R47 R48 R49 R50 R51 R52 R53 R54 R55 R56 R57 R58 R59 R60 R61 R62 R63 R64 R65 R66 R67 R68 R69 R70 R71 R72 R73 R74 R75 R76 R77 R78 R79 R80 R81 R82 R83 R84 R85 R86 R87 R88 R89 R90 R91 R92 R93 R94 R95 R96 R97 R98 R99 R100 R101 R102 R103 R104 R105 R106 R107, -5.5328 * hv700 -5.5328 * hv680 -0.0020187 * H2S -0.11218 * HNO3 -1.1252 * CO2 1.3712 * O2 -0.88436 * H2O 1.1251 * biomass
50,0,100, R2 R3 R5 R6 R7 R8 R9 R12 R13 R14 R15 R16 R17 R18 R19 R20 R21 R22 R24 R25 R26 R27 R28 R29 R30 R31 R32 R33 R34 R35 R36 R38 R39 R40 R41 R42 R44 R45 R46 R47 R48 R49 R50 R51 R52 R53 R54 R55 R56 R57 R58 R59 R60 R61 R62 R63 R64 R65 R66 R67 R68 R69 R70 R71 R72 R73 R74 R75 R76 R77 R78 R79 R80 R81 R82 R83 R84 R85 R86 R87 R88 R89 R90 R91 R92 R93 R94 R95 R96 R97 R98 R99 R100 R101 R102 R103 R104 R105 R106 R107, -5.5328 * hv700 -5.5328 * hv680 -0.0020187 * H2S -0.11218 * HNO3 -1.1252 * CO2 1.3712 * O2 -0.88436 * H2O 1.1251 * biomass
51,0,100, R2 R3 R5 R6 R7 R8 R9 R12 R13 R14 R15 R16 R17 R18 R19 R20 R21 R22 R24 R25 R26 R27 R28 R29 R30 R31 R32 R33 R34 R35 R36 R38 R39 R40 R41 R43 R44 R45 R46 R47 R48 R49 R50 R51 R52 R53 R54 R55 R56 R57 R58 R59 R60 R61 R62 R63 R64 R65 R66 R67 R68 R69 R70 R71 R72 R73 R74 R75 R76 R77 R78 R79 R80 R81 R82 R83

R84 R85 R86 R87 R88 R89 R90 R91 R92 R93 R94 R95 R96 R97 R98 R99 R100 R101 R102 R103 R104 R105 R106 R107, -5.5328 * hv700 -5.5328 * hv680 -0.0020187 * H2S -0.11218 * HNO3 -1.1252 * CO2 1.3712 * O2 -0.88436 * H2O 1.1251 * biomass

52,0,100, R2 R3 R5 R6 R7 R8 R9 R12 R13 R14 R15 R16 R17 R18 R19 R20 R21 R22 R24 R25 R26 R28 R29 R30 R31 R32 R33 R34 R35 R36 R38 R39 R40 R41 R42 R43 R44 R45 R46 R47 R48 R49 R50 R51 R52 R53 R54 R55 R56 R57 R58 R59 R60 R61 R62 R63 R64 R65 R66 R67 R68 R69 R70 R71 R72 R73 R74 R75 R76 R77 R78 R79 R80 R81 R82 R83 R84 R85 R86 R87 R88 R89 R90 R91 R92 R93 R94 R95 R96 R97 R98 R99 R100 R101 R102 R103 R104 R105 R106 R107, -5.5328 * hv700 -5.5328 * hv680 -0.0020187 * H2S -0.11218 * HNO3 -1.1252 * CO2 1.3712 * O2 -0.88436 * H2O 1.1251 * biomass

53,0,100, R2 R3 R4 R5 R6 R7 R8 R9 R10 R11 R12 R13 R14 R17 R18 R19 R20 R21 R22 R24 R25 R26 R27 R28 R29 R30 R31 R32 R33 R34 R35 R36 R39 R40 R41 R42 R44 R45 R46 R47 R48 R49 R50 R51 R52 R53 R54 R55 R56 R57 R58 R59 R60 R61 R62 R63 R64 R65 R66 R67 R68 R69 R70 R71 R72 R73 R74 R75 R76 R77 R78 R79 R80 R81 R82 R83 R84 R85 R86 R87 R88 R89 R90 R91 R92 R93 R94 R95 R96 R97 R98 R99 R100 R101 R102 R103 R104 R105 R106 R107, -5.309 * hv700 -5.309 * hv680 -0.0019243 * H2S -0.10693 * HNO3 -1.0726 * CO2 1.307 * O2 -0.84298 * H2O 1.0725 * biomass

54,0,100, R2 R3 R4 R5 R6 R7 R8 R9 R10 R11 R12 R13 R14 R17 R18 R19 R20 R21 R22 R24 R25 R26 R27 R28 R29 R30 R31 R32 R33 R34 R35 R36 R39 R40 R41 R43 R44 R45 R46 R47 R48 R49 R50 R51 R52 R53 R54 R55 R56 R57 R58 R59 R60 R61 R62 R63 R64 R65 R66 R67 R68 R69 R70 R71 R72 R73 R74 R75 R76 R77 R78 R79 R80 R81 R82 R83 R84 R85 R86 R87 R88 R89 R90 R91 R92 R93 R94 R95 R96 R97 R98 R99 R100 R101 R102 R103 R104 R105 R106 R107, -5.4011 * hv700 -5.4011 * hv680 -0.0019631 * H2S -0.10909 * HNO3 -1.0942 * CO2 1.3335 * O2 -0.86002 * H2O 1.0942 * biomass

55,0,100, R2 R3 R4 R5 R6 R7 R8 R9 R10 R11 R12 R13 R14 R17 R18 R19 R20 R21 R23 R24 R25 R26 R27 R28 R29 R30 R31 R32 R33 R34 R35 R36 R39 R40 R41 R42 R44 R45 R46 R47 R48 R49 R50 R51 R52 R53 R54 R55 R56 R57 R58 R59 R60 R61 R62 R63 R64 R65 R66 R67 R68 R69 R70 R71 R72 R73 R74 R75 R76 R77 R78 R79 R80 R81 R82 R83 R84 R85 R86 R87 R88 R89 R90 R91 R92 R93 R94 R95 R96 R97 R98 R99 R100 R101 R102 R103 R104 R105 R106 R107, -100.6175 * hv700 -100.6175 * hv680 -0.036469 * H2S -2.0265 * HNO3 -20.3272 * CO2 24.7715 * O2 -15.9763 * H2O 20.3262 * biomass

56,0,100, R2 R3 R4 R5 R6 R7 R8 R9 R10 R11 R12 R13 R14 R17 R18 R19 R20 R21 R23 R24 R25 R26 R27 R28 R29 R30 R31 R32 R33 R34 R35 R36 R39 R40 R41 R43 R44 R45 R46 R47 R48 R49 R50 R51 R52 R53 R54 R55 R56 R57 R58 R59 R60 R61 R62 R63 R64

R65 R66 R67 R68 R69 R70 R71 R72 R73 R74 R75 R76 R77 R78 R79 R80 R81 R82 R83 R84 R85 R86 R87 R88 R89 R90 R91 R92 R93 R94 R95 R96 R97 R98 R99 R100 R101 R102 R103 R104 R105 R106 R107, -5.4011 * hv700 -5.4011 * hv680 -0.0019631 * H2S -0.10909 * HNO3 -1.0942 * CO2 1.3335 * O2 -0.86002 * H2O 1.0942 * biomass
57,0,100, R2 R3 R5 R6 R7 R8 R9 R10 R11 R12 R13 R14 R17 R18 R19 R20 R21 R22 R24 R25 R26 R27 R28 R29 R30 R31 R32 R33 R34 R35 R36 R39 R40 R41 R42 R43 R44 R45 R46 R47 R48 R49 R50 R51 R52 R53 R54 R55 R56 R57 R58 R59 R60 R61 R62 R63 R64 R65 R66 R67 R68 R69 R70 R71 R72 R73 R74 R75 R76 R77 R78 R79 R80 R81 R82 R83 R84 R85 R86 R87 R88 R89 R90 R91 R92 R93 R94 R95 R96 R97 R98 R99 R100 R101 R102 R103 R104 R105 R106 R107, -5.5328 * hv700 -5.5328 * hv680 -0.0020187 * H2S -0.11218 * HNO3 -1.1252 * CO2 1.3712 * O2 -0.88436 * H2O 1.1251 * biomass
58,0,100, R2 R3 R5 R6 R7 R8 R9 R10 R11 R12 R13 R14 R17 R18 R19 R20 R21 R22 R24 R25 R26 R27 R28 R29 R30 R31 R32 R33 R34 R35 R36 R38 R39 R40 R41 R42 R44 R45 R46 R47 R48 R49 R50 R51 R52 R53 R54 R55 R56 R57 R58 R59 R60 R61 R62 R63 R64 R65 R66 R67 R68 R69 R70 R71 R72 R73 R74 R75 R76 R77 R78 R79 R80 R81 R82 R83 R84 R85 R86 R87 R88 R89 R90 R91 R92 R93 R94 R95 R96 R97 R98 R99 R100 R101 R102 R103 R104 R105 R106 R107, -100.2108 * hv700 -100.2108 * hv680 -0.036563 * H2S -2.0318 * HNO3 -20.3799 * CO2 24.8356 * O2 -16.0177 * H2O 20.3788 * biomass
59,0,100, R2 R3 R5 R6 R7 R8 R9 R10 R11 R12 R13 R14 R17 R18 R19 R20 R21 R22 R24 R25 R26 R27 R28 R29 R30 R31 R32 R33 R34 R35 R36 R38 R39 R40 R41 R43 R44 R45 R46 R47 R48 R49 R50 R51 R52 R53 R54 R55 R56 R57 R58 R59 R60 R61 R62 R63 R64 R65 R66 R67 R68 R69 R70 R71 R72 R73 R74 R75 R76 R77 R78 R79 R80 R81 R82 R83 R84 R85 R86 R87 R88 R89 R90 R91 R92 R93 R94 R95 R96 R97 R98 R99 R100 R101 R102 R103 R104 R105 R106 R107, -5.5328 * hv700 -5.5328 * hv680 -0.0020187 * H2S -0.11218 * HNO3 -1.1252 * CO2 1.3712 * O2 -0.88436 * H2O 1.1251 * biomass
60,0,100, R2 R3 R5 R6 R7 R8 R9 R10 R11 R12 R13 R14 R17 R18 R19 R20 R21 R22 R24 R25 R26 R28 R29 R30 R31 R32 R33 R34 R35 R36 R38 R39 R40 R41 R42 R43 R44 R45 R46 R47 R48 R49 R50 R51 R52 R53 R54 R55 R56 R57 R58 R59 R60 R61 R62 R63 R64 R65 R66 R67 R68 R69 R70 R71 R72 R73 R74 R75 R76 R77 R78 R79 R80 R81 R82 R83 R84 R85 R86 R87 R88 R89 R90 R91 R92 R93 R94 R95 R96 R97 R98 R99 R100 R101 R102 R103 R104 R105 R106 R107, -5.5328 * hv700 -5.5328 * hv680 -0.0020187 * H2S -0.11218 * HNO3 -1.1252 * CO2 1.3712 * O2 -0.88436 * H2O 1.1251 * biomass
61,0,100, R2 R3 R5 R6 R7 R8 R9 R10 R11 R12 R13 R14 R17 R18 R19 R20 R21 R23 R24 R25 R26 R27 R28 R29 R30 R31 R32 R33 R34 R35 R36 R39 R40 R41 R42 R43 R44 R45

R46 R47 R48 R49 R50 R51 R52 R53 R54 R55 R56 R57 R58 R59 R60 R61 R62 R63 R64 R65 R66 R67 R68 R69 R70 R71 R72 R73 R74 R75 R76 R77 R78 R79 R80 R81 R82 R83 R84 R85 R86 R87 R88 R89 R90 R91 R92 R93 R94 R95 R96 R97 R98 R99 R100 R101 R102 R103 R104 R105 R106 R107, -5.5328 * hv700 -5.5328 * hv680 -0.0020187 * H2S -0.11218 * HNO3 -1.1252 * CO2 1.3712 * O2 -0.88436 * H2O 1.1251 * biomass

62,0,100, R2 R3 R5 R6 R7 R8 R9 R10 R11 R12 R13 R14 R17 R18 R19 R20 R21 R23 R24 R25 R26 R27 R28 R29 R30 R31 R32 R33 R34 R35 R36 R38 R39 R40 R41 R42 R44 R45 R46 R47 R48 R49 R50 R51 R52 R53 R54 R55 R56 R57 R58 R59 R60 R61 R62 R63 R64 R65 R66 R67 R68 R69 R70 R71 R72 R73 R74 R75 R76 R77 R78 R79 R80 R81 R82 R83 R84 R85 R86 R87 R88 R89 R90 R91 R92 R93 R94 R95 R96 R97 R98 R99 R100 R101 R102 R103 R104 R105 R106 R107, -5.5328 * hv700 -5.5328 * hv680 -0.0020187 * H2S -0.11218 * HNO3 -1.1252 * CO2 1.3712 * O2 -0.88436 * H2O 1.1251 * biomass

63,0,100, R2 R3 R5 R6 R7 R8 R9 R10 R11 R12 R13 R14 R17 R18 R19 R20 R21 R23 R24 R25 R26 R27 R28 R29 R30 R31 R32 R33 R34 R35 R36 R38 R39 R40 R41 R43 R44 R45 R46 R47 R48 R49 R50 R51 R52 R53 R54 R55 R56 R57 R58 R59 R60 R61 R62 R63 R64 R65 R66 R67 R68 R69 R70 R71 R72 R73 R74 R75 R76 R77 R78 R79 R80 R81 R82 R83 R84 R85 R86 R87 R88 R89 R90 R91 R92 R93 R94 R95 R96 R97 R98 R99 R100 R101 R102 R103 R104 R105 R106 R107, -5.5328 * hv700 -5.5328 * hv680 -0.0020187 * H2S -0.11218 * HNO3 -1.1252 * CO2 1.3712 * O2 -0.88436 * H2O 1.1251 * biomass

64,0,100, R2 R3 R5 R6 R7 R8 R9 R10 R11 R12 R13 R14 R17 R18 R19 R20 R21 R23 R24 R25 R26 R28 R29 R30 R31 R32 R33 R34 R35 R36 R38 R39 R40 R41 R42 R43 R44 R45 R46 R47 R48 R49 R50 R51 R52 R53 R54 R55 R56 R57 R58 R59 R60 R61 R62 R63 R64 R65 R66 R67 R68 R69 R70 R71 R72 R73 R74 R75 R76 R77 R78 R79 R80 R81 R82 R83 R84 R85 R86 R87 R88 R89 R90 R91 R92 R93 R94 R95 R96 R97 R98 R99 R100 R101 R102 R103 R104 R105 R106 R107, -5.5328 * hv700 -5.5328 * hv680 -0.0020187 * H2S -0.11218 * HNO3 -1.1252 * CO2 1.3712 * O2 -0.88436 * H2O 1.1251 * biomass

65,0,100, R2 R3 R4 R5 R6 R7 R8 R9 R12 R13 R14 R15 R16 R17 R18 R19 R20 R21 R22 R24 R25 R26 R27 R28 R29 R30 R31 R32 R33 R34 R35 R36 R37 R39 R40 R41 R42 R45 R46 R47 R48 R49 R50 R51 R52 R53 R54 R55 R56 R57 R58 R59 R60 R61 R62 R63 R64 R65 R66 R67 R68 R69 R70 R71 R72 R73 R74 R75 R76 R77 R78 R79 R80 R81 R82 R83 R84 R85 R86 R87 R88 R89 R90 R91 R92 R93 R94 R95 R96 R97 R98 R99 R100 R101 R102 R103 R104 R105 R106 R107, -5.3251 * hv700 -5.3251 * hv680 -0.0019301 * H2S -0.10725 * HNO3 -1.0758 * CO2 1.311 * O2 -0.84553 * H2O 1.0757 * biomass

66,0,100, R2 R3 R4 R5 R6 R7 R8 R9 R12 R13 R14 R15 R16 R17 R18 R19 R20 R21 R22 R24 R25 R26 R27 R28 R29 R30 R31 R32 R33 R34 R35 R36 R37 R39 R40 R41 R43 R45 R46 R47 R48 R49 R50 R51 R52 R53 R54 R55 R56 R57 R58 R59 R60 R61 R62 R63 R64 R65 R66 R67 R68 R69 R70 R71 R72 R73 R74 R75 R76 R77 R78 R79 R80 R81 R82 R83 R84 R85 R86 R87 R88 R89 R90 R91 R92 R93 R94 R95 R96 R97 R98 R99 R100 R101 R102 R103 R104 R105 R106 R107, -5.4178 * hv700 -5.4178 * hv680 -0.0019692 * H2S -0.10943 * HNO3 -1.0976 * CO2 1.3376 * O2 -0.86267 * H2O 1.0976 * biomass
67,0,100, R2 R3 R5 R6 R7 R8 R9 R12 R13 R14 R15 R16 R17 R18 R19 R20 R21 R22 R24 R25 R26 R27 R28 R29 R30 R31 R32 R33 R34 R35 R36 R37 R39 R40 R41 R42 R43 R45 R46 R47 R48 R49 R50 R51 R52 R53 R54 R55 R56 R57 R58 R59 R60 R61 R62 R63 R64 R65 R66 R67 R68 R69 R70 R71 R72 R73 R74 R75 R76 R77 R78 R79 R80 R81 R82 R83 R84 R85 R86 R87 R88 R89 R90 R91 R92 R93 R94 R95 R96 R97 R98 R99 R100 R101 R102 R103 R104 R105 R106 R107, -5.5504 * hv700 -5.5504 * hv680 -0.0020251 * H2S -0.11253 * HNO3 -1.1288 * CO2 1.3756 * O2 -0.88717 * H2O 1.1287 * biomass
68,0,100, R2 R3 R5 R6 R7 R8 R9 R12 R13 R14 R15 R16 R17 R18 R19 R20 R21 R22 R24 R25 R26 R27 R28 R29 R30 R31 R32 R33 R34 R35 R36 R37 R38 R39 R40 R41 R42 R45 R46 R47 R48 R49 R50 R51 R52 R53 R54 R55 R56 R57 R58 R59 R60 R61 R62 R63 R64 R65 R66 R67 R68 R69 R70 R71 R72 R73 R74 R75 R76 R77 R78 R79 R80 R81 R82 R83 R84 R85 R86 R87 R88 R89 R90 R91 R92 R93 R94 R95 R96 R97 R98 R99 R100 R101 R102 R103 R104 R105 R106 R107, -5.5504 * hv700 -5.5504 * hv680 -0.0020251 * H2S -0.11253 * HNO3 -1.1288 * CO2 1.3756 * O2 -0.88717 * H2O 1.1287 * biomass
69,0,100, R2 R3 R5 R6 R7 R8 R9 R12 R13 R14 R15 R16 R17 R18 R19 R20 R21 R22 R24 R25 R26 R27 R28 R29 R30 R31 R32 R33 R34 R35 R36 R37 R38 R39 R40 R41 R43 R45 R46 R47 R48 R49 R50 R51 R52 R53 R54 R55 R56 R57 R58 R59 R60 R61 R62 R63 R64 R65 R66 R67 R68 R69 R70 R71 R72 R73 R74 R75 R76 R77 R78 R79 R80 R81 R82 R83 R84 R85 R86 R87 R88 R89 R90 R91 R92 R93 R94 R95 R96 R97 R98 R99 R100 R101 R102 R103 R104 R105 R106 R107, -5.5504 * hv700 -5.5504 * hv680 -0.0020251 * H2S -0.11253 * HNO3 -1.1288 * CO2 1.3756 * O2 -0.88717 * H2O 1.1287 * biomass
70,0,100, R2 R3 R5 R6 R7 R8 R9 R12 R13 R14 R15 R16 R17 R18 R19 R20 R21 R22 R24 R25 R26 R28 R29 R30 R31 R32 R33 R34 R35 R36 R37 R38 R39 R40 R41 R42 R43 R45 R46 R47 R48 R49 R50 R51 R52 R53 R54 R55 R56 R57 R58 R59 R60 R61 R62 R63 R64 R65 R66 R67 R68 R69 R70 R71 R72 R73 R74 R75 R76 R77 R78 R79 R80 R81 R82 R83 R84 R85 R86 R87 R88 R89 R90 R91 R92 R93 R94 R95 R96 R97 R98 R99 R100 R101 R102

R103 R104 R105 R106 R107, -5.5504 * hv700 -5.5504 * hv680 -0.0020251 * H2S -0.11253 * HNO3 -1.1288 * CO2 1.3756 * O2 -0.88717 * H2O 1.1287 * biomass
71,0,100, R2 R3 R4 R5 R6 R7 R8 R9 R10 R11 R12 R13 R14 R17 R18 R19 R20 R21 R22 R24 R25 R26 R27 R28 R29 R30 R31 R32 R33 R34 R35 R36 R37 R39 R40 R41 R42 R45 R46 R47 R48 R49 R50 R51 R52 R53 R54 R55 R56 R57 R58 R59 R60 R61 R62 R63 R64 R65 R66 R67 R68 R69 R70 R71 R72 R73 R74 R75 R76 R77 R78 R79 R80 R81 R82 R83 R84 R85 R86 R87 R88 R89 R90 R91 R92 R93 R94 R95 R96 R97 R98 R99 R100 R101 R102 R103 R104 R105 R106 R107, -95.7345 * hv700 -95.7345 * hv680 -0.034699 * H2S -1.9282 * HNO3 -19.3407 * CO2 23.5693 * O2 -15.201 * H2O 19.3398 * biomass
72,0,100, R2 R3 R4 R5 R6 R7 R8 R9 R10 R11 R12 R13 R14 R17 R18 R19 R20 R21 R22 R24 R25 R26 R27 R28 R29 R30 R31 R32 R33 R34 R35 R36 R37 R39 R40 R41 R43 R45 R46 R47 R48 R49 R50 R51 R52 R53 R54 R55 R56 R57 R58 R59 R60 R61 R62 R63 R64 R65 R66 R67 R68 R69 R70 R71 R72 R73 R74 R75 R76 R77 R78 R79 R80 R81 R82 R83 R84 R85 R86 R87 R88 R89 R90 R91 R92 R93 R94 R95 R96 R97 R98 R99 R100 R101 R102 R103 R104 R105 R106 R107, -95.574 * hv700 -95.574 * hv680 -0.034738 * H2S -1.9303 * HNO3 -19.3625 * CO2 23.5959 * O2 -15.2181 * H2O 19.3616 * biomass
73,0,100, R2 R3 R4 R5 R6 R7 R8 R9 R10 R11 R12 R13 R14 R17 R18 R19 R20 R21 R23 R24 R25 R26 R27 R28 R29 R30 R31 R32 R33 R34 R35 R36 R37 R39 R40 R41 R42 R45 R46 R47 R48 R49 R50 R51 R52 R53 R54 R55 R56 R57 R58 R59 R60 R61 R62 R63 R64 R65 R66 R67 R68 R69 R70 R71 R72 R73 R74 R75 R76 R77 R78 R79 R80 R81 R82 R83 R84 R85 R86 R87 R88 R89 R90 R91 R92 R93 R94 R95 R96 R97 R98 R99 R100 R101 R102 R103 R104 R105 R106 R107, -1764.187 * hv700 -1764.187 * hv680 -0.63943 * H2S -35.5323 * HNO3 -356.4091 * CO2 434.3331 * O2 -280.1218 * H2O 356.3913 * biomass
74,0,100, R2 R3 R4 R5 R6 R7 R8 R9 R10 R11 R12 R13 R14 R17 R18 R19 R20 R21 R23 R24 R25 R26 R27 R28 R29 R30 R31 R32 R33 R34 R35 R36 R37 R39 R40 R41 R43 R45 R46 R47 R48 R49 R50 R51 R52 R53 R54 R55 R56 R57 R58 R59 R60 R61 R62 R63 R64 R65 R66 R67 R68 R69 R70 R71 R72 R73 R74 R75 R76 R77 R78 R79 R80 R81 R82 R83 R84 R85 R86 R87 R88 R89 R90 R91 R92 R93 R94 R95 R96 R97 R98 R99 R100 R101 R102 R103 R104 R105 R106 R107, -95.574 * hv700 -95.574 * hv680 -0.034738 * H2S -1.9303 * HNO3 -19.3625 * CO2 23.5959 * O2 -15.2181 * H2O 19.3616 * biomass
75,0,100, R2 R3 R5 R6 R7 R8 R9 R10 R11 R12 R13 R14 R17 R18 R19 R20 R21 R22 R24 R25 R26 R27 R28 R29 R30 R31 R32 R33 R34 R35 R36 R37 R39 R40 R41 R42 R43 R45 R46 R47 R48 R49 R50 R51 R52 R53 R54 R55 R56 R57 R58 R59 R60 R61 R62 R63 R64 R65 R66 R67 R68 R69 R70 R71 R72 R73 R74 R75 R76 R77 R78 R79 R80 R81 R82 R83

R84 R85 R86 R87 R88 R89 R90 R91 R92 R93 R94 R95 R96 R97 R98 R99 R100 R101 R102 R103 R104 R105 R106 R107, -5.5504 * hv700 -5.5504 * hv680 -0.0020251 * H2S -0.11253 * HNO3 -1.1288 * CO2 1.3756 * O2 -0.88717 * H2O 1.1287 * biomass

76,0,100, R2 R3 R5 R6 R7 R8 R9 R10 R11 R12 R13 R14 R17 R18 R19 R20 R21 R22 R24 R25 R26 R27 R28 R29 R30 R31 R32 R33 R34 R35 R36 R37 R38 R39 R40 R41 R42 R45 R46 R47 R48 R49 R50 R51 R52 R53 R54 R55 R56 R57 R58 R59 R60 R61 R62 R63 R64 R65 R66 R67 R68 R69 R70 R71 R72 R73 R74 R75 R76 R77 R78 R79 R80 R81 R82 R83 R84 R85 R86 R87 R88 R89 R90 R91 R92 R93 R94 R95 R96 R97 R98 R99 R100 R101 R102 R103 R104 R105 R106 R107, -5.5504 * hv700 -5.5504 * hv680 -0.0020251 * H2S -0.11253 * HNO3 -1.1288 * CO2 1.3756 * O2 -0.88717 * H2O 1.1287 * biomass

77,0,100, R2 R3 R5 R6 R7 R8 R9 R10 R11 R12 R13 R14 R17 R18 R19 R20 R21 R22 R24 R25 R26 R27 R28 R29 R30 R31 R32 R33 R34 R35 R36 R37 R38 R39 R40 R41 R43 R45 R46 R47 R48 R49 R50 R51 R52 R53 R54 R55 R56 R57 R58 R59 R60 R61 R62 R63 R64 R65 R66 R67 R68 R69 R70 R71 R72 R73 R74 R75 R76 R77 R78 R79 R80 R81 R82 R83 R84 R85 R86 R87 R88 R89 R90 R91 R92 R93 R94 R95 R96 R97 R98 R99 R100 R101 R102 R103 R104 R105 R106 R107, -1752.7777 * hv700 -1752.7777 * hv680 -0.63953 * H2S -35.5375 * HNO3 -356.4621 * CO2 434.3976 * O2 -280.1635 * H2O 356.4442 * biomass

78,0,100, R2 R3 R5 R6 R7 R8 R9 R10 R11 R12 R13 R14 R17 R18 R19 R20 R21 R22 R24 R25 R26 R28 R29 R30 R31 R32 R33 R34 R35 R36 R37 R38 R39 R40 R41 R42 R43 R45 R46 R47 R48 R49 R50 R51 R52 R53 R54 R55 R56 R57 R58 R59 R60 R61 R62 R63 R64 R65 R66 R67 R68 R69 R70 R71 R72 R73 R74 R75 R76 R77 R78 R79 R80 R81 R82 R83 R84 R85 R86 R87 R88 R89 R90 R91 R92 R93 R94 R95 R96 R97 R98 R99 R100 R101 R102 R103 R104 R105 R106 R107, -1752.7777 * hv700 -1752.7777 * hv680 -0.63953 * H2S -35.5375 * HNO3 -356.4621 * CO2 434.3976 * O2 -280.1635 * H2O 356.4442 * biomass

79,0,100, R2 R3 R5 R6 R7 R8 R9 R10 R11 R12 R13 R14 R17 R18 R19 R20 R21 R23 R24 R25 R26 R27 R28 R29 R30 R31 R32 R33 R34 R35 R36 R37 R39 R40 R41 R42 R43 R45 R46 R47 R48 R49 R50 R51 R52 R53 R54 R55 R56 R57 R58 R59 R60 R61 R62 R63 R64 R65 R66 R67 R68 R69 R70 R71 R72 R73 R74 R75 R76 R77 R78 R79 R80 R81 R82 R83 R84 R85 R86 R87 R88 R89 R90 R91 R92 R93 R94 R95 R96 R97 R98 R99 R100 R101 R102 R103 R104 R105 R106 R107, -1752.7777 * hv700 -1752.7777 * hv680 -0.63953 * H2S -35.5375 * HNO3 -356.4621 * CO2 434.3976 * O2 -280.1635 * H2O 356.4442 * biomass

80,0,100, R2 R3 R5 R6 R7 R8 R9 R10 R11 R12 R13 R14 R17 R18 R19 R20 R21 R23 R24 R25 R26 R27 R28 R29 R30 R31 R32 R33 R34 R35 R36 R37 R38 R39 R40 R41 R42 R45 R46 R47 R48 R49 R50 R51 R52 R53 R54 R55 R56 R57 R58 R59 R60 R61 R62 R63 R64

R65 R66 R67 R68 R69 R70 R71 R72 R73 R74 R75 R76 R77 R78 R79 R80 R81 R82 R83 R84 R85 R86 R87 R88 R89 R90 R91 R92 R93 R94 R95 R96 R97 R98 R99 R100 R101 R102 R103 R104 R105 R106 R107, -5.5504 * hv700 -5.5504 * hv680 -0.0020251 * H2S -0.11253 * HNO3 -1.1288 * CO2 1.3756 * O2 -0.88717 * H2O 1.1287 * biomass
81,0,100, R2 R3 R5 R6 R7 R8 R9 R10 R11 R12 R13 R14 R17 R18 R19 R20 R21 R23 R24 R25 R26 R27 R28 R29 R30 R31 R32 R33 R34 R35 R36 R37 R38 R39 R40 R41 R43 R45 R46 R47 R48 R49 R50 R51 R52 R53 R54 R55 R56 R57 R58 R59 R60 R61 R62 R63 R64 R65 R66 R67 R68 R69 R70 R71 R72 R73 R74 R75 R76 R77 R78 R79 R80 R81 R82 R83 R84 R85 R86 R87 R88 R89 R90 R91 R92 R93 R94 R95 R96 R97 R98 R99 R100 R101 R102 R103 R104 R105 R106 R107, -1752.7777 * hv700 -1752.7777 * hv680 -0.63953 * H2S -35.5375 * HNO3 -356.4621 * CO2 434.3976 * O2 -280.1635 * H2O 356.4442 * biomass
82,0,100, R2 R3 R5 R6 R7 R8 R9 R10 R11 R12 R13 R14 R17 R18 R19 R20 R21 R23 R24 R25 R26 R28 R29 R30 R31 R32 R33 R34 R35 R36 R37 R38 R39 R40 R41 R42 R43 R45 R46 R47 R48 R49 R50 R51 R52 R53 R54 R55 R56 R57 R58 R59 R60 R61 R62 R63 R64 R65 R66 R67 R68 R69 R70 R71 R72 R73 R74 R75 R76 R77 R78 R79 R80 R81 R82 R83 R84 R85 R86 R87 R88 R89 R90 R91 R92 R93 R94 R95 R96 R97 R98 R99 R100 R101 R102 R103 R104 R105 R106 R107, -5.5504 * hv700 -5.5504 * hv680 -0.0020251 * H2S -0.11253 * HNO3 -1.1288 * CO2 1.3756 * O2 -0.88717 * H2O 1.1287 * biomass
83,0,100, R2 R3 R4 R5 R6 R7 R8 R9 R12 R13 R14 R15 R16 R17 R18 R19 R20 R21 R22 R24 R25 R26 R27 R28 R29 R30 R31 R32 R33 R34 R35 R36 R37 R39 R40 R41 R42 R44 R46 R47 R48 R49 R50 R51 R52 R53 R54 R55 R56 R57 R58 R59 R60 R61 R62 R63 R64 R65 R66 R67 R68 R69 R70 R71 R72 R73 R74 R75 R76 R77 R78 R79 R80 R81 R82 R83 R84 R85 R86 R87 R88 R89 R90 R91 R92 R93 R94 R95 R96 R97 R98 R99 R100 R101 R102 R103 R104 R105 R106 R107, -5.3176 * hv700 -5.3176 * hv680 -0.0019274 * H2S -0.1071 * HNO3 -1.0743 * CO2 1.3092 * O2 -0.84434 * H2O 1.0742 * biomass
84,0,100, R2 R3 R4 R5 R6 R7 R8 R9 R12 R13 R14 R15 R16 R17 R18 R19 R20 R21 R22 R24 R25 R26 R27 R28 R29 R30 R31 R32 R33 R34 R35 R36 R37 R39 R40 R41 R43 R44 R46 R47 R48 R49 R50 R51 R52 R53 R54 R55 R56 R57 R58 R59 R60 R61 R62 R63 R64 R65 R66 R67 R68 R69 R70 R71 R72 R73 R74 R75 R76 R77 R78 R79 R80 R81 R82 R83 R84 R85 R86 R87 R88 R89 R90 R91 R92 R93 R94 R95 R96 R97 R98 R99 R100 R101 R102 R103 R104 R105 R106 R107, -5.41 * hv700 -5.41 * hv680 -0.0019664 * H2S -0.10927 * HNO3 -1.096 * CO2 1.3357 * O2 -0.86143 * H2O 1.096 * biomass
85,0,100, R2 R3 R5 R6 R7 R8 R9 R12 R13 R14 R15 R16 R17 R18 R19 R20 R21 R22 R24 R25 R26 R27 R28 R29 R30 R31 R32 R33 R34 R35 R36 R37 R39 R40 R41 R42 R43 R44

R46 R47 R48 R49 R50 R51 R52 R53 R54 R55 R56 R57 R58 R59 R60 R61 R62 R63 R64 R65 R66 R67 R68 R69 R70 R71 R72 R73 R74 R75 R76 R77 R78 R79 R80 R81 R82 R83 R84 R85 R86 R87 R88 R89 R90 R91 R92 R93 R94 R95 R96 R97 R98 R99 R100 R101 R102 R103 R104 R105 R106 R107, -5.5422 * hv700 -5.5422 * hv680 -0.0020221 * H2S -0.11237 * HNO3 -1.1271 * CO2 1.3735 * O2 -0.88586 * H2O 1.1271 * biomass

86,0,100, R2 R3 R5 R6 R7 R8 R9 R12 R13 R14 R15 R16 R17 R18 R19 R20 R21 R22 R24 R25 R26 R27 R28 R29 R30 R31 R32 R33 R34 R35 R36 R37 R38 R39 R40 R41 R42 R44 R46 R47 R48 R49 R50 R51 R52 R53 R54 R55 R56 R57 R58 R59 R60 R61 R62 R63 R64 R65 R66 R67 R68 R69 R70 R71 R72 R73 R74 R75 R76 R77 R78 R79 R80 R81 R82 R83 R84 R85 R86 R87 R88 R89 R90 R91 R92 R93 R94 R95 R96 R97 R98 R99 R100 R101 R102 R103 R104 R105 R106 R107, -5.5422 * hv700 -5.5422 * hv680 -0.0020221 * H2S -0.11237 * HNO3 -1.1271 * CO2 1.3735 * O2 -0.88586 * H2O 1.1271 * biomass

87,0,100, R2 R3 R5 R6 R7 R8 R9 R12 R13 R14 R15 R16 R17 R18 R19 R20 R21 R22 R24 R25 R26 R27 R28 R29 R30 R31 R32 R33 R34 R35 R36 R37 R38 R39 R40 R41 R43 R44 R46 R47 R48 R49 R50 R51 R52 R53 R54 R55 R56 R57 R58 R59 R60 R61 R62 R63 R64 R65 R66 R67 R68 R69 R70 R71 R72 R73 R74 R75 R76 R77 R78 R79 R80 R81 R82 R83 R84 R85 R86 R87 R88 R89 R90 R91 R92 R93 R94 R95 R96 R97 R98 R99 R100 R101 R102 R103 R104 R105 R106 R107, -5.5422 * hv700 -5.5422 * hv680 -0.0020221 * H2S -0.11237 * HNO3 -1.1271 * CO2 1.3735 * O2 -0.88586 * H2O 1.1271 * biomass

88,0,100, R2 R3 R5 R6 R7 R8 R9 R12 R13 R14 R15 R16 R17 R18 R19 R20 R21 R22 R24 R25 R26 R28 R29 R30 R31 R32 R33 R34 R35 R36 R37 R38 R39 R40 R41 R42 R43 R44 R46 R47 R48 R49 R50 R51 R52 R53 R54 R55 R56 R57 R58 R59 R60 R61 R62 R63 R64 R65 R66 R67 R68 R69 R70 R71 R72 R73 R74 R75 R76 R77 R78 R79 R80 R81 R82 R83 R84 R85 R86 R87 R88 R89 R90 R91 R92 R93 R94 R95 R96 R97 R98 R99 R100 R101 R102 R103 R104 R105 R106 R107, -5.5422 * hv700 -5.5422 * hv680 -0.0020221 * H2S -0.11237 * HNO3 -1.1271 * CO2 1.3735 * O2 -0.88586 * H2O 1.1271 * biomass

89,0,100, R2 R3 R4 R5 R6 R7 R8 R9 R10 R11 R12 R13 R14 R17 R18 R19 R20 R21 R22 R24 R25 R26 R27 R28 R29 R30 R31 R32 R33 R34 R35 R36 R37 R39 R40 R41 R42 R44 R46 R47 R48 R49 R50 R51 R52 R53 R54 R55 R56 R57 R58 R59 R60 R61 R62 R63 R64 R65 R66 R67 R68 R69 R70 R71 R72 R73 R74 R75 R76 R77 R78 R79 R80 R81 R82 R83 R84 R85 R86 R87 R88 R89 R90 R91 R92 R93 R94 R95 R96 R97 R98 R99 R100 R101 R102 R103 R104 R105 R106 R107, -3858.6376 * hv700 -3858.6376 * hv680 -1.3986 * H2S -77.7163 * HNO3 -779.5397 * CO2 949.9752 * O2 -612.6837 * H2O 779.5005 * biomass

90,0,100, R2 R3 R4 R5 R6 R7 R8 R9 R10 R11 R12 R13 R14 R17 R18 R19 R20 R21 R22 R24 R25 R26 R27 R28 R29 R30 R31 R32 R33 R34 R35 R36 R37 R39 R40 R41 R43 R44 R46 R47 R48 R49 R50 R51 R52 R53 R54 R55 R56 R57 R58 R59 R60 R61 R62 R63 R64 R65 R66 R67 R68 R69 R70 R71 R72 R73 R74 R75 R76 R77 R78 R79 R80 R81 R82 R83 R84 R85 R86 R87 R88 R89 R90 R91 R92 R93 R94 R95 R96 R97 R98 R99 R100 R101 R102 R103 R104 R105 R106 R107, -5.41 * hv700 -5.41 * hv680 -0.0019664 * H2S -0.10927 * HNO3 -1.096 * CO2 1.3357 * O2 -0.86143 * H2O 1.096 * biomass
91,0,100, R2 R3 R4 R5 R6 R7 R8 R9 R10 R11 R12 R13 R14 R17 R18 R19 R20 R21 R23 R24 R25 R26 R27 R28 R29 R30 R31 R32 R33 R34 R35 R36 R37 R39 R40 R41 R42 R44 R46 R47 R48 R49 R50 R51 R52 R53 R54 R55 R56 R57 R58 R59 R60 R61 R62 R63 R64 R65 R66 R67 R68 R69 R70 R71 R72 R73 R74 R75 R76 R77 R78 R79 R80 R81 R82 R83 R84 R85 R86 R87 R88 R89 R90 R91 R92 R93 R94 R95 R96 R97 R98 R99 R100 R101 R102 R103 R104 R105 R106 R107, -97.9508 * hv700 -97.9508 * hv680 -0.035502 * H2S -1.9728 * HNO3 -19.7885 * CO2 24.1149 * O2 -15.5529 * H2O 19.7875 * biomass
92,0,100, R2 R3 R4 R5 R6 R7 R8 R9 R10 R11 R12 R13 R14 R17 R18 R19 R20 R21 R23 R24 R25 R26 R27 R28 R29 R30 R31 R32 R33 R34 R35 R36 R37 R39 R40 R41 R43 R44 R46 R47 R48 R49 R50 R51 R52 R53 R54 R55 R56 R57 R58 R59 R60 R61 R62 R63 R64 R65 R66 R67 R68 R69 R70 R71 R72 R73 R74 R75 R76 R77 R78 R79 R80 R81 R82 R83 R84 R85 R86 R87 R88 R89 R90 R91 R92 R93 R94 R95 R96 R97 R98 R99 R100 R101 R102 R103 R104 R105 R106 R107, -5.41 * hv700 -5.41 * hv680 -0.0019664 * H2S -0.10927 * HNO3 -1.096 * CO2 1.3357 * O2 -0.86143 * H2O 1.096 * biomass
93,0,100, R2 R3 R5 R6 R7 R8 R9 R10 R11 R12 R13 R14 R17 R18 R19 R20 R21 R22 R24 R25 R26 R27 R28 R29 R30 R31 R32 R33 R34 R35 R36 R37 R39 R40 R41 R42 R43 R44 R46 R47 R48 R49 R50 R51 R52 R53 R54 R55 R56 R57 R58 R59 R60 R61 R62 R63 R64 R65 R66 R67 R68 R69 R70 R71 R72 R73 R74 R75 R76 R77 R78 R79 R80 R81 R82 R83 R84 R85 R86 R87 R88 R89 R90 R91 R92 R93 R94 R95 R96 R97 R98 R99 R100 R101 R102 R103 R104 R105 R106 R107, -3741.0928 * hv700 -3741.0928 * hv680 -1.365 * H2S -75.8506 * HNO3 -760.8255 * CO2 927.1694 * O2 -597.9752 * H2O 760.7873 * biomass
94,0,100, R2 R3 R5 R6 R7 R8 R9 R10 R11 R12 R13 R14 R17 R18 R19 R20 R21 R22 R24 R25 R26 R27 R28 R29 R30 R31 R32 R33 R34 R35 R36 R37 R38 R39 R40 R41 R42 R44 R46 R47 R48 R49 R50 R51 R52 R53 R54 R55 R56 R57 R58 R59 R60 R61 R62 R63 R64 R65 R66 R67 R68 R69 R70 R71 R72 R73 R74 R75 R76 R77 R78 R79 R80 R81 R82 R83 R84 R85 R86 R87 R88 R89 R90 R91 R92 R93 R94 R95 R96 R97 R98 R99 R100 R101 R102

R103 R104 R105 R106 R107, -3741.0928 * hv700 -3741.0928 * hv680 -1.365 * H2S -75.8506 * HNO3 -760.8255 * CO2 927.1694 * O2 -597.9752 * H2O 760.7873 * biomass
95,0,100, R2 R3 R5 R6 R7 R8 R9 R10 R11 R12 R13 R14 R17 R18 R19 R20 R21 R22 R24 R25 R26 R27 R28 R29 R30 R31 R32 R33 R34 R35 R36 R37 R38 R39 R40 R41 R43 R44 R46 R47 R48 R49 R50 R51 R52 R53 R54 R55 R56 R57 R58 R59 R60 R61 R62 R63 R64 R65 R66 R67 R68 R69 R70 R71 R72 R73 R74 R75 R76 R77 R78 R79 R80 R81 R82 R83 R84 R85 R86 R87 R88 R89 R90 R91 R92 R93 R94 R95 R96 R97 R98 R99 R100 R101 R102 R103 R104 R105 R106 R107, -7019.4181 * hv700 -7019.4181 * hv680 -2.5611 * H2S -142.3186 * HNO3 -1427.538 * CO2 1739.6494 * O2 -1121.9818 * H2O 1427.4663 * biomass
96,0,100, R2 R3 R5 R6 R7 R8 R9 R10 R11 R12 R13 R14 R17 R18 R19 R20 R21 R22 R24 R25 R26 R28 R29 R30 R31 R32 R33 R34 R35 R36 R37 R38 R39 R40 R41 R42 R43 R44 R46 R47 R48 R49 R50 R51 R52 R53 R54 R55 R56 R57 R58 R59 R60 R61 R62 R63 R64 R65 R66 R67 R68 R69 R70 R71 R72 R73 R74 R75 R76 R77 R78 R79 R80 R81 R82 R83 R84 R85 R86 R87 R88 R89 R90 R91 R92 R93 R94 R95 R96 R97 R98 R99 R100 R101 R102 R103 R104 R105 R106 R107, -3741.0928 * hv700 -3741.0928 * hv680 -1.365 * H2S -75.8506 * HNO3 -760.8255 * CO2 927.1694 * O2 -597.9752 * H2O 760.7873 * biomass
97,0,100, R2 R3 R5 R6 R7 R8 R9 R10 R11 R12 R13 R14 R17 R18 R19 R20 R21 R23 R24 R25 R26 R27 R28 R29 R30 R31 R32 R33 R34 R35 R36 R37 R39 R40 R41 R42 R43 R44 R46 R47 R48 R49 R50 R51 R52 R53 R54 R55 R56 R57 R58 R59 R60 R61 R62 R63 R64 R65 R66 R67 R68 R69 R70 R71 R72 R73 R74 R75 R76 R77 R78 R79 R80 R81 R82 R83 R84 R85 R86 R87 R88 R89 R90 R91 R92 R93 R94 R95 R96 R97 R98 R99 R100 R101 R102 R103 R104 R105 R106 R107, -3283.8674 * hv700 -3283.8674 * hv680 -1.1982 * H2S -66.5803 * HNO3 -667.8396 * CO2 813.8535 * O2 -524.8924 * H2O 667.8061 * biomass
98,0,100, R2 R3 R5 R6 R7 R8 R9 R10 R11 R12 R13 R14 R17 R18 R19 R20 R21 R23 R24 R25 R26 R27 R28 R29 R30 R31 R32 R33 R34 R35 R36 R37 R38 R39 R40 R41 R42 R44 R46 R47 R48 R49 R50 R51 R52 R53 R54 R55 R56 R57 R58 R59 R60 R61 R62 R63 R64 R65 R66 R67 R68 R69 R70 R71 R72 R73 R74 R75 R76 R77 R78 R79 R80 R81 R82 R83 R84 R85 R86 R87 R88 R89 R90 R91 R92 R93 R94 R95 R96 R97 R98 R99 R100 R101 R102 R103 R104 R105 R106 R107, -97.5626 * hv700 -97.5626 * hv680 -0.035597 * H2S -1.9781 * HNO3 -19.8413 * CO2 24.1793 * O2 -15.5944 * H2O 19.8403 * biomass
99,0,100, R2 R3 R5 R6 R7 R8 R9 R10 R11 R12 R13 R14 R17 R18 R19 R20 R21 R23 R24 R25 R26 R27 R28 R29 R30 R31 R32 R33 R34 R35 R36 R37 R38 R39 R40 R41 R43 R44 R46 R47 R48 R49 R50 R51 R52 R53 R54 R55 R56 R57 R58 R59 R60 R61 R62 R63 R64

R65 R66 R67 R68 R69 R70 R71 R72 R73 R74 R75 R76 R77 R78 R79 R80 R81 R82 R83 R84 R85 R86 R87 R88 R89 R90 R91 R92 R93 R94 R95 R96 R97 R98 R99 R100 R101 R102 R103 R104 R105 R106 R107, -3283.8674 * hv700 -3283.8674 * hv680 -1.1982 * H2S -66.5803 * HNO3 -667.8396 * CO2 813.8535 * O2 -524.8924 * H2O 667.8061 * biomass

100,0,100, R2 R3 R5 R6 R7 R8 R9 R10 R11 R12 R13 R14 R17 R18 R19 R20 R21 R23 R24 R25 R26 R28 R29 R30 R31 R32 R33 R34 R35 R36 R37 R38 R39 R40 R41 R42 R43 R44 R46 R47 R48 R49 R50 R51 R52 R53 R54 R55 R56 R57 R58 R59 R60 R61 R62 R63 R64 R65 R66 R67 R68 R69 R70 R71 R72 R73 R74 R75 R76 R77 R78 R79 R80 R81 R82 R83 R84 R85 R86 R87 R88 R89 R90 R91 R92 R93 R94 R95 R96 R97 R98 R99 R100 R101 R102 R103 R104 R105 R106 R107, -7019.4181 * hv700 -7019.4181 * hv680 -2.5611 * H2S -142.3186 * HNO3 -1427.538 * CO2 1739.6494 * O2 -1121.9818 * H2O 1427.4663 * biomass

101,0,101, R2 R3 R5 R6 R7 R8 R9 R10 R11 R12 R13 R14 R15 R16 R17 R18 R19 R20 R24 R25 R26 R28 R29 R30 R31 R32 R33 R34 R35 R36 R37 R38 R39 R40 R41 R42 R43 R44 R45 R46 R47 R48 R49 R50 R51 R52 R53 R54 R55 R56 R57 R58 R59 R60 R61 R62 R63 R64 R65 R66 R67 R68 R69 R70 R71 R72 R73 R74 R75 R76 R77 R78 R79 R80 R81 R82 R83 R84 R85 R86 R87 R88 R89 R90 R91 R92 R93 R94 R95 R96 R97 R98 R99 R100 R101 R102 R103 R104 R105 R106 R107, -24.5661 * hv700 -24.5661 * hv680 -0.0089633 * H2S -0.49808 * HNO3 -4.996 * CO2 6.0883 * O2 -3.9266 * H2O 4.9957 * biomass

102,0,101, R2 R3 R5 R6 R7 R8 R9 R10 R11 R12 R13 R14 R15 R16 R17 R18 R19 R20 R24 R25 R26 R27 R28 R29 R30 R31 R32 R33 R34 R35 R36 R37 R38 R39 R40 R41 R43 R44 R45 R46 R47 R48 R49 R50 R51 R52 R53 R54 R55 R56 R57 R58 R59 R60 R61 R62 R63 R64 R65 R66 R67 R68 R69 R70 R71 R72 R73 R74 R75 R76 R77 R78 R79 R80 R81 R82 R83 R84 R85 R86 R87 R88 R89 R90 R91 R92 R93 R94 R95 R96 R97 R98 R99 R100 R101 R102 R103 R104 R105 R106 R107, -117.0719 * hv700 -117.0719 * hv680 -0.042715 * H2S -2.3736 * HNO3 -23.8089 * CO2 29.0144 * O2 -18.7127 * H2O 23.8077 * biomass

103,0,101, R2 R3 R5 R6 R7 R8 R9 R10 R11 R12 R13 R14 R15 R16 R17 R18 R19 R20 R24 R25 R26 R27 R28 R29 R30 R31 R32 R33 R34 R35 R36 R37 R38 R39 R40 R41 R42 R44 R45 R46 R47 R48 R49 R50 R51 R52 R53 R54 R55 R56 R57 R58 R59 R60 R61 R62 R63 R64 R65 R66 R67 R68 R69 R70 R71 R72 R73 R74 R75 R76 R77 R78 R79 R80 R81 R82 R83 R84 R85 R86 R87 R88 R89 R90 R91 R92 R93 R94 R95 R96 R97 R98 R99 R100 R101 R102 R103 R104 R105 R106 R107, -100.489 * hv700 -100.489 * hv680 -0.036665 * H2S -2.0374 * HNO3 -20.4364 * CO2 24.9046 * O2 -16.0621 * H2O 20.4354 * biomass

104,0,101, R2 R3 R4 R5 R6 R7 R8 R9 R10 R11 R12 R13 R14 R15 R16 R17 R18 R19 R20 R24 R25 R26 R27 R28 R29 R30 R31 R32 R33 R34 R35 R36 R37 R39 R40 R41 R42 R44 R45 R46 R47 R48 R49 R50 R51 R52 R53 R54 R55 R56 R57 R58 R59 R60 R61 R62 R63 R64 R65 R66 R67 R68 R69 R70 R71 R72 R73 R74 R75 R76 R77 R78 R79 R80 R81 R82 R83 R84 R85 R86 R87 R88 R89 R90 R91 R92 R93 R94 R95 R96 R97 R98 R99 R100 R101 R102 R103 R104 R105 R106 R107, -302.3506 * hv700 -302.3506 * hv680 -0.10959 * H2S -6.0896 * HNO3 -61.0822 * CO2 74.437 * O2 -48.0079 * H2O 61.0792 * biomass
105,0,101, R2 R3 R4 R5 R6 R7 R8 R9 R10 R11 R12 R13 R14 R15 R16 R17 R18 R19 R20 R24 R25 R26 R27 R28 R29 R30 R31 R32 R33 R34 R35 R36 R37 R39 R40 R41 R43 R44 R45 R46 R47 R48 R49 R50 R51 R52 R53 R54 R55 R56 R57 R58 R59 R60 R61 R62 R63 R64 R65 R66 R67 R68 R69 R70 R71 R72 R73 R74 R75 R76 R77 R78 R79 R80 R81 R82 R83 R84 R85 R86 R87 R88 R89 R90 R91 R92 R93 R94 R95 R96 R97 R98 R99 R100 R101 R102 R103 R104 R105 R106 R107, -522.8696 * hv700 -522.8696 * hv680 -0.19005 * H2S -10.5606 * HNO3 -105.9292 * CO2 129.0891 * O2 -83.2556 * H2O 105.9239 * biomass
106,0,101, R2 R3 R5 R6 R7 R8 R9 R10 R11 R12 R13 R14 R15 R16 R17 R18 R19 R20 R24 R25 R26 R27 R28 R29 R30 R31 R32 R33 R34 R35 R36 R37 R39 R40 R41 R42 R43 R44 R45 R46 R47 R48 R49 R50 R51 R52 R53 R54 R55 R56 R57 R58 R59 R60 R61 R62 R63 R64 R65 R66 R67 R68 R69 R70 R71 R72 R73 R74 R75 R76 R77 R78 R79 R80 R81 R82 R83 R84 R85 R86 R87 R88 R89 R90 R91 R92 R93 R94 R95 R96 R97 R98 R99 R100 R101 R102 R103 R104 R105 R106 R107, -151.0142 * hv700 -151.0142 * hv680 -0.0551 * H2S -3.0618 * HNO3 -30.7117 * CO2 37.4264 * O2 -24.1381 * H2O 30.7102 * biomass
107,0,101, R2 R3 R4 R5 R6 R7 R8 R9 R10 R11 R12 R13 R14 R15 R16 R17 R18 R19 R20 R22 R24 R25 R26 R27 R28 R29 R30 R31 R32 R33 R34 R35 R37 R39 R40 R41 R42 R44 R45 R46 R47 R48 R49 R50 R51 R52 R53 R54 R55 R56 R57 R58 R59 R60 R61 R62 R63 R64 R65 R66 R67 R68 R69 R70 R71 R72 R73 R74 R75 R76 R77 R78 R79 R80 R81 R82 R83 R84 R85 R86 R87 R88 R89 R90 R91 R92 R93 R94 R95 R96 R97 R98 R99 R100 R101 R102 R103 R104 R105 R106 R107, -5.0289 * hv700 -5.0289 * hv680 -0.0018227 * H2S -0.10129 * HNO3 -1.016 * CO2 1.2381 * O2 -0.7985 * H2O 1.0159 * biomass
108,0,101, R2 R3 R4 R5 R6 R7 R8 R9 R10 R11 R12 R13 R14 R15 R16 R17 R18 R19 R20 R22 R24 R25 R26 R27 R28 R29 R30 R31 R32 R33 R34 R35 R37 R39 R40 R41 R43 R44 R45 R46 R47 R48 R49 R50 R51 R52 R53 R54 R55 R56 R57 R58 R59 R60 R61 R62 R63 R64 R65 R66 R67 R68 R69 R70 R71 R72 R73 R74 R75 R76 R77 R78 R79 R80 R81 R82 R83 R84 R85 R86 R87 R88 R89 R90 R91 R92 R93 R94 R95 R96 R97 R98 R99 R100 R101

R102 R103 R104 R105 R106 R107, -5.1107 * hv700 -5.1107 * hv680 -0.0018576 * H2S -0.10322 * HNO3 -1.0354 * CO2 1.2618 * O2 -0.81377 * H2O 1.0353 * biomass
109,0,101, R2 R3 R4 R5 R6 R7 R8 R9 R10 R11 R12 R13 R14 R15 R16 R17 R18 R19 R20 R23 R24 R25 R26 R27 R28 R29 R30 R31 R32 R33 R34 R35 R37 R39 R40 R41 R42 R44 R45 R46 R47 R48 R49 R50 R51 R52 R53 R54 R55 R56 R57 R58 R59 R60 R61 R62 R63 R64 R65 R66 R67 R68 R69 R70 R71 R72 R73 R74 R75 R76 R77 R78 R79 R80 R81 R82 R83 R84 R85 R86 R87 R88 R89 R90 R91 R92 R93 R94 R95 R96 R97 R98 R99 R100 R101 R102 R103 R104 R105 R106 R107, -5.0289 * hv700 -5.0289 * hv680 -0.0018227 * H2S -0.10129 * HNO3 -1.016 * CO2 1.2381 * O2 -0.7985 * H2O 1.0159 * biomass
110,0,101, R2 R3 R4 R5 R6 R7 R8 R9 R10 R11 R12 R13 R14 R15 R16 R17 R18 R19 R20 R23 R24 R25 R26 R27 R28 R29 R30 R31 R32 R33 R34 R35 R37 R39 R40 R41 R43 R44 R45 R46 R47 R48 R49 R50 R51 R52 R53 R54 R55 R56 R57 R58 R59 R60 R61 R62 R63 R64 R65 R66 R67 R68 R69 R70 R71 R72 R73 R74 R75 R76 R77 R78 R79 R80 R81 R82 R83 R84 R85 R86 R87 R88 R89 R90 R91 R92 R93 R94 R95 R96 R97 R98 R99 R100 R101 R102 R103 R104 R105 R106 R107, -5.1107 * hv700 -5.1107 * hv680 -0.0018576 * H2S -0.10322 * HNO3 -1.0354 * CO2 1.2618 * O2 -0.81377 * H2O 1.0353 * biomass
111,0,101, R2 R3 R4 R5 R6 R7 R8 R9 R11 R12 R13 R14 R15 R16 R17 R18 R19 R20 R21 R23 R24 R25 R26 R27 R28 R29 R30 R31 R32 R33 R34 R35 R37 R39 R40 R41 R42 R44 R45 R46 R47 R48 R49 R50 R51 R52 R53 R54 R55 R56 R57 R58 R59 R60 R61 R62 R63 R64 R65 R66 R67 R68 R69 R70 R71 R72 R73 R74 R75 R76 R77 R78 R79 R80 R81 R82 R83 R84 R85 R86 R87 R88 R89 R90 R91 R92 R93 R94 R95 R96 R97 R98 R99 R100 R101 R102 R103 R104 R105 R106 R107, -5.0289 * hv700 -5.0289 * hv680 -0.0018227 * H2S -0.10129 * HNO3 -1.016 * CO2 1.2381 * O2 -0.7985 * H2O 1.0159 * biomass
112,0,101, R2 R3 R4 R5 R6 R7 R8 R9 R11 R12 R13 R14 R15 R16 R17 R18 R19 R20 R21 R23 R24 R25 R26 R27 R28 R29 R30 R31 R32 R33 R34 R35 R37 R39 R40 R41 R43 R44 R45 R46 R47 R48 R49 R50 R51 R52 R53 R54 R55 R56 R57 R58 R59 R60 R61 R62 R63 R64 R65 R66 R67 R68 R69 R70 R71 R72 R73 R74 R75 R76 R77 R78 R79 R80 R81 R82 R83 R84 R85 R86 R87 R88 R89 R90 R91 R92 R93 R94 R95 R96 R97 R98 R99 R100 R101 R102 R103 R104 R105 R106 R107, -5.1107 * hv700 -5.1107 * hv680 -0.0018576 * H2S -0.10322 * HNO3 -1.0354 * CO2 1.2618 * O2 -0.81377 * H2O 1.0353 * biomass
113,0,101, R2 R3 R4 R5 R6 R7 R8 R9 R10 R12 R13 R14 R15 R16 R17 R18 R19 R20 R21 R23 R24 R25 R26 R27 R28 R29 R30 R31 R32 R33 R34 R35 R37 R39 R40 R41 R42 R44 R45 R46 R47 R48 R49 R50 R51 R52 R53 R54 R55 R56 R57 R58 R59 R60 R61 R62 R63 R64 R65 R66 R67 R68 R69 R70 R71 R72 R73 R74 R75 R76 R77 R78 R79 R80 R81 R82

R83 R84 R85 R86 R87 R88 R89 R90 R91 R92 R93 R94 R95 R96 R97 R98 R99 R100 R101 R102 R103 R104 R105 R106 R107, -5.0289 * hv700 -5.0289 * hv680 -0.0018227 * H2S -0.10129 * HNO3 -1.016 * CO2 1.2381 * O2 -0.7985 * H2O 1.0159 * biomass

114,0,101, R2 R3 R4 R5 R6 R7 R8 R9 R10 R12 R13 R14 R15 R16 R17 R18 R19 R20 R21 R23 R24 R25 R26 R27 R28 R29 R30 R31 R32 R33 R34 R35 R37 R39 R40 R41 R43 R44 R45 R46 R47 R48 R49 R50 R51 R52 R53 R54 R55 R56 R57 R58 R59 R60 R61 R62 R63 R64 R65 R66 R67 R68 R69 R70 R71 R72 R73 R74 R75 R76 R77 R78 R79 R80 R81 R82 R83 R84 R85 R86 R87 R88 R89 R90 R91 R92 R93 R94 R95 R96 R97 R98 R99 R100 R101 R102 R103 R104 R105 R106 R107, -5.1107 * hv700 -5.1107 * hv680 -0.0018576 * H2S -0.10322 * HNO3 -1.0354 * CO2 1.2618 * O2 -0.81377 * H2O 1.0353 * biomass

115,0,101, R2 R3 R5 R6 R7 R8 R9 R10 R11 R12 R13 R14 R15 R16 R17 R18 R19 R20 R22 R24 R25 R26 R27 R28 R29 R30 R31 R32 R33 R34 R35 R37 R39 R40 R41 R42 R43 R44 R45 R46 R47 R48 R49 R50 R51 R52 R53 R54 R55 R56 R57 R58 R59 R60 R61 R62 R63 R64 R65 R66 R67 R68 R69 R70 R71 R72 R73 R74 R75 R76 R77 R78 R79 R80 R81 R82 R83 R84 R85 R86 R87 R88 R89 R90 R91 R92 R93 R94 R95 R96 R97 R98 R99 R100 R101 R102 R103 R104 R105 R106 R107, -5.2273 * hv700 -5.2273 * hv680 -0.0019073 * H2S -0.10598 * HNO3 -1.0631 * CO2 1.2955 * O2 -0.83553 * H2O 1.063 * biomass

116,0,101, R2 R3 R5 R6 R7 R8 R9 R10 R11 R12 R13 R14 R15 R16 R17 R18 R19 R20 R22 R24 R25 R26 R27 R28 R29 R30 R31 R32 R33 R34 R35 R37 R38 R39 R40 R41 R42 R44 R45 R46 R47 R48 R49 R50 R51 R52 R53 R54 R55 R56 R57 R58 R59 R60 R61 R62 R63 R64 R65 R66 R67 R68 R69 R70 R71 R72 R73 R74 R75 R76 R77 R78 R79 R80 R81 R82 R83 R84 R85 R86 R87 R88 R89 R90 R91 R92 R93 R94 R95 R96 R97 R98 R99 R100 R101 R102 R103 R104 R105 R106 R107, -5.2273 * hv700 -5.2273 * hv680 -0.0019073 * H2S -0.10598 * HNO3 -1.0631 * CO2 1.2955 * O2 -0.83553 * H2O 1.063 * biomass

117,0,101, R2 R3 R5 R6 R7 R8 R9 R10 R11 R12 R13 R14 R15 R16 R17 R18 R19 R20 R22 R24 R25 R26 R27 R28 R29 R30 R31 R32 R33 R34 R35 R37 R38 R39 R40 R41 R43 R44 R45 R46 R47 R48 R49 R50 R51 R52 R53 R54 R55 R56 R57 R58 R59 R60 R61 R62 R63 R64 R65 R66 R67 R68 R69 R70 R71 R72 R73 R74 R75 R76 R77 R78 R79 R80 R81 R82 R83 R84 R85 R86 R87 R88 R89 R90 R91 R92 R93 R94 R95 R96 R97 R98 R99 R100 R101 R102 R103 R104 R105 R106 R107, -5.2273 * hv700 -5.2273 * hv680 -0.0019073 * H2S -0.10598 * HNO3 -1.0631 * CO2 1.2955 * O2 -0.83553 * H2O 1.063 * biomass

118,0,101, R2 R3 R5 R6 R7 R8 R9 R10 R11 R12 R13 R14 R15 R16 R17 R18 R19 R20 R22 R24 R25 R26 R28 R29 R30 R31 R32 R33 R34 R35 R37 R38 R39 R40 R41 R42 R43 R44 R45 R46 R47 R48 R49 R50 R51 R52 R53 R54 R55 R56 R57 R58 R59 R60 R61 R62 R63

R64 R65 R66 R67 R68 R69 R70 R71 R72 R73 R74 R75 R76 R77 R78 R79 R80 R81 R82 R83 R84 R85 R86 R87 R88 R89 R90 R91 R92 R93 R94 R95 R96 R97 R98 R99 R100 R101 R102 R103 R104 R105 R106 R107, -5.2273 * hv700 -5.2273 * hv680 -0.0019073 * H2S -0.10598 * HNO3 -1.0631 * CO2 1.2955 * O2 -0.83553 * H2O 1.063 * biomass
119,0,101, R2 R3 R5 R6 R7 R8 R9 R10 R11 R12 R13 R14 R15 R16 R17 R18 R19 R20 R23 R24 R25 R26 R27 R28 R29 R30 R31 R32 R33 R34 R35 R37 R39 R40 R41 R42 R43 R44 R45 R46 R47 R48 R49 R50 R51 R52 R53 R54 R55 R56 R57 R58 R59 R60 R61 R62 R63 R64 R65 R66 R67 R68 R69 R70 R71 R72 R73 R74 R75 R76 R77 R78 R79 R80 R81 R82 R83 R84 R85 R86 R87 R88 R89 R90 R91 R92 R93 R94 R95 R96 R97 R98 R99 R100 R101 R102 R103 R104 R105 R106 R107, -5.2273 * hv700 -5.2273 * hv680 -0.0019073 * H2S -0.10598 * HNO3 -1.0631 * CO2 1.2955 * O2 -0.83553 * H2O 1.063 * biomass
120,0,101, R2 R3 R5 R6 R7 R8 R9 R10 R11 R12 R13 R14 R15 R16 R17 R18 R19 R20 R23 R24 R25 R26 R27 R28 R29 R30 R31 R32 R33 R34 R35 R37 R38 R39 R40 R41 R42 R44 R45 R46 R47 R48 R49 R50 R51 R52 R53 R54 R55 R56 R57 R58 R59 R60 R61 R62 R63 R64 R65 R66 R67 R68 R69 R70 R71 R72 R73 R74 R75 R76 R77 R78 R79 R80 R81 R82 R83 R84 R85 R86 R87 R88 R89 R90 R91 R92 R93 R94 R95 R96 R97 R98 R99 R100 R101 R102 R103 R104 R105 R106 R107, -5.2273 * hv700 -5.2273 * hv680 -0.0019073 * H2S -0.10598 * HNO3 -1.0631 * CO2 1.2955 * O2 -0.83553 * H2O 1.063 * biomass
121,0,101, R2 R3 R5 R6 R7 R8 R9 R10 R11 R12 R13 R14 R15 R16 R17 R18 R19 R20 R23 R24 R25 R26 R27 R28 R29 R30 R31 R32 R33 R34 R35 R37 R38 R39 R40 R41 R43 R44 R45 R46 R47 R48 R49 R50 R51 R52 R53 R54 R55 R56 R57 R58 R59 R60 R61 R62 R63 R64 R65 R66 R67 R68 R69 R70 R71 R72 R73 R74 R75 R76 R77 R78 R79 R80 R81 R82 R83 R84 R85 R86 R87 R88 R89 R90 R91 R92 R93 R94 R95 R96 R97 R98 R99 R100 R101 R102 R103 R104 R105 R106 R107, -5.2273 * hv700 -5.2273 * hv680 -0.0019073 * H2S -0.10598 * HNO3 -1.0631 * CO2 1.2955 * O2 -0.83553 * H2O 1.063 * biomass
122,0,101, R2 R3 R5 R6 R7 R8 R9 R11 R12 R13 R14 R15 R16 R17 R18 R19 R20 R21 R23 R24 R25 R26 R27 R28 R29 R30 R31 R32 R33 R34 R35 R37 R39 R40 R41 R42 R43 R44 R45 R46 R47 R48 R49 R50 R51 R52 R53 R54 R55 R56 R57 R58 R59 R60 R61 R62 R63 R64 R65 R66 R67 R68 R69 R70 R71 R72 R73 R74 R75 R76 R77 R78 R79 R80 R81 R82 R83 R84 R85 R86 R87 R88 R89 R90 R91 R92 R93 R94 R95 R96 R97 R98 R99 R100 R101 R102 R103 R104 R105 R106 R107, -5.2273 * hv700 -5.2273 * hv680 -0.0019073 * H2S -0.10598 * HNO3 -1.0631 * CO2 1.2955 * O2 -0.83553 * H2O 1.063 * biomass
123,0,101, R2 R3 R5 R6 R7 R8 R9 R11 R12 R13 R14 R15 R16 R17 R18 R19 R20 R21 R23 R24 R25 R26 R27 R28 R29 R30 R31 R32 R33 R34 R35 R37 R38 R39 R40 R41 R42 R44

R45 R46 R47 R48 R49 R50 R51 R52 R53 R54 R55 R56 R57 R58 R59 R60 R61 R62 R63 R64 R65 R66 R67 R68 R69 R70 R71 R72 R73 R74 R75 R76 R77 R78 R79 R80 R81 R82 R83 R84 R85 R86 R87 R88 R89 R90 R91 R92 R93 R94 R95 R96 R97 R98 R99 R100 R101 R102 R103 R104 R105 R106 R107, -5.2273 * hv700 -5.2273 * hv680 -0.0019073 * H2S -0.10598 * HNO3 -1.0631 * CO2 1.2955 * O2 -0.83553 * H2O 1.063 * biomass

124,0,101, R2 R3 R5 R6 R7 R8 R9 R11 R12 R13 R14 R15 R16 R17 R18 R19 R20 R21 R23 R24 R25 R26 R27 R28 R29 R30 R31 R32 R33 R34 R35 R37 R38 R39 R40 R41 R43 R44 R45 R46 R47 R48 R49 R50 R51 R52 R53 R54 R55 R56 R57 R58 R59 R60 R61 R62 R63 R64 R65 R66 R67 R68 R69 R70 R71 R72 R73 R74 R75 R76 R77 R78 R79 R80 R81 R82 R83 R84 R85 R86 R87 R88 R89 R90 R91 R92 R93 R94 R95 R96 R97 R98 R99 R100 R101 R102 R103 R104 R105 R106 R107, -5.2273 * hv700 -5.2273 * hv680 -0.0019073 * H2S -0.10598 * HNO3 -1.0631 * CO2 1.2955 * O2 -0.83553 * H2O 1.063 * biomass

125,0,101, R2 R3 R5 R6 R7 R8 R9 R10 R12 R13 R14 R15 R16 R17 R18 R19 R20 R21 R23 R24 R25 R26 R27 R28 R29 R30 R31 R32 R33 R34 R35 R37 R39 R40 R41 R42 R43 R44 R45 R46 R47 R48 R49 R50 R51 R52 R53 R54 R55 R56 R57 R58 R59 R60 R61 R62 R63 R64 R65 R66 R67 R68 R69 R70 R71 R72 R73 R74 R75 R76 R77 R78 R79 R80 R81 R82 R83 R84 R85 R86 R87 R88 R89 R90 R91 R92 R93 R94 R95 R96 R97 R98 R99 R100 R101 R102 R103 R104 R105 R106 R107, -5.2273 * hv700 -5.2273 * hv680 -0.0019073 * H2S -0.10598 * HNO3 -1.0631 * CO2 1.2955 * O2 -0.83553 * H2O 1.063 * biomass

126,0,101, R2 R3 R5 R6 R7 R8 R9 R10 R12 R13 R14 R15 R16 R17 R18 R19 R20 R21 R23 R24 R25 R26 R27 R28 R29 R30 R31 R32 R33 R34 R35 R37 R38 R39 R40 R41 R42 R44 R45 R46 R47 R48 R49 R50 R51 R52 R53 R54 R55 R56 R57 R58 R59 R60 R61 R62 R63 R64 R65 R66 R67 R68 R69 R70 R71 R72 R73 R74 R75 R76 R77 R78 R79 R80 R81 R82 R83 R84 R85 R86 R87 R88 R89 R90 R91 R92 R93 R94 R95 R96 R97 R98 R99 R100 R101 R102 R103 R104 R105 R106 R107, -5.2273 * hv700 -5.2273 * hv680 -0.0019073 * H2S -0.10598 * HNO3 -1.0631 * CO2 1.2955 * O2 -0.83553 * H2O 1.063 * biomass

127,0,101, R2 R3 R5 R6 R7 R8 R9 R10 R12 R13 R14 R15 R16 R17 R18 R19 R20 R21 R23 R24 R25 R26 R27 R28 R29 R30 R31 R32 R33 R34 R35 R37 R38 R39 R40 R41 R43 R44 R45 R46 R47 R48 R49 R50 R51 R52 R53 R54 R55 R56 R57 R58 R59 R60 R61 R62 R63 R64 R65 R66 R67 R68 R69 R70 R71 R72 R73 R74 R75 R76 R77 R78 R79 R80 R81 R82 R83 R84 R85 R86 R87 R88 R89 R90 R91 R92 R93 R94 R95 R96 R97 R98 R99 R100 R101 R102 R103 R104 R105 R106 R107, -5.2273 * hv700 -5.2273 * hv680 -0.0019073 * H2S -0.10598 * HNO3 -1.0631 * CO2 1.2955 * O2 -0.83553 * H2O 1.063 * biomass

128,0,101, R2 R3 R5 R6 R7 R8 R9 R10 R11 R12 R13 R14 R15 R16 R17 R18 R19 R20 R23 R24 R25 R26 R28 R29 R30 R31 R32 R33 R34 R35 R37 R38 R39 R40 R41 R42 R43 R44 R45 R46 R47 R48 R49 R50 R51 R52 R53 R54 R55 R56 R57 R58 R59 R60 R61 R62 R63 R64 R65 R66 R67 R68 R69 R70 R71 R72 R73 R74 R75 R76 R77 R78 R79 R80 R81 R82 R83 R84 R85 R86 R87 R88 R89 R90 R91 R92 R93 R94 R95 R96 R97 R98 R99 R100 R101 R102 R103 R104 R105 R106 R107, -5.2273 * hv700 -5.2273 * hv680 -0.0019073 * H2S -0.10598 * HNO3 -1.0631 * CO2 1.2955 * O2 -0.83553 * H2O 1.063 * biomass
129,0,101, R2 R3 R5 R6 R7 R8 R9 R11 R12 R13 R14 R15 R16 R17 R18 R19 R20 R21 R23 R24 R25 R26 R28 R29 R30 R31 R32 R33 R34 R35 R37 R38 R39 R40 R41 R42 R43 R44 R45 R46 R47 R48 R49 R50 R51 R52 R53 R54 R55 R56 R57 R58 R59 R60 R61 R62 R63 R64 R65 R66 R67 R68 R69 R70 R71 R72 R73 R74 R75 R76 R77 R78 R79 R80 R81 R82 R83 R84 R85 R86 R87 R88 R89 R90 R91 R92 R93 R94 R95 R96 R97 R98 R99 R100 R101 R102 R103 R104 R105 R106 R107, -5.2273 * hv700 -5.2273 * hv680 -0.0019073 * H2S -0.10598 * HNO3 -1.0631 * CO2 1.2955 * O2 -0.83553 * H2O 1.063 * biomass
130,0,101, R2 R3 R5 R6 R7 R8 R9 R10 R12 R13 R14 R15 R16 R17 R18 R19 R20 R21 R23 R24 R25 R26 R28 R29 R30 R31 R32 R33 R34 R35 R37 R38 R39 R40 R41 R42 R43 R44 R45 R46 R47 R48 R49 R50 R51 R52 R53 R54 R55 R56 R57 R58 R59 R60 R61 R62 R63 R64 R65 R66 R67 R68 R69 R70 R71 R72 R73 R74 R75 R76 R77 R78 R79 R80 R81 R82 R83 R84 R85 R86 R87 R88 R89 R90 R91 R92 R93 R94 R95 R96 R97 R98 R99 R100 R101 R102 R103 R104 R105 R106 R107, -5.2273 * hv700 -5.2273 * hv680 -0.0019073 * H2S -0.10598 * HNO3 -1.0631 * CO2 1.2955 * O2 -0.83553 * H2O 1.063 * biomass
131,0,101, R2 R3 R4 R5 R6 R7 R8 R9 R10 R11 R12 R13 R14 R15 R16 R17 R18 R19 R20 R22 R24 R25 R26 R27 R28 R29 R30 R31 R32 R33 R34 R35 R36 R39 R40 R41 R42 R44 R45 R46 R47 R48 R49 R50 R51 R52 R53 R54 R55 R56 R57 R58 R59 R60 R61 R62 R63 R64 R65 R66 R67 R68 R69 R70 R71 R72 R73 R74 R75 R76 R77 R78 R79 R80 R81 R82 R83 R84 R85 R86 R87 R88 R89 R90 R91 R92 R93 R94 R95 R96 R97 R98 R99 R100 R101 R102 R103 R104 R105 R106 R107, -5.309 * hv700 -5.309 * hv680 -0.0019243 * H2S -0.10693 * HNO3 -1.0726 * CO2 1.307 * O2 -0.84298 * H2O 1.0725 * biomass
132,0,101, R2 R3 R4 R5 R6 R7 R8 R9 R10 R11 R12 R13 R14 R15 R16 R17 R18 R19 R20 R22 R24 R25 R26 R27 R28 R29 R30 R31 R32 R33 R34 R35 R36 R39 R40 R41 R43 R44 R45 R46 R47 R48 R49 R50 R51 R52 R53 R54 R55 R56 R57 R58 R59 R60 R61 R62 R63 R64 R65 R66 R67 R68 R69 R70 R71 R72 R73 R74 R75 R76 R77 R78 R79 R80 R81 R82 R83 R84 R85 R86 R87 R88 R89 R90 R91 R92 R93 R94 R95 R96 R97 R98 R99 R100 R101

R102 R103 R104 R105 R106 R107, -5.4011 * hv700 -5.4011 * hv680 -0.0019631 * H2S -0.10909 * HNO3 -1.0942 * CO2 1.3335 * O2 -0.86002 * H2O 1.0942 * biomass
133,0,101, R2 R3 R4 R5 R6 R7 R8 R9 R10 R11 R12 R13 R14 R15 R16 R17 R18 R19 R20 R23 R24 R25 R26 R27 R28 R29 R30 R31 R32 R33 R34 R35 R36 R39 R40 R41 R42 R44 R45 R46 R47 R48 R49 R50 R51 R52 R53 R54 R55 R56 R57 R58 R59 R60 R61 R62 R63 R64 R65 R66 R67 R68 R69 R70 R71 R72 R73 R74 R75 R76 R77 R78 R79 R80 R81 R82 R83 R84 R85 R86 R87 R88 R89 R90 R91 R92 R93 R94 R95 R96 R97 R98 R99 R100 R101 R102 R103 R104 R105 R106 R107, -5.309 * hv700 -5.309 * hv680 -0.0019243 * H2S -0.10693 * HNO3 -1.0726 * CO2 1.307 * O2 -0.84298 * H2O 1.0725 * biomass
134,0,101, R2 R3 R4 R5 R6 R7 R8 R9 R10 R11 R12 R13 R14 R15 R16 R17 R18 R19 R20 R23 R24 R25 R26 R27 R28 R29 R30 R31 R32 R33 R34 R35 R36 R39 R40 R41 R43 R44 R45 R46 R47 R48 R49 R50 R51 R52 R53 R54 R55 R56 R57 R58 R59 R60 R61 R62 R63 R64 R65 R66 R67 R68 R69 R70 R71 R72 R73 R74 R75 R76 R77 R78 R79 R80 R81 R82 R83 R84 R85 R86 R87 R88 R89 R90 R91 R92 R93 R94 R95 R96 R97 R98 R99 R100 R101 R102 R103 R104 R105 R106 R107, -100.4427 * hv700 -100.4427 * hv680 -0.036508 * H2S -2.0287 * HNO3 -20.3489 * CO2 24.7979 * O2 -15.9933 * H2O 20.3479 * biomass
135,0,101, R2 R3 R4 R5 R6 R7 R8 R9 R11 R12 R13 R14 R15 R16 R17 R18 R19 R20 R21 R23 R24 R25 R26 R27 R28 R29 R30 R31 R32 R33 R34 R35 R36 R39 R40 R41 R42 R44 R45 R46 R47 R48 R49 R50 R51 R52 R53 R54 R55 R56 R57 R58 R59 R60 R61 R62 R63 R64 R65 R66 R67 R68 R69 R70 R71 R72 R73 R74 R75 R76 R77 R78 R79 R80 R81 R82 R83 R84 R85 R86 R87 R88 R89 R90 R91 R92 R93 R94 R95 R96 R97 R98 R99 R100 R101 R102 R103 R104 R105 R106 R107, -100.6175 * hv700 -100.6175 * hv680 -0.036469 * H2S -2.0265 * HNO3 -20.3272 * CO2 24.7715 * O2 -15.9763 * H2O 20.3262 * biomass
136,0,101, R2 R3 R4 R5 R6 R7 R8 R9 R11 R12 R13 R14 R15 R16 R17 R18 R19 R20 R21 R23 R24 R25 R26 R27 R28 R29 R30 R31 R32 R33 R34 R35 R36 R39 R40 R41 R43 R44 R45 R46 R47 R48 R49 R50 R51 R52 R53 R54 R55 R56 R57 R58 R59 R60 R61 R62 R63 R64 R65 R66 R67 R68 R69 R70 R71 R72 R73 R74 R75 R76 R77 R78 R79 R80 R81 R82 R83 R84 R85 R86 R87 R88 R89 R90 R91 R92 R93 R94 R95 R96 R97 R98 R99 R100 R101 R102 R103 R104 R105 R106 R107, -5.4011 * hv700 -5.4011 * hv680 -0.0019631 * H2S -0.10909 * HNO3 -1.0942 * CO2 1.3335 * O2 -0.86002 * H2O 1.0942 * biomass
137,0,101, R2 R3 R4 R5 R6 R7 R8 R9 R10 R12 R13 R14 R15 R16 R17 R18 R19 R20 R21 R23 R24 R25 R26 R27 R28 R29 R30 R31 R32 R33 R34 R35 R36 R39 R40 R41 R42 R44 R45 R46 R47 R48 R49 R50 R51 R52 R53 R54 R55 R56 R57 R58 R59 R60 R61 R62 R63 R64 R65 R66 R67 R68 R69 R70 R71 R72 R73 R74 R75 R76 R77 R78 R79 R80 R81 R82

R83 R84 R85 R86 R87 R88 R89 R90 R91 R92 R93 R94 R95 R96 R97 R98 R99 R100 R101 R102 R103 R104 R105 R106 R107, -100.6175 * hv700 -100.6175 * hv680 -0.036469 * H2S -2.0265 * HNO3 -20.3272 * CO2 24.7715 * O2 -15.9763 * H2O 20.3262 * biomass
138,0,101, R2 R3 R4 R5 R6 R7 R8 R9 R10 R12 R13 R14 R15 R16 R17 R18 R19 R20 R21 R23 R24 R25 R26 R27 R28 R29 R30 R31 R32 R33 R34 R35 R36 R39 R40 R41 R43 R44 R45 R46 R47 R48 R49 R50 R51 R52 R53 R54 R55 R56 R57 R58 R59 R60 R61 R62 R63 R64 R65 R66 R67 R68 R69 R70 R71 R72 R73 R74 R75 R76 R77 R78 R79 R80 R81 R82 R83 R84 R85 R86 R87 R88 R89 R90 R91 R92 R93 R94 R95 R96 R97 R98 R99 R100 R101 R102 R103 R104 R105 R106 R107, -5.4011 * hv700 -5.4011 * hv680 -0.0019631 * H2S -0.10909 * HNO3 -1.0942 * CO2 1.3335 * O2 -0.86002 * H2O 1.0942 * biomass
139,0,101, R2 R3 R5 R6 R7 R8 R9 R10 R11 R12 R13 R14 R15 R16 R17 R18 R19 R20 R22 R24 R25 R26 R27 R28 R29 R30 R31 R32 R33 R34 R35 R36 R39 R40 R41 R42 R43 R44 R45 R46 R47 R48 R49 R50 R51 R52 R53 R54 R55 R56 R57 R58 R59 R60 R61 R62 R63 R64 R65 R66 R67 R68 R69 R70 R71 R72 R73 R74 R75 R76 R77 R78 R79 R80 R81 R82 R83 R84 R85 R86 R87 R88 R89 R90 R91 R92 R93 R94 R95 R96 R97 R98 R99 R100 R101 R102 R103 R104 R105 R106 R107, -5.5328 * hv700 -5.5328 * hv680 -0.0020187 * H2S -0.11218 * HNO3 -1.1252 * CO2 1.3712 * O2 -0.88436 * H2O 1.1251 * biomass
140,0,101, R2 R3 R5 R6 R7 R8 R9 R10 R11 R12 R13 R14 R15 R16 R17 R18 R19 R20 R22 R24 R25 R26 R27 R28 R29 R30 R31 R32 R33 R34 R35 R36 R38 R39 R40 R41 R42 R44 R45 R46 R47 R48 R49 R50 R51 R52 R53 R54 R55 R56 R57 R58 R59 R60 R61 R62 R63 R64 R65 R66 R67 R68 R69 R70 R71 R72 R73 R74 R75 R76 R77 R78 R79 R80 R81 R82 R83 R84 R85 R86 R87 R88 R89 R90 R91 R92 R93 R94 R95 R96 R97 R98 R99 R100 R101 R102 R103 R104 R105 R106 R107, -5.5328 * hv700 -5.5328 * hv680 -0.0020187 * H2S -0.11218 * HNO3 -1.1252 * CO2 1.3712 * O2 -0.88436 * H2O 1.1251 * biomass
141,0,101, R2 R3 R5 R6 R7 R8 R9 R10 R11 R12 R13 R14 R15 R16 R17 R18 R19 R20 R22 R24 R25 R26 R27 R28 R29 R30 R31 R32 R33 R34 R35 R36 R38 R39 R40 R41 R43 R44 R45 R46 R47 R48 R49 R50 R51 R52 R53 R54 R55 R56 R57 R58 R59 R60 R61 R62 R63 R64 R65 R66 R67 R68 R69 R70 R71 R72 R73 R74 R75 R76 R77 R78 R79 R80 R81 R82 R83 R84 R85 R86 R87 R88 R89 R90 R91 R92 R93 R94 R95 R96 R97 R98 R99 R100 R101 R102 R103 R104 R105 R106 R107, -5.5328 * hv700 -5.5328 * hv680 -0.0020187 * H2S -0.11218 * HNO3 -1.1252 * CO2 1.3712 * O2 -0.88436 * H2O 1.1251 * biomass
142,0,101, R2 R3 R5 R6 R7 R8 R9 R10 R11 R12 R13 R14 R15 R16 R17 R18 R19 R20 R22 R24 R25 R26 R28 R29 R30 R31 R32 R33 R34 R35 R36 R38 R39 R40 R41 R42 R43 R44 R45 R46 R47 R48 R49 R50 R51 R52 R53 R54 R55 R56 R57 R58 R59 R60 R61 R62 R63

R64 R65 R66 R67 R68 R69 R70 R71 R72 R73 R74 R75 R76 R77 R78 R79 R80 R81 R82 R83 R84 R85 R86 R87 R88 R89 R90 R91 R92 R93 R94 R95 R96 R97 R98 R99 R100 R101 R102 R103 R104 R105 R106 R107, -5.5328 * hv700 -5.5328 * hv680 -0.0020187 * H2S -0.11218 * HNO3 -1.1252 * CO2 1.3712 * O2 -0.88436 * H2O 1.1251 * biomass
143,0,101, R2 R3 R5 R6 R7 R8 R9 R10 R11 R12 R13 R14 R15 R16 R17 R18 R19 R20 R23 R24 R25 R26 R27 R28 R29 R30 R31 R32 R33 R34 R35 R36 R39 R40 R41 R42 R43 R44 R45 R46 R47 R48 R49 R50 R51 R52 R53 R54 R55 R56 R57 R58 R59 R60 R61 R62 R63 R64 R65 R66 R67 R68 R69 R70 R71 R72 R73 R74 R75 R76 R77 R78 R79 R80 R81 R82 R83 R84 R85 R86 R87 R88 R89 R90 R91 R92 R93 R94 R95 R96 R97 R98 R99 R100 R101 R102 R103 R104 R105 R106 R107, -5.5328 * hv700 -5.5328 * hv680 -0.0020187 * H2S -0.11218 * HNO3 -1.1252 * CO2 1.3712 * O2 -0.88436 * H2O 1.1251 * biomass
144,0,101, R2 R3 R5 R6 R7 R8 R9 R10 R11 R12 R13 R14 R15 R16 R17 R18 R19 R20 R23 R24 R25 R26 R27 R28 R29 R30 R31 R32 R33 R34 R35 R36 R38 R39 R40 R41 R42 R44 R45 R46 R47 R48 R49 R50 R51 R52 R53 R54 R55 R56 R57 R58 R59 R60 R61 R62 R63 R64 R65 R66 R67 R68 R69 R70 R71 R72 R73 R74 R75 R76 R77 R78 R79 R80 R81 R82 R83 R84 R85 R86 R87 R88 R89 R90 R91 R92 R93 R94 R95 R96 R97 R98 R99 R100 R101 R102 R103 R104 R105 R106 R107, -5.5328 * hv700 -5.5328 * hv680 -0.0020187 * H2S -0.11218 * HNO3 -1.1252 * CO2 1.3712 * O2 -0.88436 * H2O 1.1251 * biomass
145,0,101, R2 R3 R5 R6 R7 R8 R9 R10 R11 R12 R13 R14 R15 R16 R17 R18 R19 R20 R23 R24 R25 R26 R27 R28 R29 R30 R31 R32 R33 R34 R35 R36 R38 R39 R40 R41 R43 R44 R45 R46 R47 R48 R49 R50 R51 R52 R53 R54 R55 R56 R57 R58 R59 R60 R61 R62 R63 R64 R65 R66 R67 R68 R69 R70 R71 R72 R73 R74 R75 R76 R77 R78 R79 R80 R81 R82 R83 R84 R85 R86 R87 R88 R89 R90 R91 R92 R93 R94 R95 R96 R97 R98 R99 R100 R101 R102 R103 R104 R105 R106 R107, -5.5328 * hv700 -5.5328 * hv680 -0.0020187 * H2S -0.11218 * HNO3 -1.1252 * CO2 1.3712 * O2 -0.88436 * H2O 1.1251 * biomass
146,0,101, R2 R3 R5 R6 R7 R8 R9 R11 R12 R13 R14 R15 R16 R17 R18 R19 R20 R21 R23 R24 R25 R26 R27 R28 R29 R30 R31 R32 R33 R34 R35 R36 R39 R40 R41 R42 R43 R44 R45 R46 R47 R48 R49 R50 R51 R52 R53 R54 R55 R56 R57 R58 R59 R60 R61 R62 R63 R64 R65 R66 R67 R68 R69 R70 R71 R72 R73 R74 R75 R76 R77 R78 R79 R80 R81 R82 R83 R84 R85 R86 R87 R88 R89 R90 R91 R92 R93 R94 R95 R96 R97 R98 R99 R100 R101 R102 R103 R104 R105 R106 R107, -100.2108 * hv700 -100.2108 * hv680 -0.036563 * H2S -2.0318 * HNO3 -20.3799 * CO2 24.8356 * O2 -16.0177 * H2O 20.3788 * biomass
147,0,101, R2 R3 R5 R6 R7 R8 R9 R11 R12 R13 R14 R15 R16 R17 R18 R19 R20 R21 R23 R24 R25 R26 R27 R28 R29 R30 R31 R32 R33 R34 R35 R36 R38 R39 R40 R41 R42 R44

R45 R46 R47 R48 R49 R50 R51 R52 R53 R54 R55 R56 R57 R58 R59 R60 R61 R62 R63 R64 R65 R66 R67 R68 R69 R70 R71 R72 R73 R74 R75 R76 R77 R78 R79 R80 R81 R82 R83 R84 R85 R86 R87 R88 R89 R90 R91 R92 R93 R94 R95 R96 R97 R98 R99 R100 R101 R102 R103 R104 R105 R106 R107, -100.2108 * hv700 -100.2108 * hv680 -0.036563 * H2S -2.0318 * HNO3 -20.3799 * CO2 24.8356 * O2 -16.0177 * H2O 20.3788 * biomass

148,0,101, R2 R3 R5 R6 R7 R8 R9 R11 R12 R13 R14 R15 R16 R17 R18 R19 R20 R21 R23 R24 R25 R26 R27 R28 R29 R30 R31 R32 R33 R34 R35 R36 R38 R39 R40 R41 R43 R44 R45 R46 R47 R48 R49 R50 R51 R52 R53 R54 R55 R56 R57 R58 R59 R60 R61 R62 R63 R64 R65 R66 R67 R68 R69 R70 R71 R72 R73 R74 R75 R76 R77 R78 R79 R80 R81 R82 R83 R84 R85 R86 R87 R88 R89 R90 R91 R92 R93 R94 R95 R96 R97 R98 R99 R100 R101 R102 R103 R104 R105 R106 R107, -5.5328 * hv700 -5.5328 * hv680 -0.0020187 * H2S -0.11218 * HNO3 -1.1252 * CO2 1.3712 * O2 -0.88436 * H2O 1.1251 * biomass

149,0,101, R2 R3 R5 R6 R7 R8 R9 R10 R12 R13 R14 R15 R16 R17 R18 R19 R20 R21 R23 R24 R25 R26 R27 R28 R29 R30 R31 R32 R33 R34 R35 R36 R39 R40 R41 R42 R43 R44 R45 R46 R47 R48 R49 R50 R51 R52 R53 R54 R55 R56 R57 R58 R59 R60 R61 R62 R63 R64 R65 R66 R67 R68 R69 R70 R71 R72 R73 R74 R75 R76 R77 R78 R79 R80 R81 R82 R83 R84 R85 R86 R87 R88 R89 R90 R91 R92 R93 R94 R95 R96 R97 R98 R99 R100 R101 R102 R103 R104 R105 R106 R107, -100.2108 * hv700 -100.2108 * hv680 -0.036563 * H2S -2.0318 * HNO3 -20.3799 * CO2 24.8356 * O2 -16.0177 * H2O 20.3788 * biomass

150,0,101, R2 R3 R5 R6 R7 R8 R9 R10 R12 R13 R14 R15 R16 R17 R18 R19 R20 R21 R23 R24 R25 R26 R27 R28 R29 R30 R31 R32 R33 R34 R35 R36 R38 R39 R40 R41 R42 R44 R45 R46 R47 R48 R49 R50 R51 R52 R53 R54 R55 R56 R57 R58 R59 R60 R61 R62 R63 R64 R65 R66 R67 R68 R69 R70 R71 R72 R73 R74 R75 R76 R77 R78 R79 R80 R81 R82 R83 R84 R85 R86 R87 R88 R89 R90 R91 R92 R93 R94 R95 R96 R97 R98 R99 R100 R101 R102 R103 R104 R105 R106 R107, -100.2108 * hv700 -100.2108 * hv680 -0.036563 * H2S -2.0318 * HNO3 -20.3799 * CO2 24.8356 * O2 -16.0177 * H2O 20.3788 * biomass

151,0,101, R2 R3 R5 R6 R7 R8 R9 R10 R12 R13 R14 R15 R16 R17 R18 R19 R20 R21 R23 R24 R25 R26 R27 R28 R29 R30 R31 R32 R33 R34 R35 R36 R38 R39 R40 R41 R43 R44 R45 R46 R47 R48 R49 R50 R51 R52 R53 R54 R55 R56 R57 R58 R59 R60 R61 R62 R63 R64 R65 R66 R67 R68 R69 R70 R71 R72 R73 R74 R75 R76 R77 R78 R79 R80 R81 R82 R83 R84 R85 R86 R87 R88 R89 R90 R91 R92 R93 R94 R95 R96 R97 R98 R99 R100 R101 R102 R103 R104 R105 R106 R107, -100.2108 * hv700 -100.2108 * hv680 -0.036563 * H2S -2.0318 * HNO3 -20.3799 * CO2 24.8356 * O2 -16.0177 * H2O 20.3788 * biomass

152,0,101, R2 R3 R5 R6 R7 R8 R9 R10 R11 R12 R13 R14 R15 R16 R17 R18 R19 R20 R23 R24 R25 R26 R28 R29 R30 R31 R32 R33 R34 R35 R36 R38 R39 R40 R41 R42 R43 R44 R45 R46 R47 R48 R49 R50 R51 R52 R53 R54 R55 R56 R57 R58 R59 R60 R61 R62 R63 R64 R65 R66 R67 R68 R69 R70 R71 R72 R73 R74 R75 R76 R77 R78 R79 R80 R81 R82 R83 R84 R85 R86 R87 R88 R89 R90 R91 R92 R93 R94 R95 R96 R97 R98 R99 R100 R101 R102 R103 R104 R105 R106 R107, -5.5328 * hv700 -5.5328 * hv680 -0.0020187 * H2S -0.11218 * HNO3 -1.1252 * CO2 1.3712 * O2 -0.88436 * H2O 1.1251 * biomass
153,0,101, R2 R3 R5 R6 R7 R8 R9 R11 R12 R13 R14 R15 R16 R17 R18 R19 R20 R21 R23 R24 R25 R26 R28 R29 R30 R31 R32 R33 R34 R35 R36 R38 R39 R40 R41 R42 R43 R44 R45 R46 R47 R48 R49 R50 R51 R52 R53 R54 R55 R56 R57 R58 R59 R60 R61 R62 R63 R64 R65 R66 R67 R68 R69 R70 R71 R72 R73 R74 R75 R76 R77 R78 R79 R80 R81 R82 R83 R84 R85 R86 R87 R88 R89 R90 R91 R92 R93 R94 R95 R96 R97 R98 R99 R100 R101 R102 R103 R104 R105 R106 R107, -5.5328 * hv700 -5.5328 * hv680 -0.0020187 * H2S -0.11218 * HNO3 -1.1252 * CO2 1.3712 * O2 -0.88436 * H2O 1.1251 * biomass
154,0,101, R2 R3 R5 R6 R7 R8 R9 R10 R12 R13 R14 R15 R16 R17 R18 R19 R20 R21 R23 R24 R25 R26 R28 R29 R30 R31 R32 R33 R34 R35 R36 R38 R39 R40 R41 R42 R43 R44 R45 R46 R47 R48 R49 R50 R51 R52 R53 R54 R55 R56 R57 R58 R59 R60 R61 R62 R63 R64 R65 R66 R67 R68 R69 R70 R71 R72 R73 R74 R75 R76 R77 R78 R79 R80 R81 R82 R83 R84 R85 R86 R87 R88 R89 R90 R91 R92 R93 R94 R95 R96 R97 R98 R99 R100 R101 R102 R103 R104 R105 R106 R107, -5.5328 * hv700 -5.5328 * hv680 -0.0020187 * H2S -0.11218 * HNO3 -1.1252 * CO2 1.3712 * O2 -0.88436 * H2O 1.1251 * biomass
155,0,101, R2 R3 R4 R5 R6 R7 R8 R9 R10 R11 R12 R13 R14 R15 R16 R17 R18 R19 R20 R22 R24 R25 R26 R27 R28 R29 R30 R31 R32 R33 R34 R35 R36 R37 R39 R40 R41 R42 R45 R46 R47 R48 R49 R50 R51 R52 R53 R54 R55 R56 R57 R58 R59 R60 R61 R62 R63 R64 R65 R66 R67 R68 R69 R70 R71 R72 R73 R74 R75 R76 R77 R78 R79 R80 R81 R82 R83 R84 R85 R86 R87 R88 R89 R90 R91 R92 R93 R94 R95 R96 R97 R98 R99 R100 R101 R102 R103 R104 R105 R106 R107, -1764.187 * hv700 -1764.187 * hv680 -0.63943 * H2S -35.5323 * HNO3 -356.4091 * CO2 434.3331 * O2 -280.1218 * H2O 356.3913 * biomass
156,0,101, R2 R3 R4 R5 R6 R7 R8 R9 R10 R11 R12 R13 R14 R15 R16 R17 R18 R19 R20 R22 R24 R25 R26 R27 R28 R29 R30 R31 R32 R33 R34 R35 R36 R37 R39 R40 R41 R43 R45 R46 R47 R48 R49 R50 R51 R52 R53 R54 R55 R56 R57 R58 R59 R60 R61 R62 R63 R64 R65 R66 R67 R68 R69 R70 R71 R72 R73 R74 R75 R76 R77 R78 R79 R80 R81 R82 R83 R84 R85 R86 R87 R88 R89 R90 R91 R92 R93 R94 R95 R96 R97 R98 R99 R100 R101

R102 R103 R104 R105 R106 R107, -5.4178 * hv700 -5.4178 * hv680 -0.0019692 * H2S -0.10943 * HNO3 -1.0976 * CO2 1.3376 * O2 -0.86267 * H2O 1.0976 * biomass
157,0,101, R2 R3 R4 R5 R6 R7 R8 R9 R10 R11 R12 R13 R14 R15 R16 R17 R18 R19 R20 R23 R24 R25 R26 R27 R28 R29 R30 R31 R32 R33 R34 R35 R36 R37 R39 R40 R41 R42 R45 R46 R47 R48 R49 R50 R51 R52 R53 R54 R55 R56 R57 R58 R59 R60 R61 R62 R63 R64 R65 R66 R67 R68 R69 R70 R71 R72 R73 R74 R75 R76 R77 R78 R79 R80 R81 R82 R83 R84 R85 R86 R87 R88 R89 R90 R91 R92 R93 R94 R95 R96 R97 R98 R99 R100 R101 R102 R103 R104 R105 R106 R107, -5.3251 * hv700 -5.3251 * hv680 -0.0019301 * H2S -0.10725 * HNO3 -1.0758 * CO2 1.311 * O2 -0.84553 * H2O 1.0757 * biomass
158,0,101, R2 R3 R4 R5 R6 R7 R8 R9 R10 R11 R12 R13 R14 R15 R16 R17 R18 R19 R20 R23 R24 R25 R26 R27 R28 R29 R30 R31 R32 R33 R34 R35 R36 R37 R39 R40 R41 R43 R45 R46 R47 R48 R49 R50 R51 R52 R53 R54 R55 R56 R57 R58 R59 R60 R61 R62 R63 R64 R65 R66 R67 R68 R69 R70 R71 R72 R73 R74 R75 R76 R77 R78 R79 R80 R81 R82 R83 R84 R85 R86 R87 R88 R89 R90 R91 R92 R93 R94 R95 R96 R97 R98 R99 R100 R101 R102 R103 R104 R105 R106 R107, -5.4178 * hv700 -5.4178 * hv680 -0.0019692 * H2S -0.10943 * HNO3 -1.0976 * CO2 1.3376 * O2 -0.86267 * H2O 1.0976 * biomass
159,0,101, R2 R3 R4 R5 R6 R7 R8 R9 R11 R12 R13 R14 R15 R16 R17 R18 R19 R20 R21 R23 R24 R25 R26 R27 R28 R29 R30 R31 R32 R33 R34 R35 R36 R37 R39 R40 R41 R42 R45 R46 R47 R48 R49 R50 R51 R52 R53 R54 R55 R56 R57 R58 R59 R60 R61 R62 R63 R64 R65 R66 R67 R68 R69 R70 R71 R72 R73 R74 R75 R76 R77 R78 R79 R80 R81 R82 R83 R84 R85 R86 R87 R88 R89 R90 R91 R92 R93 R94 R95 R96 R97 R98 R99 R100 R101 R102 R103 R104 R105 R106 R107, -95.7345 * hv700 -95.7345 * hv680 -0.034699 * H2S -1.9282 * HNO3 -19.3407 * CO2 23.5693 * O2 -15.201 * H2O 19.3398 * biomass
160,0,101, R2 R3 R4 R5 R6 R7 R8 R9 R11 R12 R13 R14 R15 R16 R17 R18 R19 R20 R21 R23 R24 R25 R26 R27 R28 R29 R30 R31 R32 R33 R34 R35 R36 R37 R39 R40 R41 R43 R45 R46 R47 R48 R49 R50 R51 R52 R53 R54 R55 R56 R57 R58 R59 R60 R61 R62 R63 R64 R65 R66 R67 R68 R69 R70 R71 R72 R73 R74 R75 R76 R77 R78 R79 R80 R81 R82 R83 R84 R85 R86 R87 R88 R89 R90 R91 R92 R93 R94 R95 R96 R97 R98 R99 R100 R101 R102 R103 R104 R105 R106 R107, -95.574 * hv700 -95.574 * hv680 -0.034738 * H2S -1.9303 * HNO3 -19.3625 * CO2 23.5959 * O2 -15.2181 * H2O 19.3616 * biomass
161,0,101, R2 R3 R4 R5 R6 R7 R8 R9 R10 R12 R13 R14 R15 R16 R17 R18 R19 R20 R21 R23 R24 R25 R26 R27 R28 R29 R30 R31 R32 R33 R34 R35 R36 R37 R39 R40 R41 R42 R45 R46 R47 R48 R49 R50 R51 R52 R53 R54 R55 R56 R57 R58 R59 R60 R61 R62 R63 R64 R65 R66 R67 R68 R69 R70 R71 R72 R73 R74 R75 R76 R77 R78 R79 R80 R81 R82

R83 R84 R85 R86 R87 R88 R89 R90 R91 R92 R93 R94 R95 R96 R97 R98 R99 R100 R101 R102 R103 R104 R105 R106 R107, -95.7345 * hv700 -95.7345 * hv680 -0.034699 * H2S -1.9282 * HNO3 -19.3407 * CO2 23.5693 * O2 -15.201 * H2O 19.3398 * biomass
162,0,101, R2 R3 R4 R5 R6 R7 R8 R9 R10 R12 R13 R14 R15 R16 R17 R18 R19 R20 R21 R23 R24 R25 R26 R27 R28 R29 R30 R31 R32 R33 R34 R35 R36 R37 R39 R40 R41 R43 R45 R46 R47 R48 R49 R50 R51 R52 R53 R54 R55 R56 R57 R58 R59 R60 R61 R62 R63 R64 R65 R66 R67 R68 R69 R70 R71 R72 R73 R74 R75 R76 R77 R78 R79 R80 R81 R82 R83 R84 R85 R86 R87 R88 R89 R90 R91 R92 R93 R94 R95 R96 R97 R98 R99 R100 R101 R102 R103 R104 R105 R106 R107, -95.574 * hv700 -95.574 * hv680 -0.034738 * H2S -1.9303 * HNO3 -19.3625 * CO2 23.5959 * O2 -15.2181 * H2O 19.3616 * biomass
163,0,101, R2 R3 R5 R6 R7 R8 R9 R10 R11 R12 R13 R14 R15 R16 R17 R18 R19 R20 R22 R24 R25 R26 R27 R28 R29 R30 R31 R32 R33 R34 R35 R36 R37 R39 R40 R41 R42 R43 R45 R46 R47 R48 R49 R50 R51 R52 R53 R54 R55 R56 R57 R58 R59 R60 R61 R62 R63 R64 R65 R66 R67 R68 R69 R70 R71 R72 R73 R74 R75 R76 R77 R78 R79 R80 R81 R82 R83 R84 R85 R86 R87 R88 R89 R90 R91 R92 R93 R94 R95 R96 R97 R98 R99 R100 R101 R102 R103 R104 R105 R106 R107, -1752.7777 * hv700 -1752.7777 * hv680 -0.63953 * H2S -35.5375 * HNO3 -356.4621 * CO2 434.3976 * O2 -280.1635 * H2O 356.4442 * biomass
164,0,101, R2 R3 R5 R6 R7 R8 R9 R10 R11 R12 R13 R14 R15 R16 R17 R18 R19 R20 R22 R24 R25 R26 R27 R28 R29 R30 R31 R32 R33 R34 R35 R36 R37 R38 R39 R40 R41 R42 R45 R46 R47 R48 R49 R50 R51 R52 R53 R54 R55 R56 R57 R58 R59 R60 R61 R62 R63 R64 R65 R66 R67 R68 R69 R70 R71 R72 R73 R74 R75 R76 R77 R78 R79 R80 R81 R82 R83 R84 R85 R86 R87 R88 R89 R90 R91 R92 R93 R94 R95 R96 R97 R98 R99 R100 R101 R102 R103 R104 R105 R106 R107, -1752.7777 * hv700 -1752.7777 * hv680 -0.63953 * H2S -35.5375 * HNO3 -356.4621 * CO2 434.3976 * O2 -280.1635 * H2O 356.4442 * biomass
165,0,101, R2 R3 R5 R6 R7 R8 R9 R10 R11 R12 R13 R14 R15 R16 R17 R18 R19 R20 R22 R24 R25 R26 R27 R28 R29 R30 R31 R32 R33 R34 R35 R36 R37 R38 R39 R40 R41 R43 R45 R46 R47 R48 R49 R50 R51 R52 R53 R54 R55 R56 R57 R58 R59 R60 R61 R62 R63 R64 R65 R66 R67 R68 R69 R70 R71 R72 R73 R74 R75 R76 R77 R78 R79 R80 R81 R82 R83 R84 R85 R86 R87 R88 R89 R90 R91 R92 R93 R94 R95 R96 R97 R98 R99 R100 R101 R102 R103 R104 R105 R106 R107, -1752.7777 * hv700 -1752.7777 * hv680 -0.63953 * H2S -35.5375 * HNO3 -356.4621 * CO2 434.3976 * O2 -280.1635 * H2O 356.4442 * biomass
166,0,101, R2 R3 R5 R6 R7 R8 R9 R10 R11 R12 R13 R14 R15 R16 R17 R18 R19 R20 R22 R24 R25 R26 R28 R29 R30 R31 R32 R33 R34 R35 R36 R37 R38 R39 R40 R41 R42 R43 R45 R46 R47 R48 R49 R50 R51 R52 R53 R54 R55 R56 R57 R58 R59 R60 R61 R62 R63

R64 R65 R66 R67 R68 R69 R70 R71 R72 R73 R74 R75 R76 R77 R78 R79 R80 R81 R82 R83 R84 R85 R86 R87 R88 R89 R90 R91 R92 R93 R94 R95 R96 R97 R98 R99 R100 R101 R102 R103 R104 R105 R106 R107, -95.3617 * hv700 -95.3617 * hv680 -0.034794 * H2S -1.9335 * HNO3 -19.3937 * CO2 23.6339 * O2 -15.2426 * H2O 19.3927 * biomass
167,0,101, R2 R3 R5 R6 R7 R8 R9 R10 R11 R12 R13 R14 R15 R16 R17 R18 R19 R20 R23 R24 R25 R26 R27 R28 R29 R30 R31 R32 R33 R34 R35 R36 R37 R39 R40 R41 R42 R43 R45 R46 R47 R48 R49 R50 R51 R52 R53 R54 R55 R56 R57 R58 R59 R60 R61 R62 R63 R64 R65 R66 R67 R68 R69 R70 R71 R72 R73 R74 R75 R76 R77 R78 R79 R80 R81 R82 R83 R84 R85 R86 R87 R88 R89 R90 R91 R92 R93 R94 R95 R96 R97 R98 R99 R100 R101 R102 R103 R104 R105 R106 R107, -1752.7777 * hv700 -1752.7777 * hv680 -0.63953 * H2S -35.5375 * HNO3 -356.4621 * CO2 434.3976 * O2 -280.1635 * H2O 356.4442 * biomass
168,0,101, R2 R3 R5 R6 R7 R8 R9 R10 R11 R12 R13 R14 R15 R16 R17 R18 R19 R20 R23 R24 R25 R26 R27 R28 R29 R30 R31 R32 R33 R34 R35 R36 R37 R38 R39 R40 R41 R42 R45 R46 R47 R48 R49 R50 R51 R52 R53 R54 R55 R56 R57 R58 R59 R60 R61 R62 R63 R64 R65 R66 R67 R68 R69 R70 R71 R72 R73 R74 R75 R76 R77 R78 R79 R80 R81 R82 R83 R84 R85 R86 R87 R88 R89 R90 R91 R92 R93 R94 R95 R96 R97 R98 R99 R100 R101 R102 R103 R104 R105 R106 R107, -5.5504 * hv700 -5.5504 * hv680 -0.0020251 * H2S -0.11253 * HNO3 -1.1288 * CO2 1.3756 * O2 -0.88717 * H2O 1.1287 * biomass
169,0,101, R2 R3 R5 R6 R7 R8 R9 R10 R11 R12 R13 R14 R15 R16 R17 R18 R19 R20 R23 R24 R25 R26 R27 R28 R29 R30 R31 R32 R33 R34 R35 R36 R37 R38 R39 R40 R41 R43 R45 R46 R47 R48 R49 R50 R51 R52 R53 R54 R55 R56 R57 R58 R59 R60 R61 R62 R63 R64 R65 R66 R67 R68 R69 R70 R71 R72 R73 R74 R75 R76 R77 R78 R79 R80 R81 R82 R83 R84 R85 R86 R87 R88 R89 R90 R91 R92 R93 R94 R95 R96 R97 R98 R99 R100 R101 R102 R103 R104 R105 R106 R107, -5.5504 * hv700 -5.5504 * hv680 -0.0020251 * H2S -0.11253 * HNO3 -1.1288 * CO2 1.3756 * O2 -0.88717 * H2O 1.1287 * biomass
170,0,101, R2 R3 R5 R6 R7 R8 R9 R11 R12 R13 R14 R15 R16 R17 R18 R19 R20 R21 R23 R24 R25 R26 R27 R28 R29 R30 R31 R32 R33 R34 R35 R36 R37 R39 R40 R41 R42 R43 R45 R46 R47 R48 R49 R50 R51 R52 R53 R54 R55 R56 R57 R58 R59 R60 R61 R62 R63 R64 R65 R66 R67 R68 R69 R70 R71 R72 R73 R74 R75 R76 R77 R78 R79 R80 R81 R82 R83 R84 R85 R86 R87 R88 R89 R90 R91 R92 R93 R94 R95 R96 R97 R98 R99 R100 R101 R102 R103 R104 R105 R106 R107, -95.3617 * hv700 -95.3617 * hv680 -0.034794 * H2S -1.9335 * HNO3 -19.3937 * CO2 23.6339 * O2 -15.2426 * H2O 19.3927 * biomass
171,0,101, R2 R3 R5 R6 R7 R8 R9 R11 R12 R13 R14 R15 R16 R17 R18 R19 R20 R21 R23 R24 R25 R26 R27 R28 R29 R30 R31 R32 R33 R34 R35 R36 R37 R38 R39 R40 R41 R42

R45 R46 R47 R48 R49 R50 R51 R52 R53 R54 R55 R56 R57 R58 R59 R60 R61 R62 R63 R64 R65 R66 R67 R68 R69 R70 R71 R72 R73 R74 R75 R76 R77 R78 R79 R80 R81 R82 R83 R84 R85 R86 R87 R88 R89 R90 R91 R92 R93 R94 R95 R96 R97 R98 R99 R100 R101 R102 R103 R104 R105 R106 R107, -1752.7777 * hv700 -1752.7777 * hv680 -0.63953 * H2S -35.5375 * HNO3 -356.4621 * CO2 434.3976 * O2 -280.1635 * H2O 356.4442 * biomass

172,0,101, R2 R3 R5 R6 R7 R8 R9 R11 R12 R13 R14 R15 R16 R17 R18 R19 R20 R21 R23 R24 R25 R26 R27 R28 R29 R30 R31 R32 R33 R34 R35 R36 R37 R38 R39 R40 R41 R43 R45 R46 R47 R48 R49 R50 R51 R52 R53 R54 R55 R56 R57 R58 R59 R60 R61 R62 R63 R64 R65 R66 R67 R68 R69 R70 R71 R72 R73 R74 R75 R76 R77 R78 R79 R80 R81 R82 R83 R84 R85 R86 R87 R88 R89 R90 R91 R92 R93 R94 R95 R96 R97 R98 R99 R100 R101 R102 R103 R104 R105 R106 R107, -95.3617 * hv700 -95.3617 * hv680 -0.034794 * H2S -1.9335 * HNO3 -19.3937 * CO2 23.6339 * O2 -15.2426 * H2O 19.3927 * biomass

173,0,101, R2 R3 R5 R6 R7 R8 R9 R10 R12 R13 R14 R15 R16 R17 R18 R19 R20 R21 R23 R24 R25 R26 R27 R28 R29 R30 R31 R32 R33 R34 R35 R36 R37 R39 R40 R41 R42 R43 R45 R46 R47 R48 R49 R50 R51 R52 R53 R54 R55 R56 R57 R58 R59 R60 R61 R62 R63 R64 R65 R66 R67 R68 R69 R70 R71 R72 R73 R74 R75 R76 R77 R78 R79 R80 R81 R82 R83 R84 R85 R86 R87 R88 R89 R90 R91 R92 R93 R94 R95 R96 R97 R98 R99 R100 R101 R102 R103 R104 R105 R106 R107, -5.5504 * hv700 -5.5504 * hv680 -0.0020251 * H2S -0.11253 * HNO3 -1.1288 * CO2 1.3756 * O2 -0.88717 * H2O 1.1287 * biomass

174,0,101, R2 R3 R5 R6 R7 R8 R9 R10 R12 R13 R14 R15 R16 R17 R18 R19 R20 R21 R23 R24 R25 R26 R27 R28 R29 R30 R31 R32 R33 R34 R35 R36 R37 R38 R39 R40 R41 R42 R45 R46 R47 R48 R49 R50 R51 R52 R53 R54 R55 R56 R57 R58 R59 R60 R61 R62 R63 R64 R65 R66 R67 R68 R69 R70 R71 R72 R73 R74 R75 R76 R77 R78 R79 R80 R81 R82 R83 R84 R85 R86 R87 R88 R89 R90 R91 R92 R93 R94 R95 R96 R97 R98 R99 R100 R101 R102 R103 R104 R105 R106 R107, -1752.7777 * hv700 -1752.7777 * hv680 -0.63953 * H2S -35.5375 * HNO3 -356.4621 * CO2 434.3976 * O2 -280.1635 * H2O 356.4442 * biomass

175,0,101, R2 R3 R5 R6 R7 R8 R9 R10 R12 R13 R14 R15 R16 R17 R18 R19 R20 R21 R23 R24 R25 R26 R27 R28 R29 R30 R31 R32 R33 R34 R35 R36 R37 R38 R39 R40 R41 R43 R45 R46 R47 R48 R49 R50 R51 R52 R53 R54 R55 R56 R57 R58 R59 R60 R61 R62 R63 R64 R65 R66 R67 R68 R69 R70 R71 R72 R73 R74 R75 R76 R77 R78 R79 R80 R81 R82 R83 R84 R85 R86 R87 R88 R89 R90 R91 R92 R93 R94 R95 R96 R97 R98 R99 R100 R101 R102 R103 R104 R105 R106 R107, -95.3617 * hv700 -95.3617 * hv680 -0.034794 * H2S -1.9335 * HNO3 -19.3937 * CO2 23.6339 * O2 -15.2426 * H2O 19.3927 * biomass

176,0,101, R2 R3 R5 R6 R7 R8 R9 R10 R11 R12 R13 R14 R15 R16 R17 R18 R19 R20 R23 R24 R25 R26 R28 R29 R30 R31 R32 R33 R34 R35 R36 R37 R38 R39 R40 R41 R42 R43 R45 R46 R47 R48 R49 R50 R51 R52 R53 R54 R55 R56 R57 R58 R59 R60 R61 R62 R63 R64 R65 R66 R67 R68 R69 R70 R71 R72 R73 R74 R75 R76 R77 R78 R79 R80 R81 R82 R83 R84 R85 R86 R87 R88 R89 R90 R91 R92 R93 R94 R95 R96 R97 R98 R99 R100 R101 R102 R103 R104 R105 R106 R107, -1752.7777 * hv700 -1752.7777 * hv680 -0.63953 * H2S -35.5375 * HNO3 -356.4621 * CO2 434.3976 * O2 -280.1635 * H2O 356.4442 * biomass
177,0,101, R2 R3 R5 R6 R7 R8 R9 R11 R12 R13 R14 R15 R16 R17 R18 R19 R20 R21 R23 R24 R25 R26 R28 R29 R30 R31 R32 R33 R34 R35 R36 R37 R38 R39 R40 R41 R42 R43 R45 R46 R47 R48 R49 R50 R51 R52 R53 R54 R55 R56 R57 R58 R59 R60 R61 R62 R63 R64 R65 R66 R67 R68 R69 R70 R71 R72 R73 R74 R75 R76 R77 R78 R79 R80 R81 R82 R83 R84 R85 R86 R87 R88 R89 R90 R91 R92 R93 R94 R95 R96 R97 R98 R99 R100 R101 R102 R103 R104 R105 R106 R107, -1752.7777 * hv700 -1752.7777 * hv680 -0.63953 * H2S -35.5375 * HNO3 -356.4621 * CO2 434.3976 * O2 -280.1635 * H2O 356.4442 * biomass
178,0,101, R2 R3 R5 R6 R7 R8 R9 R10 R12 R13 R14 R15 R16 R17 R18 R19 R20 R21 R23 R24 R25 R26 R28 R29 R30 R31 R32 R33 R34 R35 R36 R37 R38 R39 R40 R41 R42 R43 R45 R46 R47 R48 R49 R50 R51 R52 R53 R54 R55 R56 R57 R58 R59 R60 R61 R62 R63 R64 R65 R66 R67 R68 R69 R70 R71 R72 R73 R74 R75 R76 R77 R78 R79 R80 R81 R82 R83 R84 R85 R86 R87 R88 R89 R90 R91 R92 R93 R94 R95 R96 R97 R98 R99 R100 R101 R102 R103 R104 R105 R106 R107, -95.3617 * hv700 -95.3617 * hv680 -0.034794 * H2S -1.9335 * HNO3 -19.3937 * CO2 23.6339 * O2 -15.2426 * H2O 19.3927 * biomass
179,0,101, R2 R3 R4 R5 R6 R7 R8 R9 R10 R11 R12 R13 R14 R15 R16 R17 R18 R19 R20 R22 R24 R25 R26 R27 R28 R29 R30 R31 R32 R33 R34 R35 R36 R37 R39 R40 R41 R42 R44 R46 R47 R48 R49 R50 R51 R52 R53 R54 R55 R56 R57 R58 R59 R60 R61 R62 R63 R64 R65 R66 R67 R68 R69 R70 R71 R72 R73 R74 R75 R76 R77 R78 R79 R80 R81 R82 R83 R84 R85 R86 R87 R88 R89 R90 R91 R92 R93 R94 R95 R96 R97 R98 R99 R100 R101 R102 R103 R104 R105 R106 R107, -3766.0043 * hv700 -3766.0043 * hv680 -1.365 * H2S -75.8506 * HNO3 -760.8255 * CO2 927.1694 * O2 -597.9752 * H2O 760.7873 * biomass
180,0,101, R2 R3 R4 R5 R6 R7 R8 R9 R10 R11 R12 R13 R14 R15 R16 R17 R18 R19 R20 R22 R24 R25 R26 R27 R28 R29 R30 R31 R32 R33 R34 R35 R36 R37 R39 R40 R41 R43 R44 R46 R47 R48 R49 R50 R51 R52 R53 R54 R55 R56 R57 R58 R59 R60 R61 R62 R63 R64 R65 R66 R67 R68 R69 R70 R71 R72 R73 R74 R75 R76 R77 R78 R79 R80 R81 R82 R83 R84 R85 R86 R87 R88 R89 R90 R91 R92 R93 R94 R95 R96 R97 R98 R99 R100 R101

R102 R103 R104 R105 R106 R107, -3755.4576 * hv700 -3755.4576 * hv680 -1.365 * H2S -75.8506 * HNO3 -760.8255 * CO2 927.1694 * O2 -597.9752 * H2O 760.7873 * biomass
181,0,101, R2 R3 R4 R5 R6 R7 R8 R9 R10 R11 R12 R13 R14 R15 R16 R17 R18 R19 R20 R23 R24 R25 R26 R27 R28 R29 R30 R31 R32 R33 R34 R35 R36 R37 R39 R40 R41 R42 R44 R46 R47 R48 R49 R50 R51 R52 R53 R54 R55 R56 R57 R58 R59 R60 R61 R62 R63 R64 R65 R66 R67 R68 R69 R70 R71 R72 R73 R74 R75 R76 R77 R78 R79 R80 R81 R82 R83 R84 R85 R86 R87 R88 R89 R90 R91 R92 R93 R94 R95 R96 R97 R98 R99 R100 R101 R102 R103 R104 R105 R106 R107, -5.3176 * hv700 -5.3176 * hv680 -0.0019274 * H2S -0.1071 * HNO3 -1.0743 * CO2 1.3092 * O2 -0.84434 * H2O 1.0742 * biomass
182,0,101, R2 R3 R4 R5 R6 R7 R8 R9 R10 R11 R12 R13 R14 R15 R16 R17 R18 R19 R20 R23 R24 R25 R26 R27 R28 R29 R30 R31 R32 R33 R34 R35 R36 R37 R39 R40 R41 R43 R44 R46 R47 R48 R49 R50 R51 R52 R53 R54 R55 R56 R57 R58 R59 R60 R61 R62 R63 R64 R65 R66 R67 R68 R69 R70 R71 R72 R73 R74 R75 R76 R77 R78 R79 R80 R81 R82 R83 R84 R85 R86 R87 R88 R89 R90 R91 R92 R93 R94 R95 R96 R97 R98 R99 R100 R101 R102 R103 R104 R105 R106 R107, -5.41 * hv700 -5.41 * hv680 -0.0019664 * H2S -0.10927 * HNO3 -1.096 * CO2 1.3357 * O2 -0.86143 * H2O 1.096 * biomass
183,0,101, R2 R3 R4 R5 R6 R7 R8 R9 R11 R12 R13 R14 R15 R16 R17 R18 R19 R20 R21 R23 R24 R25 R26 R27 R28 R29 R30 R31 R32 R33 R34 R35 R36 R37 R39 R40 R41 R42 R44 R46 R47 R48 R49 R50 R51 R52 R53 R54 R55 R56 R57 R58 R59 R60 R61 R62 R63 R64 R65 R66 R67 R68 R69 R70 R71 R72 R73 R74 R75 R76 R77 R78 R79 R80 R81 R82 R83 R84 R85 R86 R87 R88 R89 R90 R91 R92 R93 R94 R95 R96 R97 R98 R99 R100 R101 R102 R103 R104 R105 R106 R107, -5.3176 * hv700 -5.3176 * hv680 -0.0019274 * H2S -0.1071 * HNO3 -1.0743 * CO2 1.3092 * O2 -0.84434 * H2O 1.0742 * biomass
184,0,101, R2 R3 R4 R5 R6 R7 R8 R9 R11 R12 R13 R14 R15 R16 R17 R18 R19 R20 R21 R23 R24 R25 R26 R27 R28 R29 R30 R31 R32 R33 R34 R35 R36 R37 R39 R40 R41 R43 R44 R46 R47 R48 R49 R50 R51 R52 R53 R54 R55 R56 R57 R58 R59 R60 R61 R62 R63 R64 R65 R66 R67 R68 R69 R70 R71 R72 R73 R74 R75 R76 R77 R78 R79 R80 R81 R82 R83 R84 R85 R86 R87 R88 R89 R90 R91 R92 R93 R94 R95 R96 R97 R98 R99 R100 R101 R102 R103 R104 R105 R106 R107, -97.7838 * hv700 -97.7838 * hv680 -0.035541 * H2S -1.975 * HNO3 -19.8102 * CO2 24.1414 * O2 -15.57 * H2O 19.8092 * biomass
185,0,101, R2 R3 R4 R5 R6 R7 R8 R9 R10 R12 R13 R14 R15 R16 R17 R18 R19 R20 R21 R23 R24 R25 R26 R27 R28 R29 R30 R31 R32 R33 R34 R35 R36 R37 R39 R40 R41 R42 R44 R46 R47 R48 R49 R50 R51 R52 R53 R54 R55 R56 R57 R58 R59 R60 R61 R62 R63 R64 R65 R66 R67 R68 R69 R70 R71 R72 R73 R74 R75 R76 R77 R78 R79 R80 R81 R82

R83 R84 R85 R86 R87 R88 R89 R90 R91 R92 R93 R94 R95 R96 R97 R98 R99 R100 R101 R102 R103 R104 R105 R106 R107, -3766.0043 * hv700 -3766.0043 * hv680 -1.365 * H2S -75.8506 * HNO3 -760.8255 * CO2 927.1694 * O2 -597.9752 * H2O 760.7873 * biomass
186,0,101, R2 R3 R4 R5 R6 R7 R8 R9 R10 R12 R13 R14 R15 R16 R17 R18 R19 R20 R21 R23 R24 R25 R26 R27 R28 R29 R30 R31 R32 R33 R34 R35 R36 R37 R39 R40 R41 R43 R44 R46 R47 R48 R49 R50 R51 R52 R53 R54 R55 R56 R57 R58 R59 R60 R61 R62 R63 R64 R65 R66 R67 R68 R69 R70 R71 R72 R73 R74 R75 R76 R77 R78 R79 R80 R81 R82 R83 R84 R85 R86 R87 R88 R89 R90 R91 R92 R93 R94 R95 R96 R97 R98 R99 R100 R101 R102 R103 R104 R105 R106 R107, -3755.4576 * hv700 -3755.4576 * hv680 -1.365 * H2S -75.8506 * HNO3 -760.8255 * CO2 927.1694 * O2 -597.9752 * H2O 760.7873 * biomass
187,0,101, R2 R3 R5 R6 R7 R8 R9 R10 R11 R12 R13 R14 R15 R16 R17 R18 R19 R20 R22 R24 R25 R26 R27 R28 R29 R30 R31 R32 R33 R34 R35 R36 R37 R39 R40 R41 R42 R43 R44 R46 R47 R48 R49 R50 R51 R52 R53 R54 R55 R56 R57 R58 R59 R60 R61 R62 R63 R64 R65 R66 R67 R68 R69 R70 R71 R72 R73 R74 R75 R76 R77 R78 R79 R80 R81 R82 R83 R84 R85 R86 R87 R88 R89 R90 R91 R92 R93 R94 R95 R96 R97 R98 R99 R100 R101 R102 R103 R104 R105 R106 R107, -5.5422 * hv700 -5.5422 * hv680 -0.0020221 * H2S -0.11237 * HNO3 -1.1271 * CO2 1.3735 * O2 -0.88586 * H2O 1.1271 * biomass
188,0,101, R2 R3 R5 R6 R7 R8 R9 R10 R11 R12 R13 R14 R15 R16 R17 R18 R19 R20 R22 R24 R25 R26 R27 R28 R29 R30 R31 R32 R33 R34 R35 R36 R37 R38 R39 R40 R41 R42 R44 R46 R47 R48 R49 R50 R51 R52 R53 R54 R55 R56 R57 R58 R59 R60 R61 R62 R63 R64 R65 R66 R67 R68 R69 R70 R71 R72 R73 R74 R75 R76 R77 R78 R79 R80 R81 R82 R83 R84 R85 R86 R87 R88 R89 R90 R91 R92 R93 R94 R95 R96 R97 R98 R99 R100 R101 R102 R103 R104 R105 R106 R107, -5.5422 * hv700 -5.5422 * hv680 -0.0020221 * H2S -0.11237 * HNO3 -1.1271 * CO2 1.3735 * O2 -0.88586 * H2O 1.1271 * biomass
189,0,101, R2 R3 R5 R6 R7 R8 R9 R10 R11 R12 R13 R14 R15 R16 R17 R18 R19 R20 R22 R24 R25 R26 R27 R28 R29 R30 R31 R32 R33 R34 R35 R36 R37 R38 R39 R40 R41 R43 R44 R46 R47 R48 R49 R50 R51 R52 R53 R54 R55 R56 R57 R58 R59 R60 R61 R62 R63 R64 R65 R66 R67 R68 R69 R70 R71 R72 R73 R74 R75 R76 R77 R78 R79 R80 R81 R82 R83 R84 R85 R86 R87 R88 R89 R90 R91 R92 R93 R94 R95 R96 R97 R98 R99 R100 R101 R102 R103 R104 R105 R106 R107, -5.5422 * hv700 -5.5422 * hv680 -0.0020221 * H2S -0.11237 * HNO3 -1.1271 * CO2 1.3735 * O2 -0.88586 * H2O 1.1271 * biomass
190,0,101, R2 R3 R5 R6 R7 R8 R9 R10 R11 R12 R13 R14 R15 R16 R17 R18 R19 R20 R22 R24 R25 R26 R28 R29 R30 R31 R32 R33 R34 R35 R36 R37 R38 R39 R40 R41 R42 R43 R44 R46 R47 R48 R49 R50 R51 R52 R53 R54 R55 R56 R57 R58 R59 R60 R61 R62 R63

R64 R65 R66 R67 R68 R69 R70 R71 R72 R73 R74 R75 R76 R77 R78 R79 R80 R81 R82 R83 R84 R85 R86 R87 R88 R89 R90 R91 R92 R93 R94 R95 R96 R97 R98 R99 R100 R101 R102 R103 R104 R105 R106 R107, -3833.1133 * hv700 -3833.1133 * hv680 -1.3986 * H2S -77.7163 * HNO3 -779.5397 * CO2 949.9752 * O2 -612.6837 * H2O 779.5005 * biomass
191,0,101, R2 R3 R5 R6 R7 R8 R9 R10 R11 R12 R13 R14 R15 R16 R17 R18 R19 R20 R23 R24 R25 R26 R27 R28 R29 R30 R31 R32 R33 R34 R35 R36 R37 R39 R40 R41 R42 R43 R44 R46 R47 R48 R49 R50 R51 R52 R53 R54 R55 R56 R57 R58 R59 R60 R61 R62 R63 R64 R65 R66 R67 R68 R69 R70 R71 R72 R73 R74 R75 R76 R77 R78 R79 R80 R81 R82 R83 R84 R85 R86 R87 R88 R89 R90 R91 R92 R93 R94 R95 R96 R97 R98 R99 R100 R101 R102 R103 R104 R105 R106 R107, -5.5422 * hv700 -5.5422 * hv680 -0.0020221 * H2S -0.11237 * HNO3 -1.1271 * CO2 1.3735 * O2 -0.88586 * H2O 1.1271 * biomass
192,0,101, R2 R3 R5 R6 R7 R8 R9 R10 R11 R12 R13 R14 R15 R16 R17 R18 R19 R20 R23 R24 R25 R26 R27 R28 R29 R30 R31 R32 R33 R34 R35 R36 R37 R38 R39 R40 R41 R42 R44 R46 R47 R48 R49 R50 R51 R52 R53 R54 R55 R56 R57 R58 R59 R60 R61 R62 R63 R64 R65 R66 R67 R68 R69 R70 R71 R72 R73 R74 R75 R76 R77 R78 R79 R80 R81 R82 R83 R84 R85 R86 R87 R88 R89 R90 R91 R92 R93 R94 R95 R96 R97 R98 R99 R100 R101 R102 R103 R104 R105 R106 R107, -3283.8674 * hv700 -3283.8674 * hv680 -1.1982 * H2S -66.5803 * HNO3 -667.8396 * CO2 813.8535 * O2 -524.8924 * H2O 667.8061 * biomass
193,0,101, R2 R3 R5 R6 R7 R8 R9 R10 R11 R12 R13 R14 R15 R16 R17 R18 R19 R20 R23 R24 R25 R26 R27 R28 R29 R30 R31 R32 R33 R34 R35 R36 R37 R38 R39 R40 R41 R43 R44 R46 R47 R48 R49 R50 R51 R52 R53 R54 R55 R56 R57 R58 R59 R60 R61 R62 R63 R64 R65 R66 R67 R68 R69 R70 R71 R72 R73 R74 R75 R76 R77 R78 R79 R80 R81 R82 R83 R84 R85 R86 R87 R88 R89 R90 R91 R92 R93 R94 R95 R96 R97 R98 R99 R100 R101 R102 R103 R104 R105 R106 R107, -5.5422 * hv700 -5.5422 * hv680 -0.0020221 * H2S -0.11237 * HNO3 -1.1271 * CO2 1.3735 * O2 -0.88586 * H2O 1.1271 * biomass
194,0,101, R2 R3 R5 R6 R7 R8 R9 R11 R12 R13 R14 R15 R16 R17 R18 R19 R20 R21 R23 R24 R25 R26 R27 R28 R29 R30 R31 R32 R33 R34 R35 R36 R37 R39 R40 R41 R42 R43 R44 R46 R47 R48 R49 R50 R51 R52 R53 R54 R55 R56 R57 R58 R59 R60 R61 R62 R63 R64 R65 R66 R67 R68 R69 R70 R71 R72 R73 R74 R75 R76 R77 R78 R79 R80 R81 R82 R83 R84 R85 R86 R87 R88 R89 R90 R91 R92 R93 R94 R95 R96 R97 R98 R99 R100 R101 R102 R103 R104 R105 R106 R107, -5.5422 * hv700 -5.5422 * hv680 -0.0020221 * H2S -0.11237 * HNO3 -1.1271 * CO2 1.3735 * O2 -0.88586 * H2O 1.1271 * biomass
195,0,101, R2 R3 R5 R6 R7 R8 R9 R11 R12 R13 R14 R15 R16 R17 R18 R19 R20 R21 R23 R24 R25 R26 R27 R28 R29 R30 R31 R32 R33 R34 R35 R36 R37 R38 R39 R40 R41 R42

R44 R46 R47 R48 R49 R50 R51 R52 R53 R54 R55 R56 R57 R58 R59 R60 R61 R62 R63 R64 R65 R66 R67 R68 R69 R70 R71 R72 R73 R74 R75 R76 R77 R78 R79 R80 R81 R82 R83 R84 R85 R86 R87 R88 R89 R90 R91 R92 R93 R94 R95 R96 R97 R98 R99 R100 R101 R102 R103 R104 R105 R106 R107, -3741.0928 * hv700 -3741.0928 * hv680 -1.365 * H2S -75.8506 * HNO3 -760.8255 * CO2 927.1694 * O2 -597.9752 * H2O 760.7873 * biomass

196,0,101, R2 R3 R5 R6 R7 R8 R9 R11 R12 R13 R14 R15 R16 R17 R18 R19 R20 R21 R23 R24 R25 R26 R27 R28 R29 R30 R31 R32 R33 R34 R35 R36 R37 R38 R39 R40 R41 R43 R44 R46 R47 R48 R49 R50 R51 R52 R53 R54 R55 R56 R57 R58 R59 R60 R61 R62 R63 R64 R65 R66 R67 R68 R69 R70 R71 R72 R73 R74 R75 R76 R77 R78 R79 R80 R81 R82 R83 R84 R85 R86 R87 R88 R89 R90 R91 R92 R93 R94 R95 R96 R97 R98 R99 R100 R101 R102 R103 R104 R105 R106 R107, -3283.8674 * hv700 -3283.8674 * hv680 -1.1982 * H2S -66.5803 * HNO3 -667.8396 * CO2 813.8535 * O2 -524.8924 * H2O 667.8061 * biomass

197,0,101, R2 R3 R5 R6 R7 R8 R9 R10 R12 R13 R14 R15 R16 R17 R18 R19 R20 R21 R23 R24 R25 R26 R27 R28 R29 R30 R31 R32 R33 R34 R35 R36 R37 R39 R40 R41 R42 R43 R44 R46 R47 R48 R49 R50 R51 R52 R53 R54 R55 R56 R57 R58 R59 R60 R61 R62 R63 R64 R65 R66 R67 R68 R69 R70 R71 R72 R73 R74 R75 R76 R77 R78 R79 R80 R81 R82 R83 R84 R85 R86 R87 R88 R89 R90 R91 R92 R93 R94 R95 R96 R97 R98 R99 R100 R101 R102 R103 R104 R105 R106 R107, -3833.1133 * hv700 -3833.1133 * hv680 -1.3986 * H2S -77.7163 * HNO3 -779.5397 * CO2 949.9752 * O2 -612.6837 * H2O 779.5005 * biomass

198,0,101, R2 R3 R5 R6 R7 R8 R9 R10 R12 R13 R14 R15 R16 R17 R18 R19 R20 R21 R23 R24 R25 R26 R27 R28 R29 R30 R31 R32 R33 R34 R35 R36 R37 R38 R39 R40 R41 R42 R44 R46 R47 R48 R49 R50 R51 R52 R53 R54 R55 R56 R57 R58 R59 R60 R61 R62 R63 R64 R65 R66 R67 R68 R69 R70 R71 R72 R73 R74 R75 R76 R77 R78 R79 R80 R81 R82 R83 R84 R85 R86 R87 R88 R89 R90 R91 R92 R93 R94 R95 R96 R97 R98 R99 R100 R101 R102 R103 R104 R105 R106 R107, -5.5422 * hv700 -5.5422 * hv680 -0.0020221 * H2S -0.11237 * HNO3 -1.1271 * CO2 1.3735 * O2 -0.88586 * H2O 1.1271 * biomass

199,0,101, R2 R3 R5 R6 R7 R8 R9 R10 R12 R13 R14 R15 R16 R17 R18 R19 R20 R21 R23 R24 R25 R26 R27 R28 R29 R30 R31 R32 R33 R34 R35 R36 R37 R38 R39 R40 R41 R43 R44 R46 R47 R48 R49 R50 R51 R52 R53 R54 R55 R56 R57 R58 R59 R60 R61 R62 R63 R64 R65 R66 R67 R68 R69 R70 R71 R72 R73 R74 R75 R76 R77 R78 R79 R80 R81 R82 R83 R84 R85 R86 R87 R88 R89 R90 R91 R92 R93 R94 R95 R96 R97 R98 R99 R100 R101 R102 R103 R104 R105 R106 R107, -5.5422 * hv700 -5.5422 * hv680 -0.0020221 * H2S -0.11237 * HNO3 -1.1271 * CO2 1.3735 * O2 -0.88586 * H2O 1.1271 * biomass

200,0,101, R2 R3 R5 R6 R7 R8 R9 R10 R11 R12 R13 R14 R15 R16 R17 R18 R19 R20 R23 R24 R25 R26 R28 R29 R30 R31 R32 R33 R34 R35 R36 R37 R38 R39 R40 R41 R42 R43 R44 R46 R47 R48 R49 R50 R51 R52 R53 R54 R55 R56 R57 R58 R59 R60 R61 R62 R63 R64 R65 R66 R67 R68 R69 R70 R71 R72 R73 R74 R75 R76 R77 R78 R79 R80 R81 R82 R83 R84 R85 R86 R87 R88 R89 R90 R91 R92 R93 R94 R95 R96 R97 R98 R99 R100 R101 R102 R103 R104 R105 R106 R107, -3833.1133 * hv700 -3833.1133 * hv680 -1.3986 * H2S -77.7163 * HNO3 -779.5397 * CO2 949.9752 * O2 -612.6837 * H2O 779.5005 * biomass

201,0,101, R2 R3 R5 R6 R7 R8 R9 R11 R12 R13 R14 R15 R16 R17 R18 R19 R20 R21 R23 R24 R25 R26 R28 R29 R30 R31 R32 R33 R34 R35 R36 R37 R38 R39 R40 R41 R42 R43 R44 R46 R47 R48 R49 R50 R51 R52 R53 R54 R55 R56 R57 R58 R59 R60 R61 R62 R63 R64 R65 R66 R67 R68 R69 R70 R71 R72 R73 R74 R75 R76 R77 R78 R79 R80 R81 R82 R83 R84 R85 R86 R87 R88 R89 R90 R91 R92 R93 R94 R95 R96 R97 R98 R99 R100 R101 R102 R103 R104 R105 R106 R107, -97.5626 * hv700 -97.5626 * hv680 -0.035597 * H2S -1.9781 * HNO3 -19.8413 * CO2 24.1793 * O2 -15.5944 * H2O 19.8403 * biomass

202,0,101, R2 R3 R5 R6 R7 R8 R9 R10 R12 R13 R14 R15 R16 R17 R18 R19 R20 R21 R23 R24 R25 R26 R28 R29 R30 R31 R32 R33 R34 R35 R36 R37 R38 R39 R40 R41 R42 R43 R44 R46 R47 R48 R49 R50 R51 R52 R53 R54 R55 R56 R57 R58 R59 R60 R61 R62 R63 R64 R65 R66 R67 R68 R69 R70 R71 R72 R73 R74 R75 R76 R77 R78 R79 R80 R81 R82 R83 R84 R85 R86 R87 R88 R89 R90 R91 R92 R93 R94 R95 R96 R97 R98 R99 R100 R101 R102 R103 R104 R105 R106 R107, -3283.8674 * hv700 -3283.8674 * hv680 -1.1982 * H2S -66.5803 * HNO3 -667.8396 * CO2 813.8535 * O2 -524.8924 * H2O 667.8061 * biomass

d. MFA results

Flux distribution for leaf metabolic network

The metabolic flux distribution values for reactions involved in the leaf metabolic network are given below.

R1 = 0.26868
R2 = 2.4182
R3 = 0.0091171
R4 = 0.013676
R5 = 0.097502
R6 = 1.0468
R7 = 1.9604
R8 = 1.9604
R9 = 0.80324
R10 = 0.32629
R11 = 0.7337
R12 = 0.35142
R13 = -0.69927
R14 = -0.34785
R15 = 0.46928
R16 = 0.46928
R17 = 0.3475
R18 = 1.0468
R19 = 0.096295
R20 = 0.58642
R21 = 0.12143
R22 = 0.55469
R23 = 0.40741
R24 = 0.13311
R25 = 0.13311
R26 = 0.080746
R27 = 0.033613
R28 = 0.032271
R29 = 0.032271
R30 = 0.032271
R31 = 0.032271
R32 = 0.0091171
R33 = 0.011869
R34 = 0.011869
R35 = 0.0091171
R36 = 0.6097
R36 = 0.6097
R37 = 0.55891
R38 = 0.011907
R39 = 0.0081882
R40 = 0.045207
R41 = 0.00034404
R42 = -0.0074638
R43 = -0.014242
R44 = 0.55616
R45 = -0.55744
R46 = 0.023098
R47 = 0.013126
R48 = 0.013126
R49 = 0.013126
R50 = 0.013126
R51 = 0.26952
R52 = 0.30209
R53 = 0.0025115
R54 = 0.003406
R55 = 0.0044038
R56 = 0.0040941
R57 = 0.0043349
R58 = 0.0040941
R59 = -0.00289
R60 = 0.00048166
R61 = -0.0054015
R62 = 0.075139
R63 = 0.0056079
R64 = 0.0028556
R65 = 0.0028556
R66 = 0.0027523
R67 = 0.0027523
R68 = 0.0027523
R69 = 0.003578
R70 = 0.0011009
R71 = 0.0011009
R72 = 0.0021331
R73 = 0.00034404
R74 = 0.00034404
R75 = 0.0039221
R76 = 0.0086011
R77 = 0.0086011
R78 = 0.00099773
R79 = 0.0021331
R80 = 0.084394
R81 = 0.02515
R82 = 0.0051951
R83 = 0.0051951
R84 = 0.0038533
R85 = -0.0072937
R86 = 0.0013771
R87 = 0.34404
R88 = 0.0067786
R89 = 0.0067786
R90 = 0.0067786
R91 = 0.0013771
R92 = 0.0076734
R93 = 0.0076734
R94 = 1.9902e-005
R95 = 0.00099098
R96 = 0.00074413
R97 = 0.0012854
R98 = 0.010205
R99 = 0.0010309
R100 = 0.0012068
R101 = 0.00058584
R102 = 0.01641
R103 = 0.0041096
R104 = 0.0010366
R105 = 0.017888
R106 = 0.045866
R107 = 0.97795

The listed flux distributions are obtained while CO_2 consumption (input) is taken as -0.978 moles for the model. The last value R107 represents the formation of biomass. R1 and R2 stand for cyclic and non cyclic photophosphyrylation (conversion of light energy into chemical energy), while R3 and R4 represent the mitochondrial electron transport and oxidative phosphorylation. Thus, the reactions R1 to R4 provide the required energy for the entire metabolic network; any change in these reactions causes total perturbation of the leaf metabolic network and influence the leaf metabolic model.

Publications

Publications

- Hézard Pauline., **Sasidharan L. Swathy**, Poughon Laurent, Fontaine Jean-Pierre and Dussap Claude-Gilles, 'Experimental set up, modelling design and preliminary results for plant growth control in the bioregenerative life support system' (2012): Proc. of *42nd International Conference on Environmental Systems* (ICES).
- **Sasidharan L. Swathy**, Hezard Pauline, Laurent Poughon and Dussap Claude-Gilles, 'Higher plant modelling for Bio regenerative life support including metabolic pathway description', (2010): Proc. of 40th *International Conference on Environmental Systems* (ICES).
- Hézard Pauline., **Sasidharan L. Swathy**, Creuly Catherine, Dussap Claude-Gilles, 'Higher plant modelling for Bio regenerative life support applications: General structure of modelling', (2010): Proc. of *40th International Conference on Environmental Systems* (ICES).
- Sebastián Torres, Mario D. Baigorí, **S.L. Swathy,** Ashok Pandey and Guillermo R. Castro (2009) : Enzymatic synthesis of banana flavour (isoamyl acetate) by *Bacillus licheniformis* S-86 esterase, *Food Research International* Volume 42, Issue 4, 454-460.
- Syed Ubaid Ahmed, Kunduru Konda Reddy, **Sasidharan L. Swathy,** Sudheer K. Singh, Sanjit Kanjilal, Rachapudi B.N. Prasad and Ashok Pandey (2009) : Enrichment of γ-linolenic acid in the lipid extracted from *Mucor zychae* MTCC 5420, *Food Research International*, Volume 42, Issue 4, 449-453.

Technical notes

- **Sasidharan L. Swathy**, Hezard Pauline and Dussap Claude-Gilles, TN 83.14: Biochemical and chemical approaches to plant growth (2010)
- Hézard Pauline, Farges Berangere **Sasidharan L. Swathy** and Dussap Claude-Gilles, TN 83.15: Definition of a roadmap for modelling and operating a controlled higher plant compartment (2010)
- Hézard Pauline, **Sasidharan L. Swathy** and Dussap Claude-Gilles, TN 83.12: Modelling approaches for higher plant cultures (2011)

Manuscript under correction and submission

- **Sasidharan L. Swathy**, Hezard Pauline, Laurent Poughon and Dussap Claude-Gilles, 'Biochemical significance of photosynthesis in terms of metabolic network analysis techniques', under correction.
- **Sasidharan L. Swathy**, Hezard Pauline, Laurent Poughon and Dussap Claude-Gilles, 'Metabolic network model and system level insights into plant respiration energy metabolism by thermodynamic analysis and metabolic network analysis techniques', under correction.

National and international conferences participated

- **Sasidharan L. Swathy,** Hezard Pauline, Laurent Poughon and Dussap Claude-Gilles, 'Higher plant modelling for Bio regenerative life support including metabolic pathway description' (2010): (Oral) *40th International Conference on Environmental Systems* (ICES), Barcelona, Spain.
- **Sasidharan L. Swathy** and Dussap Claude-Gilles, 'Plant growth modelling for life support chamber- simple metabolic model of the leaf sub system' (2010): (Oral) *Journée de l'école doctorale* (JED-SVS), Clermont Ferrand, France.
- **Sasidharan L. Swathy**, Hézard Pauline, Farges Bérangère, Laurent Poughon and Dussap Claude-Gilles, 'Life support in space: Generic model of higher plant production for MELiSSA project' (2011): (Oral) *7th International Microbial Space Workshop* (IMSW), Clermont- Ferrand, France.
- **Sasidharan L. Swathy**, Hézard Pauline, Laurent Poughon and Dussap Claude-Gilles, 'Elementary flux mode analysis in plants: Physiological plant growth model for life support system in space' (2011): (Poster) *Réseau Français de Métabolomique et Fluxomique (RFMF)*, Paris, France.
- **Sasidharan L. Swathy**, Hézard Pauline, Laurent Poughon and Dussap Claude-Gilles, 'Metabolic flux analysis –Application in plant modelling for life support systems' (2010): (Oral) *38th Scientific assembly of the committee on space research* (COSPAR), Bremen, Germany.
- **Sasidharan L. Swathy**, Hézard Pauline, Dussap Claude-Gilles, 'Prelimary results of Physiological plant growth modelling for human life support in space (will be held in July 2012): (Oral) *39th Scientific assembly of the committee on space research* (COSPAR), Mysore, India.
- Hézard Pauline., **Sasidharan L. Swathy**, Creuly Catherine., Dussap Claude-Gilles, 'Higher plant modelling for Bio regenerative life support applications: general structure of modelling', (2010): (Poster) *40th International Conference on Environmental Systems* (ICES), Barcelona, Spain. (**First prize for the best poster presentation**).
- Hézard Pauline, Farges Bérangère, **Sasidharan L. Swathy**, Dussap Claude-Gilles, 'Higher plants in life support systems: design of a model and experimental compartment' (2010): (Oral) *38th Scientific assembly of the committee on space research* (COSPAR), Bremen, Germany.
- Hézard Pauline., **Sasidharan L. Swathy**, Poughon Laurent, Fontaine Jean-Pierre and Dussap Claude-Gilles, 'Experimental set up, modelling design and preliminary results for plant growth control in the bioregenerative life support system' (will be held in July 2012): (Oral) *42nd International Conference on Environmental Systems* (ICES).
- **Sasidharan L. Swathy**, Hézard Pauline, Dussap Claude-Gilles, 'Higher plant modelling for life support applications: first results of a simple mechanistic model' (will be held in July 2012): (Oral) *39th Scientific assembly of the committee on space research* (COSPAR), Mysore, India.

Abstract

For long term space missions, higher plants are necessary to be included in life support systems. The Micro Ecological Life Support System Alternative (MELiSSA) project of European Space Agency (ESA) is based on a closed life support system where microbial and higher plant compartments support the consumer's compartment. Plants consume the possible recycling wastes (waste water and CO_2) and provide fresh food, potable water and oxygen to the crew. One of the key points for this kind of study is to maintain a system which recycles all the elements C, H, O, N, S, P, etc. That is why, the study is based on the modelling of conversion stoichiometries; they are the results of the control parameters of the system (physical limitations of mass and energy exchanges). As a preliminary step, we have established leaf metabolic model (a sub model of the plant biochemical model) involving central carbon metabolism using metabolic techniques, elementary flux mode analysis (EFMA) and metabolic flux analysis (MFA). It is associated to an integrated approach of energetics and central metabolism. Due to data limitations, the leaf metabolic model was constructed taking the biomass composition of lettuce (Lactuca sativa) from United States Department of Agriculture (USDA) and validated with the experimental data where lettuce grown in controlled Environment Systems Research Facility (CESRF) of University of Guelph (Canada). For the first approach, the model is satisfying and promising; it can predict the biomass production connecting the physical plant growth factors (light, CO_2 and water availability, etc.) along with time course growth and biomass composition. However, our results show the lack of sufficient data; hence, various kinds of measurements required for more accurate model predictions are proposed. The future model must be able to control and manage the plant growth for human survival knowing the fluxes from other compartments of MELiSSA loop. Further, the approach described here can be used more generically in all kinds of metabolic studies and modeling, especially for studying simultaneous and/or consecutive photosynthetic and respiratory metabolisms.

Résumé

Pour des missions spatiales de longue durée, les plantes supérieures doivent faire partie des systèmes de support-vie. Le projet Micro-Ecological Life Support System Alternative (MELiSSA, alternative de système de support-vie micro-écologique) de l'Agence Spatiale Européenne est basé sur un système clos de support vie qui inclut, autour d'un compartiment consommateur, des compartiments microbiens et des plantes supérieures. Les plantes consomment les déchets pouvant être recyclés (les eaux usées et du CO_2) et produisent de la nourriture fraîche, de l'eau potable et de l'oxygène pour l'équipage. Un des points clé pour ce type d'étude est le maintien d'un système qui assure le recyclage de tous les éléments C, H, O, N, S, P, … C'est pourquoi la base de l'étude repose sur une modélisation des stœchiométries de conversion qui doit traduire les échanges de matière et d'énergie en fonction des limitations physiques qui sont les paramètres de contrôle du système. L'étape préliminaire a été d'établir un modèle métabolique de feuille (un sous-modèle du modèle biochimique), comprenant le métabolisme central et utilisant les techniques métaboliques d'analyse des modes élémentaires (EFMA) et d'analyse des flux métaboliques (MFA) associé à une vision intégrée de l'énergétique du métabolisme central. En l'absence de données expérimentales suffisantes, le modèle métabolique de feuille a été construit à partir de la composition de la biomasse référencée par le Département Americain de l'Agriculture (USDA) et validé avec les données expérimentales de laitues (Lactuca sativa) cultivées dans l'installation de recherche des systèmes à environnement contrôlé (CESRF) de l'Université de Guelph (Canada). Pour la première approche, le modèle est satisfaisant et prometteur; il peut prédire la production de biomasse une fois connecté aux facteurs physiques de la croissance de plante (lumière, disponibilité en CO_2 et en eau,…) au cours du temps et à la composition de la biomasse. Cependant, nos résultats souffrent d'un manque de données pour vérifier les modèles métaboliques; ainsi, différents types de mesures pour des prédictions plus précises sont proposés. Le futur modèle doit être en mesure de contrôler la croissance de la plante pour la survie des humains, connaissant les flux provenant des autres compartiments de la boucle MELiSSA. Par ailleurs, l'approche décrite ici peut être utilisée de manière plus générale pour tous types d'études et modélisations du métabolisme, en particulier pour étudier le fonctionnement simultané et/ou consécutif des métabolismes photosynthétique et respiratoire.